

# Life Cycle of the X Chromosome

Through meiosis and embryonic  
development in mammals

Federica Federici

---

ISBN: 978-94-6299-030-2

Layout: Fabrizia Carofiglio and Federica Federici

Cover design: Otello Federici and Federica Federici

Printing: Ridderprint BV, Ridderkerk, the Netherlands

The work described in this thesis was performed at the Department of Reproduction and Development at the Erasmus MC in Rotterdam, the Netherlands.

Printing of this thesis was financially supported by Erasmus University Rotterdam, and Department of Reproduction and Development, Erasmus MC.

Copyright © 2015 by F. Federici. All rights reserved. No part of this book may be reproduced, stored in a retrieval system or transmitted in any form or by any means, without prior permission of the author.



**Life Cycle of the X Chromosome**  
**Through meiosis and embryonic development in mammals**

**Levenscyclus van het X chromosoom**  
**Door meiose en embryonale ontwikkeling bij zoogdieren**

Thesis

to obtain the degree of Doctor from the Erasmus University Rotterdam  
by command of the rector magnificus

Prof.dr. H.A.P. Pols

and in accordance with the decision of the Doctorate Board.

The public defense shall be held on  
Wednesday 11 March 2015 at 11.30 hrs

by

**Federica Federici**  
born in San Doná di Piave, Italy



## **DOCTORAL COMMITTEE**

**Promotors:** Prof.dr. J.A. Grootegoed  
Prof.dr. J.S.E. Laven

**Other members:** Dr.ir. T. Mahmoudi  
Prof.dr. S. Repping  
Prof.dr. B. van Steensel

**Copromotor:** Dr.ir. W.M. Baarends

## TABLE OF CONTENTS

<b>Chapter 1</b>	Introduction	7
	Aims and outline of this thesis	35
<b>Chapter 2</b>	Round spermatid injection (ROSI) into oocytes: what can we learn from it?	43
	Addendum: ROSI protocol	57
<b>Chapter 3</b>	Round spermatid injection into mouse oocytes rescues female lethality of a paternally inherited <i>Xist</i> deletion	65
<b>Chapter 4</b>	Incomplete meiotic sex chromosome inactivation in the dog	89
<b>Chapter 5</b>	Male specific response to unsynapsed chromatin in meiotic prophase of mammals	133
<b>Chapter 6</b>	General discussion	153
<b>Addendum</b>	Summary	173
	Samenvatting	177
	List of abbreviations	183
	Curriculum vitae	185
	PhD portfolio	187
	Acknowledgements	189



# 1

## Introduction and scope of the thesis



## INTRODUCTION

Each individual from a specific animal species has a characteristic number of chromosomes in the cells composing its body. All chromosomes within a cell are present in pairs: one chromosome of each pair comes from the mother and one from the father. In mammals, while most pairs of chromosomes, called autosomes, look the same in both males and females, one particular pair differs between the sexes. Females have two copies of the X chromosome, one from each parent, while males inherit one X chromosome from their mother and one Y chromosome from their father. Thus, it is the presence or absence of the Y chromosome that determines male or female sex, respectively. Usually the X and Y are very different in structural appearance, and they share little sequence similarity. The regulation and functions of the sex chromosomes differ in quite many aspects from those of the autosomes. The most relevant special features of sex chromosomes will be described in this chapter, embedded in an overview of important chromatin regulatory events during spermatogenesis and early embryonic development.

### 1.1 X and Y chromosome evolution in mammals

Virtually all therian mammals (eutherians, the placental mammals, and metatherians, the marsupials) have an XY/XX sex-determining system, where male sex is determined by the dominant Y-borne *Sry* gene that triggers a cascade of events leading to testis development. *Sry* is a homolog of the X-linked *Sox3* gene, and is not present in the genome of species other than the therian mammals.

How the X and Y chromosomes initially evolved has been debated for decades. The most accredited hypothesis suggests that they have differentiated from a pair of autosomes carrying the *Sox3* gene, after one of these autosomes acquired the sex determining *Sry* gene by mutation of the respective *Sox3* allele. Confirmation of this assumption has been provided, among others, by the finding that all genes on the human and marsupial X are autosomal in platypus, one of the egg-laying monotremes (prototheria), implying that the therian X and Y began their differentiation from a pair of autosomes around 165 million years ago (MYA), soon after the divergence from the monotremes (Veyrunes et al., 2008).

But how then, in the course of evolution, did an identical pair of autosomes end up being so different from each other, morphologically and genetically, as the X and Y nowadays are?

After the initial acquisition of the male-determining gene on one member of a pair of autosomes, which gave rise to a proto-Y chromosome, recombination must have become suppressed between the homomorphic proto-sex chromosomes, as a first step leading to the two heteromorphic chromosomes (Charlesworth, 1996; Rice, 1996). Currently available evidence

suggests that the elimination of recombination might have been achieved through chromosomal inversions on the proto-sex chromosomes (Lahn and Page, 1999). In therian mammals, suppression of recombination seems to have progressed in multiple steps along the proto-sex chromosomes (Lahn and Page, 1999), allowing them to accumulate mutations independently and to become genetically distinct.

Beyond their heterogeneity in gene content, the most striking difference between the X and Y chromosomes resides in their physical size, with the Y chromosome being smaller than the X. Since there is no possibility for two Y chromosomes to be present in the same nucleus during the mammalian life cycle, this chromosome is completely sheltered from genetic recombination with another Y chromosome, so that it is inherited from father to son in a clonal fashion. The X chromosome, on the other hand, can still recombine along its entire length in female meiosis, in oocytes. Various models have been proposed to explain the degeneration of the Y chromosome (Charlesworth, 1978; Orr and Kim, 1998; Rice, 1987). A common feature of these models is that the efficacy of natural positive or negative selection acting on individual Y-chromosomal genes becomes reduced on such a non-recombining chromosome, resulting into an increased accumulation of deleterious mutations, loss of function of most of its genes and final degeneration. Rapid loss of many Y chromosomal genes may have occurred already at the very beginning of mammalian X and Y evolution (reviewed in (Bachtrog, 2013)).

The best known mammalian sex chromosomes are the human X and Y, closely followed by those of several other primates and the mouse. The human X is a medium sized chromosome (about 155 Mb) containing about 800 protein-coding genes (Ensembl Human genome assembly GRCh38). The X of other placental mammals has a similar size and gene content, as predicted by Ohno (Ohno, 1967), and even gene order (Raudsepp et al., 2004), except for the mouse X, which is highly rearranged. The marsupial X chromosome is about two-thirds the size of the X of placental mammals. Comparative gene mapping has shown that the marsupial X is equivalent to the long arm and a proximal portion of the short arm of the human X, the X-conserved region (XCR) (Glas et al., 1999). The short arm of the human X is autosomal in marsupials (Graves, 1995), which means that it originated by translocation of an autosomal region to the eutherian sex chromosomes after divergence of marsupials and placental mammals. This region has therefore been called the X-added region (XAR).

In man, the Y chromosome is about 60 Mb in size. Investigating the composition and gene content of Y chromosomes of different species is challenging, because their high content of repetitive sequences and their degenerative nature has excluded them from most genome sequencing projects. It was generally thought that the Y chromosome would be poorly conserved, both in its gene content and arrangement among different species (Marshall Graves, 2008), until two very recent studies found evidence for long-term conservation of a key set of



ancestral mammalian Y-linked genes (Bellott et al., 2014; Cortez et al., 2014). Comparison of Y-chromosomal sequences in various mammals revealed that, after abundant gene loss early in the evolution of the Y chromosome (with only 3% of the ancestral proto-sex chromosomal genes surviving on the “modern” Y chromosomes), a subsequent remarkable gene stability has been maintained across the Y chromosomes of extant mammals.

### **BOX1. Meiosis**

In mammals, the transmission of genetic information from one generation to the next is achieved through sexual reproduction. Each new individual arises from fusion of a spermatozoon produced by the father with an egg derived from the mother. To generate a normal diploid organism ( $2n$ ,  $2C$ ), gametes (spermatozoa and oocytes) must have a haploid DNA content ( $1n$ ,  $1C$ ). To achieve this, a single round of DNA replication, producing diploid cells with doubled DNA content ( $2n$ ,  $4C$ ), is followed by two successive rounds of cell division during meiosis ( $1C$  is the amount of DNA in a haploid gamete generated by the two meiotic divisions) (as represented in Figure 1A and B).

DNA replication takes place at the very beginning of meiotic prophase, so that all individual homologous chromosomes are present as two sister chromatids. In order to successfully segregate chromosomes to haploid daughter cells in the first meiotic cell division, the homologous chromosomes (homologs) of the diploid genome must find each other and stably pair. Homolog recognition and pairing is promoted by DNA recombination interactions that are initiated upon formation of developmentally programmed DNA double strand breaks (DSBs). Following DSB formation, a specialized homologous recombination repair mechanism ensures that the proper partner (the respective homologous chromosome) becomes engaged in a stable pairing interaction. This interaction is then secured by the assembly of a proteinaceous structure between the homologs, the synaptonemal complex (SC). The formation of the SC starts with the accumulation of SYCP2 and SYCP3 protein filaments along the chromosomal axes of the sister chromatids. These proteins form stretches of the axial elements (AE) of the SC at the beginning of meiotic prophase, in the meiotic prophase stage called leptotene. Subsequently, in zygotene, when homologous chromosome alignment is achieved, the transverse element (TE) protein SYCP1, in cooperation with the central element (CE) components SYCE1, SYCE2, and TEX12, connects the homologous AEs. The appearance of SYCP1 defines the moment of synapsis and the AEs in the completed SC are termed lateral elements (LEs). When synapsis is complete, the lengthy pachytene stage begins, and crossovers are formed. When DSBs have been repaired, leading to the formation of crossovers or noncrossovers, the SC starts to disas-



semble at diplotene, and the homologous chromosomes, now held together at chiasmata (the X-shaped connections between the homologs, which are the visual representations of crossovers at metaphase), begin to separate. The segregation of the homologous chromosomes during the subsequent first meiotic division will give rise to two daughter cells containing only one copy of each chromosome, consisting of two sister chromatids (that are in fact no longer identical because crossing over has occurred) ( $1n, 2C$ ). Subsequently, during the second meiotic division, the sister chromatids are separated from each other, in a process mechanically identical to separation of sister chromatids in mitosis. Together, the first and second meiotic divisions produce four genetically different haploid cells ( $1n, 1C$ ) (Figure 1A and B).

Although the overall progression through the meiotic prophase stages and meiotic divisions is fundamentally comparable in male and female germ cells, significant sex specific differences are present. In mice, the first morphological difference between male and female gonads begins at embryonic day 11.5 (E11.5) with the migration of mesonephric cells into the male gonads, soon followed by formation of testis cords with precursor Sertoli cells, which enclose the primordial germ cells. These events do not occur in the gonads of female embryos, where the supporting cells differentiate a few days later to become the first granulosa precursor cells associated with germ cells passing through meiotic prophase up to an arrest in diplotene (dictyotene or dictyate arrest) around the time of birth (McLaren, 2003; Peters, 1970). In contrast, the germ cells enclosed in the testis cords in the developing male testes undergo mitotic arrest (McLaren, 2000). Meiosis in the male will first start at the onset of puberty and from then on will regularly initiate in cycles throughout further adult life, leading to the continuous production of spermatozoa (Figure 1B). In females, oocytes remain in dictyotene arrest until sexual maturity is reached, when during each reproductive cycle a small percentage of the pool of arrested oocytes (non-growing oocytes) begin to grow progressively, increasing more than 200-fold in volume. At the time when full growth is achieved (the diameter of a fully grown oocyte reaches  $80\ \mu\text{m}$ ), the oocytes become capable of re-entering the cell cycle but are maintained in meiotic arrest by the surrounding follicular cells. At ovulation, under strict hormonal control, the oocytes are stimulated to resume the first meiotic cell cycle and undergo the first meiotic division, which results in the production of a haploid secondary oocyte and a smaller haploid cell, which is the first polar body (Figure 1A). The secondary oocyte begins the second meiotic division and then arrests again, now at the metaphase of meiosis II. When triggered by fertilization, the second meiotic division will be completed, producing the female pronucleus and a second polar body (Figure 1A).

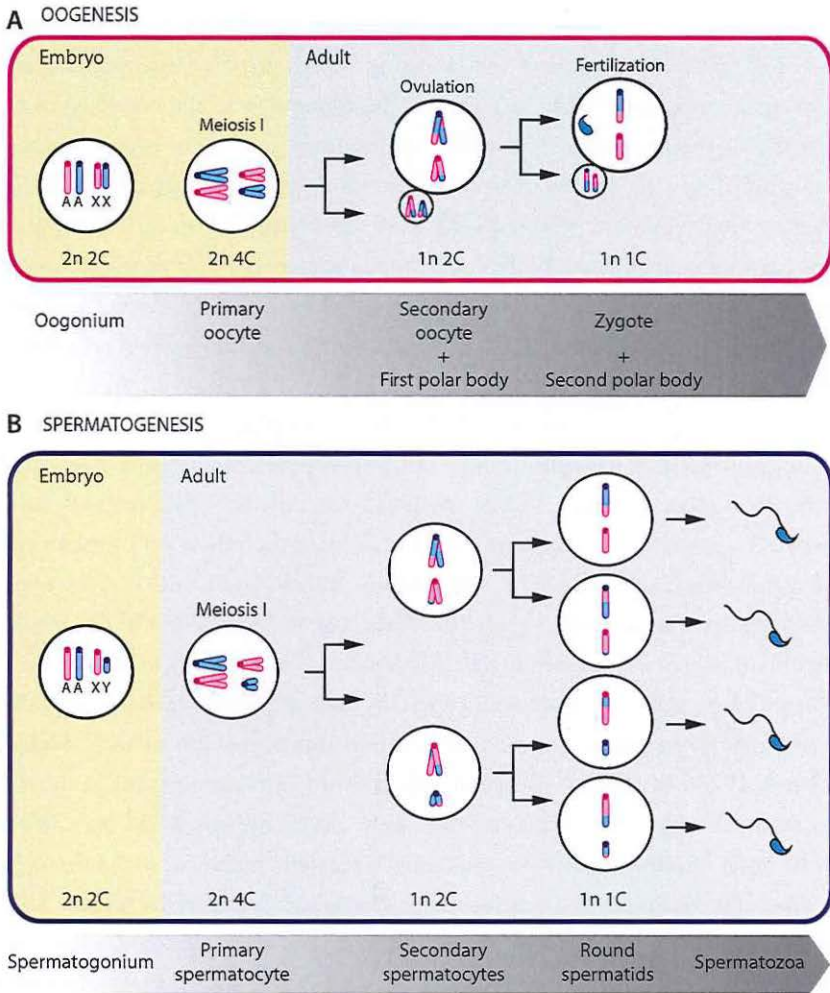


**Figure 1: Gametogenesis in female and male mouse**

Schematic drawing showing analogies in the process of maturation of the oocyte and the development of spermatozoa, following their respective pathways.

(A) During oogenesis, oogonia enter the first meiotic division after a pre-meiotic DNA replication event. These meiotic cells, called the primary oocytes, progress through the first meiotic prophase until the diplotene stage, at which point they are arrested (dictyotene or dictyate arrest) and are maintained until puberty or even longer. With the onset of puberty, groups of oocytes periodically resume and complete meiosis I upon ovulation. Cell division in meiosis I is asymmetric: almost all of the cytoplasm ends up in one cell with half the chromosomes, called the secondary oocyte. The remaining cell with little cytoplasm and the other half of the chromosomes, called the first polar body, is discarded. The oocyte then proceeds to enter meiosis II, but becomes arrested again, now at metaphase II. Fertilization induces the transition from metaphase II to anaphase



## 1.2 XY regulation in male meiosis: pairing of two heteromorphic sex chromosomes

Being genetically and structurally very different, the fact that meiotic prophase has to deal with the X and Y chromosomes has been defined as the Achilles's heel of male meiosis (BOX1) (Kauppi et al., 2011). While autosomes are entirely homologous and are hence able to pair from end to end, the X and Y are heterologous chromosomes which share only a small region of homology that enables pairing, the pseudoautosomal region (PAR). The human Y chromosome has two PARs: a large PAR1 (2.6 Mb) and a much smaller PAR2 (320 kb). Thus far, human is the only eutherian species known to have two PARs. Only PAR1 is required for pairing of the X and Y chromosomes during meiosis in men, and this region is common to most eutherian mammals (Figure 2), with a gene order that has been fairly well conserved since its addition, together with the XAR, after the divergence of placental mammals and marsupials. However, the boundary between PAR1 and the non-recombining region has shifted over evolutionary time, and both the size and the gene content of PAR1 differ among species (Raudsepp and Chowdhary, 2008; Raudsepp et al., 2012; Skinner et al., 2013) (Figure 2). Marsupials do not have a PAR region at all, and a different strategy to physically connect their sex chromosomes has evolved in this infraclass of mammals (Sharp, 1982). The single mouse PAR is very small in size (around 700 Kb) (Perry et al., 2001), and contains only 3 genes (*Srs*, *Asmt*, and part of *Mid1*) (Kasahara et al., 2010), much fewer than the 24 genes in the human PAR1. Genes located within human PAR1, when mapped in the mouse, are autosomal (Disteche et al., 1992; Gianfrancesco et al., 2001). Rearrangements and rapid evolution have shaped the PAR in the mouse lineage in a different manner (Perry et al., 2001). However, the mouse PAR, like the human PAR1, plays an essential role in pairing and partial synapsis of the sex chromosomes in male meiotic prophase.

II, leading to completion of oocyte meiosis and emission of a second polar body (which will degenerate). The production of egg cells via oogenesis occurs only from puberty to menopause.

**(B)** The basic function of spermatogenesis is to turn each one of the diploid spermatogonia into four haploid spermatozoa. This quadrupling is accomplished through two subsequent and symmetric meiotic cell divisions, without loss of cells. During interphase before onset of meiotic prophase, the spermatogonial diploid chromosomal set is replicated to form chromosomes composed of two sister chromatids, giving rise to a primary spermatocyte that will go through the first meiotic division to form two haploid secondary spermatocytes. In meiosis II, these two cells go through a second division to yield four round spermatids, containing a unique set of haploid chromosomes, that ultimately mature into four spermatozoa. Starting at puberty, a male will produce literally millions of sperm every single day for the rest of his life.

n = ploidy number; C = DNA content.

As a consequence of the presence of the (largely) unsynapsed sex chromosomes during male meiosis (Figure 3A), an essential process defined as meiotic sex chromosome inactivation (MSCI) has been called into action in the therian lineage.

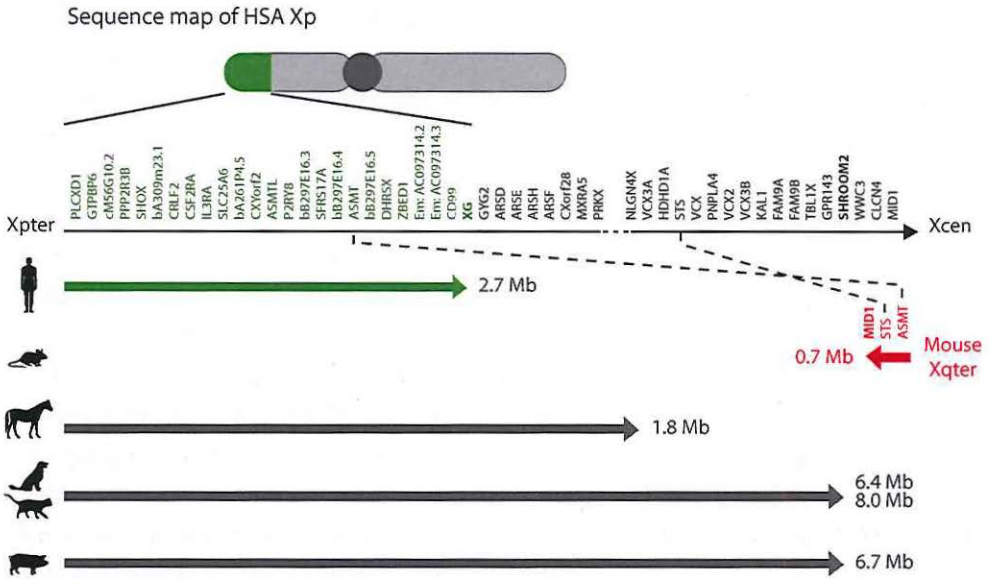


**Figure 2: Pseudoautosomal regions of some eutherian species**

The physical domain of the pseudoautosomal region (PAR) lies between the terminal ends of the sex chromosomes and the pseudoautosomal boundary (PAB), a border across which the sequence homology between the X and Y chromosomes decreases. The PAB of the human PAR1 contains 24 genes and is demarcated by the *XG* gene (in bold characters) at 2.6 Mb from the tip of HSAXp. The mouse PAR is approximately 700 kb and contains only 3 known protein coding genes. The mouse PAB is spanned by the *Mid1* gene (in bold characters). Thus far, the mouse PAR is the smallest and the gene poorest known among eutherians.

The horse PAR is about 1.8 Mb in size and contains 18 genes, its PAB is located between *PRRX* and *NLGN4X*. Even though the equine PAR contains loci from an additional region beyond the human PAR1, it is smaller than the human counterpart. The larger size of the human PAR1 is probably due to a greater abundance of intergenic repetitive sequences. The canine PAR is 6.6 Mb, contains at least 34 protein coding genes and extends proximal to *SHROOM2*. Similarly the cat PAB is also located between *SHROOM2* and *WWC3*. The porcine PAR is approximately 6.7 Mb and *SHROOM2* represents the PAB also in this species.



**BOX2. Epigenetics**

Chromosomal DNA is compacted by proteins called histones, and the resulting DNA-protein complex, which includes also many other proteins interacting with histones or DNA, is called chromatin. There are five major families of histones: H1, H3, H4, H2A, and H2B. Histones H3, H4, H2A, and H2B are also defined as the core histones, while histone H1 is known as the linker histone. Two each of the core histones come together to form a histone octamer core around which 146 bp of DNA is wrapped. This forms the basic structural entity of chromatin that is defined as a nucleosome.

So far, only one H4 isoform has been identified, whereas the H1, H3, H2A, and H2B families are composed of many histone variants, which can replace the canonical histones, thereby altering nucleosome structure, stability, and, ultimately, DNA accessibility. Mammalian histone variants are classified into two major groups: those enriched in somatic cells, which can further be divided into replication-dependent and replication-independent histones; and another group consisting of testis-specific histones (reviewed in (Maze et al., 2014)).

Nucleosomes are assembled with the aid of specific histone chaperone proteins. For example, canonical histone H3 (which refers to H3.1 and H3.2) is deposited onto DNA by the histone chaperone CAF1 during DNA replication-dependent nucleosome assembly, while the histone variant H3.3 is deposited by the histone chaperones HIRA and ATRX-DAXX complex in a replication-independent manner.

Chromatin structure can be altered by modification of either DNA or histones, or both, affecting the way they interact with each other, and resulting in conformational changes and increased accessibility of the DNA to other factors. These non-genetic alterations are tightly regulated by two major modifications: chemical modifications of the histone proteins (histone modifications) and of specific cytosine residues of DNA (DNA methylation). Together, these non-genetic alterations form the basis for the so-called epigenetic information, which can be heritable when cells divide or even across generations.

Histone modifications act in diverse biological processes such as gene regulation, DNA repair, and chromosome condensation. Several distinct classes of histone-modifying enzyme can modify histones at multiple sites. There are at least eight distinct types of chemical modifications found on histones (Tan et al., 2011). Covalent attachment to histones can create binding sites for other proteins or change the physical properties of the nucleosome. Combinations of different histone modifications are thought to constitute a code, the so-called histone code. Histones can also directly be displaced by chromatin remodeling complexes, thereby exposing underlying DNA sequences to polymerases and other



enzymes (Smith and Peterson, 2005).

DNA methylation is a biochemical process where a methyl group is added to specific cytosine residues of DNA (5-mC), and it generally relates to gene silencing. The addition of methyl groups to DNA is carried out by a family of enzymes called DNA methyltransferases (DNMTs). *De novo* DNMTs set new marks, leading to epigenetic programming, and maintenance DNMTs copy the methylation marks on the newly synthesized DNA strand in replication, making the marks heritable. Equally important is DNA demethylation, the removal of a methyl group, which is necessary for the epigenetic reprogramming of genes. Demethylation of DNA can either be passive or active, or a combination of both. Passive DNA demethylation usually takes place during replication rounds, when methylation is not maintained by DNMT1 on the newly synthesized DNA strands. Active DNA demethylation mainly occurs by the removal of 5-methylcytosine via the sequential modification of cytosine bases that have been converted by ten-eleven translocation (TET) enzyme-mediated oxidation. The TET family of 5-mC hydroxylases includes TET1, TET2, and TET3. These proteins may promote DNA demethylation by converting 5-mC to 5-hydroxymethylcytosine (5-hmC), 5-hmC to 5-formylcytosine (5-fC), and 5-fC to 5-carboxylcytosine (5-caC) through hydroxylase activity. The oxidized forms of 5mC can then be passively diluted (Inoue et al., 2011; Inoue and Zhang, 2011). In addition, 5fC and 5caC can also be removed through the base excision repair pathway which is triggered by the enzyme thymidine DNA glycosylase (TDG) (He et al., 2011; Kohli and Zhang, 2013). These processes collectively result in a hypomethylated state.

One of the best studied epigenetic processes that usually involves generation of specific DNA methylation is known as genomic imprinting. Although one might expect that genes from both parents contribute equally to embryo development, this expectation is contravened by genomic imprinting, where a subset of genes exhibits monoallelic, parental-specific expression. The imprinting marks that generate such an expression pattern are established in either the male or female germline, depending on the gene, they are heritable, and can be maintained after fertilization and through mitotic divisions. Parental genomic imprints can be erased only in the germline of the offspring, where new epigenetic marks are established depending on the sex of the offspring. Uniparental embryos, constructed to contain only maternal (gynogenetic/parthenogenetic embryos) or paternal (androgenetic embryos) diploid genome complements, fail to survive beyond mid-gestation (McGrath and Solter, 1984; Surani et al., 1984) as a consequence of misregulated expression of imprinted genes.

### 1.2.1 Meiotic sex chromosome inactivation

Chromosomes and chromosomal regions that do not become synapsed during meiosis undergo transcriptional silencing, in therian mammals (Kelly and Aramayo, 2007). In the case of the unsynapsed X and Y chromosomes during male meiosis (Figure 3A), this silencing mechanism is called meiotic sex chromosome inactivation (MSCI) (Burgoyne et al., 2009; Monesi, 1965). MSCI is the best-studied example of a more general epigenetic silencing mechanism that silences sequences without pairing partners, known as meiotic silencing of unsynapsed chromatin (MSUC) (Baarends et al., 2005; Turner et al., 2005). MSUC in mammals takes place in chromosomal regions that fail to synapse, for example in the case when certain autosomal translocations are present, or when there is (partial) aneuploidy of autosomes or sex chromosomes. The downstream consequences of MSUC, in particular in the female, are not clear, but in theory MSUC would be a potentially hazardous process, especially if crucial genes are switched off. Thus, while MSCI is solely and always occurring during male meiosis, MSUC takes place in meiosis of both sexes, but only in aberrant situations, when certain pairing problems arise.

In contrast with male and female infertility or reduced fertility that is associated with the occurrence of MSUC, males have evolved mechanisms to tolerate sex chromosome silencing, and MSCI has in fact become absolutely essential for male meiosis. Spermatocytes are able to cope with the loss of X-chromosomal gene transcription due to evolutionary adaptations which include the testis-specific expression of retrotransposed autosomal copies of several essential X-linked genes (Wang, 2004). Mutations that disrupt synaptic pairing of autosomes, and thereby induce massive MSUC, usually disrupt MSCI. This is caused by the fact that, when chromosome pairing is affected in a global manner, the proteins that mediate MSCI are redistributed to many autosomal sites and fail to accumulate to a high enough density at the sex chromosomes, allowing significant escape from MSCI, leading to X and Y gene transcription (Homolka et al., 2007; Turner, 2007; Zamudio et al., 2008). This then leads to illegitimate toxic expression of X- and Y-linked genes, and to a specific phenotype that is called pachytene arrest. Thus, if MSUC is activated and as a consequence MSCI fails, this invariably results in male-limited sterility. For example, when YY pairing was achieved in XYY spermatocytes, thus preventing inactivation of the Y, this caused arrest and subsequent loss of these spermatocytes, most probably because of inappropriate Y-linked gene transcription (Royo et al., 2010; Turner et al., 2006).

MSCI and MSUC seem to be the result of a similar molecular cascade, which involves the persistence of meiotic DSBs, in combination with the recognition of unsynapsed regions by proteins such as HORMAD1/2 (Wojtasz et al., 2009). This activates a DNA damage response

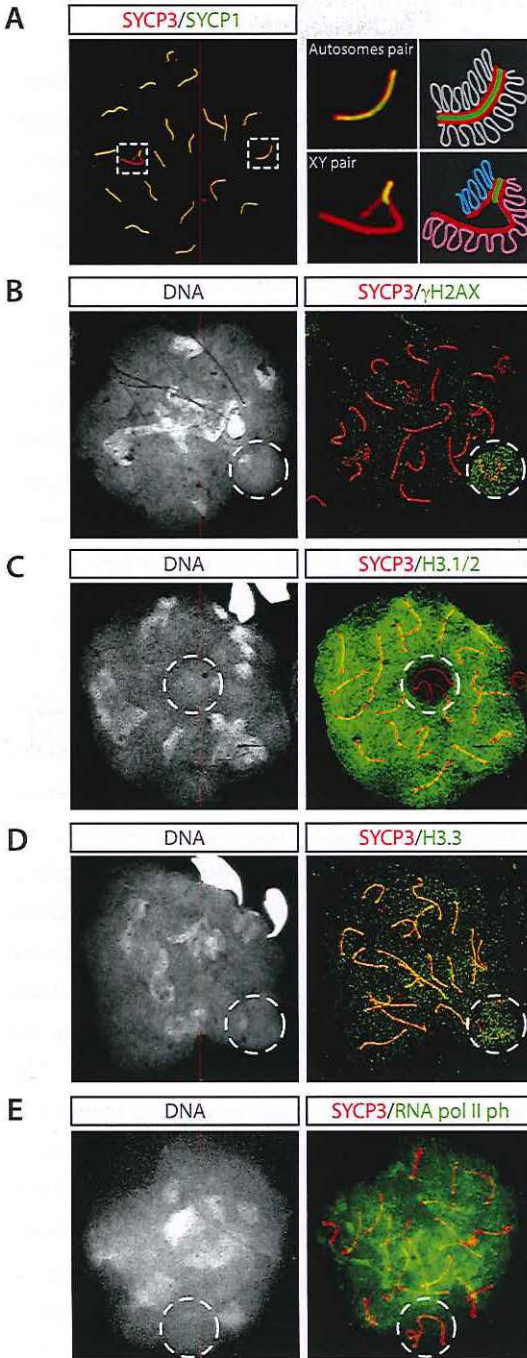


pathway which leads to accumulation of BRCA1 on the unsynapsed axes, and interdependent recruitment of MDC1 and the ATM and Rad3-related kinase, ATR, to the XY axes as well as to the surrounding chromatin (Ichijima et al., 2011; Scully et al., 1997; Turner et al., 2006). This cascade of events leads to the MDC1-dependent widespread phosphorylation of the histone variant H2AX at serine-139 ( $\gamma$ H2AX) (Figure 3B) (Ichijima et al., 2011; Mahadevaiah et al., 2001). The accumulation of  $\gamma$ H2AX represents an important epigenetic signal for triggering MSCI (Turner et al., 2004), as both H2AX and MDC1 knockout mice fail to properly form XY bodies and to undergo MSCI, leading to male sterility (Fernandez-Capetillo et al., 2003; Ichijima et al., 2011). A recent study has also shown that ATR is the main kinase phosphorylating H2AX to initiate XY inactivation, since conditional *Atr* ablation causes meiotic arrest and defective H2AX phosphorylation (Royo et al., 2013). Remarkably, once H2AX phosphorylation and XY silencing are established early in pachytene, absence of ATR in later meiotic sub-stages does not affect meiotic silencing stability (Royo et al., 2013).

Subsequent to the accumulation of  $\gamma$ H2AX, other chromosome-wide histone changes occur on the heterochromatic XY chromosome pair, the so-called XY body, including the substitution of the canonical histone H3 (Figure 3C) by the variant H3.3 (Figure 3D) (van der Heijden et al., 2007) and enrichment of macroH2A (mH2A) (Hoyer-Fender et al., 2000). In addition, several repressive histone marks (e.g., H3K9me3) become specifically enriched on the XY body in pachytene spermatocytes, whereas other histone modifications normally associated with transcriptional activity are depleted compared to the surrounding autosomal chromatin (van der Heijden et al., 2007). Furthermore, the transcriptional silencing established on the XY body via MSCI, becomes visible as a region depleted of RNA polymerase II (Figure 3E) and Cot1 DNA by mid-pachytene. The Cot-1 DNA probe is used to perform RNA FISH and allows to visualize repetitive sequences in intronic and 3' untranslated regions which emerge, upon gene transcription, into pre-spliced RNA (Turner et al., 2005). It is not clear if similar epigenetic dynamics accompany MSUC in both spermatocytes and oocytes. While transcriptional inactivation during male meiosis in mouse is cytologically marked by a more dense DAPI staining of the DNA in the region encompassing unsynapsed chromatin, in female meiosis unsynapsed chromatin is not compartmentalized in a clearly condensed region.

For man, establishment of MSCI has also been reported, although X-linked gene silencing appears to be less complete compared to chimpanzee (Mulugeta Achame et al., 2010a). This evidence is supported by immunocytological studies that point to a variation in the distribution of the RNA polymerase II and Cot1 DNA signal on the human XY body (de Vries et al., 2012). Moreover, the human sex chromosomes in late pachytene spermatocytes, miss an overt heterochromatic signature as based on the histone modification profiles normally observed on



**Figure 3: MSCI**

Representative images of spread pachytene spermatocyte nuclei immunostained for proteins of interest. On the left, the DNA is counterstained with DAPI (white), the compartmentalization and heterochromatic state of the sex chromosomes enclosed in the dashed white circle can be visually appreciated. On the right, double immunostaining with (A) anti-SYCP3 and anti-SYCP1, (B) anti-SYCP3 (red) and anti- $\gamma$ H2AX (green), (C) anti-SYCP3 (red) and anti-H3.1/2 (green), (D) anti-SYCP3 (red) and anti-H3.3 (green), (E) anti-SYCP3 (red) and anti-RNA polymerase II CTD repeat YSPTSPS (phospho S5) (green).

(A) The X and Y chromosomes (dashed white circle) are largely unsynapsed (SYCP1 accumulation is observed only in the PAR region), as shown in the enlarged areas and explanatory drawings on the right. (B) The XY body is undergoing MSCI and therefore accumulates  $\gamma$ H2AX. (C) By the time MSCI is initiated, histone H3.1/2 are evicted from sex chromosome chromatin and replaced by H3.3 (D). (E) When transcriptional reactivation occurs on autosomal chromatin in spermatocytes, the X and Y chromosomes (dashed white circle) are transcriptionally silenced by MSCI. Clear depletion of the phosphorylated (active) form of RNA polymerase II can be observed on the XY chromatin, compared to the overall level in the nucleus.

the mouse XY body (de Vries et al., 2012). Taken together, these observations evidence some levels of relaxation of MSCI in human.

In contrast to eutherian mammals, the marsupial X and Y chromosomes do not share a PAR, so that XY pairing during male meiosis occurs in the absence of complete SC formation between any region of the two sex chromosomes. In this case, the physical interaction between the heteromorphic sex chromosomes is then assured by the formation of a dense plate which attaches the ends of X and Y chromosomes. MSCI has been shown to occur also in marsupials during spermatogenesis, by Cot-1 RNA FISH and semiquantitative reverse transcriptase-polymerase chain reaction (RT-PCR) (Hornecker et al., 2007; Mahadevaiah et al., 2009; Namekawa et al., 2007). Levels of expression of X-linked housekeeping genes decline in meiotic spermatocytes in the opossum *Monodelphis domestica* (a much investigated marsupial) similarly to the reduction in levels of expression observed in mouse (Namekawa et al., 2006). Also in opossum, this X-linked gene silencing coincides with an increase in the level of expression of BRCA1 and ATR, and the association of  $\gamma$ H2AX with the X and Y chromosomes in early pachytene. This suggests that the mechanisms by which MSCI is achieved might be fairly well conserved in all therian mammals.

### 1.2.2 Post-meiotic sex chromosome repression

Once the long meiotic prophase has been completed, the first and second meiotic divisions occur in rapid succession, generating haploid round spermatids. In these cells, the silencing of the X and Y chromosomes established through MSCI in meiotic prophase partially persists in a process known as post-meiotic sex chromosome repression (PSCR) (Namekawa et al., 2006). Through microarray studies focusing on X-linked genes, it has been found that 87% of 676 genes on the X chromosome remain suppressed post-meiotically in mouse (Namekawa et al., 2006). This was comparable with pachytene spermatocytes, where 92% of X-linked genes were repressed. Yet, a significant number of X-linked genes become post-meiotically reactivated. These include many multi-copy genes (Mueller et al., 2008), but also some single-copy X-linked genes have been found to be re-expressed (Hendriksen et al., 1995; Mulugeta Achame et al., 2010b). The specific reactivation of these single-copy genes might serve important functions during spermiogenesis (see below) and early embryonic development.

In a haploid round spermatid, either the X or the Y chromosome can be visualized as a DAPI-dense domain located next to the chromocenter. The chromocenter is a cluster of constitutive heterochromatin, which typically includes the centromeric and pericentromeric regions of chromosomes. The persistence of an overall repressive state on these chromosomes can be identified by means of histone modifications associated with a heterochromatic state, such as H3K9me<sub>3</sub>, which remain on the sex chromosomes post-meiotically (Khalil et al., 2004; van





der Heijden et al., 2007). The histone variant H2A.Z is also enriched at heterochromatin domains of postmeiotic haploid spermatids, including at the sex chromosomes (Greaves et al., 2006), although its functional role during spermatogenesis remains unknown.

PSCR is maintained also in human round spermatids (Mulugeta Achame et al., 2010a; Sin et al., 2012), although the stringency of the transcriptional silencing imposed on X- and Y-linked genes compared to mouse is still under debate. In addition, the profiles of genes escaping from postmeiotic silencing are significantly divergent between human and mouse (Sin et al., 2012). This raises some questions about the possible implications of these changes and the actual relevance of maintenance of PSCR or escape from PSCR at the single-gene level.

In opossum, PSCR shares features with eutherian PSCR (Hornecker et al., 2007; Namekawa et al., 2007). As observed in mouse and man, sex chromosomes in opossum spermatids are depleted for Cot-1, retain their DAPI-intense staining, and continue to be enriched for heterochromatic marks (Namekawa et al., 2007). These data provided strong support for the hypothesis that, just as in eutherians, the postmeiotic X of opossum, and possibly also that of other marsupials, is transcriptionally suppressed.

### 1.3 Spermiogenesis

Spermiogenesis, the final stage of spermatogenesis, is a unique process during which haploid round spermatids develop into testicular spermatozoa. Its successful completion, followed by maturation of spermatozoa in the epididymis (which includes a gain of the capacity for forward motility), is necessary for the generation of sperm with fertilizing capability.

Fully developed testicular spermatozoa are formed by condensation of nuclear chromatin, elongation of the nucleus, formation of the acrosome, formation of a single and large flagellum and loss of residual cytoplasm. In addition to extensive morphological and cytoplasmic changes, the haploid round spermatids undergo extensive chromatin remodeling to develop into spermatozoa.

#### 1.3.1 The histone-to-protamine transition

To reach the oocyte, the sperm must travel along both the male and female reproductive tracts. The sperm nucleus adopts an extreme state of condensation, made possible via the replacement of canonical histone proteins (BOX2) by smaller and highly basic arginine-rich proteins, called protamines (Doenecke et al., 1997; Govin et al., 2004). This condensation enhances motility of the spermatozoon and protects its DNA content from damage. When round spermatid elongation commences, a wave of histone hyperacetylation most likely provides an accessible environment for the final histone eviction and substitution with transition proteins (TPs) and subsequently protamines (Gaucher et al., 2010).

The TPs are intermediate proteins between the histone-to-protamine transition. In mouse, there are two major TPs, TP1 and TP2, that first replace the majority of histones during spermatid elongation and the initiation of condensation. Single *Tp1* or *Tp2* knockout mouse models are fertile (displaying only minor sperm abnormalities), and this indicates that these two proteins might perform complementary functions (Yu et al., 2000; Zhao et al., 2001). Indeed, mice lacking both TPs are sterile and show major problems in spermatid nuclear condensation and genome integrity (Zhao et al., 2004).

The mouse genome encodes two protamines, PRM1 and PRM2, that replace the TPs as spermatid condensation proceeds. Attempts to generate single-gene knockouts failed, due to haploinsufficiency of either gene, resulting in severely aberrant spermatogenesis and male infertility (Cho et al., 2001). The link between abnormal protamine levels and infertility is intriguing, because abnormal protamine expression has been associated with low sperm counts, decreased sperm motility and loss of normal morphology, diminished fertilization ability and increased sperm chromatin damage also in man (reviewed in (Oliva, 2006)).

Protamine incorporation induces a conformational change in the packaging of the chromatin. The protamine bound DNA in sperm is approximately 6-20 folds more compact than a chromatin structure built from nucleosomes (Balhorn et al., 2000; Ward and Coffey, 1991).

Although the replacement of histones by protamines occurs in a genome-wide fashion, a certain fraction of histone-based nucleosomes remains associated with the sperm genome. The amount of residual nucleosomes that are retained in mature sperm ranges from approximately 1% in the mouse (Balhorn et al., 1977) and 15% in human (Bench et al., 1996; Gatewood et al., 1987) to over 50% in some marsupial species (Soon et al., 1997). Nucleosomes retained in spermatozoa may influence development of early embryos and epigenetic inheritance (BOX2). Therefore, the genomic loci associated with retained nucleosomes in sperm are of great interest. Several studies examining histone retention in mouse and human sperm reported marked retention of nucleosomes in the promoter regions of genes implicated in early development (Erkek et al., 2013; Hammoud et al., 2009). Contrary to these previous reports, very recently, two independent groups provided evidence for the predominant retention of sperm nucleosomes at genome regions devoid of protein-coding sequences, gene deserts, in mouse, human, and bovine sperm (Carone et al., 2014; Samans et al., 2014). Another line of evidence suggesting that histone retention in sperm might primarily occur over repeat elements comes from immunostaining studies on mature mouse sperm, which revealed colocalization of histones with the repeat-rich sperm chromocenter (Govin et al., 2007; van der Heijden et al., 2006). Some of the discrepancies between studies on nucleosome retention in mouse spermatozoa might result from differences in the extent of micrococcal nuclease (MNase) digestion of the isolated sperm chromatin, and the debate about the localization



and significance of sperm-retained histones is still ongoing. Consensus on the genome-wide distribution of the nucleosomes retained in mammalian spermatozoa, including a comparison of species from different orders, would provide an important basis for understanding the mechanisms of early development and epigenetic inheritance.

#### 1.4 Fertilization

At fertilization, one oocyte and one spermatozoon fuse to give rise to the 1-cell zygote (Figure 4A). Before reaching its final destination, there is still one major obstacle that the sperm cell must overcome: the zona pellucida (ZP), a relatively thick extracellular coat that surrounds the plasma membrane of mammalian eggs, with the perivitelline space in between the ZP and the plasma membrane. The ZP is laid down during the final stages of oogenesis when the non-growing oocytes enter their growth phase. As oocytes increase in diameter, the ZP increases in thickness. The mouse egg ZP is around 7  $\mu\text{m}$  thick and consists of an extensive network of interconnected filaments of glycoproteins (Wassarman and Mortillo, 1991). Free-swimming spermatozoa must recognize the ZP and stably bind to it. Once bound, spermatozoa are induced to undergo the acrosome reaction, which releases proteolytic enzymes, and together with tail movement this enables the sperm to traverse the ZP and reach the plasma membrane. Fusion of the cellular membranes constitutes the key fertilization event and allows the sperm nucleus, with the paternal genome, to enter the oocyte.

A key event resulting from sperm-oocyte fusion is an increase in the level of  $\text{Ca}^{2+}$  in the oocyte cytoplasm. This activates the oocyte, arrested at metaphase II, and triggers the resumption of the second meiotic division. Oocytes can also be activated artificially by mimicking the calcium oscillations induced during natural fertilization. In the mouse, strontium chloride ( $\text{SrCl}_2$ ), which is able to induce repetitive calcium rises, is most commonly used as activating agent. Artificial activation can be used, for example, to obtain parthenogenetic mammalian embryos, with only a maternally inherited diploid genome. A diploid genomic constitution can be maintained in these embryos because extrusion of the second polar body is inhibited by exposing the oocytes to cytochalasin B during artificial activation.

After the  $\text{Ca}^{2+}$ -dependent activation triggers the metaphase II to anaphase transition, meiosis is completed and a second polar body is extruded into the perivitelline space. At this point, the haploid parental genomes remain physically separated in the paternal and maternal pronuclei, and start undergoing structural and chemical changes. In particular, rapidly after entry into the ooplasm, the highly condensed chromatin of the sperm head becomes remodeled into the decondensed chromatin of the male pronucleus. This remarkable morphological change depends on the replacement of the sperm-specific protamines by oocyte-supplied histones and the organization of the chromatin into nucleosomes, a process defined as the

protamine-to-histone transition (Figure 4A and B). This chromatin reorganization leads to an epigenetic asymmetry between the two parental genomes (see below).

After this, the haploid genomes enclosed in the female and male pronuclei are replicated. Then, the membranes of the pronuclei are broken down, and the genomes organize into the first mitotic spindle of the zygote. The first mitotic division marks the progress from the zygote to the embryo.

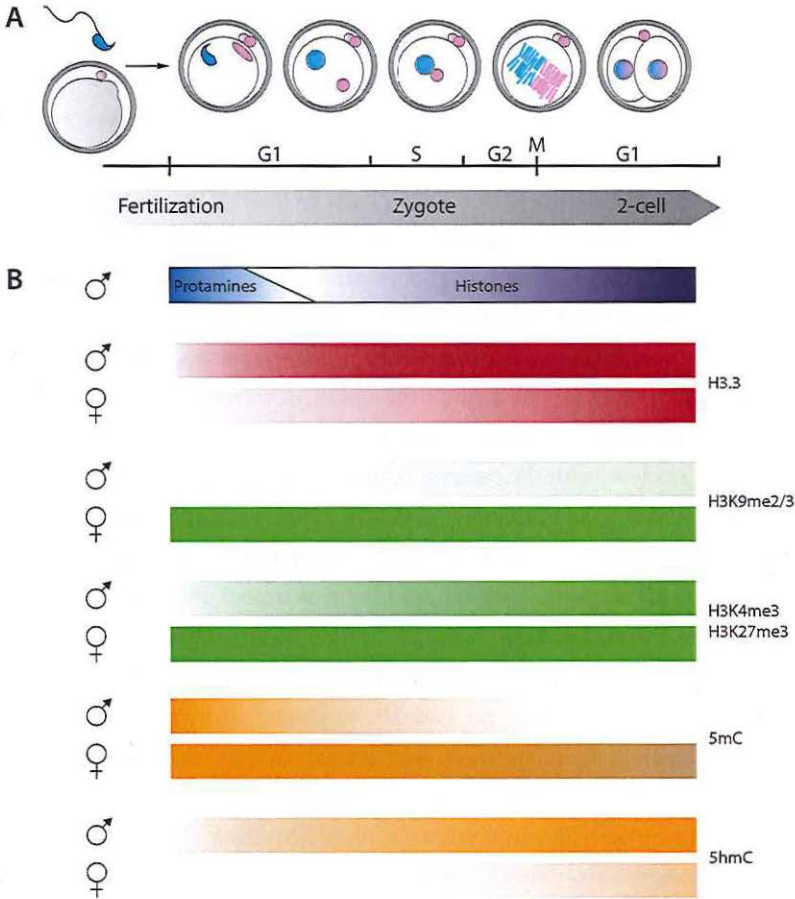


**Figure 4: Parental epigenetic asymmetry in the zygote**

(A) Before penetration of the oocyte by the spermatozoa, the maternal chromosomes are aligned on the metaphase II spindle (MII bump). Embryonic development starts with fertilization, when a single sperm cell penetrates the plasma membrane of the oocyte and delivers its haploid genome into the oocyte. This event triggers the oocyte to complete the second meiotic division, followed by the extrusion of the second polar body, and leads to the formation of a diploid cell, the zygote. In mice the paternal pronucleus is larger than the maternal one. During the progression of the cell cycle, the two pronuclei approach each other toward the center of the oocyte. The subsequent mitotic division generates the 2-cell stage embryo.

### 1.4.1 The epigenetic asymmetry between maternal and paternal chromatin

Within the first 3 hours after entry into the oocyte, the sperm chromatin undergoes extensive, active remodeling, while the maternal chromatin is relatively stable. Since paternal protamines are stripped off the DNA and replaced with oocyte-supplied histones, this contributes to an epigenetic asymmetry between the maternal and paternal chromatin, which comes in addition to an epigenetic asymmetry at the level of DNA methylation (described below).

One major difference in chromatin composition between the two pronuclei arises from the obligatory incorporation of the H3.3 histone variants into the “naked” paternal DNA, since this is the only H3 variant that can be incorporated in a DNA replication-independent manner (Loppin et al., 2005; Torres-Padilla et al., 2006). The maternal pronucleus, on the other hand, is loaded mainly with canonical H3 histones, H3.1 and H3.2, and maintains the same chromatin state of the oocyte (Figure 4B) (van der Heijden et al., 2005).

Before the onset of the first S phase, the parental pronuclei display also different histone modifications (Burton and Torres-Padilla, 2010). Compared to maternal chromatin, the newly formed paternal chromatin contains hyperacetylated histones (Adenot et al., 1997; Santos et al., 2005). In terms of histone methylation, with the exception of mono-methylated histone H3K4, H3K9 and H4K20, no methylated histone residues have been detected in the paternal pronucleus, while the maternal pronucleus contains regions enriched for different histone methylation marks, similar to what can be observed in oocytes (van der Heijden et al., 2005).

Following replication of DNA in the pronuclei and incorporation of replication-dependent histones in the zygotic genome, the asymmetry between the two parental genomes, in terms of histone variants and histone acetylation and methylation marks, mostly disappears. H3K9me2/3 marks represent an exception, as this modification continues to specifically decorate only the maternal genome after the first S phase (Liu et al., 2004), up to the 8-cell stage (Figure 4B) (Puschendorf et al., 2008).

On top of the epigenetic parental asymmetry at the level of chromatin composition, there is also a differential reprogramming of global DNA methylation between the paternally and maternally inherited genomes. In fact, the paternal genome undergoes a remarkable global oxidation event converting 5mC to 5hmC through TET3-dependent activity (Gu et al.,

**(B)** Concurrent with sperm decondensation and formation of the paternal pronucleus, protamines are exchanged for histones, resulting in nucleosomal chromatin. At this developmental time point, histone H3.3 is preferentially deposited into the male pronucleus. H3.3 incorporation in the maternal genome is not observed until the late pronuclear stage. Furthermore, the paternal genome is devoid of trimethylation marks. This asymmetry is completely lost at the 2-cell stage, except for H3K9me2/3 marks. The paternal DNA also shows a high level of cytosine hydroxymethylation and seems to undergo demethylation much faster than the maternal genome.



2011; Iqbal et al., 2011; Wossidlo et al., 2011). In contrast, the maternal genome does not acquire any significant amount of 5hmC (Figure 4B). This has led to the general view that the paternal genome is actively demethylated, while the maternal genome undergoes gradual passive 5mC dilution over subsequent cleavage divisions and DNA replication in the absence of maintenance methylation (Rougier et al., 1998). In this respect, it has been hypothesized that the specific H3K9me2 enrichment on the maternal pronucleus may function to protect it from the active removal of 5mC marks, which occurs on the paternal pronucleus during the early phase of zygotic development (Nakamura et al., 2007; Nakamura et al., 2012; Szabo and Pfeifer, 2012).

New light has been shed by two independent recent works (Guo et al., 2014; Shen et al., 2014) on the DNA demethylation dynamics in mouse zygotes. Both studies demonstrated that, in the paternal genome, demethylation downstream of 5hmC occurs mostly by a 5hmC-replication-dependent pathway. Furthermore, both maternal and paternal genomes seem to use a combination of active and passive (at the 5mC or 5hmC level) demethylation processes before the first mitotic division, although the extent of TET3-dependent maternal DNA demethylation is much less pronounced compared to that for paternal DNA (Guo et al., 2014; Shen et al., 2014).

Some other striking differences in histone modifications between the male and female pronuclei can be observed on the heterochromatic domains containing pericentric satellite DNA. Maternal pericentric regions exhibit classical constitutive heterochromatic marks, such as H3K9me3 and the associated HP1 $\beta$ , inherited from the oocyte (Probst and Almouzni, 2011; Santos et al., 2005). These features are not present on paternal pericentric regions, which are originally devoid of heterochromatic marks after fertilization. At the time of the first round of DNA replication, paternal pericentric regions acquire a form of facultative heterochromatin under the control of the Polycomb repressive complex 2 (PRC2) (Puschendorf et al., 2008). This complex has histone methyltransferase activity and catalyzes H3K27me3 on paternal heterochromatin (Puschendorf et al., 2008). Remarkably, this parental asymmetry becomes abolished when the H3K9 methyltransferase SUV39H2 is inactivated. In this case, the maternal heterochromatin becomes also coated by H3K27me3 marks, similarly to the paternal heterochromatin (Puschendorf et al., 2008).



**BOX3. Pre-implantation embryo development**

During its development, the early embryo undergoes a series of cleavage divisions which produce increasing numbers of progressively smaller cells, known as blastomeres, without increasing the overall volume of the embryo, which remains enclosed by the ZP until hatching and implantation (Figure 5A).

Soon after fertilization, the zygote is transcriptionally quiescent, and development is directed by maternally provided proteins and mRNAs present in the oocyte cytoplasm (Figure 5B) (Wang et al., 2004). Subsequently, transcription of mRNA encoded by the zygotic genome begins around the time of the first cleavage division during a process known as zygotic genome activation (ZGA) (Schultz, 2002). ZGA takes place in two phases, in the mouse: an initial minor burst of zygotic transcription begins before the first mitosis, followed by a second, larger burst at the two-cell stage, which is accompanied by degradation of maternal transcripts (Figure 5B) (Aoki et al., 1997; Hamarani et al., 2004).

Following two additional cleavages, the eight-cell embryo undergoes compaction through the development of intercellular adhesion and junctions, producing a tightly organized morula, where individual cells are no longer loosely attached to each other. When a morula has about 32 cells, some fluid starts to accumulate in the intercellular space between blastomeres forming a cavity, in the process of cavitation (Smith and McLaren, 1977), and the embryo is now called blastocyst. By this point, a first differentiation event segregates the outer trophoblast (TE) from the pluripotent inner cell mass (ICM) (Figure 5B).

The blastocyst keeps expanding and growing in cell number, until by E4.5 it “hatches” from the zona pellucida, ready to implant into the uterine wall. At this time point, the blastocyst is composed of three distinct cell lineages. Only one of these lineages, the pluripotent epiblast (EPI), contributes to the embryo itself, while the other two lineages, the trophoblast (TE) and the primitive endoderm (PE), become extra-embryonic tissues (Figure 5B). The TE is responsible for the implantation of the embryo into the uterus and will form the fetal part of the placenta. The PE becomes the parietal and visceral endoderm after implantation, which later contributes to the umbilical vesicle (formerly known as the yolk sac) (Gardner, 1983).

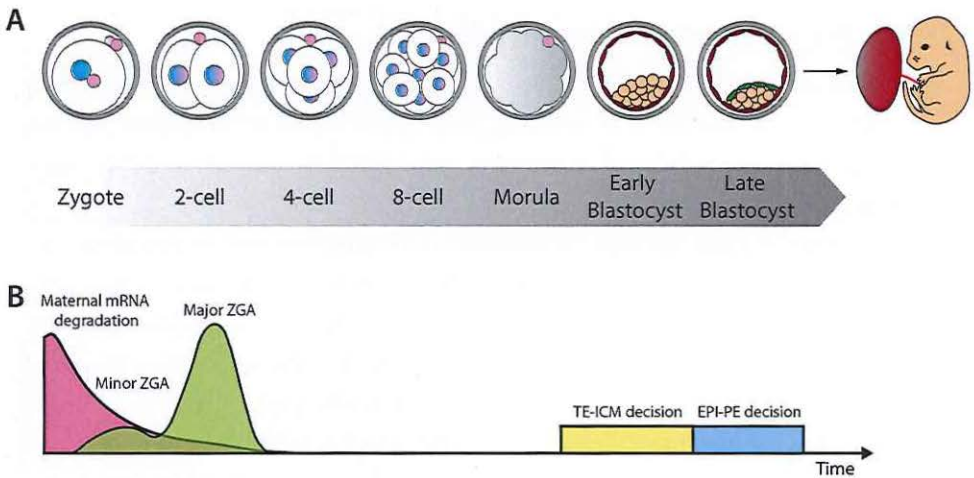


**Figure 5: Pre-implantation embryo development**

(A) In pre-implantation mouse embryos, subsequent mitotic divisions (known as cleavages) generate blastomeres without increasing the total cytoplasmic volume of the embryo. After the 8-cell stage, cell adhesion increases and blastomeres flatten up on each other, a compaction process which results in a spherical cell aggregate known as the morula. Around the 16-cell to 32-cell stage of the morula, outer cells mature into an epithelium with tight junctions between cells, and start to pump fluid from the outside into the inside of the embryo. The fluid accumulates in the intercellular spaces, leading to the formation of a cavity of gradually increasing size. The embryo is now called a blastocyst. Clustered on one side of this cavity is the pluripotent inner cell mass (ICM) (pink colored cluster), and the epithelial outer cells form the trophectoderm (TE) (red colored cells). The mature blastocyst continues to pump fluid into the cavity, hatches from the zona pellucida and eventually makes contact with the uterus, which marks the start of implantation. Around the same time, the ICM has completed a second lineage divergence into the primitive endoderm (PE) (green cell layer) and the pluripotent epiblast (EPI) (which is surrounded by primitive endoderm and trophectoderm). Only cells of the EPI form the embryo proper, whereas the TE and the PE develop into extra-embryonic tissues, such as the placenta.

(B) Representation of major events during preimplantation development that line up with the stages shown in (A). Maternal mRNA degradation, the minor and major phases of zygotic genome activation (ZGA), and the temporal onset of the first and second cell fate decisions.



## 1.5 Equalizing X-linked gene expression between sex chromosomes and autosomes in both sexes

An intriguing consequence of having unequal sex chromosomes in males versus females is the dosage difference in X-linked genes between males and females. Because males have only one X, single-copy genes on this chromosome are present in single copy in XY cells, whereas two copies of these genes are present in female cells (XX). Female cells also have twice the number of multi-copy X-linked genes.

It has always been expected that appropriate dosage compensation of X-linked gene expression between the sexes (Lyon, 1961), and relative to the autosomes, would be critical for life (Nguyen and Disteché, 2006). It is thought that X-linked genes are upregulated to achieve a two-fold increase in their expression, which will equalize X-linked gene expression with that of autosomal genes (Deng et al., 2011). In view of the imbalance in the number of X chromosomes between the sexes in mammals, this has led to the co-evolution of a dosage compensation mechanism involving the transcriptional inactivation of one X chromosome in female cells, a phenomenon defined as X chromosome inactivation (XCI).

In order for XCI to occur, the presence of the X-linked X inactivation center (Xic) is necessary. In particular, two genes producing noncoding RNAs and located in the Xic are the major players in this process: *Xist* and *Tsix*. The *Xist* gene, or X-inactive specific transcript, was discovered due to its specific expression from the inactive X chromosome in female cells. This RNA has the unique property to “coat” the chromosome from which it is produced, leading to transcriptional inactivation of the coated X, by the recruitment of various chromatin-modifying proteins. *Xist* RNA is known to recruit the Polycomb repressive complexes 1 (PRC1) and 2 (PRC2), which then mediate enrichment of the entire inactive X with repressive histone modifications, such H2AK119ub and H3K27me3.

*Tsix* (“*Xist*” backwards) is *Xist*’s antisense partner. The term “antisense” refers to the fact that part of *Tsix* is complementary in sequence to *Xist*, because the genes are partly overlapping but transcribed in opposite directions. There is an inverse relationship between *Tsix* and *Xist* expression: when *Tsix* transcription is reduced on one X, *Xist* expression increases on that same chromosome and then the *Xist* RNA mediates inactivation of the X chromosome *in cis* (Lee and Lu, 1999; Sado et al., 2001). In contrast, overexpression of *Tsix* prevents an increase in *Xist* expression and blocks inactivation of that same X (Luikenhuis et al., 2001; Stavropoulos et al., 2001). Expression of *Tsix* is thus required to antagonize *Xist* on the future active X.

In addition to these two non-coding and cis-acting genes, XCI is mediated also by X-linked XCI activators that act in a dose-dependent fashion to sense the number of X chromosomes present per diploid genome (Monkhorst et al., 2008). In particular, the X-encoded E3 ubiquitin ligase RNF12 is an important trans-acting XCI-activator (Jonkers et al., 2009; Shin et al.,

2010). RNF12 is responsible for the ubiquitination and proteasomal degradation of REX1, a pluripotency factor that, when present at the appropriate threshold concentration, inhibits *Xist* transcription, thereby blocking initiation of XCI (Gontan et al., 2012).

In mouse preimplantation female embryos, the X chromosome of paternal origin always becomes specifically inactivated. Because of this parental bias, this type of X-inactivation has been defined as imprinted XCI (iXCI). Studies on *Xist* expression, using RT-qPCR analysis, demonstrated that paternally imprinted *Xist* expression occurs from the 4-cell stage onwards in female preimplantation embryos (Kay et al., 1993). These results have been subsequently confirmed also by RNA-FISH analysis, which showed that *Xist* expression from the Xp is manifested as *cis*-accumulation of stable transcripts in cells of 8-cell stage female preimplantation embryos (Okamoto et al., 2004).

At the blastocyst stage, the extra-embryonic tissues, including the primitive endoderm (PE) and the trophoblast (TE), maintain the imprinted state of Xp inactivation (Takagi and Sasaki, 1975). However, the epiblast lineage reactivates the Xp and undergoes a new round of XCI without a dominant parent-of-origin bias, thus defined as random XCI (rXCI). The epiblast will give rise to the somatic cells of the developing embryo, where this pattern of randomly inactivated X chromosomes will be maintained throughout further cell divisions during embryogenesis.

To investigate *Xist* function, two groups engineered large deletions, removing either the promoter and first exon of the *Xist* gene (Penny et al., 1996) or the majority of exon 1 through exon 5 (Marahrens et al., 1997). *Xist* deletions are always lethal when inherited from the father (Xp $\Delta$ Xist), but not when inherited from the mother. This parent-of-origin-specific lethality is due to the total lack of XCI in the extraembryonic tissues, indicating that *Xist* is required for imprinted silencing of the Xp (Marahrens et al., 1997). Since the Xm, which bears a functional *Xist* allele, does not upregulate *Xist* to compensate for the lack of inactivation of the Xp, it appears that the imprinting mechanism cannot be overridden. Conversely, *Tsix* promoter deletions have the opposite parent-of-origin effect. *Tsix* deletions are lethal only when inherited from the mother (Xm $\Delta$ Tsix), owing to ectopic *Xist* expression and X inactivation of the Xm (as well as of the Xp) in most extraembryonic cells (Lee, 2000; Sado et al., 2001). As expected for genes with opposite effects on the same process, a paternally inherited *Xist* deletion can be rescued by maternal inheritance of a *Tsix* deleted allele (Sado et al., 2001). The defects associated with either a paternal *Xist* or a maternal *Tsix* deletion are limited to the extraembryonic tissues, as XCI in the embryonic tissues in these genetically manipulated embryos can be initiated on either X chromosome due to the random choice mechanism, meaning that the one X carrying an intact *Xic* will be inactivated in all cells. In such a situation, embryonic lethality is thus due to extraembryonic defects.



Although major progress has been made in our understanding of *Xist* regulation, very little is known about the nature or location of the imprint(s) that regulate iXCI. Theoretically, it can be proposed that the maternal X chromosome ( $X_m$ ) is imprinted, by some mechanism (see below), to remain active, or that the paternal X chromosome ( $X_p$ ) is imprinted to be inactivated (Lyon and Rastan, 1984). These possibilities are not mutually exclusive.

Important mechanistic insights into iXCI in mice have come from studies on embryos showing uniparental disomy for the X (summarized in Table 1). In androgenetic embryos, where the X chromosomes are always of paternal origin ( $X_pX_p$  and  $X_pY$ ), *Xist* up-regulation has been shown for each  $X_p$ , regardless of the number of X chromosomes present in the embryos (Okamoto et al., 2000). In contrast, in gynogenetic and parthenogenetic embryos ( $X_mX_m$ ), maternal *Xist* expression has never been reported until the 16-cell stage (Goto and Takagi, 2000; Matsui et al., 2001; Nesterova et al., 2001). Furthermore, in gynogenetic embryos generated by fusion of haploid genomes from non-growing (ng) and fully grown (fg) oocytes, the X chromosome derived from ng oocytes is inactivated in the extra-embryonic lineages, whereas the fg X chromosome never undergoes imprinted XCI. This would be consistent with the acquisition of an epigenetic mark on  $X_m$  during oocyte growth (Tada et al., 2000), which presumably acts to repress expression of *Xist* from  $X_m$ .

Taken together, these studies indicate that early *Xist* expression is governed entirely by parent of origin effects. Furthermore they suggest the presence of a strong imprint on the maternal X chromosome to remain active early on during embryogenesis. However, in the field, the nature of the imprint of the *Xci* on the  $X_m$  is still controversial and does not seem to rely on DNA methylation as one would expect based on autosomal imprinted loci (Chiba et al., 2008; Kaneda et al., 2004). Conditional deletion of both *Dnmt3a* and *Dnmt3b* in the female germline (which abolishes the methylation of imprinted loci) did not lead to *Xist* expression from the  $X_m$  in the progeny (Kaneda et al., 2004). Furthermore, an inactive X chromosome has been detected in parthenogenetic  $X_mX_m$  embryos at the morula stage (Nesterova et al., 2001), indicating that the  $X_m$  imprint can be overridden at some point, only when the  $X_p$  is absent. Instability of the possible parental imprint of the *Xic* also during normal development is indicated by the fact that when cells of the epiblast differentiate and initiate X chromosome inactivation during postimplantation embryogenesis, they undergo random XCI.

Only very recently, Fukuda et al. (2014) has provided evidence that the *Xist* promoter on the  $X_m$  is repressed by H3K9me3 enrichment (Fukuda et al., 2014). In order to facilitate the analysis of  $X_m$ -*Xist* expression, these authors used parthenogenetic embryos, thus possessing two X chromosomes of maternal origin. By ectopically expressing *Kdm4b*, which encodes a lysine demethylase enzyme, it was demonstrated that loss of H3K9me3 at the *Xist* promoter leads to precocious  $X_m$ -*Xist* activation at the 4-cell stage (Fukuda et al., 2014). Furthermore,

a high H3K9me3 level was detected in the *Xm-Xist* promoter region of 4-cell parthenogenetic embryos, by ChIP-qPCR (Fukuda et al., 2014). This enrichment was subsequently markedly reduced by the morula stage, which is consistent with the *Xm-Xist* derepression observed in parthenogenetic morulas by this stage (Nesterova et al., 2001). Inhibition of histone deacetylase by trichostatin A (TSA) treatment, also activated *Xm-Xist*, indicating that there is also an histone acetylation-mediated *Xm-Xist* activation (Fukuda et al., 2014). This finding was not specifically addressed by the authors, and it cannot be excluded that other repressive marks may regulate the *Xm-Xist* promoter, since the level of *Xm-Xist* expression reached in parthenogenetic blastocysts injected with *Kdm4b* mRNA and/or treated with TSA was not as high as compared to normal female blastocysts. Further studies aimed at deciphering *Xist* regulation during iXCI will thus be very important.

The possibility of a paternal imprint, which leads to the Xp being more prone to inactivation, is not definitely excluded. Studies on embryos with a Xp0 genotype demonstrated that the Xp is not irrevocably destined to become inactivated, allowing normal embryonic development of Xp0 embryos, with an active X chromosome (Papaioannou and West, 1981). Nevertheless, Xp0 embryos develop less well than Xm0 embryos and exhibit underdevelopment of the ectoplacental cone (Thornhill and Burgoyne, 1993). Thus, it is plausible that an Xp imprint leads to a tendency to inactivate Xp, regardless of X chromosome number, but it seems that, ultimately, this signal can be overridden, so that development can proceed based on cells in which the Xp has remained active.

Alternatively, it has also been proposed that the imprint leading to iXCI of Xp may rely on the different chromatin states of the two parental genomes, that have been reported to exist during early embryogenesis, with the Xp being inherited in a pre-inactivated state as a result of meiotic sex chromosome inactivation (MSCI) (Huynh and Lee, 2003). However, this hypothesis was contradicted when it was later shown that some paternal X-linked genes are active in two-cell stage female embryos and are then gradually inactivated during pre-implantation development (Okamoto et al., 2005). Yet the existence of a transgenerational epigenetic transmission from the paternal germline to the zygote through maintenance of pre-inactivated intergenic repeat regions on the Xp, which would subsequently predispose the Xp for iXCI, cannot be excluded (Namekawa et al., 2010). Interestingly, in marsupials, XCI occurs for the Xp in all cells of the embryo (Sharman, 1971). Although *Xist* is not found in this infraclass of mammals, a different and unrelated noncoding RNA, named *Rsx* (RNA-on-the-silent X), was recently identified in the opossum and reported to display *Xist*-like properties which would support its possible role in X-chromosome inactivation (Grant et al., 2012). *Xist* may have evolved from LNX3, a protein-coding gene with functions still extant, but unrelated to dosage compensation, in marsupials (Duret et al., 2006). It will be interesting to see how

accumulation of *Rsx* RNA on the  $X_p$  in female embryos is regulated. Interestingly, transient reactivation of the  $X_p$  has also been reported to occur in early opossum embryos, suggesting that a carry-over effect of PSCR, as an important mechanistic factor leading to iXCI of  $X_p$ , is unlikely also in the methatherian lineage (Mahadevaiah et al., 2009).

**Table 1: *Xist* expression in wild-type and uniparental embryos**

Genotype	<i>Xist</i> expression at 4-cell stage	<i>Xist</i> expression at morula stage	References
$X_M X_P$	● ●	● ●	
$X_M Y$	Never	Never	
$X_M X_M$	Never	● ● or ● ●*	Nesterova, 2001
$X_P X_P$	● ●	● ● or ● ●*	Okamoto, 2000
$X_P Y$	●	●	Okamoto, 2000
$X_P O$	●	●	Matsui, 2001

● *Xist* expression

● *Xist* repression

Each dot represents  
*Xist* status/X chromosome

\* = not in all cells





## AIMS AND OUTLINE OF THIS THESIS

Mammalian sex chromosomes encounter quite many special challenges, travelling through the life cycle.

The work presented in this thesis has focused on obtaining more insight in the biological relevance of the specific regulation of the sex chromosomes during the male and female life cycle. One central aspect that we focused on involves the possible functional link between PSCR and iXCI in pre-implantation mouse female embryos. To study the possible influence of Xp chromatin on iXCI, we made use of round spermatid injection into oocytes (ROSI). This technique is described from an historical, clinical and biological perspective in Chapter 2.

Immature round spermatids have a chromatin organization which is vastly different from that of spermatozoa. In Chapter 3, through fertilization of mouse oocytes with round spermatids obtained from mice bearing an *Xist* deletion ( $Xp\Delta Xist$ ), we aimed to verify if transmission of an Xp from round spermatids, silenced through PSCR, would allow iXCI establishment in the absence of a paternally inherited *Xist* gene.

Another central topic of the present thesis concerns the regulation of the sex chromosomes during meiosis from an evolutionary perspective. In most studies, the mouse has been “the model” species to study sex chromosomal pairing behavior and transcriptional regulation during meiosis. However, previous observations indicate that MSCI and PSCR are less stringent and more variable in human compared to mouse. This prompted us to broaden our understanding of these phenomena by studying XY pairing dynamics, MSCI, and PSCR in a more distant mammalian species, *Canis familiaris*, from the Carnivora order (Chapter 4). In this context we performed a comparative analysis of MSCI and PSCR between dog, human and mouse.

Persistence of unsynapsed chromatin in meiotic cells leads to transcriptional silencing, but also triggers a chromosome-wide histone exchange of H3.1/.2 by the variant H3.3. The precise function of this extensive remodeling is not fully clear. In Chapter 5, we aimed to unravel the relevance and conservation of this remodeling event during male meiosis in different species, including two marsupials (representing the metatheria), and in female mouse meiosis when unsynapsed chromatin is present.

In Chapter 6 we discuss the findings presented in the previous chapters and address possible further directions of the work presented in this thesis.

## REFERENCES

- Adenot, P.G., Mercier, Y., Renard, J.P., and Thompson, E.M. (1997). Differential H4 acetylation of paternal and maternal chromatin precedes DNA replication and differential transcriptional activity in pronuclei of 1-cell mouse embryos. *Development* 124, 4615-4625.
- Aoki, F., Worrad, D.M., and Schultz, R.M. (1997). Regulation of transcriptional activity during the first and second cell cycles in the pre-implantation mouse embryo. *Dev Biol* 181, 296-307.
- Baarends, W.M., Wassenaar, E., van der Laan, R., Hoogerbrugge, J.W., Sleddens-Linkels, E., Hoesjmakers, J.H., de Boer, P., and Grootegoed, J.A. (2005). Silencing of unpaired chromatin and histone H2A ubiquitination in mammalian meiosis. *Mol Cell Biol* 25, 1041-1053.
- Bachtrog, D. (2013). Y-chromosome evolution: emerging insights into processes of Y-chromosome degeneration. *Nat Rev Genet* 14, 113-124.
- Balhorn, R., Brewer, L., and Corzett, M. (2000). DNA condensation by protamine and arginine-rich peptides: analysis of toroid stability using single DNA molecules. *Mol Reprod Dev* 56, 230-234.
- Balhorn, R., Gledhill, B.L., and Wyrobek, A.J. (1977). Mouse sperm chromatin proteins: quantitative isolation and partial characterization. *Biochemistry* 16, 4074-4080.
- Bellott, D.W., Hughes, J.F., Skaletsky, H., Brown, L.G., Pyntikova, T., Cho, T.J., Koutseva, N., Zaghul, S., Graves, T., Rock, S., et al. (2014). Mammalian Y chromosomes retain widely expressed dosage-sensitive regulators. *Nature* 508, 494-499.
- Bench, G.S., Friz, A.M., Corzett, M.H., Morse, D.H., and Balhorn, R. (1996). DNA and total protamine masses in individual sperm from fertile mammalian subjects. *Cytometry* 23, 263-271.
- Burgoyne, P.S., Mahadevaiah, S.K., and Turner, J.M. (2009). The consequences of asynapsis for mammalian meiosis. *Nat Rev Genet* 10, 207-216.
- Burton, A., and Torres-Padilla, M.E. (2010). Epigenetic reprogramming and development: a unique heterochromatin organization in the pre-implantation mouse embryo. *Brief Funct Genomics* 9, 444-454.
- Carone, B.R., Hung, J.H., Hainer, S.J., Chou, M.T., Carone, D.M., Weng, Z., Fazio, T.G., and Rando, O.J. (2014). High-resolution mapping of chromatin packaging in mouse embryonic stem cells and sperm. *Dev Cell* 30, 11-22.
- Charlesworth, B. (1978). Model for evolution of Y chromosomes and dosage compensation. *Proc Natl Acad Sci U S A* 75, 5618-5622.
- Charlesworth, B. (1996). The evolution of chromosomal sex determination and dosage compensation. *Curr Biol* 6, 149-162.
- Chiba, H., Hirasawa, R., Kaneda, M., Amakawa, Y., Li, E., Sado, T., and Sasaki, H. (2008). De novo DNA methylation independent establishment of maternal imprint on X chromosome in mouse oocytes. *Genesis* 46, 768-774.
- Cho, C., Willis, W.D., Goulding, E.H., Jung-Ha, H., Choi, Y.C., Hecht, N.B., and Eddy, E.M. (2001). Haploinsufficiency of protamine-1 or -2 causes infertility in mice. *Nat Genet* 28, 82-86.
- Cortez, D., Marin, R., Toledo-Flores, D., Froidevaux, L., Liechti, A., Waters, P.D., Grutzner, F., and Kaessmann, H. (2014). Origins and functional evolution of Y chromosomes across mammals. *Nature* 508, 488-493.
- de Vries, M., Vosters, S., Merks, G., D'Hauwers, K., Wansink, D.G., Ramos, L., and de Boer, P. (2012). Human male meiotic sex chromosome inactivation. *PLoS One* 7, e31485.
- Deng, X., Hiatt, J.B., Nguyen, D.K., Ercan, S., Sturgill, D., Hillier, L.W., Schlesinger, F., Davis, C.A., Reinke, V.J., Gingeras, T.R., et al. (2011). Evidence for compensatory upregulation of expressed X-linked genes in mammals, *Caenorhabditis elegans* and *Drosophila melanogaster*. *Nat Genet* 43, 1179-1185.
- Disteche, C.M., Brannan, C.I., Larsen, A., Adler, D.A., Schorderet, D.F., Gearing, D., Copeland, N.G., Jenkins, N.A., and Park, L.S. (1992). The human pseudoautosomal GM-CSF receptor alpha subunit gene is autosomal in mouse. *Nat Genet* 1, 333-336.
- Doenecke, D., Drabent, B., Bode, C., Bramlage, B., Franke, K., Gavenis, K., Kosciessa, U., and Witt, O. (1997). Histone gene expression and chromatin structure during spermatogenesis. *Adv Exp Med Biol* 424, 37-48.
- Duret, L., Chureau, C., Samain, S., Weissenbach, J., and Avner, P. (2006). The Xist RNA gene



evolved in eutherians by pseudogenization of a protein-coding gene. *Science* 312, 1653-1655.

Erkek, S., Hisano, M., Liang, C.Y., Gill, M., Murr, R., Dieker, J., Schubeler, D., van der Vlag, J., Stadler, M.B., and Peters, A.H. (2013). Molecular determinants of nucleosome retention at CpG-rich sequences in mouse spermatozoa. *Nat Struct Mol Biol* 20, 868-875.

Fernandez-Capetillo, O., Mahadevaiah, S.K., Celeste, A., Romanienko, P.J., Camerini-Otero, R.D., Bonner, W.M., Manova, K., Burgoyne, P., and Nussenzweig, A. (2003). H2AX is required for chromatin remodeling and inactivation of sex chromosomes in male mouse meiosis. *Dev Cell* 4, 497-508.

Fukuda, A., Tomikawa, J., Miura, T., Hata, K., Nakabayashi, K., Eggan, K., Akutsu, H., and Umezawa, A. (2014). The role of maternal-specific H3K9me3 modification in establishing imprinted X-chromosome inactivation and embryogenesis in mice. *Nat Commun* 5, 5464.

Gardner, R.L. (1983). Origin and differentiation of extraembryonic tissues in the mouse. *Int Rev Exp Pathol* 24, 63-133.

Gatewood, J.M., Cook, G.R., Balhorn, R., Bradbury, E.M., and Schmid, C.W. (1987). Sequence specific packaging of DNA in human sperm chromatin. *Science* 236, 962-964.

Gaucher, J., Reynoird, N., Montellier, E., Boussoar, F., Rousseaux, S., and Khochbin, S. (2010). From meiosis to postmeiotic events: the secrets of histone disappearance. *FEBS J* 277, 599-604.

Gianfrancesco, F., Sanges, R., Esposito, T., Tempesta, S., Rao, E., Rappold, G., Archidiacono, N., Graves, J.A., Forabosco, A., and D'Urso, M. (2001). Differential divergence of three human pseudoautosomal genes and their mouse homologs: implications for sex chromosome evolution. *Genome Res* 11, 2095-2100.

Glas, R., Marshall Graves, J.A., Toder, R., Ferguson-Smith, M., and O'Brien, P.C. (1999). Cross-species chromosome painting between human and marsupial directly demonstrates the ancient region of the mammalian X. *Mamm Genome* 10, 1115-1116.

Gontan, C., Achame, E.M., Demmers, J., Barakat, T.S., Rentmeester, E., van, I.W., Grootegoed, J.A., and Gribnau, J. (2012). RNF12 initiates X-chromosome inactivation by targeting REX1

for degradation. *Nature* 485, 386-390.

Goto, Y., and Takagi, N. (2000). Maternally inherited X chromosome is not inactivated in mouse blastocysts due to parental imprinting. *Chromosome Res* 8, 101-109.

Govin, J., Caron, C., Lestrat, C., Rousseaux, S., and Khochbin, S. (2004). The role of histones in chromatin remodelling during mammalian spermiogenesis. *Eur J Biochem* 271, 3459-3469.

Govin, J., Escoffier, E., Rousseaux, S., Kuhn, L., Ferro, M., Thevenon, J., Catena, R., Davidson, I., Garin, J., Khochbin, S., et al. (2007). Pericentric heterochromatin reprogramming by new histone variants during mouse spermiogenesis. *J Cell Biol* 176, 283-294.

Grant, J., Mahadevaiah, S.K., Khil, P., Sangrithi, M.N., Royo, H., Duckworth, J., McCarrey, J.R., VandeBerg, J.L., Renfree, M.B., Taylor, W., et al. (2012). Rxs is a metatherian RNA with Xist-like properties in X-chromosome inactivation. *Nature* 487, 254-258.

Graves, J.A. (1995). The evolution of mammalian sex chromosomes and the origin of sex determining genes. *Philos Trans R Soc Lond B Biol Sci* 350, 305-311; discussion 311-302.

Greaves, I.K., Rangasamy, D., Devoy, M., Marshall Graves, J.A., and Tremethick, D.J. (2006). The X and Y chromosomes assemble into H2A.Z-containing [corrected] facultative heterochromatin [corrected] following meiosis. *Mol Cell Biol* 26, 5394-5405.

Gu, T.P., Guo, F., Yang, H., Wu, H.P., Xu, G.F., Liu, W., Xie, Z.G., Shi, L., He, X., Jin, S.G., et al. (2011). The role of Tet3 DNA dioxygenase in epigenetic reprogramming by oocytes. *Nature* 477, 606-610.

Guo, F., Li, X., Liang, D., Li, T., Zhu, P., Guo, H., Wu, X., Wen, L., Gu, T.P., Hu, B., et al. (2014). Active and passive demethylation of male and female pronuclear DNA in the mammalian zygote. *Cell Stem Cell* 15, 447-458.

Hamatani, T., Carter, M.G., Sharov, A.A., and Ko, M.S. (2004). Dynamics of global gene expression changes during mouse preimplantation development. *Dev Cell* 6, 117-131.

Hammoud, S.S., Nix, D.A., Zhang, H., Purwar, J., Carrell, D.T., and Cairns, B.R. (2009). Distinctive chromatin in human sperm packages genes for embryo development. *Nature* 460, 473-478.

Acad Sci U S A 104, 9730-9735.

Nesterova, T.B., Barton, S.C., Surani, M.A., and Brockdorff, N. (2001). Loss of Xist imprinting in diploid parthenogenetic preimplantation embryos. *Dev Biol* 235, 343-350.

Nguyen, D.K., and Disteché, C.M. (2006). Dosage compensation of the active X chromosome in mammals. *Nat Genet* 38, 47-53.

Ohno, S. (1967). Sex chromosomes and sex-linked genes (Springer-Verlag).

Okamoto, I., Arnaud, D., Le Baccon, P., Otte, A.P., Disteché, C.M., Avner, P., and Heard, E. (2005). Evidence for de novo imprinted X-chromosome inactivation independent of meiotic inactivation in mice. *Nature* 438, 369-373.

Okamoto, I., Otte, A.P., Allis, C.D., Reinberg, D., and Heard, E. (2004). Epigenetic dynamics of imprinted X inactivation during early mouse development. *Science* 303, 644-649.

Okamoto, I., Tan, S., and Takagi, N. (2000). X-chromosome inactivation in XX androgenetic mouse embryos surviving implantation. *Development* 127, 4137-4145.

Oliva, R. (2006). Protamines and male infertility. *Hum Reprod Update* 12, 417-435.

Orr, H.A., and Kim, Y. (1998). An adaptive hypothesis for the evolution of the Y chromosome. *Genetics* 150, 1693-1698.

Papaioannou, V.E., and West, J.D. (1981). Relationship between the parental origin of the X chromosomes, embryonic cell lineage and X chromosome expression in mice. *Genet Res* 37, 183-197.

Penny, G.D., Kay, G.F., Sheardown, S.A., Rastan, S., and Brockdorff, N. (1996). Requirement for Xist in X chromosome inactivation. *Nature* 379, 131-137.

Perry, J., Palmer, S., Gabriel, A., and Ashworth, A. (2001). A short pseudoautosomal region in laboratory mice. *Genome Res* 11, 1826-1832.

Peters, H. (1970). Migration of gonocytes into the mammalian gonad and their differentiation. *Philos Trans R Soc Lond B Biol Sci* 259, 91-101.

Probst, A.V., and Almouzni, G. (2011). Heterochromatin establishment in the context of genome-wide epigenetic reprogramming. *Trends Genet* 27, 177-185.

Puschendorf, M., Terranova, R., Boutsma, E., Mao, X., Isono, K., Brykczynska, U., Kolb, C., Otte, A.P., Koseki, H., Orkin, S.H., et al. (2008). PRC1 and Suv39h specify parental asymmetry at constitutive heterochromatin in early mouse embryos. *Nat Genet* 40, 411-420.

Raudsepp, T., and Chowdhary, B.P. (2008). The horse pseudoautosomal region (PAR): characterization and comparison with the human, chimp and mouse PARs. *Cytogenet Genome Res* 121, 102-109.

Raudsepp, T., Das, P.J., Avila, F., and Chowdhary, B.P. (2012). The pseudoautosomal region and sex chromosome aneuploidies in domestic species. *Sex Dev* 6, 72-83.

Raudsepp, T., Lee, E.J., Kata, S.R., Brinkmeyer, C., Mickelson, J.R., Skow, L.C., Womack, J.E., and Chowdhary, B.P. (2004). Exceptional conservation of horse-human gene order on X chromosome revealed by high-resolution radiation hybrid mapping. *Proc Natl Acad Sci U S A* 101, 2386-2391.

Rice, W.R. (1987). Genetic hitchhiking and the evolution of reduced genetic activity of the Y sex chromosome. *Genetics* 116, 161-167.

Rice, W.R. (1996). Sexually antagonistic male adaptation triggered by experimental arrest of female evolution. *Nature* 381, 232-234.

Rougier, N., Bourc'his, D., Gomes, D.M., Niveleau, A., Plachot, M., Paldi, A., and Viegas-Pequignot, E. (1998). Chromosome methylation patterns during mammalian preimplantation development. *Genes Dev* 12, 2108-2113.

Royo, H., Polikiewicz, G., Mahadevaiah, S.K., Prosser, H., Mitchell, M., Bradley, A., de Rooij, D.G., Burgoyne, P.S., and Turner, J.M. (2010). Evidence that meiotic sex chromosome inactivation is essential for male fertility. *Curr Biol* 20, 2117-2123.

Royo, H., Prosser, H., Ruzankina, Y., Mahadevaiah, S.K., Cloutier, J.M., Baumann, M., Fukuda, T., Hoog, C., Toth, A., de Rooij, D.G., et al. (2013). ATR acts stage specifically to regulate multiple aspects of mammalian meiotic silencing. *Genes Dev* 27, 1484-1494.

Sado, T., Wang, Z., Sasaki, H., and Li, E. (2001). Regulation of imprinted X-chromosome inactivation in mice by Tsix. *Development* 128, 1275-1286.



Samans, B., Yang, Y., Krebs, S., Sarode, G.V., Blum, H., Reichenbach, M., Wolf, E., Steger, K., Dansranjav, T., and Schagdarsurengin, U. (2014). Uniformity of nucleosome preservation pattern in Mammalian sperm and its connection to repetitive DNA elements. *Dev Cell* 30, 23-35.

Santos, F., Peters, A.H., Orte, A.P., Reik, W., and Dean, W. (2005). Dynamic chromatin modifications characterise the first cell cycle in mouse embryos. *Dev Biol* 280, 225-236.

Schultz, R.M. (2002). The molecular foundations of the maternal to zygotic transition in the preimplantation embryo. *Hum Reprod Update* 8, 323-331.

Scully, R., Chen, J., Plug, A., Xiao, Y., Weaver, D., Feunteun, J., Ashley, T., and Livingston, D.M. (1997). Association of BRCA1 with Rad51 in mitotic and meiotic cells. *Cell* 88, 265-275.

Sharman, G.B. (1971). Late DNA replication in the paternally derived X chromosome of female kangaroos. *Nature* 230, 231-232.

Sharp, P. (1982). Sex chromosome pairing during male meiosis in marsupials. *Chromosoma* 86, 27-47.

Shen, L., Inoue, A., He, J., Liu, Y., Lu, F., and Zhang, Y. (2014). Tet3 and DNA replication mediate demethylation of both the maternal and paternal genomes in mouse zygotes. *Cell Stem Cell* 15, 459-470.

Shin, J., Bossenz, M., Chung, Y., Ma, H., Byron, M., Taniguchi-Ishigaki, N., Zhu, X., Jiao, B., Hall, L.L., Green, M.R., et al. (2010). Maternal Rnf12/RLIM is required for imprinted X-chromosome inactivation in mice. *Nature* 467, 977-981.

Sin, H.S., Ichijima, Y., Koh, E., Namiki, M., and Namekawa, S.H. (2012). Human postmeiotic sex chromatin and its impact on sex chromosome evolution. *Genome Res* 22, 827-836.

Skinner, B.M., Lachani, K., Sargent, C.A., and Affara, N.A. (2013). Regions of XY homology in the pig X chromosome and the boundary of the pseudoautosomal region. *BMC Genet* 14, 3.

Smith, C.L., and Peterson, C.L. (2005). ATP-dependent chromatin remodeling. *Curr Top Dev Biol* 65, 115-148.

Smith, R., and McLaren, A. (1977). Factors affecting the time of formation of the mouse blastocoele. *J Embryol Exp Morphol* 41, 79-92.

Soon, L.L., Ausio, J., Breed, W.G., Power, J.H., and Muller, S. (1997). Isolation of histones and related chromatin structures from spermatozoa nuclei of a dasyurid marsupial, *Sminthopsis crassicaudata*. *J Exp Zool* 278, 322-332.

Stavropoulos, N., Lu, N., and Lee, J.T. (2001). A functional role for Tsix transcription in blocking Xist RNA accumulation but not in X-chromosome choice. *Proc Natl Acad Sci U S A* 98, 10232-10237.

Surani, M.A., Barton, S.C., and Norris, M.L. (1984). Development of reconstituted mouse eggs suggests imprinting of the genome during gametogenesis. *Nature* 308, 548-550.

Szabo, P.E., and Pfeifer, G.P. (2012). H3K9me2 attracts PGC7 in the zygote to prevent Tet3-mediated oxidation of 5-methylcytosine. *J Mol Cell Biol* 4, 427-429.

Tada, T., Obata, Y., Tada, M., Goto, Y., Nakatsuji, N., Tan, S., Kono, T., and Takagi, N. (2000). Imprint switching for non-random X-chromosome inactivation during mouse oocyte growth. *Development* 127, 3101-3105.

Takagi, N., and Sasaki, M. (1975). Preferential inactivation of the paternally derived X chromosome in the extraembryonic membranes of the mouse. *Nature* 256, 640-642.

Tan, M., Luo, H., Lee, S., Jin, F., Yang, J.S., Montellier, E., Buchou, T., Cheng, Z., Rousseaux, S., Rajagopal, N., et al. (2011). Identification of 67 histone marks and histone lysine crotonylation as a new type of histone modification. *Cell* 146, 1016-1028.

Thornhill, A.R., and Burgoyne, P.S. (1993). A paternally imprinted X chromosome retards the development of the early mouse embryo. *Development* 118, 171-174.

Torres-Padilla, M.E., Bannister, A.J., Hurd, P.J., Kouzarides, T., and Zernicka-Goetz, M. (2006). Dynamic distribution of the replacement histone variant H3.3 in the mouse oocyte and preimplantation embryos. *Int J Dev Biol* 50, 455-461.

Turner, J.M. (2007). Meiotic sex chromosome inactivation. *Development* 134, 1823-1831.

Turner, J.M., Aprelikova, O., Xu, X., Wang, R., Kim, S., Chandramouli, G.V., Barrett, J.C., Burgoyne, P.S., and Deng, C.X. (2004). BRCA1, histone H2AX phosphorylation, and male meiotic sex chromosome inactivation. *Curr Biol* 14,

2135-2142.

Turner, J.M., Mahadevaiah, S.K., Ellis, P.J., Mitchell, M.J., and Burgoyne, P.S. (2006). Pachytene asynapsis drives meiotic sex chromosome inactivation and leads to substantial postmeiotic repression in spermatids. *Dev Cell* 10, 521-529.

Turner, J.M., Mahadevaiah, S.K., Fernandez-Capetillo, O., Nussenzweig, A., Xu, X., Deng, C.X., and Burgoyne, P.S. (2005). Silencing of unsynapsed meiotic chromosomes in the mouse. *Nat Genet* 37, 41-47.

van der Heijden, G.W., Derijck, A.A., Posfai, E., Giele, M., Pelczar, P., Ramos, L., Wansink, D.G., van der Vlag, J., Peters, A.H., and de Boer, P. (2007). Chromosome-wide nucleosome replacement and H3.3 incorporation during mammalian meiotic sex chromosome inactivation. *Nat Genet* 39, 251-258.

van der Heijden, G.W., Derijck, A.A., Ramos, L., Giele, M., van der Vlag, J., and de Boer, P. (2006). Transmission of modified nucleosomes from the mouse male germline to the zygote and subsequent remodeling of paternal chromatin. *Dev Biol* 298, 458-469.

van der Heijden, G.W., Dieker, J.W., Derijck, A.A., Muller, S., Berden, J.H., Braat, D.D., van der Vlag, J., and de Boer, P. (2005). Asymmetry in histone H3 variants and lysine methylation between paternal and maternal chromatin of early mouse zygotes. *Mech Dev* 122, 1008.

Veyrunes, F., Waters, P.D., Miethke, P., Rens, W., McMillan, D., Alsop, A.E., Grutzner, F., Deakin, J.E., Whittington, C.M., Schatzkamer, K., et al. (2008). Bird-like sex chromosomes of platypus imply recent origin of mammal sex chromosomes. *Genome Res* 18, 965-973.

Wang, P.J. (2004). X chromosomes, retrogenes and their role in male reproduction. *Trends Endocrinol Metab* 15, 79-83.

Wang, Q.T., Piotrowska, K., Ciemerych, M.A., Milenkovic, L., Scott, M.P., Davis, R.W., and Zernicka-Goetz, M. (2004). A genome-wide study of gene activity reveals developmental signaling pathways in the preimplantation mouse embryo. *Dev Cell* 6, 133-144.

Ward, W.S., and Coffey, D.S. (1991). DNA packaging and organization in mammalian spermatozoa: comparison with somatic cells. *Biol Reprod* 44, 569-574.

Wassarman, P.M., and Mortillo, S. (1991). Structure of the mouse egg extracellular coat, the zona pellucida. *Int Rev Cytol* 130, 85-110.

Wojtasz, L., Daniel, K., Roig, I., Bolcun-Filas, E., Xu, H., Boonsanay, V., Eckmann, C.R., Cooke, H.J., Jasin, M., Keeney, S., et al. (2009). Mouse *HORMAD1* and *HORMAD2*, two conserved meiotic chromosomal proteins, are depleted from synapsed chromosome axes with the help of *TRIP13* AAA-ATPase. *PLoS Genet* 5, e1000702.

Wossidlo, M., Nakamura, T., Lepikhov, K., Marques, C.J., Zakhartchenko, V., Boiani, M., Arand, J., Nakano, T., Reik, W., and Walter, J. (2011). 5-Hydroxymethylcytosine in the mammalian zygote is linked with epigenetic reprogramming. *Nat Commun* 2, 241.

Yu, Y.E., Zhang, Y., Unni, E., Shirley, C.R., Deng, J.M., Russell, L.D., Weil, M.M., Behringer, R.R., and Meistrich, M.L. (2000). Abnormal spermatogenesis and reduced fertility in transition nuclear protein 1-deficient mice. *Proc Natl Acad Sci U S A* 97, 4683-4688.

Zamudio, N.M., Chong, S., and O'Bryan, M.K. (2008). Epigenetic regulation in male germ cells. *Reproduction* 136, 131-146.

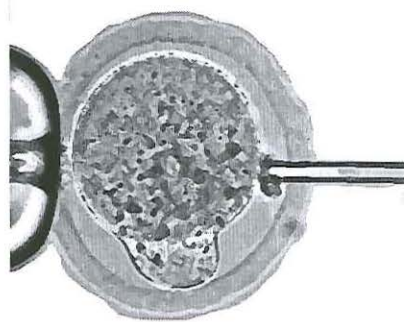
Zhao, M., Shirley, C.R., Hayashi, S., Marcon, L., Mohapatra, B., Sukanuma, R., Behringer, R.R., Boissonneault, G., Yanagimachi, R., and Meistrich, M.L. (2004). Transition nuclear proteins are required for normal chromatin condensation and functional sperm development. *Genesis* 38, 200-213.

Zhao, M., Shirley, C.R., Yu, Y.E., Mohapatra, B., Zhang, Y., Unni, E., Deng, J.M., Arango, N.A., Terry, N.H., Weil, M.M., et al. (2001). Targeted disruption of the transition protein 2 gene affects sperm chromatin structure and reduces fertility in mice. *Mol Cell Biol* 21, 7243-7255.



# 2

Round spermatid injection (ROSI) into oocytes:  
what can we learn from it?





## The journey towards the development of ROSI

The birth of Louise Brown, the world's first baby conceived by in vitro fertilization (IVF) in 1978, made the headlines, and immediately led to a general public awareness of the potentiality of assisted reproduction. Soon afterwards, thousands of infertile couples could benefit from IVF, and obtain children generated from their own gametes. IVF involves incubation of sperm and egg in a culture dish, and requires a proper concentration of moving sperm for fertilization to be successful. Therefore, males that produced semen samples with very few (motile) sperm could still not conceive a child through IVF. Some years after the introduction of IVF, embryologists started to apply a technique called subzonal insemination (SUZI) in cases when sperm concentration was low, and IVF attempts had previously failed (Metka et al., 1985). By mechanically introducing a few sperm through the zona pellucida into the perivitelline space, they were leaving it up to the sperm to complete the journey and fuse with the oocyte membrane. Despite this advancement, SUZI was still a highly inefficient technique for resolving cases of severe male infertility (Bertrand et al., 1996).

In the early nineties, while performing SUZI in the Centre for Reproductive Medicine in Belgium, the embryologists Gianpiero Palermo and André van Steirteghem accidentally injected a sperm directly into the ooplasm of the oocyte. Surprisingly, the fertilized egg not only survived the injection, but also developed into a normal embryo. Once transferred back to the mother's uterus, it resulted in a pregnancy with delivery of a healthy baby (Palermo et al., 1992). Thus, more or less by serendipity, a revolutionary treatment emerged, and only two years later intracytoplasmic sperm injection (ICSI) was in clinical practice.

However, for patients without sperm in the ejaculate (azoospermic), neither IVF nor ICSI could be attempted. Although azoospermic individuals do not have any spermatozoa in their ejaculate, they might have (patchy) areas in their testes where spermatogenesis still occurs. If some mature sperm cells are detected in a testis biopsy, those can be isolated by testicular sperm extraction (TESE) and ICSI can still be performed. However, in many cases only immature haploid germ cells can be detected in a testis biopsy of an azoospermic patient. To test if it might be feasible to develop assisted reproduction techniques for this group of patients, injection of such "immature" haploid germ cells into oocytes was tested first in animal models.

A round spermatid represents the earliest haploid male germ cell type, and might become a functional male gamete if its nucleus is mechanically introduced into an oocyte. Round spermatid injection (ROSI) was first attempted in 1993 by Ogura and colleagues, using the golden hamster and the mouse as model organisms (Ogura and Yanagimachi, 1993; Ogura et al., 1993). They reported that the spermatid nuclei were able to duplicate their DNA and participate in syngamy with the female pronucleus when incorporated into oocytes either

by microsurgery or through electrofusion. Later on, the birth of four normal mice following ROSI showed that mouse round spermatids can support full-term embryo development (Ogura et al., 1994). Moreover, some years later it was even shown that several subsequent generations of ROSI-derived mice did not display any overt abnormalities (Tamashiro et al., 1999). ROSI in other animals, including rabbit (Sofikitis et al., 1994) and rat (Hirabayashi et al., 2002), was also reported to result in the birth of normal offspring. Based upon these promising results it was anticipated that it was only a matter of time before its efficacy would have been proven also in human.

The first successful injection of human oocytes with round spermatids from a man for whom the testis biopsy lacked more mature stages of germ cells, was reported by Vanderzwalmen et al. (1995). This led to the formation of a zygote which developed up to the 4-cell stage (Vanderzwalmen et al., 1995). This publication was rapidly followed by the first report of two successful childbirths resulting from injection of round spermatids into human oocytes (Tesarik et al., 1995). After these first live births had been achieved using ROSI, only a few other centers were able to obtain successful pregnancies following ROSI (Antinori et al., 1997a; Antinori et al., 1997b; Vanderzwalmen et al., 1997).

Meanwhile many other clinics experienced very low fertilization rates following ROSI (Levrán et al., 2000; Vicdan et al., 2001; Yamanaka et al., 1997). In addition, attempts to perform ROSI using non-human primates were reported to be largely unsuccessful (Hewitson et al., 2000). Based on the frequent failure of achieving a pregnancy following ROSI, the use of round spermatids as substitute gametes in humans started to become very controversial. In fact, after the publication of Antinori's work, no pregnancies have been reported that resulted from the use of round spermatids from patients with a complete absence of elongated spermatids or spermatozoa from the preliminary ejaculate or from diagnostic testicular biopsies (Balaban et al., 2000; Benkhalifa et al., 2004; Khalili et al., 2002; Levrán et al., 2000; Urman et al., 2002; Vicdan et al., 2001). In total, only about 12 children have been reported worldwide to have been born following ROSI, and since 2002, no clinical ROSI-derived pregnancies have been reported. Nowadays, IVF clinics worldwide have abandoned performing round spermatid injection.

### **ROSI in mouse: what can we learn from it?**

If all a male gamete needs to achieve is the delivery of an intact, haploid genome to the oocyte, and to activate the oocyte to trigger meiotic resumption, this should also be possible upon artificial oocyte activation followed by injection of a round spermatid. However, the developmental failure reported to occur in many ROSI-derived embryos before and after implantation, not only in human but also in mouse, suggests that apparently more than the



DNA sequence is required for proper embryonic development (Ohta et al., 2009). This is not at all surprising, given the current knowledge on the intricate regulatory mechanisms that accompany early embryonic development. Such regulation depends on many epigenetic signals, in order to constitute the correct chromatin structure that orchestrates gene expression to be executed in a timely manner. Preimplantation embryo development is marked by dramatic and differential changes in the chromatin structure and epigenetic make-up of the paternal and maternal genomes. Furthermore, parental imprints, set during gametogenesis, need to be maintained during this very dynamic epigenetic regulation of the genome in the early embryo, to ensure correct gene expression later on.

To shed light on the causes of the poor ROSI outcome, several groups have investigated some fundamental processes (summarized in Table 1) that, if misregulated, may cause the early embryonic developmental failure in ROSI-derived mouse embryos. These processes will now be discussed in the context of the major events that occur during mouse preimplantation development.

### **Protamine-to-histone transition**

After fertilization of the egg by a mature spermatozoa, the paternal genome rapidly undergoes dramatic structural changes and acquires newly provided hypomethylated histones. However, as explained above, round spermatids are presented to the “maternal environment” with a chromatin constitution that is completely histone-based.

In order to verify if the histones transmitted through ROSI would be removed or preserved in the zygote, H3K9me3 patterns, a histone modification that is always present in round spermatids but absent in mouse sperm-derived paternal pronuclei, have been analyzed in the paternal pronuclei of ROSI-derived zygotes. Using this marker, it was demonstrated that most of the histones present in the spermatid-derived paternal pronucleus were those that were originally carried by the spermatid (Kishigami et al., 2006; Polanski et al., 2008). In fact, it was found that H3K9me3 enrichment in paternal pericentromeric regions persisted at least until the first mitotic division upon ROSI (Kishigami et al., 2006). In contrast, upon normal fertilization in the mouse, paternal pericentromeric heterochromatin lacks this posttranslational modification, and an alternative form of facultative heterochromatin is established by progressive acquisition of H3K27me3 (Puschendorf et al., 2008). Thus, it appears that round spermatid-derived histones in the paternal pronucleus are not exchanged for maternal histones.

It could be envisioned that the aberrant epigenetic signature on the paternal pericentromeric heterochromatin in early preimplantation ROSI-derived mouse embryos could be associated with an increased chance of mis-segregation errors and subsequent occurrence of embryonic

chromosomal abnormalities, which are generally considered to be a major cause of the low survival rate of ROSI derived embryos (Yamagata et al., 2009). By live-cell imaging, one study recorded an extremely high frequency (77.5%) of abnormal chromosome segregation (ACS) at the first mitosis in ROSI-generated mouse embryos (Yamagata et al., 2009). To assess the capacity of implantation and post-implantation development of ROSI-derived embryos displaying ACS at the 2-cell stage, those embryos were transferred to the oviducts of pseudopregnant females. Although embryos with ACS could implant and form deciduae, at E7.5 there were no viable embryos and the deciduae were reabsorbed around E9.5, suggesting that embryos with ACS underwent spontaneous miscarriage. The authors provided evidence for the presence of DNA double strand breaks in the spermatid-derived genome of embryos displaying ACS. However, they also reported that the incidence of ACS depended strongly on the skill of the operator that performed the ROSI (Yamagata et al., 2009). Due to this apparent operator-dependent variability, it is difficult to draw a definite conclusion from this work. It is important to note that, *in vivo*, mouse round spermatids do not appear to have a significant number of DNA double strand breaks. It is only later, during spermatid elongation, when the histone-to-protamine transition commences, that multiple DSBs are transiently formed (Marcon and Boissonneault, 2004). This could be related to DNA uncoiling mediated by topoisomerases (Leduc et al., 2008). Thus, if such spermatids are injected, they might give rise to embryos with increased levels of DSBs compared to those obtained with spermatids that are at an earlier step of differentiation, or mature sperm. Alternatively, or in addition, round spermatids may acquire damage during isolation and preparation for microinjection. There is a need for research that can provide more insight in the link between spermatozoal or spermatid histone content and the presence of DNA damage in the male pronucleus.

### **Paternal DNA demethylation**

In mouse, active demethylation of the paternal genome, except for the imprinted regions, normally takes place in the male pronucleus of the zygote soon after fertilization and various aberrant methylation patterns at the 2-cell stage have been reported to be an indicator of early developmental failure (Shi and Haaf, 2002). It has been hypothesized that paternal DNA demethylation could be linked to, and helped, by the protamine-to-histone exchange, that would render the paternal DNA accessible to putative demethylases, when the protamines are off and before the new histones are on the DNA (Haaf, 2006). If this is the case, the histone-associated DNA of round spermatids might be resistant to global demethylation after ROSI. To assess this, the DNA methylation status of the paternal pronucleus has been assessed after ICSI and ROSI. In several studies, ROSI-derived embryos were found to develop with genome-wide, aberrant DNA methylation states (Kishigami et al., 2006; Polanski et al.,



2008). Using an anti-5-methyl-cytosine antibody, the paternal pronucleus of ROSI-derived zygotes was marked by a high overall DNA methylation level up to the first mitosis, whereas the paternal pronucleus derived from mature sperm normally was devoid of such a signal (Kishigami et al., 2006; Polanski et al., 2008). Hence, the presence of paternal histones in ROSI-derived paternal pronuclei may interfere with normal paternal DNA demethylation occurring in the zygote. In particular, the presence of certain histone modifications may be relevant in this context. Previous studies have shown an interaction between DNMTs and H3K9 methyltransferases (Freitag and Selker, 2005; Geiman and Robertson, 2002). Furthermore, recent studies have shown that retention of a small amount of H3K9me2-marked histones at imprinted loci in normal mature sperm plays a role in protecting these regions in the paternal genome from cytosine demethylation in normal mouse zygotes (Nakamura et al., 2012).

Interestingly, time-lapse analysis of DNA methylation status in ROSI-derived zygotes was performed by microinjection of a synthetic RNA encoding enhanced green fluorescence protein (EGFP) fused to the methyl-CpG-binding domain and nuclear localization signal of methyl-CpG binding protein 1 (MBD1). This experiment showed abnormal localization of methylated chromatin in the nucleoplasm of the male pronucleus upon ROSI (Yamazaki et al., 2007). These mislocalized dotted structures seem to correspond to the pericentromeric regions, which are highly H3K9me3-positive in round spermatid-derived pronuclei, and also failed to be recruited to their normal location near the nucleolus during pronuclear formation. After analysis of the fluorescence pattern at the pronuclear stage, each ROSI-derived embryo was allowed to develop to the 2-cell stage for further assessment. Less than 50% of the zygotes that initially contained mislocalized methylated dots in the male nucleoplasm reached the 2-cell stage, while more than 70% of ROSI-derived zygotes with normal localization of methylated DNA within the male pronucleus developed to the 2-cell stage (Yamazaki et al., 2007).

Together, these results suggest that an abnormally high genome-wide methylation level of the paternal genome, in combination with aberrant localization of the methylated DNA, might interfere with the normal development of ROSI-derived embryos.

### Parental imprints

Misregulation of parental imprints is generally known to have profound consequences for embryonic development (Schulz et al., 2010). Acquisition of the paternal methylation imprints occurs early during spermatogenesis, some imprints are already established at the spermatogonial stage and other loci undergo acquisition and loss of methylation marks in spermatocytes (Davis et al., 2000; Lucifero et al., 2004). To analyze whether round spermatids carry correct genomic imprinting marks, and if these imprints can be properly maintained after ROSI, expression of 6 imprinted genes has been assessed in ROSI-derived mouse embryos



(Shamanski et al., 1999). In this study, all tested paternally (*Igf2*, *Snrpn*, and *Peg1*) and maternally expressed imprinted genes (*H19*, *Igf2r*, and *Mash2*) did not show any differences in mRNA expression levels in ROSI-derived embryos compared to controls. These results have been confirmed by another group (Miki et al., 2004). Together, these observations demonstrate that acquisition of imprinted DNA methylation patterns is complete by the round spermatid stage and can be maintained upon performing ROSI. Thus, the generally poor outcome of ROSI is less likely to be a result of defects in expression of imprinted genes.

### Zygotic genome activation

Following fertilization, proper initiation of zygotic genome activation (ZGA) by the 2-cell stage is essential for continued embryonic development. While mature spermatozoa are generally considered to be transcriptionally inert, round spermatids enter the oocyte in a fully transcriptionally active state, which might interfere with the normal gene expression reprogramming established during the ZGA. Indeed it has been shown that fertilization with sperm derived from mice in which the histone-to-protamine transition is somewhat aberrant leads to altered gene expression (Ihara et al., 2014). If such an effect is already evident with mature sperm, that could have even more dramatic consequences in the case of using round spermatids.

To study if ZGA occurred normally in ROSI-derived embryos compared to controls, expression of two zygotic genes, *Hsp70.1* and *Smcy*, was analyzed at the 2-cell stage (Ziyyat and Lefevre, 2001). Significantly decreased levels of expression of *Hsp70.1* were detected in ROSI-derived 2-cell stage embryos, where *Smcy* had a normal expression profile. In another study, transcript analysis of 4 other zygotic genes was performed (Hayashi et al., 2003). Compared to controls, similar patterns of transcriptional activation were found for most of the genes analyzed: the translation initiation factor gene *eIF-1A* (previously named *eIF-4C*), the histone deacetylase gene *Hdac-1* and the murine endogenous retrovirus-like element *ERV-L*. However, ROSI-derived embryos expressed abnormally elevated levels of the retrovirus-like mobile element intracisternal A particle (IAP) from the 2-cell to the blastocyst stages (Hayashi et al., 2003). The biological effects of IAP expression on mouse embryo development are unknown and this result remains difficult to interpret. Taken together, although single gene expression analysis has been performed on a very limited number of zygotic genes, both these studies suggest some misregulation of ZGA.

Through another experimental approach, ZGA was verified using 5-bromouridine-5'-triphosphate (BrUTP) labeling of newly synthesized RNAs. In this study it was reported that more than 70% of the ROSI-derived 2-cell stage embryos exhibited a lower overall level of transcriptional activity compared to those generated with ICSI (Bui et al., 2011). This indicates

that ZGA initiation might be delayed or incomplete in the majority of ROSI-derived embryos. Although BrUTP incorporation does not offer any qualitative information, this study also confirms the existence of some ZGA disturbances in ROSI-derived embryos. Follow up studies using genome-wide RNA sequencing approaches would certainly provide very useful data in order to better understand this particular aspect. For now, the link between the reported abnormal gene expression patterns and the low success rate after ROSI remains unclear and should be further investigated.

### Regulation of the early developmental gene expression pattern

In contrast to the highly condensed mature sperm, injection of a round spermatid (especially if cytoplasm is not removed) into an oocyte represents the massive arrival of mRNA from various genes, some of which might be deleterious to the development of the embryo if translated. In addition, continued transcription of genes that are involved in round spermatid development might occur. The ectopic expression of many proteins encoded by round spermatid mRNAs, such as the protamines, could interfere with normal cellular function.

Expression of round spermatid specific genes in ROSI-derived embryos was analyzed by measurement of transcript levels for *transition protein 1 (Tp1)*, *protamine 1 (Prm1)*, *protamine 2 (Prm2)*, *Gapds* and *ropporin (Ropn1)*, which are normally not present at any moment during embryonic development (Borghol et al., 2008; Hayashi et al., 2003; Ziyat and Lefevre, 2001). Furthermore, mRNA expression of *Ube1Y*, a Y-linked gene that escapes the general repression of X- and Y-linked gene transcription in spermatids (Hendriksen et al., 1995; Odorisio et al., 1996), was also observed. In control embryos, *Ube1Y* was not expressed before post-implantation development (Ziyat and Lefevre, 2001).

In general, all tested round spermatid-specific mRNAs were found to be expressed immediately following fertilization in ROSI-derived zygotes, but became rapidly down-regulated by the 2-cell stage, with only some minor differences in their temporal expression pattern. These results led the authors to suggest that, in mouse, regulatory mechanisms are activated soon after ROSI to inhibit the inappropriate transcription of male post-meiotically expressed genes. Thus, transient misexpression of spermatidal genes following ROSI is not expected to have a major impact on the execution of the normal developmental gene expression program.

**Table 1: Possible causes of the poor ROSI outcome**

Process analyzed	Status	References
Parental imprints	V	(Miki et al. 2004; Shamanski et al. 1999)
ZGA	X	(Bui et al., 2011; Hayashi et al., 2003; Ziyat and Lefevre, 2001)
Repression of RS specific genes	V*	(Borghol et al., 2008; Hayashi et al., 2003; Ziyat and Lefevre, 2001)
Paternal DNA demethylation	X	(Kishigami et al., 2006; Polanski et al., 2008; Yamazaki et al., 2007)
Paternal DNA epigenetic profile	X	(Kishigami et al., 2006; Polanski et al., 2008)
Chromosome segregation	X	(Yamagata et al., 2009)

\* = initially misregulated



## ROSI as a tool to study the consequences of marked variation in paternal chromatin composition

Analyses of molecular processes in ROSI-derived mouse embryos can help us to obtain clinically relevant insight, applicable to sperm or spermatid selection in the application of TESE in man, if we view the round spermatid as an extreme example of a gamete with incomplete removal of histones. As described in Chapter 1, during normal spermatogenesis, most but not all histones are replaced by protamines. The percentage of retained histones is much lower in mouse compared to man, and also much more variable in man. In the Netherlands, a quality standard consensus document for assisted reproduction using surgically obtained sperm has been published by the three associations involved in assisted reproduction (Dutch Societies for Gynaecology & Obstetrics, Urology, and Clinical Embryology ([http://www.nvog.nl/Sites/Files/0000003313\\_Kwaliteitsnorm%20ICSI%20chirurgisch%20verkregen%20zaadcellen%2020130702.pdf](http://www.nvog.nl/Sites/Files/0000003313_Kwaliteitsnorm%20ICSI%20chirurgisch%20verkregen%20zaadcellen%2020130702.pdf))). That consensus document indicated that, when motile sperm cannot be retrieved, immotile sperm with normal morphology, or elongated spermatids may be used for ICSI. The use of round spermatids is not allowed. Elongated spermatids that are not fully condensed, most likely still contain a higher relative proportion of nucleosome-packaged DNA compared to normal mature sperm (De Vries et al., 2012). There are no reports of studies that investigated whether elongated spermatid injection (ELSI), compared to ICSI with mature and motile sperm, could be associated with more frequent aberrations in embryonic development, that might be attributed to some form of epigenetic misregulation.

Thus, it is clear that more fundamental research, aimed at deciphering what are the critical aspects of chromatin structure that are required to support normal embryo development is needed.

Application of ROSI in mouse, followed by detailed analyses of the consequences for genome integrity, epigenetic constitution, and gene expression patterns both in preimplantation embryos but also at later stages of development could help us to unravel critical parameters for epigenetic sperm quality. Furthermore, since chromosome aneuploidy is one of the major causes for embryo loss in human embryology, and studies on human embryos are difficult to perform due to ethical reasons, it would be very important to investigate this further by using mouse ROSI as a model for this phenomenon.

Taken together, we feel that mouse ROSI could be a valuable research tool for evaluation of the importance of spermatozoal chromatin composition and properties in human ICSI, but also to be able to provide deep insight in the biological relevance of the epigenetic conformation of the paternal genome for normal embryo development. In the future, this type of basic research may help to develop better tests for gamete quality in all assisted reproduction techniques aimed at overcoming male infertility.

### Technical aspects of ROSI in our lab

Although ROSI success rate is rather low also in mouse, ranging in different studies from efficiencies of 1.7% to 28.2% (Kimura and Yanagimachi, 1995; Ogura et al., 1994), it still represents a feasible approach. In our hands, normally around 10% of the fertilized oocytes that survive the injection will develop into normal embryos after transfer into pseudopregnant females. Microinjection of mouse oocytes is technically much more challenging than human oocyte microinjection. While conventional microinjection into human oocytes is very successful, in mice this has been proven to be very difficult, mainly because the oolemma (the oocyte plasma membrane) of mouse oocytes is much more elastic compared to that of human oocytes. Piezo-actuated micromanipulation appeared indispensable to pierce through the oolemma, to perform microinjections into mouse oocytes. By generating ultrasonic mechanical pulses that travel longitudinally along the pipette and vibrate the tip of the injection needle, piezo-drilling permits more easy penetration of the zona pellucida and of the oolemma. Detailed protocols have been described to successfully execute piezo-actuated mouse ICSI (Yoshida and Perry, 2007).

In our group, we adapted the published ICSI protocol (Yoshida and Perry, 2007) to perform ROSI (detailed protocol described in the Addendum to this Chapter 2). Mouse round spermatids do not possess oocyte activation capacity, so prior to ROSI small batches of oocytes (10-15) have to be pre-activated for one hour by incubation in calcium-free medium supplemented with 15 mM strontium chloride ( $\text{SrCl}_2$ ). Mouse round spermatids can be easily identified in a testicular cell suspension by their small size (about 10  $\mu\text{m}$  in diameter) and round nucleus with a centrally located dense structure that contains the centromeric DNA (Ogura and Yanagimachi, 1993). Gentle pipetting using a 5  $\mu\text{m}$  injection needle can be applied to release the nuclei of the round spermatids and these can then be collected and directly used for microinjection (Figure 1A). In our setup, the microscope is equipped with an XYclone laser system (Hamilton Thorne), that is used to create a hole in the zona pellucida (Figure 1B). This is a very helpful tool because it allows one to penetrate the zona pellucida more quickly and easily than through piezo-drilling. Operating within very short time spans when working outside the environmentally controlled conditions of an incubator (5%  $\text{CO}_2$  in air, and constant temperature at 37°C) is particularly important to assure oocyte survival and improve the chance of normal further embryonic development. Once the zona pellucida has been pierced, the injection needle, containing the previously collected round spermatid nucleus, is introduced into the perivitelline space. At this point, the piezo-drill is used to penetrate the oocyte membrane as in performing mouse ICSI (Figure 1C) (Yoshida and Perry, 2007).

In Chapter 3 we made extensive use of this technique to study if the epigenetic and tran-



scriptional status of a round spermatid X chromosome, that carries heterochromatic marks as a consequence of MSC1, could affect imprinted X chromosome inactivation dynamics in early female mouse embryos.

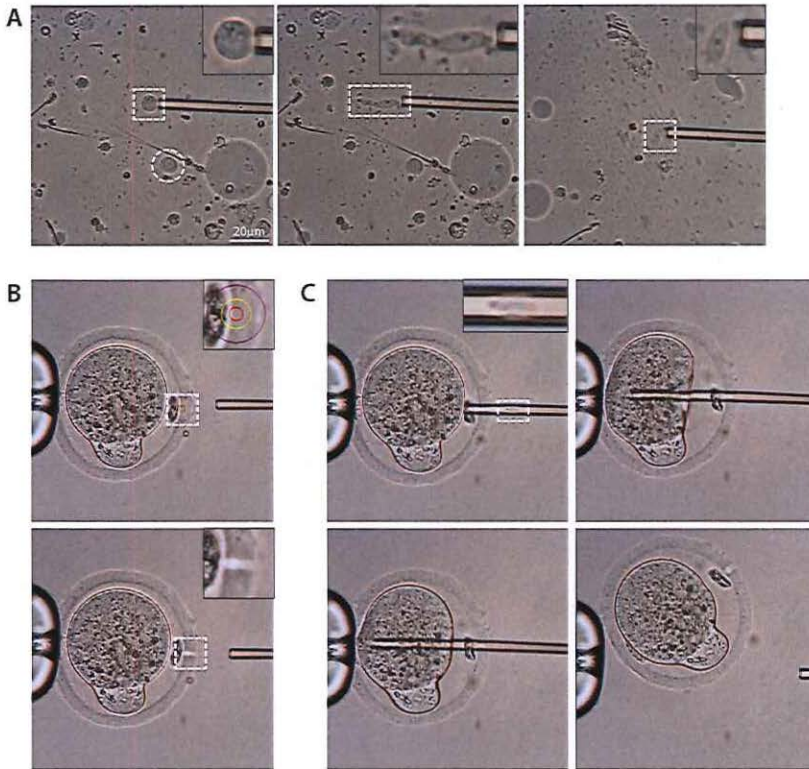


**Figure 1: Technical aspects of ROSI**

(A) Left: the  $5\mu\text{m}$  microinjection pipette is lowered into the testicular cell suspension. Two round spermatids are highlighted in the indicated areas (circle and square). Enlargement of the round spermatid in the squared box is shown in the top right corner. Middle: after the round spermatid has been drawn into the injection pipette followed by expelling in the medium, its nucleus separates from the cytoplasm, which remains loosely attached on the left side of the nucleus. Right: clean round spermatid nucleus obtained after repeated pipetting. (B) Top: oocyte held by holding pipette on the left side. In this case, the cortical bump over the chromosomes in anaphase II (from which the second polar body will be extruded) is oriented at 6 o'clock position (on an imaged clock face). White squared area shows the highly degenerated first polar body and the target of the XY clone laser system on a portion of the zona pellucida. Bottom: laser-pierced zona pellucida. (C) Top left: the injection needle, containing the previously collected round spermatid nucleus (shown in the enlargement), is introduced into the perivitelline space through the gate created in the zona pellucida. Top right: the tip of the microinjection needle is advanced towards the opposite side of the oocyte. This produces a deep invagination in the oocyte plasma membrane. Bottom left: the piezo-drill is used to penetrate the oocyte membrane which now visibly relaxes along the shaft of the needle. The round spermatid nucleus is quickly released into the cytoplasm. Bottom right: the needle is smoothly withdrawn from the oocyte and the oocyte is released from the holding pipette. Scale bar is  $20\mu\text{m}$  throughout.





## ROSI protocol (adapted from Yoshida and Perry, 2007)

### Reagents

- Mice of the strain B6D2F1, female C57BL/6 × male DBA/2 F1 hybrid (supplier Harlan)
- G-1 PLUS (Vitrolife)
- G-MOPS PLUS (Vitrolife)
- MEM- $\alpha$  Complete (LIFE-TECHNOLOGIES/GIBCO cat. no. 22571)
- Ca<sup>2+</sup>-free M16 (homemade)
- Strontium Chloride (SrCl<sub>2</sub>) (Sigma Company)
- Embryo-tested bovine testis hyaluronidase (Sigma, cat. no. H-4272)
- Polyvinylpyrrolidone (PVP) (Irvine scientific, cat. no. 99219), dissolved in G-MOPS
- Mineral oil (Sigma, cat. no. M8410-500ml)
- Elemental mercury (Hg<sup>0</sup>) (Sigma, cat. no. 215457-100G)
- Human chorionic gonadotropin (hCG) (cat. no. REG NL 1249) and pregnant mare serum gonadotropin (PMSG) (cat. no. REG NL 1396) (MSD Animal Health (Intervet))

### Equipment

- Forceps, watchmaker's #5, two pairs (Meekers Medical, cat. no. HB105)
- Blunt ended curved forceps, two pairs (Meekers Medical, cat. no. HB210)
- Glass capillaries (Harvard Apparatus, 1,5 OD x 1,17 ID x 150L, GC150T-10, part. no. 30-0062)
- Transfer needles obtained by pulled glass capillaries
- Holding needles (MPH-SM-20, ORIGIO)
- Microinjection needles (PIEZO-5-20, ORIGIO)
- The STRIPPER BP Stainless Steel Slimline embryo-handling micropipetter (MXL3-STR-BP-SW, ORIGIO) with silicone bulb (MXL3-BULB, ORIGIO)
- Precision pipettes, such as the P200 Pipetman (Gilson, Inc.)
- Stereomicroscope, SZH10 Olympus
- Heated platform
- Workstation comprising inverted microscope (Olympus LH50A) equipped with Eppendorf micromanipulators (CellTram Air and vario) and injectors (Narishige)
- Piezo micromanipulator controller (PMAS-CT140; Prime Tech)
- XYclone laser system (LWD 40x objective, Hamilton Thorne), which attaches to the turret of the inverted microscope just like a typical objective
- Humidified CO<sub>2</sub> (5% (v/v) in air) incubator (Sanyo MCO-17AIC)
- Eppendorf tubes
- Centered-well organ culture dishes (Falcon, cat. no. 353037, 60 x 15 mm style)
- Easy grip tissue culture dishes (BD Falcon, cat. no. 353004, 60 x 15 mm style)
- 1-ml syringe
- 26 G needle

### Reagent setup

Supplemented MEM- $\alpha$  complete contains 44 ml MEM- $\alpha$ , 113  $\mu$ l Sodium-Lactate, 1 ml stock solution (0.006 g Sodium-Pyruvate, 0.25 g HEPES, 0.007 g L-Glutamin), 5 ml Fetal Calf Serum (FCS); pH is set at 7.2 with 1 N NaOH. Final solution is 0.22  $\mu$ m sterile-filtered. Freshly prepared the day before ROSI and stored at 4 °C.

Ca<sup>2+</sup>-free M16 10X stock (in -20 °C, 5ml/falcon tube) contains 5.68 g NaCl, 0.356 g KCl, 0.162 g KH<sub>2</sub>PO<sub>4</sub>, 0.293 g SO<sub>4</sub>.7H<sub>2</sub>O, 2.101 g NaHCO<sub>3</sub>, 4.35 ml Sodium lactate, 0.036 g Sodium pyruvate, 1 g Glucose, 4 g BSA, 2 ml Phenol Red, up to 100 ml with sterile water.

Ca<sup>2+</sup>-free M16 1X contains 5 ml Ca<sup>2+</sup>-free M16 10X stock + 45 ml H<sub>2</sub>O.

PVP solution is obtained by dissolving it in 1 ml MOPS on a roller, at room temperature for at least one hour. Store in 0.2 ml aliquots at -20 °C (for up to months). The 'in-use' aliquot of PVP solution is useable for several weeks stored at 4 °C.

Embryo-tested bovine testes hyaluronidase (Sigma H3884) stock is prepared by dissolving 30 mg of bovine testis hyaluronidase in water (to give 10 mg/ml). Store in 50  $\mu$ l aliquots at -20°C. Use at a final concentration of 300  $\mu$ g/ml by diluting it in supplemented MEM- $\alpha$  complete.

PMSG and hCG for superovulation are prepared by dissolving PMSG and hCG separately at 50 IU/ml in 0.9% (w/v) NaCl solution. 0.22  $\mu$ m-filter and store in 1 ml aliquots at -20°C for 1–2 months.

### Equipment setup

#### Preparation of the microscope for micromanipulation

A single holding pipette may be used for many sessions without changing it. At least one change of microinjection needle is recommended per session. Mount the microinjection needle firmly on a piezo workstation and use the injector to apply positive pressure and advance the Hg0 front so that it approaches the needle tip. Lower the assembly into the mineral oil of the collection dish and examine it at 200 $\times$  magnification. The Hg0 (microinjection pipette) front should be static unless caused to move by the injector. Draw some mineral oil into the pipette, then move to a drop of the PVP solution and draw some into the pipette.

#### Procedure overview of piezo-actuated round spermatid injection (ROSI)

##### Preparation of oocytes

To obtain relatively large numbers of oocytes (25–35/B6D2F1), superovulate by serial intra-



peritoneal injection (26 G needle) of 5 IU PMSG followed 48 h later by 5 IU hCG. Typically (with standard mouse room light/dark cycles), administer hormone injections at 5–6 pm. Females of 8–10 weeks give good yields, but the optimum varies. 12–15 h post-hCG injection, sacrifice the mice (3–5 per experiment usually suffices), collect their oviducts and place them separately in supplemented MEM- $\alpha$  complete drops (100  $\mu$ l) in the cover of a culture dish.

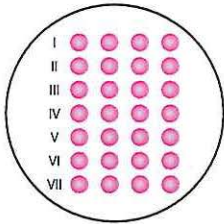
Working under the stereomicroscope, hold the oviduct wall with one pair of forceps and tear the evidently swollen ampulla containing the oocyte-cumulus complex. Tease the oocyte-cumulus complex from the oviduct; it should emerge as a single mass. Discard the oviductal remnant and repeat the process for the remaining oviducts.

Move the oocyte-cumulus masses by using a glass capillary attached to the hand pipette in a new centered-well dish containing supplemented MEM- $\alpha$  complete with bovine testis hyaluronidase stock solution at a final concentration of 300  $\mu$ g/ml. To allow the hyaluronidase to digest the intercellular matrix, oocytes can be pipetted repeatedly. Cumulus cells will fall away from the complexes, leaving the oocytes on a cumulus cell carpet.

Remove oocytes with a transfer pipette and place them in a centered-well dish with fresh supplemented MEM- $\alpha$  complete (without hyaluronidase). Wash the oocytes by pipetting repeatedly.

Transfer the oocytes to a drop (10  $\mu$ l) of pre-equilibrated G1 culture medium under mineral oil in a culture dish (from now on called storage dish), washing three times to remove traces of supplemented MEM- $\alpha$  complete. Place the storage dish containing the oocytes in the incubator for at least 15 min until required.

### Oocytes activation



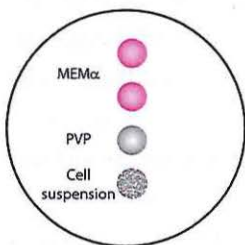
Activation dish setup is shown in Figure.

Place one batch of oocytes (10–15) into the first row of the activation dish containing drops of  $\text{Ca}^{2+}$ -free M16 with 10 mM  $\text{SrCl}_2$  and leave for 60 minutes in the incubator. Keep activating a new batch of 10–15 oocytes every 30 minutes, until the oocytes in the G1 storage dish are finished. During oocyte activation, a testicular cell suspension may be prepared as follows.

### Preparation of testicular cell suspension

Collect one testis from a male that is at least 8 weeks old and place it on a clean culture dish. Remove the tunica albuginea with fine forceps and then add 500  $\mu$ l of G-MOPS. Mince gently the tissue in between blunt ended curved forceps. The solution becomes milky as the cells disperse. Transfer solution in an Eppendorf tube. Make 1:10 dilution in a new Eppendorf tube.

### Microinjection dish setup



The cover of a plastic dish is used as a microinjection chamber. A vertical row of four small drops (10  $\mu$ l each), of which the first two are supplemented MEM- $\alpha$  complete (for oocytes), the subsequent drop is PVP in buffered MOPS, and the last is an aliquot of the 1:10 diluted testicular cell suspension, is placed on the bottom of the dish and covered with mineral oil (as shown in Figure).

With a transfer pipette, remove the first batch of activated oocytes (after completion of 60 minutes activation) from the activation dish and place them into the microinjection dish in the first droplet of supplemented MEM- $\alpha$  Complete. Then, move them to the second supplemented MEM- $\alpha$  complete drop and arrange them precisely in a vertical row. Place the microinjection dish on the microscope stage.

### Round spermatid nuclei collection

Mouse round spermatids can be easily identified in the last drop of 1:10 diluted testicular cell suspension by their small size (about 10  $\mu$ m in diameter) and round nucleus with a centrally located dense structure that contains the centromeric DNA (Ogura and Yanagimachi, 1993). Gentle pipetting was applied until the nuclei of the round spermatids lose all cytoplasm and can then be collected, transferred to the clean PVP drop.

Draw one or more RS nuclei into the microinjection pipette in the PVP drop. With experience, multiple (5) nuclei can be accumulated within a pipette at intervals of around 100  $\mu$ m; although only a single nucleus is subsequently injected per oocyte. Collecting multiple nuclei removes the need to return to the PVP droplet each time between injections. Working at 40 $\times$  magnification, move the microscope stage so that the pipette is in the microinjection droplet (supplemented MEM- $\alpha$  complete) containing 10–15 oocytes.

### Oocytes microinjection

Lower the holding pipette into the microinjection droplet (supplemented MEM- $\alpha$  complete) containing the oocytes and position the holding and microinjection pipettes so that their tips are on either side (usually with the holding pipette on the left) of a selected oocyte (the first or last of the vertical row). Use the microinjection needle to orientate the oocyte so that its MII plate is located straight up or down along the y-axis (12 o'clock or 6 o'clock). Either orientation minimizes the risk of damaging the MII plate during microinjection. Select an orientation that gives the largest space between the plasma membrane and the zona pellucida (perivitelline space) on the side of the microinjection pipette.

At 40 $\times$  XYclone laser objective, bring the oocyte plasma membrane into sharp focus. Use the

fine z-axis control to move the pipettes up or down so that their ends are in focus.

Applying gentle suction within the holding pipette, push the oocyte against the holding pipette aperture with the microinjection pipette. Pushing causes the oocyte zona and plasma membrane to engage the holding pipette aperture and cover it, anchoring the oocyte and making it easier to inject.

Move the most advanced RS nucleus so that it is 50–100  $\mu\text{m}$  from the pipette tip. Check the focus and Pierce the zona pellucida by laser applied pulse (XYclone).

The injection needle tip can now rapidly pass through the zona into the perivitelline space. Sustain positive pressure until the end-most RS nucleus is 10–50  $\mu\text{m}$  from the tip and ensure that the plasma membrane is in sharp focus.

Steadily advance the tip towards the opposite side of the oocyte, where it is being anchored by the holding pipette. Stop when the tip has advanced ~95% of the oocyte diameter. This produces a deep invagination in the (remarkably elastic) oocyte plasma membrane, which is now stretched around the microinjection needle.

While maintaining zero net pressure (or a very small negative one) within the microinjection pipette, apply a single piezo pulse. Ensure that the oocyte plasma membrane visibly relaxes along the shaft of the needle. This is an indispensable indication that the membrane has been punctured.

Deposit the RS nucleus in the cytoplasm with the application of small positive pressure in the microinjection pipette. Introduce the minimum amount of medium and do not suck cytoplasm into the pipette.

As soon as the RS nucleus has been deposited, withdraw the needle smoothly from the oocyte. The membrane should return to its original position and seal.

Release the injected oocyte by gently applying positive pressure within the holding pipette and proceed with the injection of the next oocyte. Once all oocytes have been injected, allow them at least 5 min to recover before being returned to the  $\text{CO}_2$  incubator. Fatal mechanical trauma to the oocyte during micromanipulation usually results in the onset of lysis within few minutes. Remove dead oocytes from the survivors during transfer to the G1 culture dish, wash the oocytes 4 times in equilibrated G1 culture medium to remove supplemented MEM- $\alpha$  complete (HEPES is toxic at 37°C) before placing them in the  $\text{CO}_2$  incubator. For optimal development, limit the time the oocytes are out of the incubator; less than 40 minutes is a guideline. Oocytes can then further cultured in the same G1 culture dish until the desired developmental stage is reached.

Experienced workers inject 15–20 oocytes sequentially, which takes 20–30 min. From oocyte collection to injection of the final sample, ROSI typically takes 3–6 h for 40–100 oocytes.



## REFERENCES

- Antinori, S., Versaci, C., Dani, G., Antinori, M., Pozza, D., and Selman, H.A. (1997a). Fertilization with human testicular spermatids: four successful pregnancies. *Hum Reprod* 12, 286-291.
- Antinori, S., Versaci, C., Dani, G., Antinori, M., and Selman, H.A. (1997b). Successful fertilization and pregnancy after injection of frozen-thawed round spermatids into human oocytes. *Hum Reprod* 12, 554-556.
- Balaban, B., Urman, B., Isiklar, A., Alatas, C., Aksoy, S., Mercan, R., and Nuhoglu, A. (2000). Progression to the blastocyst stage of embryos derived from testicular round spermatids. *Hum Reprod* 15, 1377-1382.
- Benkhalifa, M., Kahraman, S., Biricik, A., Serteyil, S., Domez, E., Kumtepe, Y., and Qumsiyeh, M.B. (2004). Cytogenetic abnormalities and the failure of development after round spermatid injections. *Fertil Steril* 81, 1283-1288.
- Bertrand, E., Devreker, F., van den Bergh, M., and Englert, Y. (1996). Is the subzonal-insemination procedure an efficient technique in the treatment of extreme oligoasthenoteratozoospermia? *Eur J Morphol* 34, 245-255.
- Borghol, N., Blachere, T., and Lefevre, A. (2008). Transcriptional and epigenetic status of protamine 1 and 2 genes following round spermatids injection into mouse oocytes. *Genomics* 91, 415-422.
- Bui, H.T., Wakayama, S., Mizutani, E., Park, K.K., Kim, J.H., Van Thuan, N., and Wakayama, T. (2011). Essential role of paternal chromatin in the regulation of transcriptional activity during mouse preimplantation development. *Reproduction* 141, 67-77.
- Davis, T.L., Yang, G.J., McCarrey, J.R., and Bartolomei, M.S. (2000). The H19 methylation imprint is erased and re-established differentially on the parental alleles during male germ cell development. *Hum Mol Genet* 9, 2885-2894.
- De Vries, M., Ramos, L., Housein, Z., and De Boer, P. (2012). Chromatin remodelling initiation during human spermiogenesis. *Biol Open* 1, 446-457.
- Freitag, M., and Selker, E.U. (2005). Controlling DNA methylation: many roads to one modification. *Curr Opin Genet Dev* 15, 191-199.
- Geiman, T.M., and Robertson, K.D. (2002). Chromatin remodeling, histone modifications, and DNA methylation-how does it all fit together? *J Cell Biochem* 87, 117-125.
- Haaf, T. (2006). Methylation dynamics in the early mammalian embryo: implications of genome reprogramming defects for development. *Curr Top Microbiol Immunol* 310, 13-22.
- Hayashi, S., Yang, J., Christenson, L., Yanagimachi, R., and Hecht, N.B. (2003). Mouse preimplantation embryos developed from oocytes injected with round spermatids or spermatozoa have similar but distinct patterns of early messenger RNA expression. *Biol Reprod* 69, 1170-1176.
- Hendriksen, P.J.M., Hoogerbrugge, J.W., Themmen, A.P.N., Koken, M.H.M., Hoeijmakers, J.H.J., Oostra, B.A., Van der Lende, T., and Grootegoed, J.A. (1995). Postmeiotic transcription of X and Y chromosomal genes during spermatogenesis in the mouse. *Dev Biol* 170, 730-733.
- Hewitson, L., Martinovich, C., Simerly, C., Dominko, T., and Schatten, G. (2000). Is round spermatid injection (ROSI) a therapy for male infertility? ROSI in the rhesus monkey is unsuccessful. *Fertility and Sterility* 74, S68.
- Hirabayashi, M., Kato, M., Aoto, T., Ueda, M., and Hochi, S. (2002). Rescue of infertile transgenic rat lines by intracytoplasmic injection of cryopreserved round spermatids. *Mol Reprod Dev* 62, 295-299.
- Ihara, M., Meyer-Ficca, M.L., Leu, N.A., Rao, S., Li, F., Gregory, B.D., Zalenskaya, I.A., Schultz, R.M., and Meyer, R.G. (2014). Paternal poly (ADP-ribose) metabolism modulates retention of inheritable sperm histones and early embryonic gene expression. *PLoS Genet* 10, e1004317.
- Khalili, M.A., Aflatoonian, A., and Zavos, P.M. (2002). Intracytoplasmic injection using spermatids and subsequent pregnancies: round versus elongated spermatids. *J Assist Reprod Genet* 19, 84-86.
- Kimura, Y., and Yanagimachi, R. (1995). Mouse oocytes injected with testicular spermatozoa or round spermatids can develop into normal offspring. *Development* 121, 2397-2405.
- Kishigami, S., Van Thuan, N., Hikichi, T., Ohta,

- H., Wakayama, S., Mizutani, E., and Wakayama, T. (2006). Epigenetic abnormalities of the mouse paternal zygotic genome associated with microinsemination of round spermatids. *Dev Biol* 289, 195-205.
- Leduc, F., Maquennehan, V., Nkoma, G.B., and Boissonneault, G. (2008). DNA damage response during chromatin remodeling in elongating spermatids of mice. *Biol Reprod* 78, 324-332.
- Levrin, D., Nahum, H., Farhi, J., and Weissman, A. (2000). Poor outcome with round spermatid injection in azoospermic patients with maturation arrest. *Fertil Steril* 74, 443-449.
- Lucifero, D., Chaillet, J.R., and Trasler, J.M. (2004). Potential significance of genomic imprinting defects for reproduction and assisted reproductive technology. *Hum Reprod Update* 10, 3-18.
- Marcon, L., and Boissonneault, G. (2004). Transient DNA strand breaks during mouse and human spermiogenesis new insights in stage specificity and link to chromatin remodeling. *Biol Reprod* 70, 910-918.
- Metka, M., Haromy, T., and Huber, J. (1985). Micromanipulatory sperm injection—a new method in the treatment of infertile males. *Wien Med Wochenschr* 135, 55-59.
- Miki, H., Lee, J., Inoue, K., Ogonuki, N., Noguchi, Y., Mochida, K., Kohda, T., Nagashima, H., Ishino, F., and Ogura, A. (2004). Microinsemination with first-wave round spermatids from immature male mice. *J Reprod Dev* 50, 131-137.
- Nakamura, T., Liu, Y.J., Nakashima, H., Ume-hara, H., Inoue, K., Matoba, S., Tachibana, M., Ogura, A., Shinkai, Y., and Nakano, T. (2012). PGC7 binds histone H3K9me2 to protect against conversion of 5mC to 5hmC in early embryos. *Nature* 486, 415-419.
- Odorisio, T., Mahadevaiah, S.K., McCarrey, J.R., and Burgoyne, P.S. (1996). Transcriptional analysis of the candidate spermatogenesis gene *Ube1y* and of the closely related *Ube1x* shows that they are coexpressed in spermatogonia and spermatids but are repressed in pachytene spermatocytes. *Dev Biol* 180, 336-343.
- Ogura, A., Matsuda, J., and Yanagimachi, R. (1994). Birth of normal young after electrofusion of mouse oocytes with round spermatids. *Proc Natl Acad Sci U S A* 91, 7460-7462.
- Ogura, A., and Yanagimachi, R. (1993). Round spermatid nuclei injected into hamster oocytes from pronuclei and participate in syngamy. *Biol Reprod* 48, 219-225.
- Ogura, A., Yanagimachi, R., and Usui, N. (1993). Behaviour of hamster and mouse round spermatid nuclei incorporated into mature oocytes by electrofusion. *Zygote* 1, 1-8.
- Ohta, H., Sakaide, Y., and Wakayama, T. (2009). Functional analysis of male mouse haploid germ cells of various differentiation stages: early and late round spermatids are functionally equivalent in producing progeny. *Biol Reprod* 80, 511-517.
- Palermo, G., Joris, H., Devroey, P., and Van Steirteghem, A.C. (1992). Pregnancies after intracytoplasmic injection of single spermatozoon into an oocyte. *Lancet* 340, 17-18.
- Polanski, Z., Motosugi, N., Tsurumi, C., Hiiragi, T., and Hoffmann, S. (2008). Hypomethylation of paternal DNA in the late mouse zygote is not essential for development. *Int J Dev Biol* 52, 295-298.
- Puschendorf, M., Terranova, R., Boutsma, E., Mao, X., Isono, K., Brykczynska, U., Kolb, C., Otte, A.P., Koseki, H., Orkin, S.H., et al. (2008). PRC1 and Suv39h specify parental asymmetry at constitutive heterochromatin in early mouse embryos. *Nat Genet* 40, 411-420.
- Schulz, R., Proudhon, C., Bestor, T.H., Woodfine, K., Lin, C.S., Lin, S.P., Prissette, M., Oakey, R.J., and Bourc'his, D. (2010). The parental non-equivalence of imprinting control regions during mammalian development and evolution. *PLoS Genet* 6, e1001214.
- Shamanski, F.L., Kimura, Y., Lavoit, M.C., Pedersen, R.A., and Yanagimachi, R. (1999). Status of genomic imprinting in mouse spermatids. *Hum Reprod* 14, 1050-1056.
- Shi, W., and Haaf, T. (2002). Aberrant methylation patterns at the two-cell stage as an indicator of early developmental failure. *Mol Reprod Dev* 63, 329-334.
- Sofikitis, N.V., Miyagawa, I., Agapitos, E., Pasyanos, P., Toda, T., Hellstrom, W.J., and Kawamura, H. (1994). Reproductive capacity of the nucleus of the male gamete after completion of meiosis. *J Assist Reprod Genet* 11, 335-341.
- Tamashiro, K.L., Kimura, Y., Blanchard, R.J.,



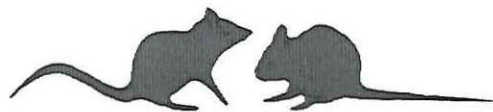
- Blanchard, D.C., and Yanagimachi, R. (1999). Bypassing spermiogenesis for several generations does not have detrimental consequences on the fertility and neurobehavior of offspring: a study using the mouse. *J Assist Reprod Genet* 16, 315-324.
- Tesarik, J., Mendoza, C., and Testart, J. (1995). Viable embryos from injection of round spermatids into oocytes. *N Engl J Med* 333, 525.
- Urman, B., Alatas, C., Aksoy, S., Mercan, R., Nuhoglu, A., Mumcu, A., Isiklar, A., and Balaban, B. (2002). Transfer at the blastocyst stage of embryos derived from testicular round spermatid injection. *Hum Reprod* 17, 741-743.
- Vanderzwalmen, P., Lejeune, B., Nijs, M., Segal-Bertin, G., Vandamme, B., and Schoysman, R. (1995). Fertilization of an oocyte microinseminated with a spermatid in an in-vitro fertilization programme. *Human Reproduction* 10, 502-503.
- Vanderzwalmen, P., Zech, H., Birkenfeld, A., Yemini, M., Bertin, G., Lejeune, B., Nijs, M., Segal, L., Stecher, A., Vandamme, B., et al. (1997). Intracytoplasmic injection of spermatids retrieved from testicular tissue: influence of testicular pathology, type of selected spermatids and oocyte activation. *Hum Reprod* 12, 1203-1213.
- Vicdan, K., Isik, A.Z., and Delilbasi, L. (2001). Development of blastocyst-stage embryos after round spermatid injection in patients with complete spermiogenesis failure. *J Assist Reprod Genet* 18, 78-86.
- Yamagata, K., Suetsugu, R., and Wakayama, T. (2009). Assessment of chromosomal integrity using a novel live-cell imaging technique in mouse embryos produced by intracytoplasmic sperm injection. *Hum Reprod* 24, 2490-2499.
- Yamanaka, K., Sofikitis, N.V., Miyagawa, I., Yamamoto, Y., Toda, T., Antypas, S., Dimitriadis, D., Takenaka, M., Taniguchi, K., Takahashi, K., et al. (1997). Ooplasmic round spermatid nuclear injection procedures as an experimental treatment for nonobstructive azoospermia. *J Assist Reprod Genet* 14, 55-62.
- Yamazaki, T., Yamagata, K., and Baba, T. (2007). Time-lapse and retrospective analysis of DNA methylation in mouse preimplantation embryos by live cell imaging. *Dev Biol* 304, 409-419.
- Yoshida, N., and Perry, A.C. (2007). Piezo-actuated mouse intracytoplasmic sperm injection (ICSI). *Nat Protoc* 2, 296-304.
- Ziyyat, A., and Lefevre, A. (2001). Differential gene expression in pre-implantation embryos from mouse oocytes injected with round spermatids or spermatozoa. *Hum Reprod* 16, 1449-1456.



# 3

Round spermatid injection into mouse oocytes  
rescues female lethality  
of a paternally inherited *Xist* deletion

Submitted





**Round spermatid injection into mouse oocytes rescues female lethality of a paternally inherited *Xist* deletion**

Federica Federici<sup>1</sup>, Evelyne Wassenaar<sup>1</sup>, Christine van de Werken<sup>2</sup>, Esther Baart<sup>2</sup>, Joop SE Laven<sup>2</sup>, J Anton Grootegoed<sup>1</sup>, Joost Gribnau<sup>1</sup> and Willy M Baarends<sup>1\*</sup>

<sup>1</sup>Department of Reproduction and Development, Erasmus MC, University Medical Center, Rotterdam, The Netherlands

<sup>2</sup>Department of Obstetrics and Gynaecology, Erasmus MC, University Medical Center, Rotterdam, The Netherlands

\* Corresponding author





**ABSTRACT**

Imprinted X chromosome inactivation (iXCI) is essential for development of mouse female embryos. In iXCI, the paternal X (X<sub>p</sub>) chromosome is silenced through *Xist* RNA coating in cis. Paternal inheritance of an *Xist* deletion ( $\Delta Xist$ ) is embryonic lethal to female embryos, due to iXCI abolishment. Here, we show that fertilization by intracytoplasmic injection of  $\Delta Xist$  round spermatids into mature oocytes allows survival of female embryos. This is not mediated by *Xist*-independent X<sub>p</sub> silencing, but by a shift to inactivation of the maternal X (X<sub>m</sub>). Intracytoplasmic injection of  $\Delta Xist$  mature spermatozoa did not result in such an effect. We suggest that the epigenetic state and/or the transcriptional activity of the X chromosome of round spermatids exerts a profound effect on the iXCI process in pre-implantation embryos.

## INTRODUCTION

In mice, the heterologous X and Y chromosomes undergo meiotic sex chromosome inactivation (MSCI) in the male germ line (reviewed by (Turner, 2007)). After meiosis, silencing of X- and Y-linked genes is largely maintained during spermatid differentiation through post-meiotic sex chromatin repression (PSCR) (Namekawa et al., 2006). Noteworthy, a number of X- and Y-linked genes, single and multi-copy, escape PSCR and become specifically reactivated (Hendriksen et al., 1995; Mulugeta Achame et al., 2010; Namekawa et al., 2006). Subsequently, after fertilization, the X chromosome of paternal origin (Xp) will always be inactivated in female pre-implantation embryos. This event is defined as imprinted X chromosome inactivation (iXCI) and depends on expression of the *Xist* noncoding RNA (Okamoto et al., 2004). During iXCI, *Xist* RNA spreads in cis on the Xp and forms an RNA cloud coating the entire chromosome. This triggers the recruitment of chromatin-modifying protein complexes on the Xp, which in turn will establish repressive epigenetic marks on the Xp, rendering it transcriptionally inactive. At the blastocyst stage, while iXCI is stably maintained in extraembryonic tissues, the Xp becomes reactivated in the epiblast and a new round of inactivation starts without a parent-of-origin bias (random XCI) (Mak et al., 2004).

A possible link between MSCI and iXCI has been previously proposed (Huynh and Lee, 2003). This model suggests that iXCI could be a downstream consequence of MSCI and that a pre-inactivated X-chromosome would thus be inherited directly from father to daughter in mice (pre-inactivation hypothesis). However, it was later shown that paternal X-linked genes are active at the 2-cell stage and are then gradually inactivated during pre-implantation development (Deng et al., 2014; Namekawa et al., 2010; Okamoto et al., 2005; Patrat et al., 2009). Furthermore, while MSCI takes place independently from *Xist* (Turner et al., 2002), iXCI is completely abolished in the absence of a paternal *Xist* gene (Marahrens et al., 1997), indicating that de novo *Xist*-dependent silencing occurs in the pre-implantation embryo. Thus, inheritance of a paternal *Xist* deletion ( $\Delta Xist$ ) precludes iXCI of the Xp, and therefore results in poor extra-embryonic tissue development. This leads to complete reabsorption of mutant female embryos by E12.5 (Mugford et al., 2012). In contrast, female embryos inheriting the mutated allele through the mother develop normally (Marahrens et al., 1997).

To explain the parental bias towards Xp inactivation, it can be proposed that either the maternal X chromosome (Xm) carries an imprinting mark that prevents it from expressing *Xist*, or that the Xp is imprinted to be preferentially inactivated. Alternatively, both the maternal and the paternal *Xist* alleles can carry an imprinting mark. While the presence of an imprinting mark on the Xm has already been demonstrated (Fukuda et al., 2014; Tada et al., 2000), the existence and possible nature of an imprint leading to exclusive paternal *Xist* ex-

pression remain elusive. Recently, it has been proposed that iXCI occurs as a two-step process (Namekawa et al., 2010). First, pre-inactivated intergenic repeat regions on the Xp may carry transgenerational epigenetic information from the paternal germline to the zygote, predisposing the Xp for iXCI independently of *Xist* (Namekawa et al., 2010). This might rely on the inheritance of sperm-derived nucleosomes and their associated modifications. Second, subsequent establishment of genic silencing strictly depends on *Xist* expression from the paternal allele (Namekawa et al., 2010). Alternatively, it has been suggested that the preferential inactivation of the paternal X chromosome may simply rely on early and robust activation of the paternal *Xist* gene (Heard et al., 2004). This may be facilitated, upon fertilization, by the protamine-to-histone transition, during which the highly condensed sperm DNA acquires newly deposited histones lacking most heterochromatic marks. The transcriptionally permissive chromatin signature deposited on the paternal pronucleus would then allow higher gene expression of paternal compared to the maternal genes, possibly including the *Xist* gene. Conclusive evidence for the contribution of either the repeat-based silencing established during spermatogenesis or the protamine-to-histone transition, in the control of iXCI of Xp, is lacking.

To test if the chromatin rearrangement in spermatids impacts on iXCI, we made use of mouse round spermatids to fertilize oocytes. Contrary to the protamine-based chromatin structure of spermatozoa, round spermatids have an histone-packaged genome. Thus, when round spermatid are injected into a mouse oocyte (ROSI), the paternal genome already has a histone-based chromatin constitution, contrary to the protamine-packaged chromatin of spermatozoa. Hence, ROSI evades the protamine-to-histone replacement in the male pronucleus, which in normal fertilization leads to global de novo histone coverage of the paternal genome (Kishigami et al., 2006), although this aspect remains to be specifically assessed at the single chromosome level. Here, by using ROSI as an experimental tool, we have first established if the chromatin constitution of round spermatids is maintained at the single chromosome level in ROSI-derived zygotes. Next, we observed whether such an absence of genome wide paternal chromatin remodelling affected the timing of paternal *Xist* expression in ROSI-derived female zygotes, on a wild type background.

In addition, we determined if the transcriptionally repressed state and the heterochromatic marks already present on the X chromosome of round spermatids because of PSCR, might be sufficient to establish iXCI independently of *Xist*-mediated silencing. Using round spermatids from male mice lacking a functional *Xist* gene ( $Xp\Delta Xist$ ) for ROSI, we would expect to rescue the early embryonic lethality of  $Xp\Delta Xist$  female embryos through *Xist*-independent Xp inactivation.



Our results show that paternal histones and their associated histone modification persist in ROSI-derived early pre-implantation embryos, as previously demonstrated (Kishigami et al., 2006). However, the lack of maternal histone incorporation into the round spermatid-derived chromatin of the Xp does not misregulate the normal timing of paternal *Xist* expression on a wild type background.

Using Xp $\Delta$ *Xist* male mice as round spermatids donors for ROSI, we prevented the female lethality that is observed upon fertilization with mature Xp $\Delta$ *Xist* spermatozoa. Surprisingly, this was not mediated by *Xist*-independent Xp silencing, but by a shift to inactivation of the Xm. We speculate that the round spermatid-derived Xp expresses XCI trans activator(s) at higher levels compared to the spermatozoa-derived Xp, thus overcoming the refractory epigenetic signature that is associated with the maternal *Xist* gene. This allows proper dosage compensation of X-linked genes through inactivation of the Xm instead of the Xp in extraembryonic cells of Xp $\Delta$ *Xist* female ROSI-derived embryos.

## RESULTS AND DISCUSSION

### Histones and associated epigenetic modifications are transmitted from round spermatids to ROSI-derived zygotes

To analyze the histone modification patterns of round spermatid-derived paternal chromatin in early embryos, and in particular the epigenetic profile of the Xp, we arrested ROSI-derived mouse embryos at the pro-metaphase stage of the first and second cleavage divisions (Avo Santos et al., 2011). This allows the visualization of epigenetic marks on individual chromosomes. As a control for staining specificity, zygotes obtained by intracytoplasmic sperm injection (ICSI), using epididymal spermatozoa, were subjected to the same experimental procedure.

Resulting from the histone-to-protamine transition in spermatids, mouse epididymal spermatozoa contain approximately only 1% of residual histones (Balhorn et al., 1977; van der Heijden et al., 2006). After sperm decondensation by heparin treatment and immunostaining for histone H3.1/2 and centromeres (with anti-centromere antibody, ACA), limited histone retention associated with pericentromeric regions was visible (Figure 1 A, left panel), as previously shown (van der Heijden et al., 2006). After fertilization, when the protamine-to-histone transition has taken place, we did not detect any H3K9me3 at paternal prometaphase chromosomes of ICSI-derived zygotes (Figure 1A), while prometaphase chromosomes of maternal origin were strongly enriched for H3K9me3 at pericentromeric regions and displayed moderate H3K9me3 levels along the chromosome arms. These results are in accordance with results from previous studies on *in vivo* fertilized embryos, that showed epigenetic asymmetry between maternally and paternally inherited chromatin up to the third cleavage division (Arney et al., 2002; Puschendorf et al., 2008; Santos et al., 2005; van der Heijden et al., 2005).

In round spermatids, the X and Y chromosomes, as well as the constitutive pericentric heterochromatin clustered in the chromocenter, are enriched for H3K9me3 (Figure 1B, left panel), in accordance with previously published data (van der Heijden et al., 2007). In ROSI-derived zygotes at the first cleavage division, we detected persistence of H3K9me3 at the DAPI-dense heterochromatic chromosome ends of paternal origin and on the entire Xp (Figure 1B). This epigenetic profile mirrors exactly the H3K9me3 pattern observed in round spermatids. ROSI-derived 2-cell stage female embryos that were arrested at the pro-metaphase of the second cleavage division displayed maintenance of a high enrichment for H3K9me3 in particular on one of the two X chromosomes (Figure 1C). We verified by *Xist* DNA FISH that the highly H3K9me3 enriched chromosomes in both blastomeres from one 2-cell stage embryo were indeed X chromosomes as expected (Figure 1C, right panel and enlargements). One blastomere (the lower one, in Figure 1C) showed DNA FISH staining also on the Xm, confirming that the embryo was indeed female. Some leakage of H3K9me3 staining remained

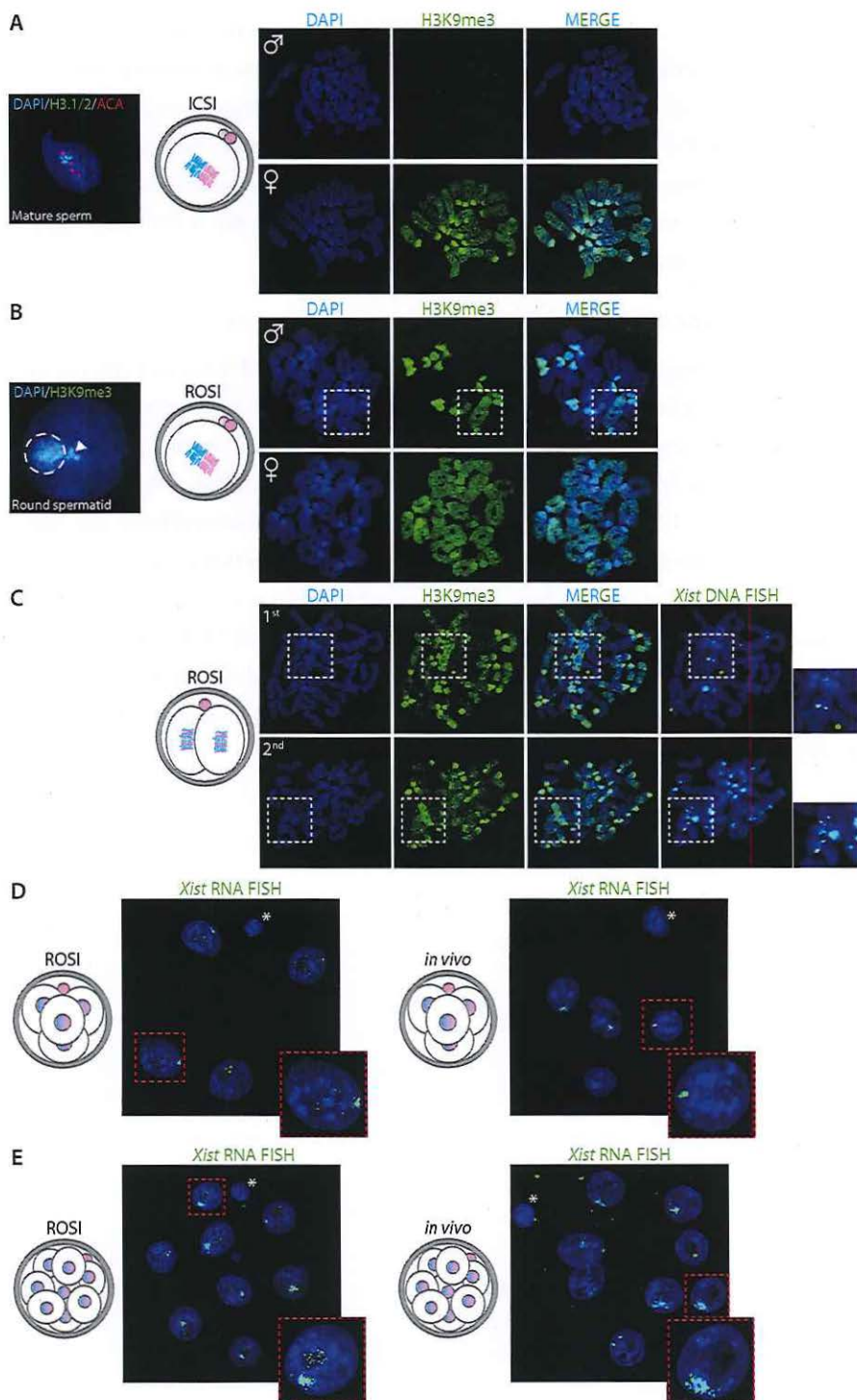
visible as background fluorescence, even after DNA FISH has been performed.

These data confirm previous observations that a substantial fraction of modified histones which are present on round spermatid chromatin are maintained in the early pre-implantation embryo generated by ROSI (Kishigami et al., 2006). Here we have observed that this concerns in particular the X chromosome, where the H3K9me3 chromatin signature covers the entire chromosome, in contrast to the histones that are incorporated along the X chromatin upon normal fertilization, that are devoid of H3K9me3.

### **Normal establishment of iXCI in ROSI-derived female zygotes**

We then aimed to investigate if absent or limited remodeling of round spermatid-derived paternal chromatin, and the heterochromatic epigenetic signature of the X chromosome specifically, might affect the timing of *Xist* expression in ROSI-derived female zygotes, and interfere with iXCI establishment. In ROSI-derived female embryos, *Xist* expression started normally at the 4-cell stage (Figure 1D), followed by *Xist* spreading at the 8-cell stage (Figure 1E), similarly to what has been described for in vivo fertilized control embryos (Okamoto and Heard, 2006). This suggests that the protamine-to-histone transition does not play a major role in the activation of the paternal *Xist* gene. In addition, the enrichment of H3K9me3 along the X chromosome does not appear to interfere with *Xist* transcription. It therefore seems more likely that another type of imprint, or a different mechanism, controls preferential *Xist* expression from Xp.





◀ **Figure 1. Chromatin remodeling and *Xist* expression in ROSI-derived embryos**

**A)** Left panel: Representative image of a decondensed nucleus of a mature mouse spermatozoon stained with H3.1/2 (in green) and anti-centromere antibody (ACA) (in red), to illustrate the limited presence of histones in association with pericentromeric chromatin in mature mouse sperm, as shown previously by others (van der Heijden et al., 2006).

Right panels: immunolocalization of H3K9me3 (green) in chromosome spreads of prometaphase-arrested zygotes obtained by ICSI (as represented in the drawing). The condensed chromosomes of paternal and maternal origin are cutouts from the whole zygote images (paternal chromosome set on top; maternal below). DNA is counterstained with DAPI (blue).

**B)** Left panel: representative nucleus of a round spermatid immunostained for H3K9me3 (green) to illustrate the enrichment of H3K9me3 on the chomocenter (encircled) and adjacent sex chromosome (arrowhead) as described previously (van der Heijden et al., 2007).

Right panels: immunolocalization of H3K9me3 (green) in chromosome spreads of prometaphase-arrested zygotes obtained by ROSI (as represented in the drawing, n=20 zygotes). The condensed chromosomes of paternal and maternal origin are cutouts from the whole zygote images (paternal chromosome set on top; maternal below). The X chromosome is indicated by a white dashed square box.

**C)** Immunofluorescence analysis for H3K9me3 (green) on chromosome spreads of a representative prometaphase-arrested 2-cell stage embryo obtained by ROSI (as indicated by the drawing on the left, n=2). Each blastomere from the same embryo is cutout into separate images (1st blastomere on top; 2nd blastomere below). The X chromosome is indicated by a white dashed square box. *Xist* DNA FISH (right panel) was performed on the same chromosome spreads represented on the left. Square boxes on the right are blowups of each corresponding boxed area containing one X chromosome (1st blastomere) or two X chromosomes (2nd blastomere).

**D)** Representative *Xist* RNA FISH on a ROSI-derived 4-cell stage embryo on the left (n=5), and a 4-cell stage embryo derived by *in vivo* fertilization (n=4). Dashed red square boxes are blowups of each corresponding boxed area.

**E)** Representative *Xist* RNA FISH on a ROSI-derived 8-cell stage embryo on the left (n= 5), and an 8-cell stage embryo derived by *in vivo* fertilization. Dashed red square boxes are blowups of each corresponding boxed area.

### Transmission of Xp $\Delta$ *Xist* through round spermatids rescues female embryonic lethality

Female embryos inheriting an *Xist* deletion on the paternal X chromosome can no longer be recovered by E12, because lack of iXCI of Xp leads to embryonic lethality (Marahrens et al., 1997). We tested if transmission of an Xp carrying the *Xist* deletion through ROSI instead of fertilization with mature sperm, might rescue the embryonic lethal phenotype. This experiment was based on the hypothesis that inheritance of a Xp that had already been transcriptionally inactivated during meiosis, and carries a pre-established heterochromatic signature, might provide sufficient dosage compensation in extraembryonic tissues in the absence of *Xist*, and thereby would allow female embryo survival. We performed ROSI with Xp $\Delta$ *Xist* spermatids obtained from a c57bl6  $\Delta$ *Xist* mouse line, generated by Csankovszki (Csankovszki et al., 1999). In control experiments, we performed ICSI with Xp $\Delta$ *Xist* mature sperm from the same mouse line. At E15, we obtained 17 pups after ROSI and 11 after ICSI (Table 1 and Supplemental Table 1). This was approximately 10% of the number of 2-cell stage embryos that were transferred to pseudopregnant females, for both techniques. The sex of the embryos was determined by visual inspection of the isolated gonads and confirmed by PCR for *UbeX* and *UbeY* (data not shown). The ICSI experiments yielded only males, as expected. In contrast, 5 out of the 17 E15 embryos generated by ROSI were female ( $p < 0.05$ , chi square test).

**Table 1: Experimental outcomes**

	ICSI (E15)	ROSI (E15)	ROSI (P0)
N of independent experiments	4	4	2
N of 2-cell embryos transferred	104	163	64
N of pups	11	17	7
Males	11	12	5
Females	0	4	2
XO females	0	1	0

We genotyped all ROSI-derived female embryos, and found both a wt and deleted *Xist* allele in embryonic and extraembryonic tissues of 4 of the female embryos, while one embryo was an XO female which had lost the mutated paternal X chromosome (Figure 2A). Next, we analysed the X chromosome to autosome (X:A) ratio for all embryos using quantitative PCR on genomic DNA, and observed the expected 1:1 ratio for the four XX embryos, placentas and isolated gonads (Figure 2B).

We then verified if ROSI-derived Xp $\Delta$ *Xist* female embryos might develop to term. To this



end, we collected pups on the morning after birth (P0). We obtained 7 live born pups (10% survival of 2-cell embryos that were transferred), of which 5 were males and 2 were females, as shown in Table 1. Sex was confirmed by PCR for *UbeX* and *UbeY* (data not shown). The two *XpΔXist* females were comparable in size and body weight to the male siblings (Figure 2C). Genotyping for the mutated and wild type *Xist* allele confirmed heterozygosity of the females (Figure 2C).

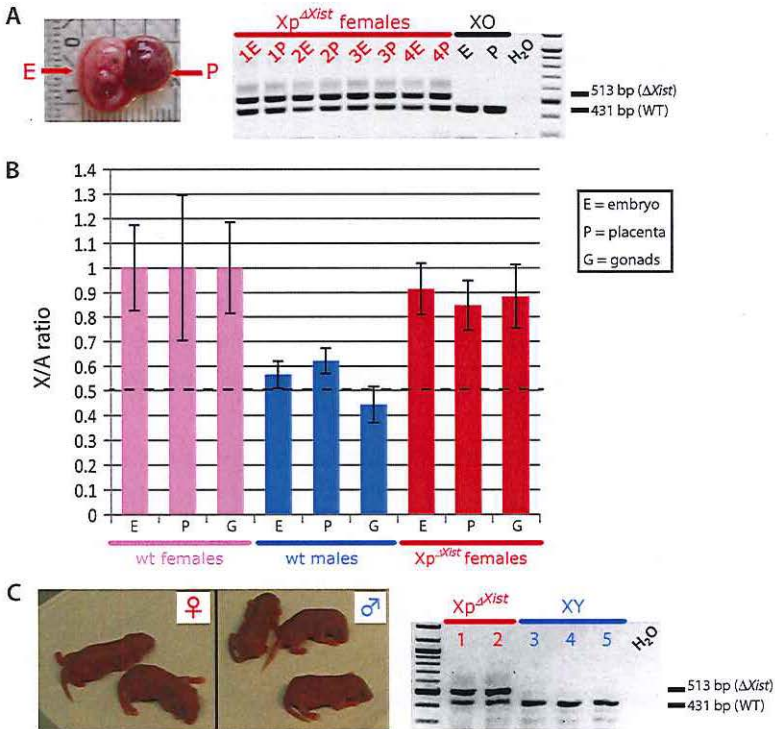


**Figure 2. ROSI rescues female-specific lethality of a paternally inherited *Xist* deletion (*XpΔXist*)**

**A**) Representative E15 *XpΔXist* ROSI-derived female embryo (E) and attached placenta (P). Genotypes on DNA isolated from embryo and placenta of 4 ROSI-derived *XpΔXist* E15 female embryos and one ROSI-derived XO embryo are shown on the right. Genotype was determined by the presence of a PCR product for the wt *Xist* allele (431bp band) and deleted allele (513 bp band). Water negative control and 100 bp marker were also loaded. **B**) qPCR on genomic DNA isolated from E15 embryos, placentas and gonads for *Xist* (chromosome X) and *Rex1* (chromosome 8). X chromosome to autosome (X/A) ratio was determined for each individual tissue in 4 control females. Results were averaged and the ratio was arbitrarily set to 1. The X/A ratio was determined for each individual tissue in 4 control males in 4 *XpΔXist* ROSI-derived female embryos, and ratios for each tissue were averaged and normalized to 1. Results for each individual tissue are shown as dots. **C**) Image of 5 newborn pups with normal appearance derived with ROSI using *XpΔXist* round spermatids (2 females on the left and 3 males on the right). Genotypes for the wt and deleted *Xist* alleles are shown to the right. As expected, both females were heterozygotes, while the males only had the wt *Xist* allele inherited from the mother.

### ROSI with Xp $\Delta$ *Xist* allows initiation of XCI on the maternal X chromosome

The exceptional survival of Xp $\Delta$ *Xist* female embryos might be explained by maintenance of the meiotically pre-inactivated state of the round spermatid-derived Xp, as we initially hypothesized. However, it cannot be excluded that survival of the embryos might be explained by XCI of the (wild type) X chromosome of maternal origin, replacing iXCI of Xp. In order to distinguish between these different possibilities, we analyzed *Xist* expression levels by qPCR in E15 control male and female placentas and in the three ROSI-derived Xp $\Delta$ *Xist* female placentas for which RNA samples were available. As expected, male placentas showed very low *Xist* expression, which most probably reflects expression from a very small amount of maternal decidua contamination (Figure 3A). Conversely, *Xist* expression was very high in wild type female placentas, in accordance with maintenance of stable iXCI of Xp in this tissue, required for proper extraembryonic tissue development. Surprisingly, *Xist* RNA levels of ROSI-derived Xp $\Delta$ *Xist* female placentas were comparable to those of wild type female placentas. Since the *Xist* gene has been deleted from the paternal allele, this expression can only be explained by robust transcription occurring from the wild type maternal X chromosome. This indicates that a switch from Xp inactivation to Xm inactivation has occurred in the Xp $\Delta$ *Xist* female embryos that were obtained by ROSI.

To assess if *Xist* transcription from Xm was occurring homogeneously throughout the extraembryonic tissues, we then checked *Xist* expression by RNA FISH on E15 placenta sections obtained from one ROSI-derived Xp $\Delta$ *Xist* female (Figure 3B). By using the Reichert's membrane as reference for the embryonic side of the placenta, we verified that *Xist* clouds formed on the whole population of labyrinth cells of embryonic origin.

The onset of Xm inactivation in the Xp $\Delta$ *Xist* female embryos was analysed through qRT-PCR analysis of *Xist* expression on RNA isolated from morulas obtained from pluggings with wild type and Xp $\Delta$ *Xist* males, and from morulas generated by ROSI with Xp $\Delta$ *Xist* round spermatids. We determined the sex of the embryos by presence or absence of the Y-specific transcript, *Eif2s3y*. As expected, *Xist* was expressed at very high levels in wild type female morulas, but absent from males. In contrast, none of the in vivo fertilized Xp $\Delta$ *Xist* male and female morulas showed any *Xist* expression above background (n=11 females, from two independent experiments, 5 are shown in Figure 3C). Interestingly, *Xist* levels were variable in ROSI-derived Xp $\Delta$ *Xist* female morulas, and only one out of 11 analysed female embryos did not display any *Xist* expression (Figure 3C). This variability is consistent with the fact that we did not rescue all Xp $\Delta$ *Xist* females by performing ROSI, but only approximately half of them. This estimation is based on an expected equal chance to obtain either a male or female embryo, where in our ROSI experiments with Xp $\Delta$ *Xist* spermatids 4 out of 17 total E15 pups,

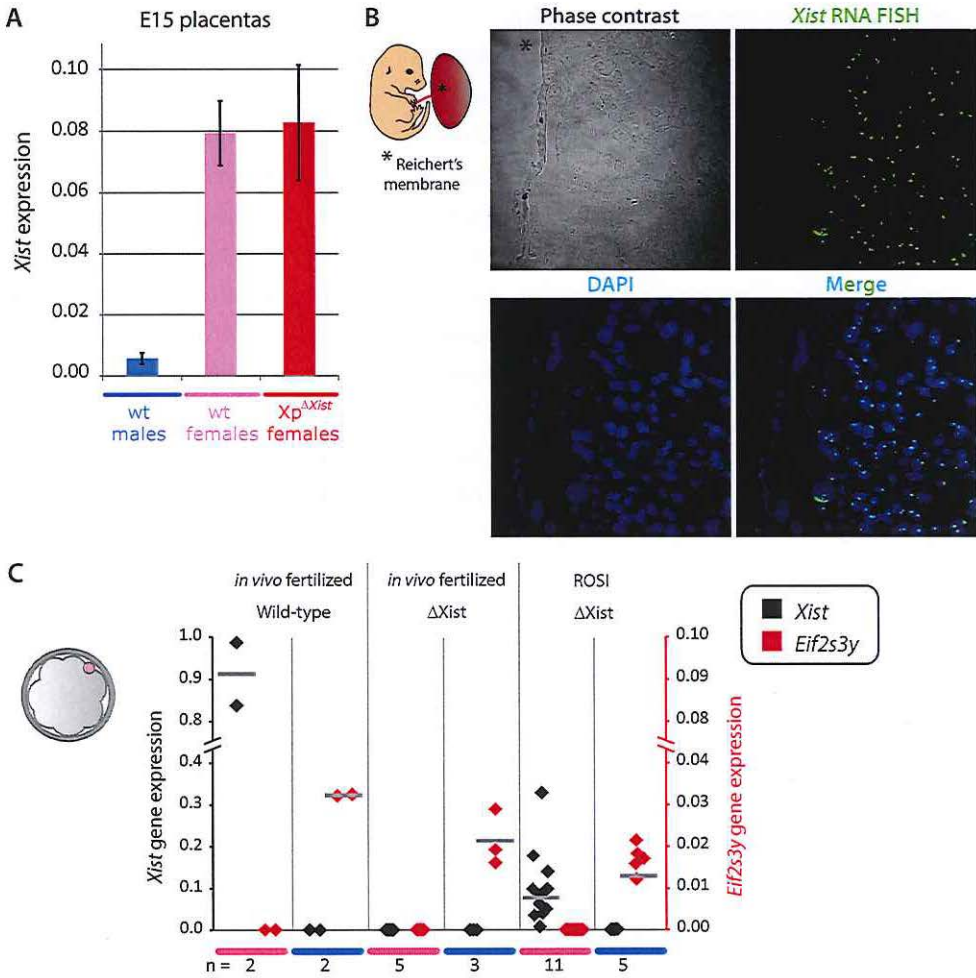


**Figure 3.  $XmXp^{\Delta Xist}$  female survival is mediated by a shift to inactivation of the maternal X ( $Xm$ )**

**A**) Average *Xist* gene expression levels  $\pm$  s.d. on RNA isolated from E15 placentas of 3 control males (light blue bars), 3 control females (pink bars) and 3 ROSI-derived Xp $\Delta Xist$  females (red bars). The data were normalized to *Actin*.

**B**) Representative image of the *Xist* RNA FISH (in green) on cryosections from a E15 ROSI-derived Xp $\Delta Xist$  female placenta (n=2). From the phase contrast image on top (right), the Reichert's membrane on the embryonic side of the placenta can be visualized (marked by asterisk). DNA is counterstained with DAPI.

**C**) Dot plot showing *Xist* (black) and *Eif2s3y* (red) mRNA expression levels for RNA isolated from individual in vivo fertilized wt and Xp $\Delta Xist$  male (blue) and female (pink) mouse morulas, and from ROSI-derived Xp $\Delta Xist$  male and female morulas. Expression levels were normalized to *Actin*. Grey lines indicate the average values, n values are indicated below the graph.



and 2 out of 7 total live born pups were female.

Previous reports have shown that also in diploid parthenogenetic embryos the Xm starts to express *Xist* around the morula stage (Kay et al., 1994; Nesterova et al., 2001). It was then suggested that this could occur simply because the repressive imprint on the Xm *Xist* allele, preventing its expression, was not retained throughout pre-implantation development. The present experiments indicate that the situation is more complicated. If removal of the repressive imprint on the *Xist* promoter of the Xm, would play per se a prominent role in allowing Xm inactivation, *Xist* expression from Xm should occur in the in vivo fertilized Xp $\Delta$ *Xist* female embryos with similar dynamics as observed for parthenogenetic embryos. However, this is not what happens, since *Xist* expression was not observed in any of the Xp $\Delta$ *Xist* female morulas obtained by natural mating (Figure 3C).

In the model in Figure 4, we propose that when iXCI is initiated in embryos carrying an Xp and an Xm, the Xp is more responsive to XCI trans activator(s) than the Xm. This differential response is most likely related to an imprint of the *Xist* promoter on the Xm, which prevents *Xist* expression, and which is absent from the promoter on Xp (Fukuda et al., 2014). In other words, the threshold for activation of *Xist* expression by XCI trans activator(s) is intrinsically higher for Xm than for Xp. In a wild type embryo, transcription of the XCI activator(s) would reach the threshold for *Xist* expression from the Xp in all blastomeres by the 4-cell stage, but virtually never reach the threshold for activation of *Xist* expression from Xm. To explain *Xist* expression from the Xm in ROSI-derived Xp $\Delta$ *Xist* female morulas, we propose that the XCI activator(s) are expressed at higher levels from the Xp derived from a round spermatid compared to the Xp delivered by mature spermatozoa. Therefore there would be a higher chance that a threshold for activation of *Xist* expression from Xm, by X-linked XCI trans activators, will be reached, compared to the normal situation, when a sperm-derived Xp chromosome is present (Figure 4). While transcriptional suppression is maintained for most Xp genes during PSCR, some X-linked genes are known to escape and become specifically reactivated. One of these reactivated genes is RNF12, which is a known XCI trans activator (Jonkers et al., 2009). Hence, the X-linked *Rnf12* gene represents a good candidate to be expressed at higher levels from the Xp derived from a round spermatid, and to act as XCI trans activator on the Xm. However, we do not exclude that other and multiple X-linked factors are involved. In addition, changes in autosomal gene expression in ROSI-derived embryos compared to normally fertilized or ICSI-derived embryos also may contribute to inactivation of the Xm. However, such a contribution of autosomal genes is expected to play a minor role, because we did not observe *Xist* expression from the Xm in wild type ROSI-derived male embryos (n=5).

Taken together, the present experiments have demonstrated that injection of round spermatids into oocytes allows activation of *Xist* transcription from the Xm in preimplantation mouse embryos in the absence of a paternal *Xist* gene. Our data point to critical differences in epigenetic aspects of control of X-linked gene expression in round spermatids versus mature spermatozoa.

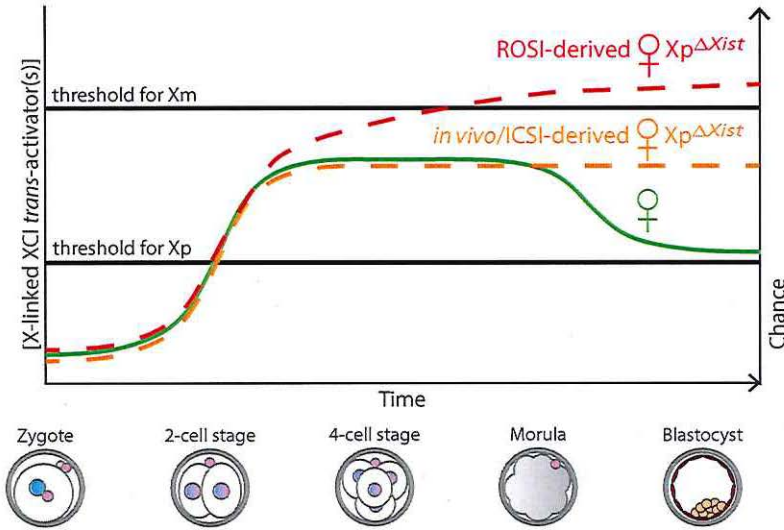


**Figure 4. Model of XCI initiation in pre-implantation embryos**

Depicted are the different thresholds for *Xist* expression from Xm and for Xp (black horizontal lines). Combined expression of gene(s) encoding X-linked XCI trans activator(s) from both Xp and Xm in female pre-implantation embryos throughout their development is represented as green line (for wt), yellow dashed line (for ICSI-derived or in vivo fertilized  $Xp\Delta Xist$ ) and red dashed line (for ROSI-derived  $Xp\Delta Xist$ ).

3

## MATERIALS AND METHODS

### Animals

B6D2F1 mice (C57BL/6 × DBA/2) were used as oocyte donors. We used B10CBA females that were mated with vasectomized males as pseudopregnant surrogates for transfer of ICSI- and ROSI-derived two-cell stage embryos. C57Bl6 mice carrying an *Xist* deletion ( $\Delta Xist$ ) were those originally generated by Csankovszki and colleagues (Csankovszki et al., 1999). Control wild type C56Bl6 males were also used as spermatid and spermatozoa donors. All animal experiments were approved by the local animal experiments committee DEC Consult and animals were maintained under the supervision of the Animal Welfare Officer. To obtain embryos from in vivo fertilized oocytes, superovulated B6D2F1 females were mated with wild type or  $\Delta Xist$  males and zygotes were retrieved from the oviduct and cultured for different applications.

### Oocyte collection

Mature oocytes were collected from the oviducts of 6- to 16-wk-old B6D2F1 female mice (Harlan) that had been induced to superovulate with 5 IU pregnant mare's serum gonadotropin (PMSG; Intervet), followed by 5 IU human chorionic gonadotropin (hCG; Intervet) 48 h later. Oocytes were collected from oviducts approximately 16 h after hCG injection and treated with 80 IU ml<sup>-1</sup> hyaluronidase (Sigma) until the cumulus cells dispersed. The oocytes were then placed in G1 medium (Vitrolife), covered with mineral oil, and stored at 37°C (5% CO<sub>2</sub>:95% air). Before injection, oocytes were placed into Ca<sup>2+</sup>-free M16 containing 10 mM SrCl<sub>2</sub> for 60 min.

### Round spermatid preparation

To collect round spermatids, seminiferous tubules of the testes from male mice were gently minced using two blunt ended curved forceps, and single cells were suspended in G-MOPS PLUS medium (Vitrolife).

### Microinsemination with round spermatids

ROSI was carried out as described in the Addendum to Chapter 2.

### Microinsemination with mature spermatozoa (ICSI)

ICSI was carried out as described previously (Yoshida and Perry, 2007).

### Embryo culture and transfer

Injected oocytes were cultured for 24–30 h in G-1 PLUS medium until the two-cell stage. Thereafter, 10–15 two-cell embryos were transferred to each oviduct of surrogate females on day 1 of pseudopregnancy. Alternatively, embryos were cultured up to the 4-cell, 8-cell, or



morula stage in G-1 PLUS medium and further processed for different applications as described below.

### Chromosome spread preparations

Zygotes or two-cell embryos were incubated with colcemid (1.5 µg/ml) to arrest cells at prometaphase until pronuclei had disappeared. To obtain chromosome spreads, after zona pellucida removal with Acidic Tyrode's Solution (Sigma), arrested zygotes were incubated in hyposolution (25 % v/v FCS, 0.5 % w/v sodium citrate) for 5 min and subsequently transferred to a drop of fixative (1 % v/v paraformaldehyde, 0.2 % v/v Triton X-100, 0.1 mM dithiothreitol, pH 9.2) on a glass slide. After horizontal drying for 1 h, the slides were washed with 0.08 % Photo-Flo (Kodak) and air dried. All slides were stored at -20 °C until further use.

### Decondensation of mouse caput sperm

Decondensation of mouse caput sperm was performed as described previously (van der Heijden et al., 2006).

### Preparation of spread spermatid nuclei

Nuclei of wild type mouse spermatogenic cells were spread as previously described (Peters et al., 1997).

### Immunofluorescence

For immunofluorescence stainings, slides containing zygote or embryos chromosome spreads, decondensed sperm, or spread spermatid nuclei, were rinsed in phosphate-buffered saline PBS-T (PBS, 0.01% v/v Tween-20) and locked with blocking solution (PBS-T, 2% w/v bovine serum albumin (BSA fraction V), 5% v/v normal goat serum) for 30 minutes and incubated with primary antibodies at 4°C overnight. The following antibodies were used in this study: rabbit polyclonal against H3K9me3 (1:200, Abcam), mouse monoclonal anti H3.1/2 (1:1000, gift from dr. P. de Boer, for validation see (van der Heijden et al., 2007)) and human centromere autoantigen (ACA, 1:1000, Fitzgerald Industries, 90C-CS1058). After washing with PBS-T, chromosome spreads were incubated with the appropriate secondary antibodies for 1 hour, washed with PBS-T and mounted with ProLon Gold mounting solution for DNA counterstaining. Images were obtained using a LSM700 confocal laser scanning microscope (Zeiss) and processed with Fiji and Adobe Photoshop CS3 software.

### RNA/DNA FISH

Pre-implantation embryos were treated with acid Tyrode's solution (Sigma) to remove the zona pellucida. Method and probe for *Xist* RNA-FISH have been described (Barakat and Gribnau, 2014; Jonkers et al., 2008). For DNA FISH, chromosome spreads of prometaphase arrested embryos were denatured in 80% v/v formamide for 1 minute before the same *Xist*

probe used for RNA FISH was applied on the slide. Detection was performed as for RNA FISH.

### Placenta cryosections

Placentas were removed at E15. The tissues were snap frozen and stored at  $-80^{\circ}\text{C}$  until use. For RNA FISH, 14  $\mu\text{m}$ -thick frozen sections were made from frozen tissues on a cryostat and mounted on glass slides. Sections were briefly air-dried, extracted with 0.5% Triton X-100 in phosphate-buffered saline (PBS) on ice, fixed in 4% formaldehyde, 5% acetic acid for 18 min at room temperature, washed 3 times in PBS for 5 min each, dehydrated in 70-100% ethanol series and air-dried.

### Genotyping PCR for Xist deletion

The primer pairs used to assess the genotype of the mice for the presence or absence of the Xist deletion have been previously described (Gribnau et al., 2005).

### qRT-PCR analysis

For quantitative RT-PCR (RT-qPCR) of single embryos, the Taqman<sup>®</sup> Cells-to-Ct Kit (Applied Biosystems) was used according to the manufacturer's protocol. All samples were analyzed in triplicate in a 10  $\mu\text{l}$  final reaction volume using the BioRad CFX 384 Real-time System. The reaction mixture contained SYBR Green PCR Master Mix (Applied Biosystems), primers (either *Actin*, *Xist*, or *Eif2s3y*) and 2.5  $\mu\text{l}$  of cDNA. The following primers were used: *Xist* for GGATCCTGCTTGAAGTACTGC and rev CAGGCAATCCTTCTTCTTGAG (Chureau et al., 2011), *Actin* for AACCCCTAAGGCCAACCGTGAAAAG and rev CATGGCTGGG-GTGTGAAGGTCTC, *Eif2s3y* for CCAGGGACCAAAGGAACTT and rev TAGCCT-GGCTTTCTTTTACC (Vernet et al., 2014).

For copy number qPCR on genomic DNA, primers were designed for the X chromosome on the *Tsix* promoter region (for CCGAGATATCCACGCATCTT and rev AGCTGGC-TATCACGCTCTTC) and for chromosome 12 on the *Rex1* allele (for GGTGCAAGAA-GAAGCTGAGG and rev GTTTCGAGCTCTCCGTGAAG).

After an initial hold at  $94^{\circ}\text{C}$  for 2 minutes, reaction mixtures underwent 40 cycles of 30s at  $94^{\circ}\text{C}$ , 30s at  $60^{\circ}\text{C}$ , and 30s at  $72^{\circ}\text{C}$ . Results were expressed as Cycle threshold (Ct) values. Gene expression levels were normalized over Actin gene expression, according to the  $2^{-\Delta\text{CT}}$  method (Livak and Schmittgen, 2001). In order to be able to use a relative quantification approach to compare expression levels we ensured that the primer pairs have similar amplification efficiencies ( $E = 100 \pm 10\%$ ).



## REFERENCES

- Arney KL, Bao S, Bannister AJ, Kouzarides T, and Surani MA (2002). Histone methylation defines epigenetic asymmetry in the mouse zygote. *Int J Dev Biol* 46:317-320.
- Avo Santos M, van de Werken C, de Vries M, Jahr H, Vromans MJ, Laven JS, Fauser BC, Kops GJ, Lens SM, and Baart EB (2011). A role for Aurora C in the chromosomal passenger complex during human preimplantation embryo development. *Hum Reprod* 26:1868-1881.
- Balhorn R, Gledhill BL, and Wyrobek AJ (1977). Mouse sperm chromatin proteins: quantitative isolation and partial characterization. *Biochemistry* 16:4074-4080.
- Barakat TS, and Gribnau J (2014). Combined DNA-RNA fluorescent in situ hybridization (FISH) to study X chromosome inactivation in differentiated female mouse embryonic stem cells. *J Vis Exp*.
- Chureau C, Chantalat S, Romito A, Galvani A, Duret L, Avner P, and Rougeulle C (2011). *Ftx* is a non-coding RNA which affects *Xist* expression and chromatin structure within the X-inactivation center region. *Hum Mol Genet* 20:705-718.
- Csankovszki G, Panning B, Bates B, Pehrson JR, and Jaenisch R (1999). Conditional deletion of *Xist* disrupts histone macroH2A localization but not maintenance of X inactivation. *Nat Genet* 22:323-324.
- Deng Q, Ramskold D, Reinius B, and Sandberg R (2014). Single-cell RNA-seq reveals dynamic, random monoallelic gene expression in mammalian cells. *Science* 343:193-196.
- Fukuda A, Tomikawa J, Miura T, Hata K, Nakabayashi K, Eggan K, Akutsu H, and Umezawa A (2014). The role of maternal-specific H3K9me3 modification in establishing imprinted X-chromosome inactivation and embryogenesis in mice. *Nat Commun* 5:5464.
- Gribnau J, Luikenhuis S, Hochedlinger K, Monkhorst K, and Jaenisch R (2005). X chromosome choice occurs independently of asynchronous replication timing. *J Cell Biol* 168:365-373.
- Heard E, Chaumeil J, Masui O, and Okamoto I (2004). Mammalian X-chromosome inactivation: an epigenetics paradigm. *Cold Spring Harb Symp Quant Biol* 69:89-102.
- Hendriksen PJM, Hoogerbrugge JW, Themmen APN, Koken MHM, Hoesjmakers JHJ, Oostra BA, Van der Lende T, and Grootegoed JA (1995). Postmeiotic transcription of X and Y chromosomal genes during spermatogenesis in the mouse. *Dev Biol* 170:730-733.
- Huynh KD, and Lee JT (2003). Inheritance of a pre-inactivated paternal X chromosome in early mouse embryos. *Nature* 426:857-862.
- Jonkers I, Barakat TS, Achame EM, Monkhorst K, Kenter A, Rentmeester E, Grosveld F, Grootegoed JA, and Gribnau J (2009). RNF12 is an X-Encoded dose-dependent activator of X chromosome inactivation. *Cell* 139:999-1011.
- Jonkers I, Monkhorst K, Rentmeester E, Grootegoed JA, Grosveld F, and Gribnau J (2008). *Xist* RNA is confined to the nuclear territory of the silenced X chromosome throughout the cell cycle. *Mol Cell Biol* 28:5583-5594.
- Kay GF, Barton SC, Surani MA, and Rastan S (1994). Imprinting and X chromosome counting mechanisms determine *Xist* expression in early mouse development. *Cell* 77:639-650.
- Kishigami S, Van Thuan N, Hikichi T, Ohta H, Wakayama S, Mizutani E, and Wakayama T (2006). Epigenetic abnormalities of the mouse paternal zygotic genome associated with microinsemination of round spermatids. *Dev Biol* 289:195-205.
- Livak KJ, and Schmittgen TD (2001). Analysis of relative gene expression data using real-time quantitative PCR and the 2<sup>-Delta Delta C(T)</sup> Method. *Methods* 25:402-408.
- Mak W, Nesterova TB, de Napoles M, Appanah R, Yamanaka S, Otte AP, and Brockdorff N (2004). Reactivation of the paternal X chromosome in early mouse embryos. *Science* 303:666-669.
- Marahrens Y, Panning B, Dausman J, Strauss W, and Jaenisch R (1997). *Xist*-deficient mice are defective in dosage compensation but not spermatogenesis. *Gen Dev* 11:156-166.
- Mugford JW, Yee D, and Magnuson T (2012). Failure of extra-embryonic progenitor maintenance in the absence of dosage compensation. *Development* 139:2130-2138.
- Mulugeta Achame E, Wassenaar E, Hoogerbrugge



- ge JW, Sleddens-Linkels E, Ooms M, Sun ZW, van IWF, Grootegoed JA, and Baarends WM (2010). The ubiquitin-conjugating enzyme HR6B is required for maintenance of X chromosome silencing in mouse spermatocytes and spermatids. *BMC Genomics* 11:367.
- Namekawa SH, Park PJ, Zhang LF, Shima JE, McCarrey JR, Griswold MD, and Lee JT (2006). Postmeiotic sex chromatin in the male germline of mice. *Curr Biol* 16:660-667.
- Namekawa SH, Payer B, Huynh KD, Jaenisch R, and Lee JT (2010). Two-step imprinted X-inactivation: Repeat vs genic silencing in the mouse. *Mol Cell Biol*.
- Nesterova TB, Barton SC, Surani MA, and Brockdorff N (2001). Loss of Xist imprinting in diploid parthenogenetic preimplantation embryos. *Dev Biol* 235:343-350.
- Okamoto I, Arnaud D, Le Baccon P, Otte AP, Disteche CM, Avner P, and Heard E (2005). Evidence for de novo imprinted X-chromosome inactivation independent of meiotic inactivation in mice. *Nature* 438:369-373.
- Okamoto I, and Heard E (2006). The dynamics of imprinted X inactivation during preimplantation development in mice. *Cytogenet Genome Res* 113:318-324.
- Okamoto I, Otte AP, Allis CD, Reinberg D, and Heard E (2004). Epigenetic dynamics of imprinted X inactivation during early mouse development. *Science* 303:644-649.
- Patrat C, Okamoto I, Diabanguouaya P, Vialon V, Le Baccon P, Chow J, and Heard E (2009). Dynamic changes in paternal X-chromosome activity during imprinted X-chromosome inactivation in mice. *Proc Natl Acad Sci U S A* 106:5198-5203.
- Peters AH, Plug AW, van Vugt MJ, and de Boer P (1997). A drying-down technique for the spreading of mammalian meiocytes from the male and female germline. *Chromosome Res* 5:66-68.
- Puschendorf M, Terranova R, Boutsma E, Mao X, Isono K, Brykczynska U, Kolb C, Otte AP, Kosaki H, Orkin SH, et al. (2008). PRC1 and Suv39h specify parental asymmetry at constitutive heterochromatin in early mouse embryos. *Nat Genet* 40:411-420.
- Santos F, Peters AH, Otte AP, Reik W, and Dean W (2005). Dynamic chromatin modifications characterise the first cell cycle in mouse embryos. *Dev Biol* 280:225-236.
- Tada T, Obata Y, Tada M, Goto Y, Nakatsuji N, Tan S, Kono T, and Takagi N (2000). Imprint switching for non-random X-chromosome inactivation during mouse oocyte growth. *Development* 127:3101-3105.
- Turner JM (2007). Meiotic sex chromosome inactivation. *Development* 134:1823-1831.
- Turner JM, Mahadevaiah SK, Elliott DJ, Garchon HJ, Pehrson JR, Jaenisch R, and Burgoyne PS (2002). Meiotic sex chromosome inactivation in male mice with targeted disruptions of Xist. *J Cell Sci* 115:4097-4105.
- van der Heijden GW, Derijck AA, Posfai E, Giele M, Pelczar P, Ramos L, Wansink DG, van der Vlag J, Peters AH, and de Boer P (2007). Chromosome-wide nucleosome replacement and H3.3 incorporation during mammalian meiotic sex chromosome inactivation. *Nat Genet* 39:251-258.
- van der Heijden GW, Derijck AA, Ramos L, Giele M, van der Vlag J, and de Boer P (2006). Transmission of modified nucleosomes from the mouse male germline to the zygote and subsequent remodeling of paternal chromatin. *Dev Biol* 298:458-469.
- van der Heijden GW, Dieker JW, Derijck AA, Muller S, Berden JH, Braat DD, van der Vlag J, and de Boer P (2005). Asymmetry in histone H3 variants and lysine methylation between paternal and maternal chromatin of early mouse zygotes. *Mech Dev* 122:1008.
- Vernet N, Szot M, Mahadevaiah SK, Ellis PJ, Decarpentrie F, Ojarikre OA, Rattigan A, Take-to T, and Burgoyne PS (2014). The expression of Y-linked Zfy2 in XY mouse oocytes leads to frequent meiosis 2 defects, a high incidence of subsequent early cleavage stage arrest and infertility. *Development* 141:855-866.
- Yoshida N, and Perry AC (2007). Piezo-actuated mouse intracytoplasmic sperm injection (ICSI). *Nat Protoc* 2:296-304.

**Supplemental Table 1: Individual experimental outcome**

<b>ICSI (E15)</b>	Males	Females	XO females
Outcome experiment 1	2	0	0
Outcome experiment 2	3	0	0
Outcome experiment 3	1	0	0
Outcome experiment 4	5	0	0
<b>ROSI (E15)</b>			
Outcome experiment 1	1	0	1
Outcome experiment 2	5	1	0
Outcome experiment 3	1	1	0
Outcome experiment 4	5	2	0
<b>ROSI (P0)</b>			
Outcome experiment 1	2	0	0
Outcome experiment 2	3	2	0







# 4

## Incomplete meiotic sex chromosome inactivation in the dog

Submitted





## Incomplete meiotic sex chromosome inactivation in the dog

Federica Federici\*, Eskeatnaf Mulugeta\*#, Sam Schoenmakers<sup>1</sup>, Evelyne Wassenaar, Jos W. Hoogerbrugge, Godfried W van der Heijden<sup>1</sup>, Wiggert A van Cappellen<sup>2</sup>, Johan A Slotman<sup>2</sup>, Wilfred FJ van IJcken<sup>3</sup>, Joop SE Laven<sup>1</sup>, J Anton Grootegoed, and Willy M Baarends§

Department of Reproduction and Development,

<sup>1</sup>Department of Obstetrics and Gynaecology,

<sup>2</sup>Erasmus Optical Imaging Centre, Department of Pathology,

<sup>3</sup>Erasmus Center for Biomics,

Erasmus MC, University Medical Center, 3000 CA Rotterdam, The Netherlands

#Present address: Institut Curie, Genetics and Developmental Biology Unit 11 et 13 rue Pierre et Marie Curie, 75248 Paris Cedex 05, France

\* These authors contributed equally to this manuscript

§ Corresponding author



**ABSTRACT**

In mouse male meiotic prophase, autosomes can stably associate through homologous synapsis, while the largely heterologous sex chromosomes synapse only in the short pseudoautosomal region (PAR). Homology recognition is aided by formation and repair of hundreds of programmed DNA double-strand breaks (DSBs). DSBs persist along the non-homologous arms of the sex chromosomes. Asynapsis and persistent DSBs then trigger transcriptional silencing through meiotic sex chromosome inactivation (MSCI). This inactive state is partially maintained in post-meiotic cells (postmeiotic sex chromatin repression, PSCR). For the human, establishment of MSCI and PSCR have also been reported, but X-linked gene silencing appears to be more variable compared to mouse. To gain more insight into the regulation and significance of MSCI and PSCR, we have performed a global analysis of XY pairing dynamics, DSB repair, MSCI and PSCR in the dog, for which complete high coverage genome sequencing has recently become available, allowing a thorough comparative analyses.

In addition to PAR synapsis, we observed extensive self-synapsis of the heterologous part of the dog X chromosome, and rapid loss of known markers of DSB repair and MSCI. Sequencing of RNA from purified spermatocytes and spermatids revealed establishment of MSCI, but the self-synapsing region of the X displayed higher X-linked gene expression compared to the unsynapsed area in spermatocytes, and was post-meiotically reactivated. In contrast, genes in the PAR (which are generally believed to escape MSCI) were expressed at very low levels in both spermatocytes and spermatids. Our comparative analyses was used to identify conserved X-linked genes that escape MSCI completely, or are specifically re-activated in human, mouse and dog spermatids.

Overall, our data indicate that MSCI is incomplete in the dog. This may be partially explained by transient extensive self-synapsis of the X chromosome, in association with rapid meiotic DSB repair. In addition, our comparative analysis identifies novel candidate male fertility genes.

## INTRODUCTION

In male placental mammals, the X and Y chromosomes share homology only in the pseudoautosomal regions (PAR). PAR length varies greatly among species, ranging from only 700 kb in mouse (Perry et al., 2001), to 2.7 Mb in human (Ross et al., 2005) and 6.6 Mb in dog (Li et al., 2013; Young et al., 2008). In the mouse, all chromosomes are acrocentric, and the PAR localizes at the tip of the long q-arm of the sex chromosomes. The human metacentric X and Y chromosome have two PARs, one on each end of the sex chromosomes. However, usually only PAR1, on the end of the p arm of the sex chromosomes, engages in meiotic recombination. The total length of the dog Y is only approximately 20 Mb, and the single dog PAR is located on the p arm of the sex chromosomes (Li et al., 2013). In contrast, the human and mouse Y chromosome are much longer, 60 and 95 Mb, respectively. The X chromosome is highly conserved in evolution, and measures 156, 171, and 124 Mb in human, mouse, and dog, respectively. The presence of a heterologous chromosome pair in males poses a challenge to the process of meiosis during spermatogenesis, and has specific consequences for the transcriptional activity of these chromosomes during spermatogenesis, as explained below. Here we have focused on the regulation of the sex chromosomes during male meiotic prophase in the dog, because of its long PAR, and some peculiar features of XY pairing during meiotic prophase, described in detail in this manuscript.

In the first meiotic division, homologous chromosomes need to segregate faithfully, to generate two daughter cells with a complete haploid set of chromosomes. This requires a lengthy prophase during which each chromosome pairs, and exchanges genetic information with its homologous partner. This process involves the formation of approximately 250 meiotic DNA double-strand breaks (DSBs) (Moens et al., 2002) by the transesterase SPO11 (Keeney et al., 1999; Mahadevaiah et al., 2001) at so-called hotspots (Smagulova et al., 2011) distributed throughout the genome. Subsequently, repair of these DSBs occurs via a meiosis-specific adaptation of the somatic homologous recombination (HR) repair process. HR in meiotic prophase cells is thought to prefer the use of the intact DNA from the homologous chromosome as a template for repair, whereas the sister chromatid is the favored repair template in somatic G2 cells (Schwacha and Kleckner, 1997). This preference for the homologous chromosome in meiosis is known as the interhomolog bias (Bolcun-Filas and Schimenti, 2012). Based on this bias, the meiosis-specific HR repair mechanism helps chromosome pairing and allows complete homologous synapsis through the formation of the synaptonemal complex (SC) (Yang and Wang, 2009). It also ensures formation of at least one crossover for each chromosome pair, which is required for faithful segregation of homologous chromosomes and the sex chromosomes during the first meiotic metaphase to anaphase transition. All these

events can be traced via immunocytochemical localization of key players in the HR repair process and markers of SC formation. RAD51 and DMC1 are recombinases that form foci in response to the formation of DSBs by SPO11, and each focus is thought to correspond to a DSB site (Carofiglio et al., 2013; Cole et al., 2012; Moens et al., 1997; Moens et al., 2002). SC formation reaches completion as DSB repair proceeds and the initial formation of the axial elements, that form first along each chromosomal axis, can be followed by staining for its components, such as SYCP2, SYCP3 (Lammers et al., 1994; Offenberger et al., 1998), and the HORMAD proteins (Wojtasz et al., 2009). Subsequently, formation of the central or transverse elements, that provide the “glue” between the homologous chromosomes as they synapse, can be followed by staining for components of the transverse filaments and central element such as SYCP1 (Meuwissen et al., 1992) and TEX12 (Hamer et al., 2006).

Stable XY synapsis in mouse and man is observed only for the tips of these chromosomes that contain the PAR (Solari, 1974). Detailed electron microscopic evaluation of the XY pair in mouse spermatocytes has revealed that the synapsis between X and Y is dynamic, whereby the region that displays synapsis varies between 0.2 and 3  $\mu\text{m}$ . When synapsis is maximal, approximately 90% of the *y*-chromosomal axis is synapsed (Solari, 1970; Tres, 1977). The unsynapsed configuration of the heterologous X and Y chromosomal axes is detected throughout meiotic prophase. Sex chromosomes are thus faced with a particular challenge in repairing meiotic DSBs in the non-PARs. Asynapsis and persistence of unrepaired DSBs lead to global transcriptional repression, a process called meiotic sex chromosome inactivation (MSCI) (reviewed in (Turner, 2007); (Carofiglio et al., 2013). On the other hand, PARs, where synapsis and repair can proceed normally, are generally thought to escape from MSCI (McKee and Handel, 1993), but so far this has not been analysed.

In mouse, inactive XY chromatin forms a distinct nuclear domain, the so-called XY body, which usually resides at the periphery of the nucleus and can be cytologically distinguished by its 4',6-diamidino-2-phenylindole (DAPI)-intense appearance (Monesi, 1965). XY body formation has been observed in a variety of different mammals (Ansari et al., 1993; Echeverria et al., 2003; Franco et al., 2007; Libbus, 1985; Moses, 1977; Namekawa et al., 2007; Sciarano et al., 2012; Solari and Pigozzi, 1994; Villagomez, 1993). Transcriptional suppression of X and Y has been reported to persist in post-meiotic spermatids in mouse and human, and is referred to as post-meiotic sex chromatin repression (PSCR) (Namekawa et al., 2006; Turner et al., 2006). PSCR, despite being a direct consequence of MSCI, appears to be less stringent, since a significant number of X-linked genes are post-meiotically reactivated (multi-copy genes on both sex chromosomes (Mueller et al., 2008), and ~13% to 20% of single copy genes on the X (Mulugeta Achame et al., 2010b; Namekawa et al., 2006). Transcriptomic studies of MSCI and PSCR have so far been performed only in mouse and human, using microarray analyses



of RNA purified from different germ cell types (Mulugeta Achame et al., 2010b; Namekawa et al., 2006; Sin et al., 2012), or whole testes (Mulugeta Achame et al., 2010a). More recently, also RNA sequencing approaches have been used to analyse global and sex chromosome transcriptional regulation during spermatogenesis in the mouse (Lesch et al., 2013; Soumillon et al., 2013). MSCI appears to be a specialization of a more general process, Meiotic Silencing of Unsynapsed Chromatin (MSUC), that silences chromatin that remains unsynapsed during male and female meiotic prophase in mammals (Baarends et al., 2005; Turner et al., 2005). Although MSUC shares several epigenetic characteristics with MSCI, these phenomena seem to lead to opposite end results: MSCI must successfully be installed in order for spermatocytes to progress through the meiotic prophase (Royo et al., 2010), whereas occurrence of MSUC could be detrimental to the cell (Burgoyne et al., 2009). Whether MSUC and MSCI are equally effective is not known, since no global analyses of mRNA expression from regions that are subject to MSUC are available. Based on immunocytochemical analyses, it appears that some components of the shared MSCI/MSUC machinery are limiting, and when MSUC is activated in spermatocytes, this reduces the effectiveness of MSCI (Homolka et al., 2007). Meiotic and post-meiotic X chromosome silencing was reported to be similarly effective for mouse and man (Sin et al., 2012). However, when we analyzed publicly available microarray data from human testes, the results indicated that MSCI and PSCR might be less complete in human compared to mouse (Mulugeta Achame et al., 2010a), and this notion was supported by immunocytological observations that indicated that MSCI was less stringently controlled in human compared to mouse (de Vries et al., 2012). Furthermore, the profiles of X-linked genes escaping from PSCR diverge significantly between humans and mice (Sin et al., 2012). Thus, detailed analysis of MSCI and PSCR in other mammalian species might help in understanding common and relevant features of these processes and identify new important candidate X-linked fertility genes.

Our group is interested in studying the functional links between sex chromosome pairing, DSB repair, and transcriptional silencing in several species (Mulugeta Achame et al., 2010a; Schoenmakers et al., 2009; Schoenmakers et al., 2010), including dog (*Canis familiaris*). The last common ancestor of mouse, human and the domestic dog lived around 64–65 million years ago (O’Leary et al., 2013). The diploid genome of the dog consists of 38 autosomal pairs and the sex chromosomal pair (Lindblad-Toh et al., 2005). Previously, the general pattern of meiotic recombination during dog meiotic prophase has been studied through staining for the mismatch repair protein MLH1, which also marks crossover sites in spermatocytes of mouse and man (Basheva et al., 2008).

Here, we first provide a detailed description of the assembly and disassembly of the synaptonemal complex during canine spermatogenesis. We show that the dog X chromosome

displays extensive self-synapsis during mid pachytene, contributing to a more rapid meiotic DSB repair along the self-synapsed part of the X chromosome and to early loss of MSCI marks. These observations, together with the availability of complete high coverage genome sequencing for this species, prompted us to study MSCI and PSCR more in detail by RNA sequencing. We show that X self-synapsis is associated with a partial escape from MSCI. In contrast to what has been previously suggested (McKee and Handel, 1993), the PAR, at least in dog, has very low transcriptional activity in both spermatocytes and spermatids. In addition, our comparative analysis among dog, mouse and human of post-meiotically down- and up-regulated genes, provides new potential targets in the search for candidate X-linked male fertility genes.

## RESULTS

### Extensive X self-synapsis in dog mid pachytene spermatocytes

The progression of meiotic prophase and synapsis in canine spermatocytes was studied by immunostaining for SYCP3 (lateral elements) and SYCP1 (transverse filaments) .

At leptotene ( $1.7\% \pm 0.6$  of the spread nuclei of spermatocytes;  $n=3$  (100 nuclei analysed per dog sample)), short fragments of SYCP3 appear throughout the nucleus, rapidly followed by the appearance of fragments of SYCP1, that co-localize with SYCP3, but are initially fewer in number (Figure 1A). In zygotene ( $8\% \pm 4.6$  of the spread nuclei of spermatocytes;  $n=3$  (100 nuclei analysed per dog sample)), longer stretches of SYCP3 and SYCP1 fragments are present, in agreement with the known progression of synapsis between the homologous chromosomes. However, the SYCP3 pattern appears a bit more dotted compared to what can be observed in mouse zygotene spermatocytes. In pachytene ( $85\% \pm 3.6$  of the spread nuclei of spermatocytes;  $n=3$  (100 nuclei analysed per dog sample)), SC assembly is complete on all autosomes, and SYCP3 and SYCP1 completely co-localize, indicating full synapsis. Diplotene nuclei were very rare ( $5.3\% \pm 1.5$  of the spread nuclei of spermatocytes;  $n=3$  (100 nuclei analysed per dog sample)), indicating that this stage lasts only very short in the dog (in mouse we observed that 23% of spermatocyte nuclei were at diplotene,  $n=100$ ). Again, SYCP3 is observed in a dotted pattern, whereas mouse diplotene spermatocytes still contain linear SYCP3 staining along the chromosomal axes at this stage. The XY pair could be easily detected in the majority of pachytene nuclei, due to the absence of SYCP1 along most of the X chromosomal axis detected by SYCP3 (Figure 1), but no distinct nuclear domain encompassing the XY body was observed in the DAPI staining. The chromosomal axis of the Y chromosome was very short, and frequently appeared to synapse almost completely with the X. In addition, large stretches of SYCP1, much longer than what might have been expected from XY synapsis,



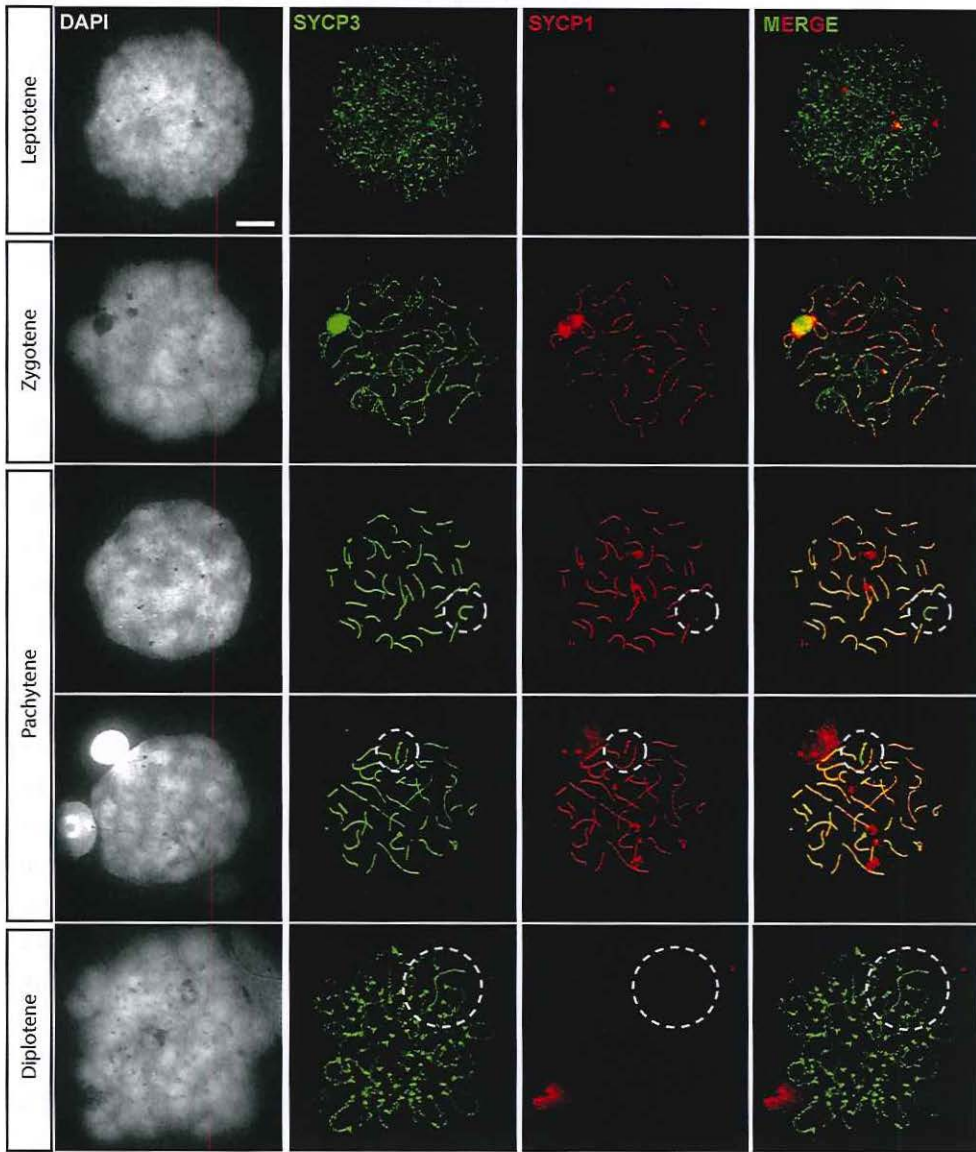


**Figure 1 - Extensive X chromosome self-synapsis in dog pachytene spermatocytes**

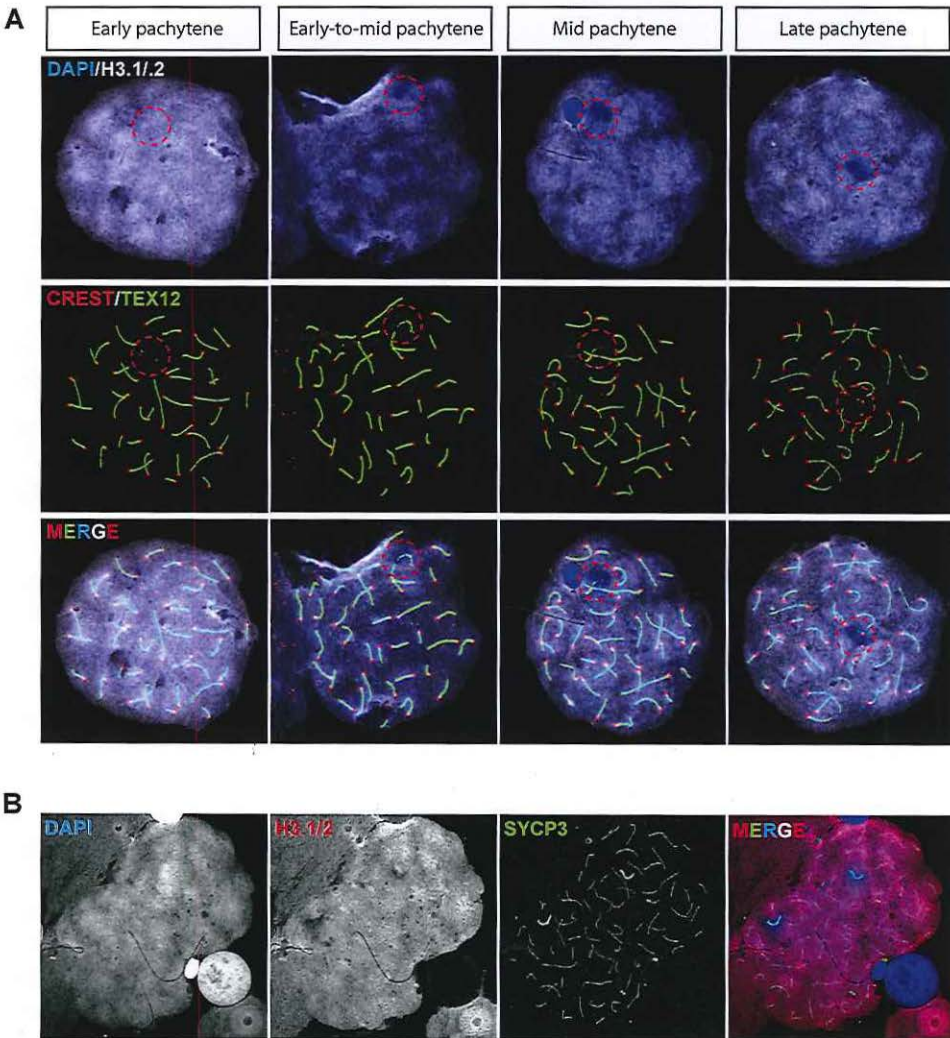
Overview of the dog male meiotic prophase and the progression of synapsis between the XY pair. The left panel shows DAPI staining of the different spermatocyte nuclei, the substages are indicated on the left. To the right of the DAPI images, images of the corresponding nuclei stained for the synaptonemal complex proteins SYCP1 (green) and SYCP3 (red) are shown, followed by the merge ( $n = 100$  nuclei analyzed in at least 3 different dog samples). The XY pair in pachytene and diplotene nuclei is encircled. Bar represents  $10 \mu\text{m}$ .



were sometimes observed (Figure 1, lower pachytene nucleus).

To study the dynamics of XY association during meiotic prophase in more detail, we first identified the different XY configurations, and their temporal appearance. To this end we made use of the fact that XY body formation is followed by a replacement of histone variants H3.1 and H3.2 by H3.3, as has been described for the mouse (van der Heijden et al., 2007), allowing a distinction between early and mid-to-late pachytene spermatocytes. Using a monoclonal antibody that specifically recognizes H3.1 and H3.2, we observed depletion of the H3.1/2 antigens from at least part of the XY body from mid pachytene onwards (Figure 2A). Costaining with the marker of the central element TEX12, and the centromere marker CREST, revealed that a short synapsed patch can be observed on the XY pair in early pachytene, before histone removal, that localizes near the Y centromere (the dog X and Y chromosomes are metacentric, but since the Y axis is so short, the PAR always appears close to the Y centromere), indicating synapsis between X and Y. Subsequently, when H3.1 removal occurs in early-to-mid pachytene and mid pachytene spermatocytes, a longer stretch of TEX12 staining is observed on the XY pair (Figure 2A). This extensive synapsis is transient, and was usually observed in the area between the PAR and the X chromosome centromere (p-arm). Finally, in late pachytene, the TEX12 signal becomes restricted again to the area close to the Y centromere. At these final stages, the X-chromosomal axis stained by SYCP3 becomes thickened (Figure 2B). When we quantified the extent of synapsis along the X chromosome in 100 pachytene nuclei, 27 displayed no synapsis, 44 had little synapsis (either restricted to the PAR or similar to the middle panel of Figure 2C), extensive synapsis up to the X centromere was observed in 21 nuclei, and even more extreme synapsis, including part of the Xq region in 8 nuclei. To understand if the extensive synapsis occurs between X and Y or represents some form of X self-synapsis, we used Structured Illumination Microscopy (SIM) which reaches a resolution of 120 (green channel)-130 nm (red channel), on samples immunostained with SYCP3 and SYCP1 (Figure 3A). This showed a short stretch of synapsis between X and Y, encompassing approximately half of the Y chromosomal axis, in early pachytene nuclei. At mid pachytene, additional synapsis was observed along two short stretches where part of the X chromosomal forms a looped structure. Thus, this configuration may represent heterologous self-synapsis of the X. In addition, some nuclei showed a split SYCP3 signal along most of the X chromosome that also showed a stretch of SYCP1 in between, indicating that in these nuclei, possible synapsis between sister chromatids of the X chromosome could occur. To verify whether these SYCP1 stretches represented true synapsis, we also stained for TEX12, a component of the central element, and HORMAD1, a marker of unsynapsed axes, which is known to be removed upon synapsis in mouse spermatocytes (Wojtasz et al., 2009). Figure 3B shows that, indeed also in dog spermatocytes, HORMAD1 signals are frequently reduced

when TEX12 is present. In addition, CREST antibody was used to verify the locations of the X and Y centromeres, and showed that the X centromere localizes at the tip of the loop that appears to display some form of heterologous synapsis.



4

**Figure 2 - Progressive remodeling of the XY body during meiotic prophase in dog spermatocytes**

**A)** Pachytene spermatocyte spread nuclei stained for DAPI (blue), H3.1/2 (white, artificial color chosen to represent the infrared signal), CREST (red) and TEX12 (green). Single immunostainings are shown in grayscale. The different substages are indicated on top.

**B)** Pachytene spermatocyte spread nucleus stained for DAPI (blue), H3.1/2 (red), SYCP3 (green). Single immunostainings are shown in grayscale.



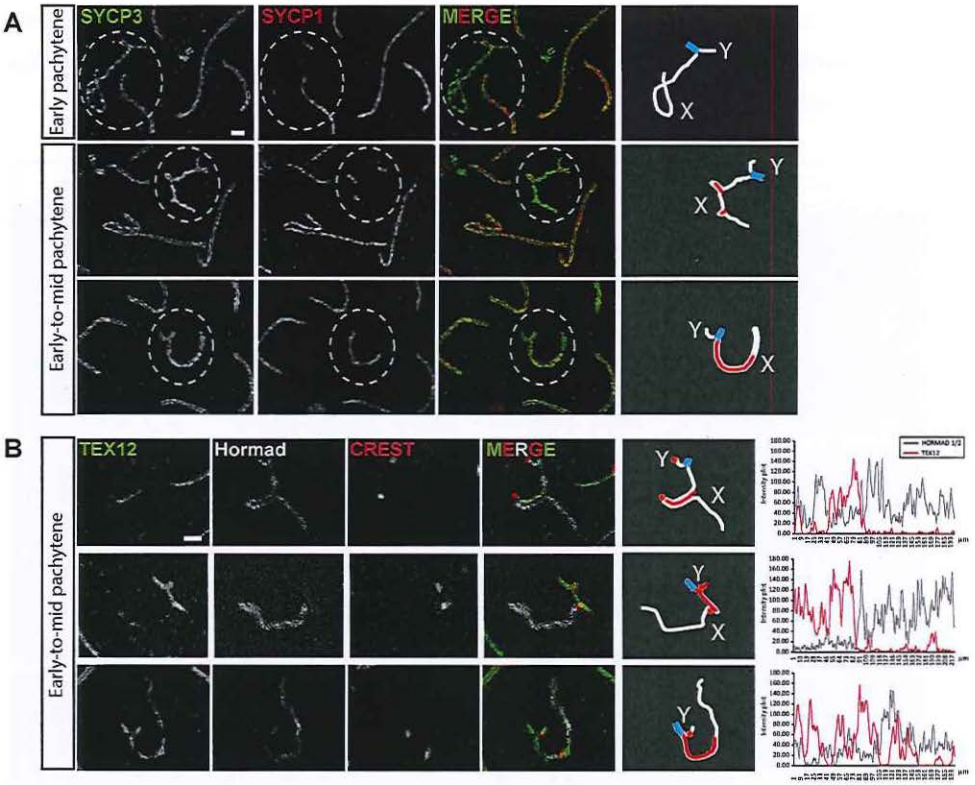


**Figure 3 - Transient X self-synapsis during pachytene in dog spermatocytes**

**A)** Subregions of spermatocyte spread nuclei containing the X and Y at different substages of pachytene indicated on the left are shown at high resolution (Structured Illumination Microscopy (SIM)) to resolve the lateral elements of the synaptonemal complex immunostained for SYCP3 (white/green). The nuclei are costained for SYCP1 to identify regions of synapsis. To the right, drawings showing in white the X-specific and the Y-specific regions, in light blue PAR homologous synapsis and in red X chromosome heterologous self-synapsis. Bar represents 1  $\mu$ m.

**B)** As in A, but these nuclei were stained with antibodies against TEX12 (marker of synapsis), HORMAD1/2 (specifically localizes on unsynapsed axes) and CREST (to mark the centromeres) as indicated. Scale bar represents 1  $\mu$ m. To the right, drawings showing in white the X-specific and the Y-specific region (in light blue PAR homologous synapsis, in red X chromosome heterologous self-synapsis, and in orange the centromere locations) and intensity plots of TEX12 (in red) and HORMAD1/2 (in gray) signals along the synaptonemal complex between the X and Y chromosomes. Intensities are measured starting from the PAR region and proceeding towards the telomeric region of the X axis.



## DNA double strand break repair appears to be completed during maximal self-synapsis along the X chromosome axis

Due to the largely heterologous state of the mouse X and Y chromosomes, DSB repair on these sex chromosomes is delayed in regions outside the PAR (reviewed in (Inagaki et al., 2010)). To visualize the dynamics of DNA double strand break formation and repair on the dog XY, we first analysed the presence of the homologous recombination repair protein RAD51, and the well-known marker of DSBs and the XY body,  $\gamma$ H2AX (Mahadevaiah et al., 2001)(Figure 4A).  $\gamma$ H2AX represents the phosphorylated form of H2AX. This variant of H2A can be phosphorylated by the checkpoint kinases ATR and ATM or by DNA-PKCs in somatic cells in response to DNA damage (Rogakou et al., 1999). During meiotic prophase in mouse, ATM phosphorylates H2AX at meiotic DSBs (Bellani et al., 2005; Mahadevaiah et al., 2001; Rogakou et al., 1999). Later, ATR is responsible for the formation of  $\gamma$ H2AX on the XY body (Bellani et al., 2005; Royo et al., 2013).

At leptotene, we observed many RAD51 foci, indicative for the presence of DSBs throughout the nucleus, and  $\gamma$ H2AX displayed a focal staining pattern colocalising with the RAD51 foci. The number of foci decreased during zygotene. In early pachytene nuclei (which represent 40.7% of the total number of pachytene nuclei (92/226 nuclei)), only a few foci remained present on the synapsed axes of autosomes, whereas the X chromosome still carried many bright RAD51 foci associated with intense  $\gamma$ H2AX staining of the XY body chromatin (Figure 4A). In mid pachytene nuclei (50.9% of the total number of pachytene nuclei),  $\gamma$ H2AX still covered most of the XY axes, but RAD51 foci had disappeared from the sex chromosomes. Quadruple staining of RAD51, SYCP3, SYCP1, and  $\gamma$ H2AX confirmed the notion that RAD51 disappears before  $\gamma$ H2AX, and also showed that RAD51 has disappeared when maximal synapsis is reached (Figure 4B). Finally, neither RAD51 foci nor  $\gamma$ H2AX were observed on the XY body of late pachytene nuclei (8.4% of the total number of pachytene nuclei), and in none of the few diplotene nuclei that were found. In cells where both  $\gamma$ H2AX and RAD51 were absent from the XY body, the SYCP3 axes of the XY pair usually had a thickened appearance, and these were defined as late pachytenes. We verified the absence of  $\gamma$ H2AX from such late pachytene nuclei using immunofluorescent staining of dog testis sections. For the spermatogenic cycle of the dog, 8 different cellular associations have been described (schematically depicted in Figure 5A, (Foote et al., 1972)), with late pachytene and diplotene spermatocytes appearing at Stages VI and VII. Indeed, we observed a few  $\gamma$ H2AX negative nuclei with one intense axis staining for SYCP3 at Stage VI, and more such nuclei were observed at Stage VII (Figure 5B).

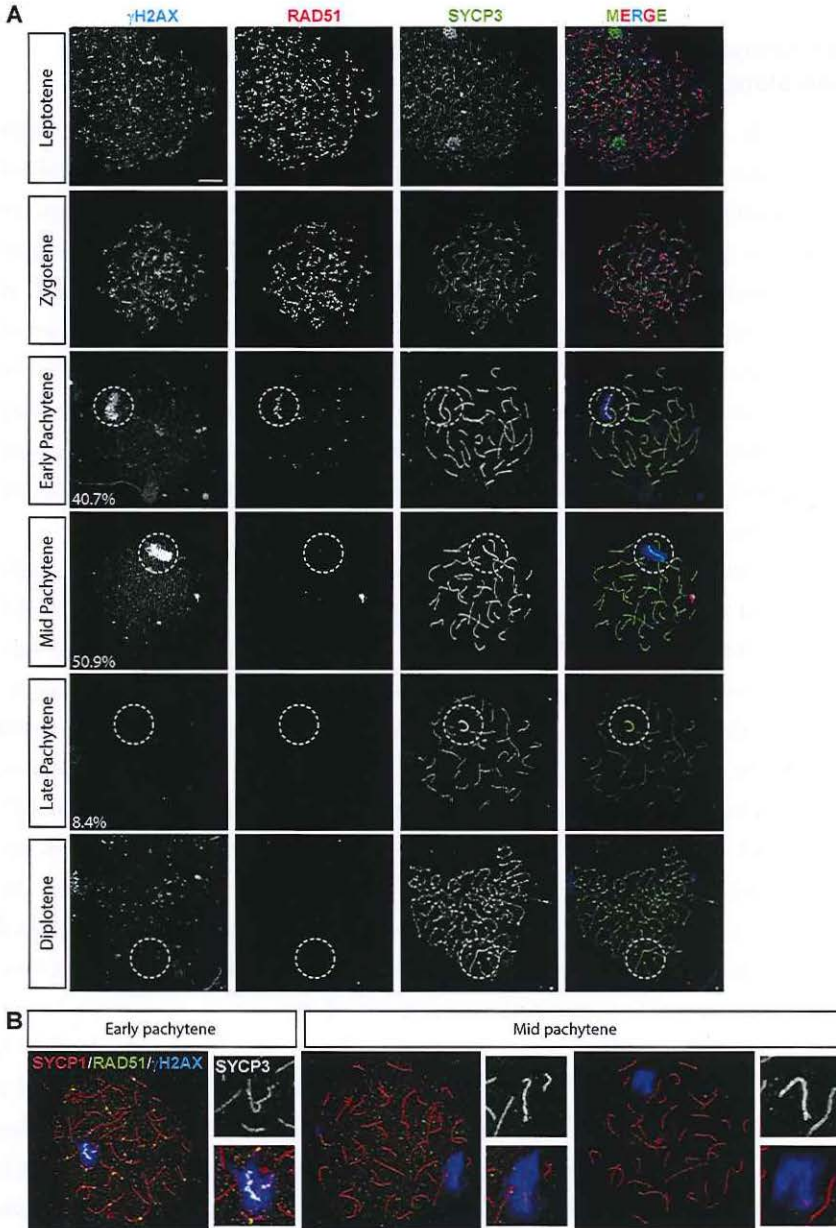
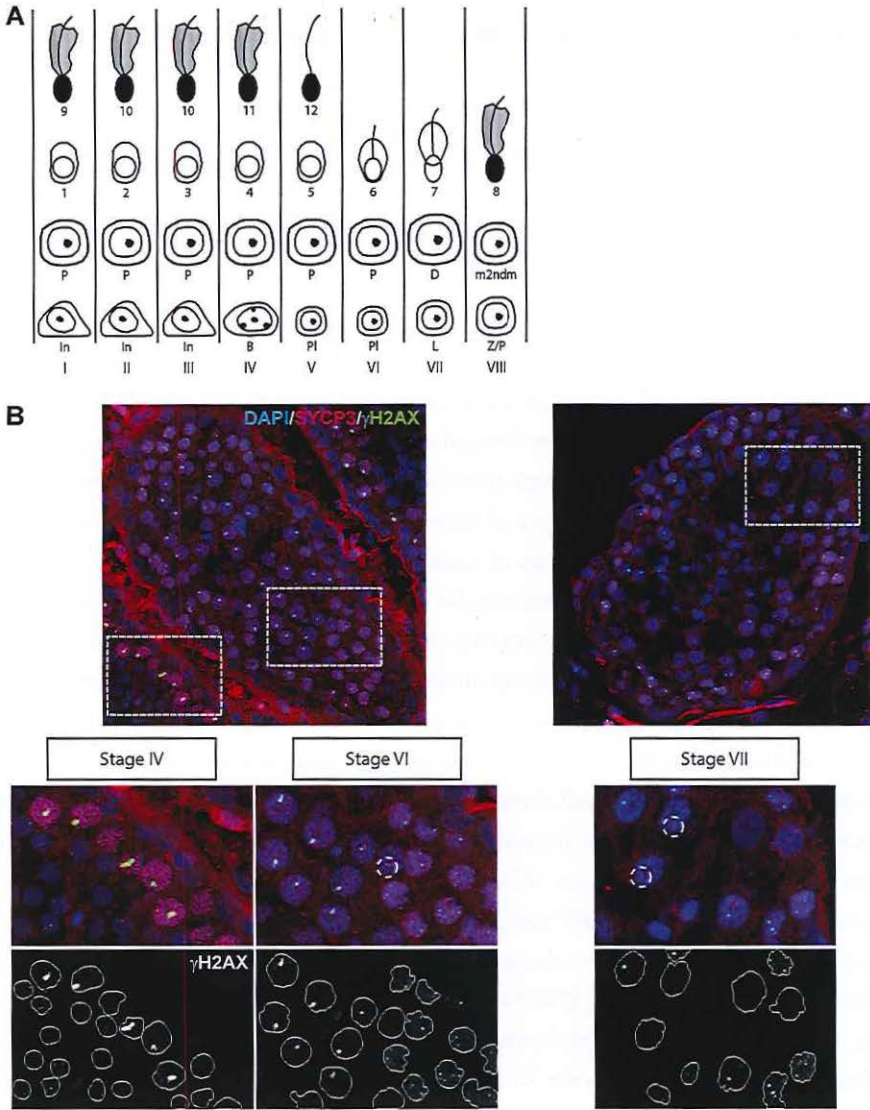


**Figure 4 - DSBs repair dynamics**

A) Spermatocyte spread nuclei stained for  $\gamma$ H2AX (blue), RAD51 (red) and SYCP3 (green). Single stainings are shown in greyscale. Percentages indicate the fraction of pachytene nuclei observed as shown. Scale bar represents 10  $\mu$ m. B) Spermatocyte spread nuclei stained for  $\gamma$ H2AX (blue), RAD51 (green), SYCP1 (green), and SYCP3 (only shown in the enlargement, in greyscale). Close-ups show a magnification of the XY body, the top image shows SYCP3 staining (greyscale) in the area, for which the merge of SYCP1, RAD51 and  $\gamma$ H2AX is shown below.



4

**Figure 5 - Loss of  $\gamma$ H2AX from the XY body in pachytene spermatocytes becomes evident at Stage VI of the spermatogenic cycle in the dog**

A) Schematic drawing of the different stages of the spermatogenic cycle of the dog (adapted from (Russell et al., 1990)).

B) Immunostaining of cryosections of dog testes for  $\gamma$ H2AX (green) and SYCP3 (red), and also stained with DAPI (blue). Stages were identified based on Russell et al. (1990) (Russell et al., 1990). Loss of  $\gamma$ H2AX and the thickened SYCP3 axes representative of late pachytene becomes evident at Stage VI. Single immunostainings are shown in grayscale. Magnifications are shown in the bottom panels, and some cells and the XY body are outlined for reference.



### Markers of MSCI on the XY body of dog pachytene spermatocytes

In addition to being the earliest known marker of the mouse XY body,  $\gamma$ H2AX is required for the initiation of MSCI in mouse spermatocytes (Fernandez-Capetillo et al., 2003). The canine XY pair is highly enriched for  $\gamma$ H2AX in early-to-mid pachytene, but loses this mark before exit from pachytene. We wondered if this early depletion of  $\gamma$ H2AX from the XY body could be associated with premature release from MSCI. Therefore, we investigated the localization pattern of additional markers of mammalian MSCI.

First, we analysed the presence of RNA polymerase II, using two different antibodies, one targeting all RNA polymerase II, and one that targets only the form that is phosphorylated at serine 2 in the heptapeptide repeats in the C-terminal domain (CTD repeat) of the large subunit in association with transcription elongation (reviewed in (Hsin and Manley, 2012)). The overall level of RNA polymerase II was quite low in dog pachytene nuclei, but nonetheless the XY-pair frequently appeared depleted of RNA polymerase II as compared to the rest of the nucleus (Figure 6A), indicating a lack of transcriptional activity. In accordance with this observation, we also observed reduced staining for phosphorylated RNA polymerase II in the region containing the XY body in the majority of pachytene nuclei (57%, n=101) (Figure 6B, C). However, surprisingly, this antibody showed an intense dotted signal adjacent to the SYPC3-stained X chromosomal axis also in a large fraction of the pachytene nuclei (41%). When we quantified the occurrence of this phenomenon, relative to the presence of a  $\gamma$ H2AX signal on the XY body and the overall depletion of phosphorylated RNA polymerase II from the XY body, it became evident that the presence or absence of the dotted signal was variable in relation to the other markers (Figure 6C). In order to provide additional evidence for overall transcriptional silencing of the XY body, at least in part of the pachytene nuclei, we performed an RNA-FISH experiment to detect nascent transcripts containing repeat DNA. This method has also been used to verify MSCI and MSUC in the mouse (Namekawa et al., 2006; Turner et al., 2005). Figure 7 indeed shows reduced hybridization of Cot1 DNA in the area of the chromatin that encompasses the XY body in comparison to the rest of the chromatin in two pachytene nuclei (Figure 7). However, also this depletion was not always evident (not shown) Next, we analysed the localisation of two different histone modifications; H3 lysine 4 dimethylation (H3K4me2), known to be associated with active or potentiated chromatin, and H3 lysine 9 trimethylation (H3K9me3) as a marker of inactive chromatin. In mouse spermatocytes, both these modifications are enriched on the XY body in late prophase nuclei (late pachytene-diplotene) and persist on the sex chromosomes in round spermatids (Khalil et al., 2004; van der Heijden et al., 2007). Methylation of H3K9 is thought to function to maintain repression of the sex chromosomes in post-meiotic cells, in the absence of  $\gamma$ H2AX (Cocquet

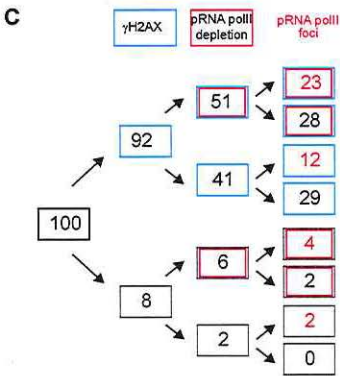
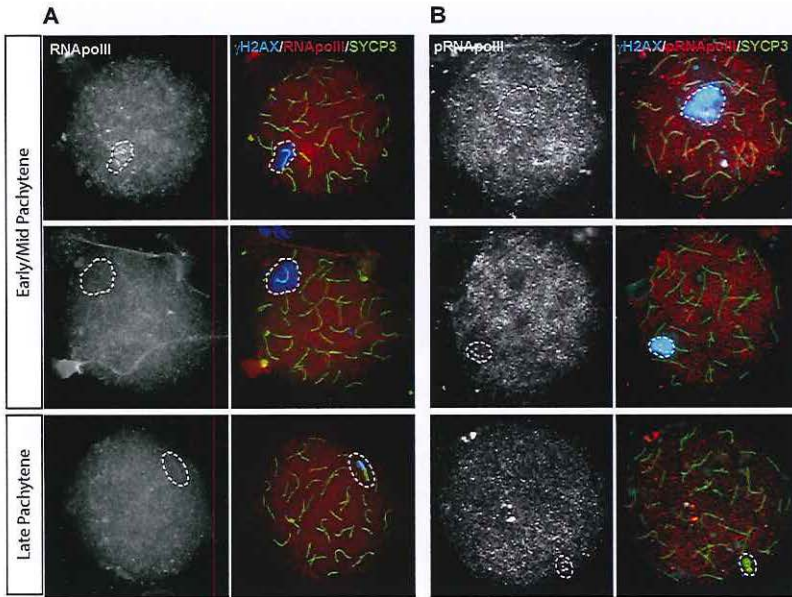


**Figure 6 - Different patterns of RNA polymerase II localization on the XY body of dog pachytene spermatocytes**

**A)** Pachytene spermatocyte spread nuclei stained for  $\gamma$ H2AX (blue), RNA polymerase II (RNAPolII, red), and SYCP3 (green), single RNA polymerase II immunostainings are shown in gray scale. The lower panel represents a late pachytene spermatocyte in which  $\gamma$ H2AX is already lost from part of the X chromosome and RNAPolII is not clearly depleted from the XY body.

**B)** Pachytene spermatocyte spread nuclei stained for  $\gamma$ H2AX (blue), phosphorylated RNA polymerase II (RNAPolIII, red), and SYCP3 (green), single RNA polymerase II immunostainings are shown in gray scale. The lower panel represents a late pachytene spermatocyte in which  $\gamma$ H2AX is already lost from part of the X chromosome. RNA polymerase II depletion from the XY body is evident in the nucleus shown in the middle. In addition, foci of phosphorylated RNA polymerase II staining are specifically observed in the XY body of the middle and the bottom nucleus.

**C)** Quantification of the percentages of pachytene nuclei ( $n=101$ ) with RNA polymerase II foci in the XY body, relative to the overall depletion of this mark from the (rest of) the XY body, and to the enrichment of  $\gamma$ H2AX in the XY body. Nuclei were immunostained as shown in panel B.



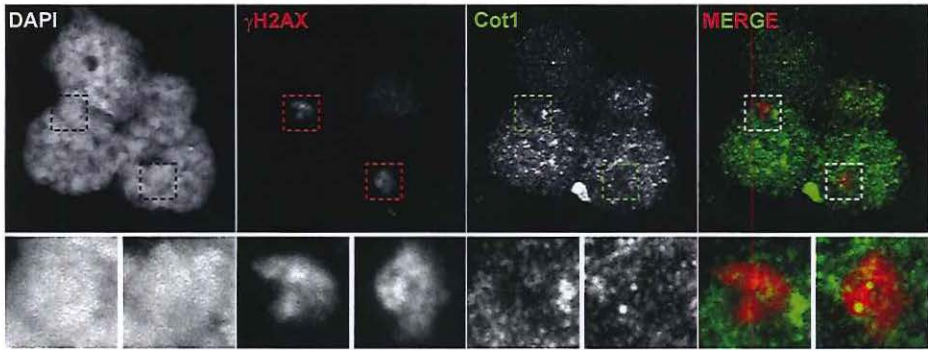


**Figure 7 - Reduced transcriptional activity in the XY body of dog pachytene spermatocytes**

Images of Cot1 RNA FISH combined with an immunostaining for  $\gamma$ H2AX on spermatocyte nuclei. High  $\gamma$ H2AX signals (covering the XY body) correspond to low Cot1 signals, indicating little transcriptional activity. Magnifications of the left and right XY body are shown below each image.

et al., 2009). In contrast, the increase in H3K4 methylation in mouse diplotene spermatocytes may contribute to reactivation of a subgroup of X- or Y-linked genes in round spermatids (Baarends et al., 2007). In dog spermatocytes, the overall level of H3K4me2 was low in pachytene nuclei. In parallel with depletion of H3.1 from the XY body chromatin, depletion of H3K4me2 from XY body chromatin was observed. In diplotene nuclei and round spermatids, H3K4me2 remained excluded from the area of the nucleus that lacks H3.1, which covers either the X or the Y chromosome (Figure 8A and 8B). We performed a similar analysis for H3K9me3, and observed a general enrichment of this modification in the centromeric regions of all chromosomes including the XY pair. Only in late pachytene, enrichment of H3K9me3 on the XY body appeared to spread a bit more, and included at least half of the XY body chromatin, but this enrichment was no longer observed at diplotene (Figure 8C). In round spermatids, enrichment of H3K9me3 was highly variable in the area lacking H3.1 (Figure 8D, compare left nucleus to right nucleus).

### mRNA sequencing reveals MSCI and PSCR in the dog

To directly compare X chromosomal and autosomal RNA expression levels in both spermatocytes and spermatids, we isolated total RNA from cell preparations enriched in either spermatocytes (79.3% pure, Additional file 1, Table S1) or spermatids (84.4% pure, Additional file 1, Table S1) from testes of 3 dogs and performed RNA sequencing analysis. After removal of genes for which mRNA was absent in 5 or more samples we detected 91% of the genes presently annotated as coding genes in the dog genome (38 autosomes and the X chromosome; the male specific region of the dog Y chromosome sequence was recently reported (Li et al., 2013), but has not been annotated). Next, we generated boxplots of the gene expression



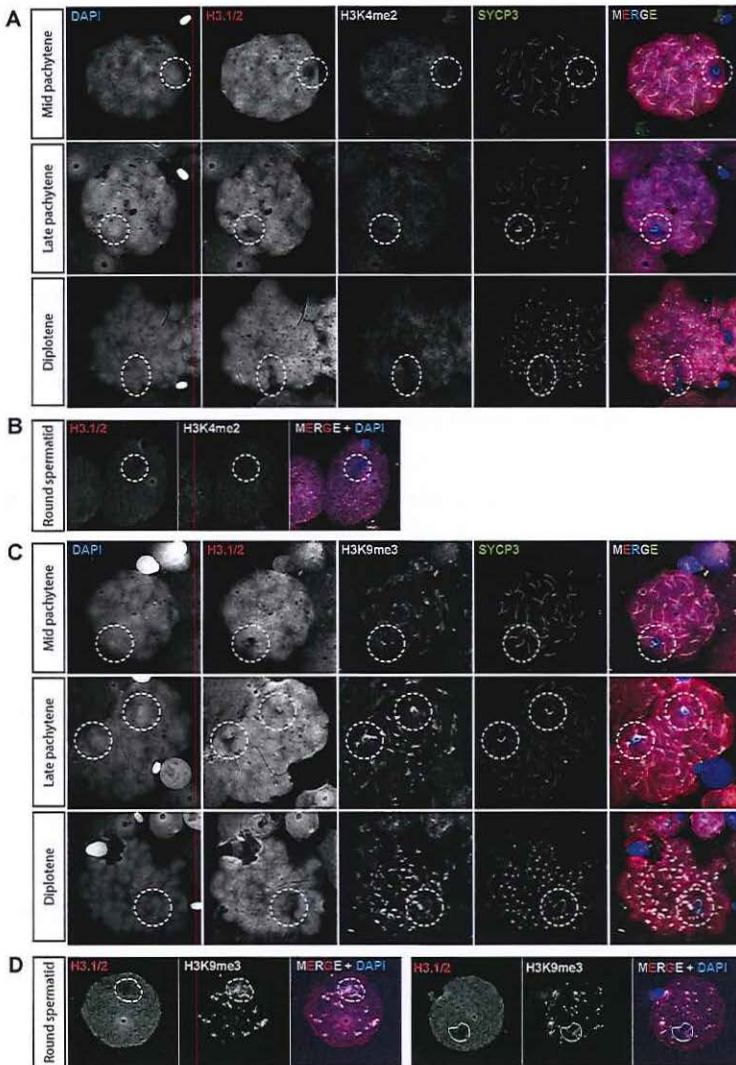


**Figure 8 - Dynamics of H3K4me2 and H3K9me3 on the XY body in dog spermatocytes**

A) Pachytene spermatocyte spread nuclei stained for DAPI (blue), H3.1/2 (red), H3K4me2 (white, artificial color chosen to represent the infrared signal) and SYCP3 (green). Single immunostainings are shown in grayscale. Subsequent substages indicated on the left are shown from top to bottom in the different panels.

B) Spermatid spread nuclei stained for DAPI (blue), H3.1/2 (red), and H3K4me2 (white, artificial color chosen to represent the infrared signal). Single immunostainings are shown in grayscale.

C) Pachytene spermatocyte spread nuclei stained for DAPI (blue), H3.1/2 (red), H3K9me3 (white, artificial color chosen to represent the infrared signal) and SYCP3 (green). Single immunostainings are shown in grayscale. Subsequent substages indicated on the left are shown from top to bottom in the different panels.

D) Representative spermatid spread nuclei stained for DAPI (blue), H3.1/2 (red), and H3K9me3 (white, artificial color chosen to represent the infrared signal). Single immunostainings are shown in grayscale.

(log<sub>2</sub> FPKM, Fragments Per Kilobase of transcript per Million fragments mapped) and observed that the expression levels for the X chromosome were significantly lower compared to autosomes both in spermatocytes (p-value < 10<sup>-14</sup>) and spermatids (p-value < 10<sup>-5</sup>), indicating that both MSCI and PSCR impact on the activity of the X chromosome (Figure 9A, left). To be able to compare the degree of MSCI and PSCR between dog and mouse, we also generated similar boxplots for mouse spermatocytes and spermatids, using the recently published RNA sequencing dataset, using purified spermatocyte and round spermatid cell fractions of similar purity to our samples (Additional file 1, Tables S2 and S3) (Soumillon et al., 2013) (Figure 9A, middle). It was found that gene expression from the X compared to the autosomes was reduced more clearly in mouse spermatocytes (p-value < 10<sup>-15</sup>). In addition, although PSCR was apparent (p-value < 10<sup>-7</sup>), a significant overall post-meiotic upregulation of X-linked gene expression was observed in mouse (p-value < 10<sup>-15</sup>), but not in dog spermatids. For the human, only results from microarray analyses are available (Sin et al., 2012), and we generated boxplots of these datasets. The results indicate that X-linked gene expression in human spermatogenesis follows a pattern with measurable MSCI (p-value < 10<sup>-6</sup>), but X-linked gene expression in round spermatids was even higher than autosomal expression (p-value < 0.01) (Figure 9A, right).

► **Figure 9 - Gene expression in mouse, dog, and human spermatocytes and round spermatids**

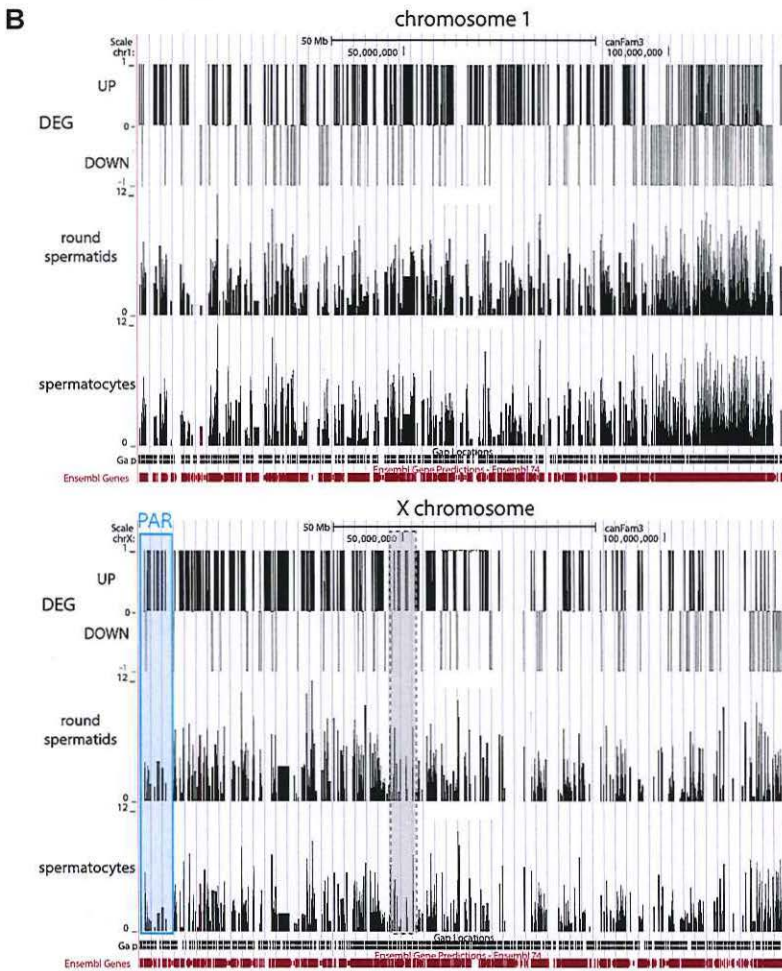
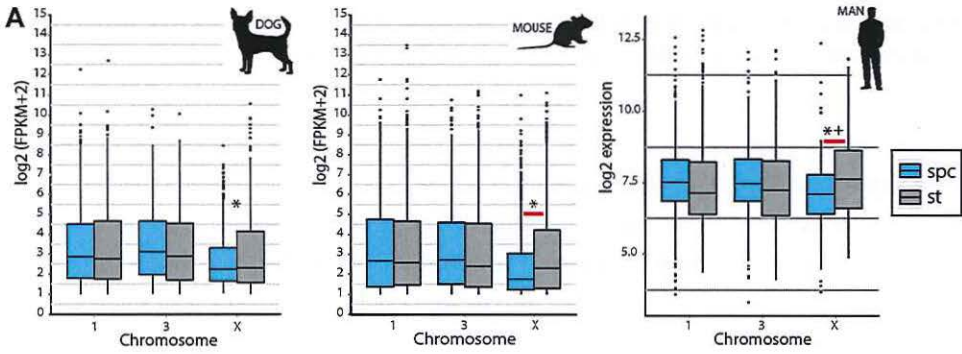
**A)** Left and middle: boxplots showing median, 25, and 75 percentile values of the mRNA levels represented as log<sub>2</sub>(FPKM+2) values obtained from RNA sequencing, of genes on chromosomes 1,3, and X in dog and mouse (using the dataset published by(Soumillon et al., 2013) spermatocytes (spc) and round spermatids (st). Genes that were expressed below the 25 percentile values of the whole genome average in both spermatocytes and spermatids were excluded from this analysis.

Right: boxplot showing median, 25, and 75 percentile values of the mRNA levels represented as log<sub>2</sub> (expression value). The values were obtained from published microarray hybridization data using mRNA isolated from human spermatocytes and spermatids (Sin et al., 2012), and shown here for chromosomes 1,3, and X. Genes with very low expression (gene expression value below 100, Affimetrix probesets with mean signal intensities lower than 100) in both spermatocytes and spermatids were excluded from this analysis. Asterisks indicate significant difference in gene expression between autosomes and the X chromosome for spermatocytes and spermatids. Plus indicates significantly higher X-linked than autosomal gene expression in spermatids. Horizontal red lines indicate significant difference in X-linked gene expression between spermatocytes and spermatids.

**B)** Overview of differentially expressed genes along chromosome 1 and chromosome X, comparing expression in spermatocytes and round spermatids from the dog. Genes that are significantly up-regulated in round spermatids compared to spermatocytes (differentially expressed genes; DEG) are indicated as +1bars, and significantly down-regulated genes are represented as -1 bars along chromosome X and along chromosome 1. In addition, the log<sub>2</sub> value of the FPKM values +2 of all genes along the chromosomes in spermatocytes and round spermatids are shown. Gene density along the chromosomes can be inferred from the density of the bar representing locations of Ensembl annotated genes along the chromosome shown at the bottom. For the X chromosome, the approximate location of the PAR border is indicated by a light blue line, and centromere location is indicated by a dashed gray line.



INCOMPLETE MEIOTIC SEX CHROMOSOME INACTIVATION IN THE DOG



4



### Reactivation of single copy X-linked genes in dog round spermatids, but also post-meiotic downregulation of a subset of X-linked genes

Next we identified differentially expressed genes between spermatocytes and spermatids using two different approaches (Cufflinks (Cuffdiff) and edgeR (see Materials and Methods). Both approaches yielded highly comparable sets of genes (Additional File 1, Table S4: 70-95 % identity of significantly up- and down-regulated autosomal and X-linked genes for the two methods), and a more detailed investigation was performed using the Cufflinks analysis results. For X-linked genes with a more than 1.5 fold change in gene expression, we observed that 207 genes were significantly up-regulated in spermatids compared to spermatocytes, and 123 were down-regulated (Table 1). Previously, we have shown that a large group of single-copy genes can escape from PSCR in mouse spermatids (Mulugeta Achame et al., 2010b), contrary to the hypothesis that post-meiotic expression of X-linked genes would require multiple copies of a gene to overcome the repressive marks (Mueller et al., 2008). Of the up-regulated genes, the only known multi-copy genes we could identify that were differentially expressed from the X chromosome were members of the MAGEA and MAGEB gene families, that are also multi-copy in mouse and man. However, the majority of these genes was down-regulated in spermatids compared to spermatocytes. In addition, 32 differentially expressed dog X-linked genes are homologous to multi-copy X-linked genes identified in mouse and human by Mueller et al. (Mueller et al., 2013), but very few of these genes are clearly multi-copy (>2 copies) in dog, and 14 are down-regulated in spermatids compared to spermatocytes (Additional file 1, Table S5).

**Table 1 - Comparison of the number of differentially expressed genes in mouse and dog spermatocytes and spermatids**

	# genes analysed	>1.5 fold change (%)*	Down (%)*	Up (%)*	# X-linked genes (%)*	>1.5 fold change X (%)*	Down X (%)*	Up X (%)*
<b>Mouse</b>	23100	8565 (37)	4305 (19)	4260 (18)	1016 (4.4)	399 (1.7)	57 (0.25)	342 (1.5)
<b>Dog</b>	19475	8851 (45)	4219 (22)	4632 (24)	768 (3.9)	330 (1.7)	123 (0.63)	207 (1.1)
<b>Common</b>	13492	2650 (20)	1340 (10)	1310 (10)	475 (3.5)	100 (0.74)	9 (0.066)	91 (0.67)

Down: down-regulated in spermatids compared to spermatocytes

Up: up-regulated in spermatids compared to spermatocytes

\*percentage relative to the #genes analysed

Next we compared the above-mentioned RNA sequencing data recently deposited for mouse spermatocytes and spermatids (Soumillon et al., 2013), to our dog dataset. Significantly differentially expressed genes were identified using the same method for both species. Table 1 shows the results that were obtained. From this, it is clear that there are more X-linked genes that become up-regulated in spermatids in mouse compared to dog. Conversely, fewer X-linked genes are specifically post-meiotically down-regulated in mouse compared to dog. Almost half of the X-linked genes that are up-regulated in spermatids in the dog share this expression pattern with the mouse. In contrast, less than 10% of the down-regulated genes are shared between mouse and dog.

### Differential regulation of gene expression along the p and q arms of the dog X chromosome

To study whether certain regions of the dog X chromosome (in relation to the observed heterologous self-synapsis) are more likely to be up- or down-regulated in round spermatids we plotted the density of differentially expressed genes and their corresponding expression level ( $\log_2$  FPKM) along the X chromosome and chromosome 1 (these two chromosomes are similar in size and gene content in dog) (Figure 9B). For the X chromosome, a higher number of up-regulated genes appears to be located on the p arm (containing the PAR) as compared to the q arm. Reciprocally, the q arm of the X chromosome contains a relatively high number of down-regulated genes. For chromosome 1, some areas are also more enriched for either up- or down-regulated genes, but here it appears to correlate better with gene density and the overall gene expression activity in those areas. A similar pattern to that found for chromosome 1 was observed for chromosomes 3 and 5 (data not shown).

To further investigate whether changes in gene expression between spermatids and spermatocytes vary along the X chromosome, we plotted the walking average of gene expression along chromosomes X and 1. The expression pattern of genes along chromosome 1 is not globally different between spermatocytes and spermatids (Figure 10A). In contrast, the expression of genes along the X chromosome is globally up-regulated in spermatids compared to spermatocytes (Figure 10B). However, we observed variability in the degree of upregulation depending on the position of genes on the chromosome. Upregulation is much more pronounced along the p arm of the X chromosome, compared to the q arm (Figure 10B). We then looked at the expression level of genes along the X chromosome in mouse, and observed a much more clear upregulation in round spermatids, compared to what we observed for the dog (Figure 10B). Along chromosome 1, the patterns of gene expression were similar in mouse and dog. To visualize the differential regulation of the p and q arms of the X chromosome in the dog more clearly, we generated separate boxplots of gene expression from the two arms in spermatocytes



and round spermatids, and compared the outcome to boxplots obtained for autosomes of the dog (Figure 10C). All dog and mouse autosomes, and also the mouse X chromosome, are acrocentric. Therefore, in this evaluation we introduced an arbitrary split of left (a) and right (b) parts of chromosomes 1, 3, and X. As expected, we observed that expression from the dog p and q arm of the X is significantly reduced compared to the split autosomes in spermatocytes (p-value  $X_p < 0.05$ ,  $X_q < 10^{-7}$ ) (Figure 10C). However, the expression from the p-arm was higher than the expression from the q arm (p-value  $< 0.05$ ). More importantly, in round spermatids, the gene expression from the p arm of the dog X even reaches a level that is not different from autosomal gene expression, whereas the q arm remains repressed (p-value  $< 10^{-3}$ ) (Figure 10C). In the mouse, no differences in gene expression between the arbitrarily split arms of the chromosomes, including the X, were observed (Figure 10C). In accordance with the results presented in Figure 9, partial reactivation is observed for both (arbitrarily chosen) parts of the X chromosome.

### Low gene expression levels in the dog PAR

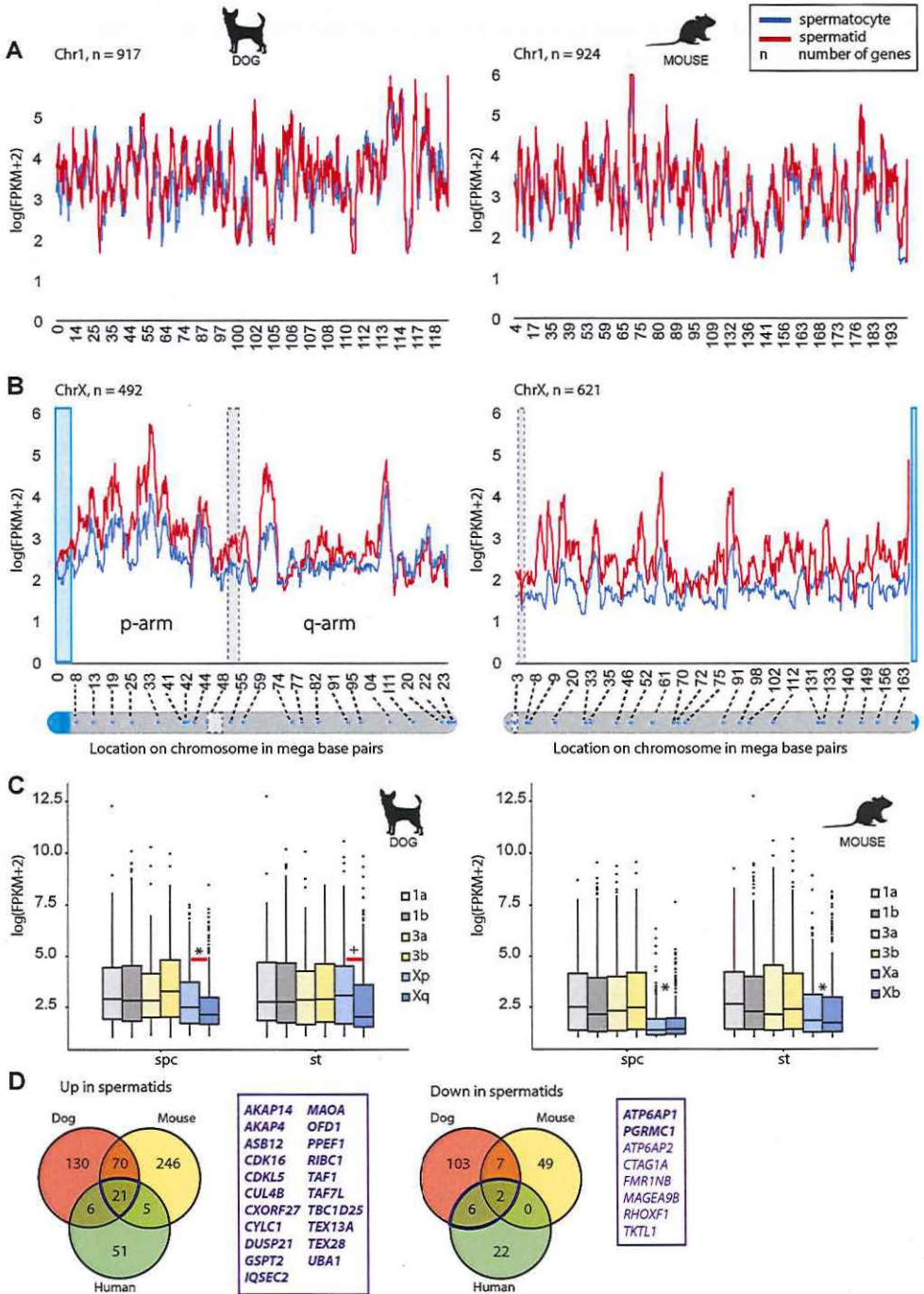
The dog has an exceptionally large PAR containing 34 annotated genes (Lindblad-Toh et al., 2005), and it was expected that this region would escape from MSCI since it is capable to fully engage in homologous synapsis and meiotic recombination. However, we found a relatively low average level of mRNA expression in this region (Additional file 1, Table S6) in both spermatocytes and spermatids. The value is more than 10-fold lower than the overall genome average, and also more than two-fold lower than the average of the whole X chromosome in spermatocytes. Thus, it appears that the dog PAR is even more repressed in spermatocytes compared to the rest of the X chromosome, and shows very little re-expression in spermatids. Interestingly, one gene, named *SLC25A6* (*ANC2*), was found to be highly expressed in dog spermatocytes (normalized FPKM= 47.19 in spermatocytes and 18.11 in spermatids), and thus appears to escape from MSCI. *SLC25A6* encodes an adenine nucleotide carrier (ANC), an ADP/ATP carrier that transports ADP into mitochondria and ATP out of mitochondria. *SLC25A6* is a member of a family of four proteins that also includes *SLC25A4* (*ANC1*), *SLC25A5* (*ANC3*) and *SLC25A31* (*ANC4*). Of these, only the gene encoding *SLC25A5* is also X-linked. The expression levels of these genes in spermatocytes and spermatids of mouse, dog and man are shown in Additional file 1, Table S7. It is clear that both the autosomal *SLC25A31* gene and the X-linked *SLC25A6* gene are the main ANCP variants that are expressed in spermatocytes in dog. *SLC25A6* has not been conserved in the mouse genome, and the autosomal *SLC25A31* variant is highly expressed in spermatocytes. In man, *SLC25A31* is also the main expressed gene, and the two X-linked variants *SLC25A5* and *SLC25A6* are expressed at levels comparable to the median for expressed genes calculated for the genome in both spermatocytes and round spermatids, indicating that they may be transcribed and escape MSCI.



### Pathway analysis of X-linked genes with common post-meiotic regulation between mouse, dog and man

To investigate if genes that are up-regulated in spermatids in both mouse and dog belong to a conserved pathway that is essential during this stage, a pathway analysis was performed using the 91 commonly up-regulated genes in spermatids. The top 5 of significantly enriched Molecular and Cellular Functions are: Cell Morphology; DNA Replication, Recombination, and Repair; Cell Signaling; Post-Translational; and Protein Synthesis (Additional file 1, Table S8). Finally, we compared the X-linked up- and down-regulated genes between dog, mouse, and human (Figure 10D), and identified 21 genes that are up-regulated in spermatids of all three species (Additional file 1, Table S9). For 8 of these genes, mouse knockout models have been described; two are embryonic-lethal, precluding direct analyses of the function of the gene in spermatogenesis, three displayed no clear reproductive defect, and three models displayed defects in post-meiotic spermatid differentiation. For the X-linked genes that were expressed at lower levels in spermatids compared to spermatocytes, very few were conserved between two species, and only two were common to mouse, dog, and man (*ATP6AP1* and *PGRMC1*) (Figure 10D).

CHAPTER 4



◀ **Figure 10 - Partial conservation of MSCI and PSCR among mouse, dog, and man**

A) Walking average of gene expression along chromosome 1 in spermatocytes and round spermatids from dog and mouse.

B) Walking average of gene expression along chromosome X in spermatocytes and round spermatids from dog and mouse. PARs are indicated in blue. Centromere positions are shown in dashed gray boxes.

C) Boxplot showing median, 25, and 75 percentile of gene expression in the p arm (Xp) and q arm (Xq) of the dog X in spermatocytes and round spermatids compared to boxplots of arbitrarily split autosomes of dog and mouse X chromosomes and autosomes. Asterisks indicate significant difference in gene expression between split autosomes and the X chromosome arms. Plus indicates significant difference between split autosomes and the q arm of the X only. Horizontal red lines indicate significant difference in X-linked gene expression between chromosome arms.

D) Venn diagram showing the number of commonly up-regulated (left) and down-regulated (right) X-linked genes in round spermatids compared to spermatocytes in dog, mouse and human. Genes commonly up-regulated or down-regulated in all three species are listed in bold. Down-regulated genes common only to dog and human, not to mouse, are listed with regular characters. Borders of the areas including listed genes are marked in blue.



## DISCUSSION

Here, we performed a detailed analysis of the dynamics of XY chromosome pairing during meiotic prophase in dog, in relation to the progression of meiotic DSB repair, and regulation of gene expression.

The dog X chromosome has two special characteristics that make this analysis particularly relevant. First, it displays transient but extensive self-synapsis during pachytene, as revealed by our immunocytochemical analyses, and second it has an exceptionally long PAR, as compared to mouse and human. We studied both these properties in relation to the dynamics of meiotic DSB repair and the MSCI/PSCR process.

### **Transient self-synapsis correlates with progression of HR repair on the X chromosome and loss of $\gamma$ H2AX**

In general, lack of synapsis is associated with persistence of markers of DSB repair (Moens et al., 1997). For the mouse XY pair, this might be attributed to the lack of homology between X and Y, in combination with the effect of an interhomolog bias, which would inhibit use of the sister chromatid as a template for HR repair. The accomplishment of extensive heterologous synapsis along the dog X during a brief period in midpachytene was associated with concomitant loss of markers of ongoing DSB repair. Loss of  $\gamma$ H2AX occurred first in the area that included both the PAR and the self-synapsed regions, occurring either heterologous in looped regions of the X chromosome, or between sister chromatids, indicating that HR repair may occur faster in this area compared to the rest of the X chromosome. This finding also nicely correlates with the fact that we observed loss of HORMAD association with the self-synapsed regions, and HORMAD activity has been clearly linked to ATR activation and subsequent  $\gamma$ H2AX formation in the mouse (Daniel et al., 2011; Wojtasz et al., 2012). The fact that all  $\gamma$ H2AX enrichment on the X is lost prior to the end of pachytene may also indicate that meiotic HR repair on the X is complete before the end of pachytene, and thus may occur overall more rapidly in dog compared to mouse. Although meiotic HR repair is thought to preferentially involve the use of an intact repair template from the homologous chromosome, this is not possible for regions that localize outside the PAR on the sex chromosome. In the mouse, it has been suggested that some DSBs may be repaired by non-homologous end-joining at the end of meiotic prophase, when components of this machinery are re-expressed (Ahmed et al., 2010). However, it is perhaps more likely that the sister chromatid is eventually used as a repair template on the sex chromosomes, because the DSB ends have been resected, and this may channel repair towards homologous recombination.

### **MSCI occurs in dog spermatocytes, but may be incomplete or transient in some regions**

Persistence of meiotic DSBs and asynapsis are detected by the machinery that induces MSCI in the mouse (Baarends et al., 2005; Carofiglio et al., 2013; Turner et al., 2005; Wojtasz et al., 2012). We observed transient extensive self-synapsis of the X and associated loss of  $\gamma$ H2AX from synapsed regions in dog pachytene spermatocytes. In addition, although H3K4me2 remains depleted from the X and Y chromosomes in diplotene nuclei, H3K9me3 enrichment on the sex chromosomes was only transiently observed, and not evident in late spermatocytes and post-meiotic cells. Also, in late pachytene and diplotene spermatocytes, RNAPolIII depletion was less clear compared to the earlier pachytene nuclei, and phosphorylated RNA polymerase was highly enriched in a focal manner along selected regions of the X chromosome in subfraction of the pachytene nuclei, apparently independent of synapsis. This contrasts with what has been observed in mouse, where the depletion of RNAPolIII on the XY body compared to autosomes is most evident in late pachytene and diplotene, mainly because overall transcription on autosomes increases (Page et al., 2012). Based on these observations, we investigated if MSCI and/or PSCR might be incomplete, or transient in the dog, using a whole genome approach.

Using RNA sequencing, we observed that MSCI occurs also in the dog. When we analysed global regulation of gene expression along the dog X chromosome in spermatocytes and round spermatids, we observed that MSCI is less clearly established along the p arm of the X chromosome, compared to the q arm. In addition, the overall level of gene expression derived from the p arm of the X chromosome was similar to that of autosomal genes in round spermatids, whereas for the q arm post-meiotic reactivation of the X-linked genes was limited or even absent. It is interesting to note that the X self-synapsis is most frequently observed along the p arm of the X chromosome, and synapsis of the tip of the q arm was almost never observed. Thus, it might be suggested that the (heterologous) synapsis facilitates not only DSB repair, but also helps to (re)activate gene expression on the X chromosome. Still, there are also regions in the q arm of the X chromosome that appear to have a relatively high expression level in both spermatocytes and round spermatids. Intriguingly, the very region for which we would expect a clear correlation between synapsis and lack of MSCI, the PAR, was expressed at very low levels in both spermatocytes and spermatids. We expected that the PAR would behave like autosomes regarding repair and synapsis, and escape from MSCI, but it appears to be subject to its own unknown specific regulatory control mechanism. Thus, although there is some degree of correlation between X self-synapsis and reduced MSCI, other, yet unknown aspects of sex chromosome regulation may differ between dog and mouse and influence MSCI.

### MSCI escapees

Little is known about X-linked genes that may escape from MSCI in mouse, except for a report on escape of miRNA genes and the noncoding *Tsix* transcript in spermatocytes (Anguera et al., 2011; Song et al., 2009).

Since MSCI is less complete in dog (and possibly also in man (de Vries et al., 2012; Mulugeta Achame et al., 2010a), and observations in this manuscript), it might be expected that true escapees of MSCI could exist in these species. In dog, 46 of the X-linked genes that are more than 1.5-fold down-regulated in spermatids have an FPKM value  $>4$  in spermatocytes, which is higher than the median FPKM value of all genes that were analysed in spermatocytes, and thus indicates ongoing transcription.

X-linked genes that are specifically expressed in spermatocytes and become down-regulated in spermatids in more than one species are expected to possibly exert a relevant function during meiosis. Mouse and dog have 9 common X-linked genes that are expressed at a level more than 1.5-fold lower in spermatids compared to spermatocytes. Two of these, *ATP6API/ Atp6ap1* and *PGRMC1/Pgrmc1* are also more than 1.5 fold down-regulated in human spermatids, based on the microarray data. Nothing is known about the putative expression or role of these proteins in spermatocytes.

Interestingly, of the 8 X-linked genes that are down-regulated both in dog and human round spermatids, 5 have been shown to be expressed in human spermatocytes and thus may represent true escapees of MSCI: *FMR1NB*, *CTAG1A* (von Kopylow et al., 2010), *MAGEA* (Chen et al., 2011), *RHOXF1* (Song et al., 2013), and *TKTL1* (Rolland et al., 2013). Out of these, *FMR1NB*, *CTAG1A* and *MAGEA9B* are cancer/testis antigens. *RHOXF1* is a homeobox protein and *TKTL1* is a transketolase involved in the pentose-phosphate pathway. These 5 genes are thus of special interest as candidate X-linked genes that may perform an important function during meiotic prophase in human spermatogenesis.

The gene encoding the ADP/ATP carrier *SLC25A6* is another interesting putative MSCI-escapee, and localizes to the PAR in dog and man. ANC proteins are of vital importance for the metabolism of the cell, and pachytene spermatocytes likely require a high rate of ATP synthesis (Brower et al., 2009; Nakada et al., 2006).

### PSCR may not reflect an active repressive process

From our whole genome analysis of mRNA expression in dog spermatocytes and spermatids, it is clear that most X-linked genes that are significantly up-regulated in spermatids compared to spermatocytes are single-copy genes. We propose that persistence of the inactivation of X-linked genes in dog and perhaps human spermatids is not primarily due to a post-meiotic repressive mechanism operating during this stage, but rather represents a carry-over of MSCI.



This is supported by the observed lack of repressive histone marks, as well as by the absence of a DAPI dense area on the sex chromosomes of spermatids, one of the markers of PSCR in mouse. This new extensive analysis of MSCI and PSCR in the dog again supports the notion that X-linked gene activation occurs frequently for single-copy genes in spermatids, and is not globally inhibited. It should also be considered that alleviation of MSCI in round spermatids does not have to automatically lead to re-expression of all X-linked genes that were previously active in spermatogonia. For some of these genes, their products may not be required for, or would be detrimental to spermatid development. Therefore, they will not be specifically (re)activated in round spermatids.

### Identification of putative X-linked male fertility genes

The pathway analysis of X-linked genes that are significantly up-regulated in spermatids both in mouse and dog, revealed that most of these genes are involved in shaping the sperm cell and maintaining genome integrity. These are important processes that require (re)activation of a specific subset of X-linked genes. In addition, it is worth mentioning that a relatively high number of reactivated genes are involved in the regulation of posttranslational modifications and of protein synthesis and degradation (in particular the ubiquitin pathway). The addition of the dog as a new species to the dataset of gene expression in spermatocytes and spermatids allows identification of X-linked genes that show post-meiotic induction of gene expression in mouse, human and dog, thus providing more evidence for an important function in spermatogenesis. For some of these genes, knockout mice have been generated. Several of these mutant animals were shown to be fertile, indicating that even conserved expression does not necessarily indicate that the gene is absolutely required for fertility, at least in the mouse. It should be kept in mind that spermatogenesis is much more efficient in mouse compared to man, yielding a much higher number of mature spermatozoa per gram testis weight per time unit, and a small selective advantage of expression of an X-linked gene in mouse spermatids may translate into an essential function in man. Therefore, all genes listed in Additional file 1, Table S9, as well as the conserved possible MSCI escapees described above should be considered candidate human fertility genes.

### CONCLUSIONS

Our results provide novel insights in the regulation and significance of sex chromosome gene expression during spermatogenesis in mammals. We show that transient but extensive heterologous self-synapsis of the X chromosome is associated with rapid DSB repair and reduced MSCI. On the other hand, the genes that are localized in the pseudoautosomal region are mostly transcriptionally inactive in both spermatocytes and spermatids, despite the normal

progression of synapsis in this region. We hypothesize that the PAR is controlled by its own specific regulatory mechanism but that specific genes in this region that exert a meiotic or post-meiotic function can be active. Furthermore, based on conserved expression patterns in mouse, human, and dog spermatocytes and/or spermatids, we identified genes that may function in spermatocytes (escapes) or round spermatids (reactivated genes), and should be considered as potential X-linked male fertility factors.

## METHODS

### Sample collection and germ cell isolation

Testes used in this study were collected from specialized veterinary clinics immediately after dog castration surgery was performed. For RNA sequencing analysis, testes were obtained from two Chihuahuas, here named dog 4 and dog 6 (respectively 9 and 16 months old), and from one German Shepherd, referred to as dog 5 (4 years old). Spermatocytes and round spermatids were purified on the same day of samples collection by using collagenase and trypsin treatment, followed by sedimentation at unit gravity (StaPut procedure) (Grootegoed et al., 1986).

### Analyses of cell purity in the isolated germ cell fractions

Purified germ cells were fixed in Bouin's fixative on glass slides and stained with eosin and hematoxylin using standard histological methods. Purity was estimated by cellular morphology (percentages are shown in Additional file 1, Table S1). In addition, we compared the RNA-seq transcript levels of five genes specifically expressed in spermatids (three protamine genes [*PRM1*, *PRM2*, and *PRM3*] and two transition protein genes [*TNP1* and *TNP2*]) and 3 genes that are specifically induced in spermatocytes (*SYCP1*, 2, and 3), between the spermatid and spermatocyte samples, and between the dog and (published) mouse samples (Tables S8 and S9). From this, it is clear that the fold changes in gene expression are similar in the mouse and dog samples, indicating comparable purities. This is also consistent with the reported purities of these mouse spermatocyte and round spermatid fractions (approximately 70 and 90%, respectively, based on morphological assessment (Soumillon et al., 2013)). Since the spermatid-specific mRNAs are not expressed in spermatocytes, the average log<sub>2</sub> of the fold-change (FC) of 3.6 of increased expression in the spermatid fraction, indicates a contamination of around 8% of spermatid mRNA in the spermatocyte mRNA preparations. This is consistent with the results of the morphological assessment. For contamination of spermatocytes in the spermatid fraction, no such calculation can be made, since RNA transcription of genes that are important in spermatocytes may continue to some extent in round spermatids.

## Antibodies

For primary antibodies, we used: mouse monoclonal antibodies anti-phosphorylated H2AX (Upstate), anti-RNA polymerase II (Abcam), anti-Ser2 phosphorylated RNA Polymerase II (H5) (Abcam) anti H3.1/2 (gift from dr. P. de Boer); rabbit polyclonal antibodies anti-RAD51 (Essers et al., 2002), anti-SYCP3 and anti-SYCP1 (gift from dr. C. Heyting), anti-HORMAD1 (gift from dr. A. Tóth), anti-H3K4me2, anti-H3K9me3; goat anti-SYCP3 (R&D System); guinea pig anti-TEX12 (gift from dr. C. Höög); human anti-centromere antibodies (CREST) (Fitzgerald Industries). For secondary antibodies, we used a goat anti-rabbit IgG alexa 405/488/546/633, goat anti-mouse alexa IgG 350/488/546/633, donkey anti-goat IgG alexa 488/555, goat-anti human IgG 555, goat anti-guinea pig IgG 488/546 (Molecular Probes).

## Meiotic spread nuclei preparations and immunocytochemistry

Testis tissues were processed to obtain spread nuclei for immunocytochemistry as described in (Peters et al., 1997). Spread nuclei of spermatocytes were stained with antibodies mentioned above. Before incubation with antibodies, slides were washed in phosphate buffered saline (PBS, 3×10 min), and non-specific sites were blocked with 0.5% w/v BSA and 0.5% w/v milk powder in PBS. Primary antibodies were diluted in 10% w/v BSA in PBS, and incubations were overnight at room temperature in a humid chamber. Subsequently, slides were washed (3×10 min) in PBS, blocked in 10% v/v normal goat serum (Sigma) in blocking buffer (supernatant of 5% w/v milk powder in PBS centrifuged at 14,000 rpm for 10 min), and incubated with secondary antibodies in 10% normal goat serum in blocking buffer at room temperature for 2 hours. Finally, slides were washed (3×10 min) in PBS (in the dark) and embedded in Prolong Gold with or without DAPI (Invitrogen).

## Imaging

Fluorescent images were observed using a fluorescence microscope (Axioplan 2; Carl Zeiss) equipped with a digital camera (Coolsnap-Pro; Photometrics). Fluorescent images were taken under identical conditions for all slides, and images were analyzed using the ImageJ (Fiji) software (Rasband, W.S., ImageJ, U.S. National Institutes of Health, Bethesda, Maryland, USA [<http://rsb.info.nih.gov/ij/>]). Confocal imaging was performed on a Zeiss LSM700 microscope (Carl Zeiss, Jena): we used a 63× oil immersion objective lens (N.A. 1.4), pinhole 1AU. DAPI was excited at 405 nm and imaged with a short pass filter (SP) 490 nm; Alexa 488 was excited at 490 nm and imaged SP 555 nm; Alexa 546 was excited at 555 nm and imaged SP 640 nm; Alexa 633 was excited at 639 nm and for the imaging no filter was required. SIM analysis was performed using a Nikon N-SIM super-resolution microscope system and



NIS-Elements 2 image processing software.

### **RNA fluorescent *in situ* hybridization (FISH)**

We carried out Cot-1 RNA FISH using a previously described method (Turner et al., 2005). Dog Cot-1 DNA was prepared from dog genomic DNA by shearing, denaturing, and reannealing under conditions that enrich for repetitive sequences (Zwick et al., 1997).

### **RNA sequencing**

Total RNA was extracted from (pure) spermatocyte and spermatid fractions using the Trizol RNA isolation protocol. Quality of extracted RNA was verified using Bioanalyzer 2100 (Agilent technologies), all samples had RIN values above 8.5. RNA sequencing library was prepared using Illumina TruSeq RNA version 1 according to the manufacturer's protocol starting with 1 µg of total RNA. RNA sequencing was performed on Illumina HiSeq2000 for single read 36 bp. Sequence reads were aligned to the dog genome (*Canis familiaris*, NCBI, build3.1) using Tophat (version Tophat-1.4.0). Transcripts were assembled and expression values (FPKM) were generated using Cufflinks (version Cufflinks-2.1.1). Data was further processed to calculate gene expression per chromosome using R and Excel. First, genes with low data and FPKM less than 0 in more than 5 samples out of 6 were removed. To remove low expressed genes, we first calculated the 25 percentile of all samples, and removed genes with FPKM below the 25 percentile in spermatocytes.

Differential expression was performed using Cufflinks (Cuffdiff) (Trapnell et al., 2010) and edgeR (Robinson et al., 2010). For Cuffdiff, Cufflinks-assembled transcripts were first merged using Cuffmerge, and differentially expressed genes were identified using Cuffdiff. Cuffdiff results were further processed using cummeRbund. For edgeR, reads per gene were first counted using HTSeq [<http://www-huber.embl.de/users/anders/HTSeq/>] and differential expression was assessed between the two groups, each with three replicates. Pathway analysis (enrichment analysis) was performed using IPA (Ingenuity® Systems, [www.ingenuity.com](http://www.ingenuity.com)). Statistical analysis (Wilcoxon rank sum test) was performed using R software.

### **ACKNOWLEDGEMENTS**

We thank the veterinarians from Baerveldt & Schuur (Gouda, The Netherlands), Dierenkliniek Rotterdam and Delft-Centrum for providing dog testes. We also thank Drs Attila Toth (Dresden, Germany) and Christer Höög (Stockholm, Sweden) for providing antibodies. We thank Dr. J. Gribnau (Erasmus MC, Rotterdam) for advice. This work was supported by the Netherlands Organisation for Scientific Research (NWO) through ALW (VIDI 864.05.003).

## REFERENCES

- Ahmed EA, Philippens ME, Kal HB, de Rooij DG, and de Boer P (2010). Genetic probing of homologous recombination and non-homologous end joining during meiotic prophase in irradiated mouse spermatocytes. *Mutat Res* 688:12-18.
- Anguera MC, Ma W, Clift D, Namekawa S, Kelleher RJ, 3rd, and Lee JT (2011). Tsx produces a long noncoding RNA and has general functions in the germline, stem cells, and brain. *PLoS Genet* 7:e1002248.
- Ansari HA, Jung HR, Hediger R, Fries R, Konig H, and Stranzinger G (1993). A balanced autosomal reciprocal translocation in an azoospermic bull. *Cytogenet Cell Genet* 62:117-123.
- Baarends WM, Wassenaar E, Hoogerbrugge JW, Schoenmakers S, Sun ZW, and Grootegoed JA (2007). Increased phosphorylation and dimethylation of XY body histones in the Hr6b-knockout mouse is associated with derepression of the X chromosome. *J Cell Sci* 120:1841-1851.
- Baarends WM, Wassenaar E, van der Laan R, Hoogerbrugge JW, Sleddens-Linkels E, Hoeijmakers JH, de Boer P, and Grootegoed JA (2005). Silencing of unpaired chromatin and histone H2A ubiquitination in mammalian meiosis. *Mol Cell Biol* 25:1041-1053.
- Basheva EA, Bidau CJ, and Borodin PM (2008). General pattern of meiotic recombination in male dogs estimated by MLH1 and RAD51 immunolocalization. *Chromosome Res* 16:709-719.
- Bellani MA, Romanienko PJ, Cairatti DA, and Camerini-Otero RD (2005). SPO11 is required for sex-body formation, and Spo11 heterozygosity rescues the prophase arrest of *Atm*<sup>-/-</sup> spermatocytes. *J Cell Sci* 118:3233-3245.
- Bolcun-Filas E, and Schimenti JC (2012). Genetics of meiosis and recombination in mice. *Int Rev Cell Mol Biol* 298:179-227.
- Brower JV, Lim CH, Jorgensen M, Oh SP, and Terada N (2009). Adenine nucleotide translocase 4 deficiency leads to early meiotic arrest of murine male germ cells. *Reproduction* 138:463-470.
- Burgoyne PS, Mahadevaiah SK, and Turner JM (2009). The consequences of asynapsis for mammalian meiosis. *Nat Rev Genet* 10:207-216.
- Carofoglio F, Inagaki A, de Vries S, Wassenaar E, Schoenmakers S, Vermeulen C, van Cappellen WA, Sleddens-Linkels E, Grootegoed JA, Te Riele HP, et al. (2013). SPO11-Independent DNA Repair Foci and Their Role in Meiotic Silencing. *PLoS Genet* 9:e1003538.
- Chen YT, Chiu R, Lee P, Beneck D, Jin B, and Old LJ (2011). Chromosome X-encoded cancer/testis antigens show distinctive expression patterns in developing gonads and in testicular seminoma. *Hum Reprod* 26:3232-3243.
- Cocquet J, Ellis PJ, Yamauchi Y, Mahadevaiah SK, Affara NA, Ward MA, and Burgoyne PS (2009). The multicopy gene *Sly* represses the sex chromosomes in the male mouse germline after meiosis. *PLoS Biol* 7:e1000244.
- Cole F, Kauppi L, Lange J, Roig I, Wang R, Keeney S, and Jasin M (2012). Homeostatic control of recombination is implemented progressively in mouse meiosis. *Nat Cell Biol* 14:424-430.
- Daniel K, Lange J, Hached K, Fu J, Anastassiadis K, Roig I, Cooke HJ, Stewart AF, Wassmann K, Jasin M, et al. (2011). Meiotic homologue alignment and its quality surveillance are controlled by mouse *HORMAD1*. *Nat Cell Biol* 13:599-610.
- de Vries M, Vosters S, Merlck G, D'Hauwers K, Wansink DG, Ramos L, and de Boer P (2012). Human male meiotic sex chromosome inactivation. *PLoS One* 7:e31485.
- Echeverria OM, Benavente R, Ortiz R, and Vazquez-Nin GH (2003). Ultrastructural and immunocytochemical analysis of the XY body in rat and Guinea pig. *Eur J Histochem* 47:45-54.
- Essers J, Hendriks RW, Wesoly J, Beerens CE, Smit B, Hoeijmakers JH, Wyman C, Dronkert ML, and Kanaar R (2002). Analysis of mouse *Rad54* expression and its implications for homologous recombination. *DNA Repair (Amst)* 1:779-793.
- Fernandez-Capetillo O, Mahadevaiah SK, Celeste A, Romanienko PJ, Camerini-Otero RD, Bonner WM, Manova K, Burgoyne P, and Nussenzweig A (2003). H2AX is required for chromatin remodeling and inactivation of sex chromosomes in male mouse meiosis. *Dev Cell* 4:497-508.



- Foote RH, Swierstra EE, and Hunt WL (1972). Spermatogenesis in the dog. *Anat Rec* 173:341-351.
- Franco MJ, Sciarano RB, and Solari AJ (2007). Protein immunolocalization supports the presence of identical mechanisms of XY body formation in eutherians and marsupials. *Chromosome Res* 15:815-824.
- Grootegoed JA, Jansen R, and van der Molen HJ (1986). Effect of glucose on ATP dephosphorylation in rat spermatids. *J Reprod Fertil* 77:99-107.
- Hamer G, Gell K, Kouznetsova A, Novak I, Benavente R, and Hoog C (2006). Characterization of a novel meiosis-specific protein within the central element of the synaptonemal complex. *J Cell Sci* 119:4025-4032.
- Homolka D, Ivanek R, Capkova J, Jansa P, and Forejt J (2007). Chromosomal rearrangement interferes with meiotic X chromosome inactivation. *Genome Res* 17:1431-1437.
- Hsin JP, and Manley JL (2012). The RNA polymerase II CTD coordinates transcription and RNA processing. *Genes Dev* 26:2119-2137.
- Inagaki A, Schoenmakers S, and Baarends WM (2010). DNA double strand break repair, chromosome synapsis and transcriptional silencing in meiosis. *Epigenetics* 5:255-266.
- Keeney S, Baudat F, Angeles M, Zhou ZH, Copeland NG, Jenkins NA, Manova K, and Jasin M (1999). A mouse homolog of the *Saccharomyces cerevisiae* meiotic recombination DNA transferase Spo11p. *Genomics* 61:170-182.
- Khalil AM, Boyar FZ, and Driscoll DJ (2004). Dynamic histone modifications mark sex chromosome inactivation and reactivation during mammalian spermatogenesis. *Proc Natl Acad Sci U S A* 101:16583-16587.
- Lammers JH, Offenberger HH, van Aalderen M, Vink AC, Dietrich AJ, and Heyting C (1994). The gene encoding a major component of the lateral elements of synaptonemal complexes of the rat is related to X-linked lymphocyte-regulated genes. *Mol Cell Biol* 14:1137-1146.
- Lesch BJ, Dokshin GA, Young RA, McCarrey JR, and Page DC (2013). A set of genes critical to development is epigenetically poised in mouse germ cells from fetal stages through completion of meiosis. *Proc Natl Acad Sci U S A* 110:16061-16066.
- Li G, Davis BW, Raudsepp T, Pearks Wilkerson AJ, Mason VC, Ferguson-Smith M, O'Brien PC, Waters PD, and Murphy WJ (2013). Comparative analysis of mammalian Y chromosomes illuminates ancestral structure and lineage-specific evolution. *Genome Res* 23:1486-1495.
- Libbus BL (1985). The ordered arrangement of chromosomes in the Chinese hamster spermatocyte nucleus. *Hum Genet* 70:130-135.
- Lindblad-Toh K, Wade CM, Mikkelsen TS, Karlsson EK, Jaffe DB, Kamal M, Clamp M, Chang JL, Kulbokas EJ, 3rd, Zody MC, et al. (2005). Genome sequence, comparative analysis and haplotype structure of the domestic dog. *Nature* 438:803-819.
- Mahadevaiah SK, Turner JM, Baudat F, Rogakou EP, de Boer P, Blanco-Rodriguez J, Jasin M, Keeney S, Bonner WM, and Burgoyne PS (2001). Recombinational DNA double-strand breaks in mice precede synapsis. *Nat Genet* 27:271-276.
- McKee BD, and Handel MA (1993). Sex chromosomes, recombination, and chromatin conformation. *Chromosoma* 102:71-80.
- Meuwissen RL, Offenberger HH, Dietrich AJ, Rieswijk A, van Iersel M, and Heyting C (1992). A coiled-coil related protein specific for synapsed regions of meiotic prophase chromosomes. *EMBO J* 11:5091-5100.
- Moens PB, Chen DJ, Shen Z, Kolas N, Tarsounas M, and Heng HHQ (1997). Rad51 immunocytology in rat and mouse spermatocytes and oocytes. *Chromosoma* 106:207-215.
- Moens PB, Kolas NK, Tarsounas M, Marcon E, Cohen PE, and Spyropoulos B (2002). The time course and chromosomal localization of recombination-related proteins at meiosis in the mouse are compatible with models that can resolve the early DNA-DNA interactions without reciprocal recombination. *J Cell Sci* 115:1611-1622.
- Monesi V (1965). Differential rate of ribonucleic acid synthesis in the autosomes and sex chromosomes during male meiosis in the mouse. *Chromosoma* 17:11-21.
- Moses MJ (1977). Synaptonemal complex karyotyping in spermatocytes of the Chinese hamster (*Cricetus griseus*). II. Morphology of the XY pair in spread preparations. *Chromosoma* 60:127-137.



- Mueller JL, Mahadevaiah SK, Park PJ, Warburton PE, Page DC, and Turner JM (2008). The mouse X chromosome is enriched for multicopy testis genes showing postmeiotic expression. *Nat Genet* 40:794-799.
- Mueller JL, Skaletsky H, Brown LG, Zaghul S, Rock S, Graves T, Auger K, Warren WC, Wilson RK, and Page DC (2013). Independent specialization of the human and mouse X chromosomes for the male germ line. *Nat Genet* 45:1083-1087.
- Mulugeta Achame E, Baarends WM, Gribnau J, and Grootegoed JA (2010a). Evaluating the relationship between spermatogenic silencing of the X chromosome and evolution of the Y chromosome in chimpanzee and human. *PLoS One* 5:e15598.
- Mulugeta Achame E, Wassenaar E, Hoogerbrugge JW, Sleddens-Linkels E, Ooms M, Sun ZW, van IWF, Grootegoed JA, and Baarends WM (2010b). The ubiquitin-conjugating enzyme HR6B is required for maintenance of X chromosome silencing in mouse spermatocytes and spermatids. *BMC Genomics* 11:367.
- Nakada K, Sato A, Yoshida K, Morita T, Tanaka H, Inoue S, Yonekawa H, and Hayashi J (2006). Mitochondria-related male infertility. *Proc Natl Acad Sci U S A* 103:15148-15153.
- Namekawa SH, Park PJ, Zhang LF, Shima JE, McCarrey JR, Griswold MD, and Lee JT (2006). Postmeiotic sex chromatin in the male germline of mice. *Curr Biol* 16:660-667.
- Namekawa SH, VandeBerg JL, McCarrey JR, and Lee JT (2007). Sex chromosome silencing in the marsupial male germ line. *Proc Natl Acad Sci U S A* 104:9730-9735.
- O'Leary MA, Bloch JI, Flynn JJ, Gaudin TJ, Gi-allombardo A, Giannini NP, Goldberg SL, Kraatz BP, Luo ZX, Meng J, et al. (2013). The placental mammal ancestor and the post-K-Pg radiation of placentals. *Science* 339:662-667.
- Offenberg HH, Schalk JA, Meuwissen RL, van Aalderen M, Kester HA, Dietrich AJ, and Heyting C (1998). SCP2: a major protein component of the axial elements of synaptonemal complexes of the rat. *Nucleic Acids Res* 26:2572-2579.
- Page J, de la Fuente R, Manterola M, Parra MT, Viera A, Berrios S, Fernandez-Donoso R, and Rufas JS (2012). Inactivation or non-reactivation: what accounts better for the silence of sex chromosomes during mammalian male meiosis? *Chromosoma* 121:307-326.
- Perry J, Palmer S, Gabriel A, and Ashworth A (2001). A short pseudoautosomal region in laboratory mice. *Genome Res* 11:1826-1832.
- Peters AH, Plug AW, van Vugt MJ, and de Boer P (1997). A drying-down technique for the spreading of mammalian meiocytes from the male and female germline. *Chromosome Res* 5:66-68.
- Robinson MD, McCarthy DJ, and Smyth GK (2010). edgeR: a Bioconductor package for differential expression analysis of digital gene expression data. *Bioinformatics* 26:139-140.
- Rogakou EP, Boon C, Redon C, and Bonner WM (1999). Megabase chromatin domains involved in DNA double-strand breaks in vivo. *J Cell Biol* 146:905-916.
- Rolland AD, Lavigne R, Daully C, Calvel P, Kervarrec C, Freour T, Evrard B, Rioux-Leclercq N, Auger J, and Pineau C (2013). Identification of genital tract markers in the human seminal plasma using an integrative genomics approach. *Hum Reprod* 28:199-209.
- Ross MT, Grafham DV, Coffey AJ, Scherer S, McLay K, Muzny D, Platzer M, Howell GR, Burrows C, Bird CP, et al. (2005). The DNA sequence of the human X chromosome. *Nature* 434:325-337.
- Royo H, Polikiewicz G, Mahadevaiah SK, Prosser H, Mitchell M, Bradley A, de Rooij DG, Burgoyne PS, and Turner JM (2010). Evidence that meiotic sex chromosome inactivation is essential for male fertility. *Curr Biol* 20:2117-2123.
- Royo H, Prosser H, Ruzankina Y, Mahadevaiah SK, Cloutier JM, Baumann M, Fukuda T, Hoog C, Toth A, de Rooij DG, et al. (2013). ATR acts stage specifically to regulate multiple aspects of mammalian meiotic silencing. *Genes Dev* 27:1484-1494.
- Russell LD, Ertlin RA, Sinha Hikim AP, and Clegg ED (1990). Histological and histopathological evaluation of the testis (Clearwater, FL, USA, Cache River Press).
- Schoenmakers S, Wassenaar E, Hoogerbrugge JW, Laven JS, Grootegoed JA, and Baarends WM (2009). Female meiotic sex chromosome inactivation in chicken. *PLoS Genet* 5:e1000466.

- Schoenmakers S, Wassenaar E, Laven JS, Grootegoed JA, and Baarends WM (2010). Meiotic silencing and fragmentation of the male germline restricted chromosome in zebra finch. *Chromosoma* 119:311-324.
- Schwacha A, and Kleckner N (1997). Interhomolog bias during meiotic recombination: meiotic functions promote a highly differentiated interhomolog-only pathway. *Cell* 90:1123-1135.
- Sciurano RB, Rahn MI, Rossi L, Luaces JB, Merani MS, and Solari AJ (2012). Synapsis, recombination, and chromatin remodeling in the XY body of armadillos. *Chromosome Res* 20:293-302.
- Sin HS, Ichijima Y, Koh E, Namiki M, and Namekawa SH (2012). Human postmeiotic sex chromatin and its impact on sex chromosome evolution. *Genome Res* 22:827-836.
- Smagulova F, Gregoret IV, Brick K, Khil P, Camerini-Otero RD, and Petukhova GV (2011). Genome-wide analysis reveals novel molecular features of mouse recombination hotspots. *Nature* 472:375-378.
- Solari AJ (1970). The spatial relationship of the X and Y chromosomes during meiotic prophase in mouse spermatocytes. *Chromosoma* 29:217-236.
- Solari AJ (1974). The behavior of the XY pair in mammals. *Int Rev Cytol* 38:273-317.
- Solari AJ, and Pigozzi MI (1994). Fine structure of the XY body in the XY1Y2 trivalent of the bat *Artibeus lituratus*. *Chromosome Res* 2:53-58.
- Song HW, Anderson RA, Bayne RA, Gromoll J, Shimasaki S, Chang RJ, Parast MM, Laurent LC, de Rooij DG, Hsieh TC, et al. (2013). The RHOX homeobox gene cluster is selectively expressed in human oocytes and male germ cells. *Hum Reprod* 28:1635-1646.
- Song R, Ro S, Michaels JD, Park C, McCarrey JR, and Yan W (2009). Many X-linked microRNAs escape meiotic sex chromosome inactivation. *Nat Genet* 41:488-493.
- Soumillon M, Necsulea A, Weier M, Brawand D, Zhang X, Gu H, Barthes P, Kokkinaki M, Nef S, Gnirke A, et al. (2013). Cellular source and mechanisms of high transcriptome complexity in the mammalian testis. *Cell Rep* 3:2179-2190.
- Trapnell C, Williams BA, Pertea G, Mortazavi A, Kwan G, van Baren MJ, Salzberg SL, Wold BJ, and Pachter L (2010). Transcript assembly and quantification by RNA-Seq reveals unannotated transcripts and isoform switching during cell differentiation. *Nat Biotechnol* 28:511-515.
- Tres LL (1977). Extensive pairing of the XY bivalent in mouse spermatocytes as visualized by whole-mount electron microscopy. *J Cell Sci* 25:1-15.
- Turner JM (2007). Meiotic sex chromosome inactivation. *Development* 134:1823-1831.
- Turner JM, Mahadevaiah SK, Ellis PJ, Mitchell MJ, and Burgoyne PS (2006). Pachytene asynapsis drives meiotic sex chromosome inactivation and leads to substantial postmeiotic repression in spermatids. *Dev Cell* 10:521-529.
- Turner JM, Mahadevaiah SK, Fernandez-Capetillo O, Nussenzweig A, Xu X, Deng CX, and Burgoyne PS (2005). Silencing of unsynapsed meiotic chromosomes in the mouse. *Nat Genet* 37:41-47.
- van der Heijden GW, Derijck AA, Posfai E, Giele M, Pelczar P, Ramos L, Wansink DG, van der Vlag J, Peters AH, and de Boer P (2007). Chromosome-wide nucleosome replacement and H3.3 incorporation during mammalian meiotic sex chromosome inactivation. *Nat Genet* 39:251-258.
- Villagomez DA (1993). Zygotene-pachytene sub-staging and synaptonemal complex karyotyping of boar spermatocytes. *Hereditas* 118:87-99.
- von Kopylow K, Kirchhoff C, Jezek D, Schulze W, Feig C, Primig M, Steinkraus V, and Spiess AN (2010). Screening for biomarkers of spermatogonia within the human testis: a whole genome approach. *Hum Reprod* 25:1104-1112.
- Wojtasz L, Cloutier JM, Baumann M, Daniel K, Varga J, Fu J, Anastassiadis K, Stewart AF, Remenyi A, Turner JM, et al. (2012). Meiotic DNA double-strand breaks and chromosome asynapsis in mice are monitored by distinct HORMAD2-independent and -dependent mechanisms. *Genes Dev* 26:958-973.
- Wojtasz L, Daniel K, Roig I, Bolcun-Filas E, Xu H, Boonsanay V, Eckmann CR, Cooke HJ, Jasin M, Keeney S, et al. (2009). Mouse HORMAD1 and HORMAD2, two conserved meiotic chromosomal proteins, are depleted from synapsed chromosome axes with the help of TRIP13 AAA-ATPase. *PLoS Genet* 5:e1000702.
- Yang F, and Wang PJ (2009). The Mammalian synaptonemal complex: a scaffold and beyond. *Genome Dyn* 5:69-80.

Young AC, Kirkness EF, and Breen M (2008). Tackling the characterization of canine chromosomal breakpoints with an integrated in-situ/in-silico approach: the canine PAR and PAB. *Chromosome Res* 16:1193-1202.

Zwick MS, Hanson RE, Islam-Faridi MN, Stelly DM, Wing RA, Price HJ, and McKnight TD (1997). A rapid procedure for the isolation of C0t-1 DNA from plants. *Genome* 40:138-142.





CHAPTER 4

Table S1: Analyses of dog germ cell purity

	Spermatocytes	Spermatids	Cytoplasm	Others	Spermatids	Spermatocytes	Cytoplasm	Others
Dog 4	86	16	2	3	140	2	17	6
Dog5	95	18	4	9	101	1	12	8
Dog6	94	9	1	7	116	1	15	4
Tot.	265 (79.3%)	43 (12.9%)	7 (2.1%)	19 (5.7%)	357 (84.4%)	4 (0.9%)	44 (10.4%)	18 (4.3%)

Table S2: Relative expression levels of spermatocyte genes in mouse and dog spermatids

Spermatocyte gene	Dog log2 fold change spt/spc	Mouse log2 fold change spt/spc
<i>Sycp1/SYCP1</i>	-0.46	-0.42
<i>Sycp2/SYCP2</i>	-2.88	-1.38
<i>Sycp3/SYCP3</i>	-1.07	-1.11
Average	-1.47	-0.97

Table S3: Relative expression levels of spermatid genes in mouse and dog spermatids

Spermatid gene	Dog log2 fold change spt/spc	Mouse log2 fold change spt/spc
<i>Tnp1/TNP1</i>	3.76	3.54
<i>Tnp2/TNP2</i>	4.02	3.51
<i>Prm1/PRM1</i>	n.a.	3.51
<i>Prm2/PRM2</i>	3.86	3.80
<i>Prm3/PRM3</i>	2.75	3.18
Average	3.60	3.51

Table S4: Comparison between Cufflinks and edgeR results

	# diff. expressed genes	# in common (%)	# sign and >1.5 fold up	# in common (%)	# sign and >1.5 fold down	# in common (%)	# sign and >1.5 fold up X	# in common (%)	# sign and >1.5 fold down X	# in common (%)
Cufflinks	9679	8661 (89)	4632	4323 (94)	4220	4094 (97)	207	197 (95)	126	116 (92)
edgeR	9904	8661 (87)	4828	4323 (90)	4919	4094 (83)	224	197 (88)	160	116 (73)

Table S5: Differentially expressed dog X-linked genes homologous to mouse and/or human multicopy genes

Down in spermatids	Up in spermatids
<i>DDX26B</i>	<i>COL4A6</i>
<i>MAGEB1</i>	<i>GLRA2</i>
<i>MAGEB4</i>	<i>GLRA4</i>
<i>MAGED1</i>	<i>H2BFWT</i>
<i>MAOB</i>	<i>MAGEB10</i>
<i>NGFRAP1</i>	<i>MAGEB5</i>
<i>RAB9A</i>	<i>MAOA</i>
<i>SHROOM2</i>	<i>MID2</i>
<i>SLC9A6</i>	<i>PHKA2</i>
<i>SSX5</i>	<i>PRPS2</i>
<i>TCEAL4</i>	<i>RAB9B</i>
<i>ZNF182</i>	<i>SCML1</i>
<i>ZNF185</i>	<i>SCML2</i>
<i>ZNF280C</i>	<i>SPACA5</i>
	<i>TGIF2LX</i>
	<i>ZCCHC12</i>
	<i>ZNF711</i>
	<i>ZNF81</i>

Table S6: Average FPKM values of gene expression in dog

	Genome	Chr 1	X	PAR
SPERMATOCYTES	27.05	28.31	6.15	2.46
SPERMATIDS	37.92	35.18	22.87	2.71

INCOMPLETE MEIOTIC SEX CHROMOSOME INACTIVATION IN THE DOG

Table S7: Expression of *SLC25A* variants in spermatocytes and spermatids of mouse man and dog

DOG (RNA-seq)				MOUSE (RNA-seq)			MAN (microarray)		
gene	chr	spc (FPKM)	spt (FPKM)	chr	spc (FPKM)	spt (FPKM)	chr	spc	spt
<i>SLC25A4</i>	16	5.77	2.06	8	6.18	2.81	4	26.44	13.83
<i>SLC25A5</i>	X	4.08	1.77	X	8.50	2.38	X	159.86	297.73
<i>SLC25A6</i>	X(PAR)	47.19	18.11	-	-	-	X(PAR)	113.95	163.43
<i>SLC25A31</i>	19	34.76	20.54	3	34.10	16.26	4	265.19	75.93

Table S8: Molecular and cellular functions associated with X-linked genes upregulated in spermatids of dog and mouse

Category	p-value	Genes
Cell Morphology	9.44E-04-4.66E-02	<i>PHEX, AKAP4, PAK3, CDK16, TAF7L, MAOA, HMGB3</i>
DNA Replication, Recombination, and Repair	2.08E-03-3.94E-02	<i>HUWE1, CUL4B, CETN2, UBE2A, TEX11, ERCC6L</i>
Cell Signaling	2.37E-03-4.33E-02	<i>PRKX, TAF1, AKAP4, PDK3, MED12, MED14</i>
Post-Translational Modification	2.37E-03-3.17E-02	<i>HUWE1, CDKL5, OGT, PRKX, TAF1, UBE2A, RLIM, UBA1, ASB9, PDK3, MAOA</i>
Protein Synthesis	2.37E-03-3.56E-02	<i>CUL4B, PRKX, TAF1, RLIM, EIF1AX, ASB9, PDK3</i>
Molecular Transport	3.49E-03-1.99E-02	<i>PHEX, SLC35A2, RPGR, MAOA</i>
Nucleic Acid Metabolism	3.49E-03-1.99E-02	<i>CTPS2, SLC35A2, RPGR</i>
Small Molecule Biochemistry	3.49E-03-4.33E-02	<i>OGT, CTPS2, SLC35A2, RPGR, SMS, MAOA</i>
Carbohydrate Metabolism	4.02E-03-2.39E-02	<i>OGT, SLC35A2</i>
Cell Death and Survival	4.02E-03-4.98E-02	<i>HUWE1, OGT, UXT, ATP11C, PAK3, BGN, SH3BP1, MAOA</i>
Cell-To-Cell Signaling and Interaction	4.02E-03-4.71E-02	<i>CDKL5, OGT, OPHN1, PAK3, RLIM, BGN, MAOA</i>
Cellular Assembly and Organization	4.02E-03-3.94E-02	<i>OPHN1, PAK3, OFD1, TEX11, MAOA</i>
Cellular Development	4.02E-03-4.71E-02	<i>CUL4B, RLIM, BGN, USP9X, CDK16, ZFX, TEX11, TAF7L</i>
Cellular Function and Maintenance	4.02E-03-1.99E-02	<i>PHEX, OPHN1, OFD1, MAOA</i>
Cellular Growth and Proliferation	4.02E-03-4.33E-02	<i>CUL4B, CETN2, RLIM, BGN</i>
Drug Metabolism	4.02E-03-2.39E-02	<i>MAOA</i>
Gene Expression	4.02E-03-1.72E-02	<i>MED12, MED14, TXLNG</i>
Cell Cycle	8.01E-03-3.17E-02	<i>RLIM, ERCC6L</i>
Cellular Movement	8.01E-03-4.11E-02	<i>CDKL5, AKAP4, TAF7L, MAOA</i>
Energy Production	8.01E-03-1.6E-02	<i>MAOA</i>
Lipid Metabolism	1.6E-02-1.6E-02	<i>SLC35A2</i>
Protein Degradation	3.06E-02-3.06E-02	<i>CUL4B, RLIM, ASB9</i>
Amino Acid Metabolism	3.17E-02-3.17E-02	<i>SMS</i>
RNA Post-Transcriptional Modification	4.71E-02-4.71E-02	<i>CSTF2</i>

Table S9: X-linked genes upregulated in spermatids of mouse, human, and dog

	Gene	Mouse knockout	Molecular function	Putative function in spermatogenesis
Structural components	<i>AKAP14</i>	-	A-kinase-anchoring protein	Ciliary beat frequency (Kultgen et al., 2002)
	<i>AKAP4</i>	immotile sperm (Miki et al., 2002)	A-kinase-anchoring protein	Fibrous sheet formation
	<i>CDK16</i>	malformed sperm , reduced motility (Mikolcevic et al., 2012)	Cyclin dependent kinase	Annulus formation
	<i>OFD1</i>	embryonic lethal (Ferrante et al., 2006) Mutations in the human ortholog are associated with Oral-facial-digital type 1 (OFD1; MIM 311200) syndrome and Simpson-Golabi-Behmel syndrome type 2	Centrosome associated proteins, involved in Cilia formation (D'Angelo et al., 2012). Removal through autophagy is essential for proper cilia function (Tang et al., 2013)	
	<i>CYLC1</i>	-	Cyclin, basic protein, structural component of cytoskeleton	Component of sperm head cytoskeleton (Hess et al., 1993)
Ubiquitin pathway	<i>ASB12</i>	-	The ankyrin repeat and SOCS box (ASB) family, forms E3 complex with Cul5-Rbx2	Ubiquitylation (Kohroki et al., 2005)
	<i>CUL4B</i>	embryonic lethal, epiblast-specific knockout is viable, reproduction not analysed (Liu et al., 2012)	Component of E3 ligase complex	Ubiquitylation
	<i>UBA1</i>	-	Ubiquitin-activating enzyme	Ubiquitylation
Mitochondrial enzymes	<i>DUSP21</i>	-	Mitochondrial membrane phosphatase (Rardin et al., 2008)	
	<i>MAOA</i>	fertile, aggressive behaviour (Cases et al., 1995)	Monoamine oxidase A degrades serotonin and norepinephrine. Mitochondrial enzyme	
Transcription regulation	<i>TAF1</i>	-	Largest subunit of TFIID, transcriptional regulation	
	<i>TAF7L</i>	reduced sperm numbers and quality, fertile (Cheng et al., 2007)	Regulation of transcription program together with TAF1	
	<i>IQSEC2</i>	human mutations cause nonsyndromic intellectual disability (Shoubridge et al., 2010)	Guanine nucleotide exchange factor for the ADP-ribosylation factor family of small GTPases, involved in membrane trafficking and actin dynamics	
	<i>TBC1D25</i>	-	Rab GTPase-activating protein involved in autophagy (Popovic et al., 2012)	
	<i>CDKL5</i>	neurodevelopmental disorder, fertile (Wang et al., 2012)	Cyclin-dependent kinase-like	
	<i>CXORF27</i>	-	Huntingtin interacting protein with histone fold (Marino-Ramirez et al., 2006)	
	<i>GSPT2</i>	-	Polypeptide release factor (translation termination) (Le Goff et al., 2002)	
	<i>TEX13A</i>	-	Testis-specific gene possibly involved in mRNA processing (Nguyen et al., 2011)	
	<i>PPEF1</i>	fertile, no clear phenotype (Ramulu et al., 2001)	Calcium binding phosphatase	
	<i>RIBC1</i>	-	The RIB43A domain with coiled coils 1 ( <i>RIBC1</i> ) gene with unknown function	
	<i>TEX28</i>	-	Testis-specific single exon gene of unknown function (Hanna et al., 1997)	



## REFERENCES

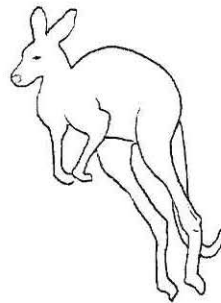
- Cases O, Seif I, Grimsby J, Gaspar P, Chen K, Pournin S, Muller U, Aguet M, Babinet C, Shih JC, et al. (1995). Aggressive behavior and altered amounts of brain serotonin and norepinephrine in mice lacking MAOA. *Science* 268:1763-1766.
- Cheng Y, Buffone MG, Kouadio M, Goodheart M, Page DC, Gerton GL, Davidson I, and Wang PJ (2007). Abnormal sperm in mice lacking the Taf71 gene. *Mol Cell Biol* 27:2582-2589.
- D'Angelo A, De Angelis A, Avallone B, Piscopo I, Tammaro R, Studer M, and Franco B (2012). *Odf1* controls dorso-ventral patterning and axoneme elongation during embryonic brain development. *PLoS One* 7:e52937.
- Ferrante MI, Zullo A, Barra A, Bimonte S, Messaddeq N, Studer M, Dolle P, and Franco B (2006). Oral-facial-digital type I protein is required for primary cilia formation and left-right axis specification. *Nat Genet* 38:112-117.
- Hanna MC, Platts JT, and Kirkness EF (1997). Identification of a gene within the tandem array of red and green color pigment genes. *Genomics* 43:384-386.
- Hess H, Heid H, and Franke WW (1993). Molecular characterization of mammalian cyclin, a basic protein of the sperm head cytoskeleton. *J Cell Biol* 122:1043-1052.
- Kohroki J, Nishiyama T, Nakamura T, and Masuho Y (2005). ASB proteins interact with Cullin5 and Rbx2 to form E3 ubiquitin ligase complexes. *FEBS Lett* 579:6796-6802.
- Kultgen PL, Byrd SK, Ostrowski LE, and Milgram SL (2002). Characterization of an A-kinase anchoring protein in human ciliary axonemes. *Mol Biol Cell* 13:4156-4166.
- Le Goff C, Zemlyanko O, Moskalenko S, Berkova N, Inge-Vechtomov S, Philippe M, and Zhouravleva G (2002). Mouse GSPT2, but not GSPT1, can substitute for yeast eRF3 in vivo. *Genes Cells* 7:1043-1057.
- Liu L, Yin Y, Li Y, Prevedel L, Lacy EH, Ma L, and Zhou P (2012). Essential role of the CUL4B ubiquitin ligase in extra-embryonic tissue development during mouse embryogenesis. *Cell Res* 22:1258-1269.
- Marino-Ramirez L, Hsu B, Baxevanis AD, and Landsman D (2006). The Histone Database: a comprehensive resource for histones and histone fold-containing proteins. *Proteins* 62:838-842.
- Miki K, Willis WD, Brown PR, Goulding EH, Fulcher KD, and Eddy EM (2002). Targeted disruption of the *Akap4* gene causes defects in sperm flagellum and motility. *Dev Biol* 248:331-342.
- Mikolcovic P, Sigl R, Rauch V, Hess MW, Pfaller K, Barisic M, Pelliniemi LJ, Boesl M, and Geley S (2012). Cyclin-dependent kinase 16/PCTAIRE kinase 1 is activated by cyclin Y and is essential for spermatogenesis. *Mol Cell Biol* 32:868-879.
- Nguyen CD, Mansfield RE, Leung W, Vaz PM, Loughlin FE, Grant RP, and Mackay JP (2011). Characterization of a family of RanBP2-type zinc fingers that can recognize single-stranded RNA. *J Mol Biol* 407:273-283.
- Popovic D, Akutsu M, Novak I, Harper JW, Behrends C, and Dikic I (2012). Rab GTPase-activating proteins in autophagy: regulation of endocytic and autophagy pathways by direct binding to human ATG8 modifiers. *Mol Cell Biol* 32:1733-1744.
- Ramulu P, Kennedy M, Xiong WH, Williams J, Cowan M, Blesh D, Yau KW, Hurley JB, and Nathans J (2001). Normal light response, photoreceptor integrity, and rhodopsin dephosphorylation in mice lacking both protein phosphatases with EF hands (PPEF-1 and PPEF-2). *Mol Cell Biol* 21:8605-8614.
- Rardin MJ, Wiley SE, Murphy AN, Pagliarini DJ, and Dixon JE (2008). Dual specificity phosphatases 18 and 21 target to opposing sides of the mitochondrial inner membrane. *J Biol Chem* 283:15440-15450.
- Shoubbridge C, Walikonis RS, Gecz J, and Harvey RJ (2010). Subtle functional defects in the Arf-specific guanine nucleotide exchange factor IQSEC2 cause non-syndromic X-linked intellectual disability. *Small GTPases* 1:98-103.
- Tang Z, Lin MG, Stowe TR, Chen S, Zhu M, Stearns T, Franco B, and Zhong Q (2013). Autophagy promotes primary ciliogenesis by removing OFD1 from centriolar satellites. *Nature* 502:254-257.
- Wang IT, Allen M, Goffin D, Zhu X, Fairless AH, Brodtkin ES, Siegel SJ, Marsh ED, Blendy JA, and Zhou Z (2012). Loss of CDKL5 disrupts kinome profile and event-related potentials leading to autistic-like phenotypes in mice. *Proc Natl Acad Sci U S A* 109:21516-21521.



# 5

Male specific response to unsynapsed  
chromatin in meiotic prophase of mammals

Work in progress







**Male specific response to unsynapsed chromatin in meiotic prophase of mammals**

Federica Federici<sup>1</sup>, Godfried W. van der Heijden<sup>2</sup>, Evelyne Wassenaar<sup>1</sup>, Andre Nussenzweig<sup>3</sup>, Joop SE Laven<sup>2</sup>, J. Anton Grootegoed<sup>1</sup>, and Willy M. Baarends<sup>1\*</sup>

<sup>1</sup>Department of Reproduction and Development, Erasmus MC University Medical Center, Rotterdam, The Netherlands

<sup>2</sup>Department of Obstetrics and Gynaecology, Erasmus MC University Medical Center, Rotterdam, The Netherlands

<sup>3</sup>Laboratory of Genome Integrity, National Cancer Institute, National Institutes of Health, Bethesda, Maryland 20892, USA

\*Corresponding author



**ABSTRACT**

Among eutherian mammals, meiotic sex chromosome inactivation (MSCI) leads to formation of the XY body in male meiotic prophase, in pachytene spermatocytes. MSCI is related to an even more widely conserved mechanism for meiotic silencing of unsynapsed chromatin (MSUC), which shuts down transcription in chromosome regions that fail to form a synaptonemal complex with a homologous partner and remain unsynapsed. MSUC can occur in both male and female meiotic prophase. MSCI and MSUC in mouse and human spermatocytes are associated with an exceptional chromosome wide remodelling of nucleosomes, by exchange of H3.1 and H3.2 by the H3.3 variant. Here, we show that this nucleosome remodelling occurs only in meiotic spermatocytes, not in oocytes. It requires formation of  $\gamma$ H2AX, but occurs independent of histone ubiquitination by the E3 ligase RNF8. The meiotic exchange of histone variants in spermatocytes, during the formation of the sex body by MSCI, was found to be conserved among eutherian mammals, and also occurs in the metatherian *Monodelphis domestica* (opossum), but not in the metatherian *Macropus rufogrisus* (Bennet's wallaby). This suggests that the MSCI-associated nucleosome remodelling, involving exchange of histone variants, evolved before the split between metatherians and eutherians.



## INTRODUCTION

Spermatogenesis in mammals is associated with major chromatin reorganization events. Next to the exchange of histones, by transition proteins first, and subsequently by protamines, during chromatin compaction in late spermatogenesis, histone variants have a prominent role in the strictly organised differentiation and maturation events that take place at earlier steps of spermatogenesis (Kimmins and Sassone-Corsi, 2005). It is well known that testis-specific or testis-enriched histone variants are expressed at specific steps to partially replace the canonical histones (reviewed by (Rathke et al., 2014)). However, the precise function of most of these variants has not yet been determined, although it was recently established that TH2B, which replaces more than 75% of canonical H2B in pachytene spermatocytes, in the prophase of the first meiotic division, is important for correct regulation of the histone-to-protamine transition that occurs later, in haploid spermatids (Montellier et al., 2013). It is thought that, by changing the physical structure of nucleosomes, TH2B may facilitate nucleosome disassembly later on. Replacement of canonical H2A and H2B involves exchange of H2A/H2B heterodimers without disruption of the nucleosome core particle. On the other hand, exchange of H3 and/or H4 leads to complete dissolution of nucleosomes. Three H3 variants are known to be expressed in both somatic and testicular cells of rat and mouse: H3.1 and H3.2, that are both incorporated during S phase, and H3.3 which is incorporated when nucleosome eviction has occurred in other phases of the cell cycle (Tagami et al., 2004). In addition, testis-specific TH3 is known to replace part of the other H3 variants during the initial phase of spermatogenesis, in mitotic spermatogonia, and remains present in the developing germ cells thereafter (Trostle-Weige et al., 1984).

Here we have investigated the extensive chromosome-wide exchange of H3.1 and H3.2 by the variant H3.3 (also termed nucleosome exchange or renewal) in the chromatin of the sex chromosomes in spermatocytes (van der Heijden et al., 2007). This chromatin remodelling process has been shown to occur concomitantly to initiation of meiotic sex chromosome inactivation (MSCI) in spermatocytes of mouse and man (de Vries et al., 2012; van der Heijden et al., 2007). MSCI is a consequence of the special properties of the XY chromosome pair. During meiotic prophase, all chromosomes need to associate with their homologous partner and exchange genetic information via homologous recombination. The sex chromosomes share homology only in a relatively short pseudoautosomal region (PAR). Thus, actual chromosome pairing and stable association is limited to this region, and the synaptonemal complex, a protein structure that connects paired chromosomal axes, is completely formed only in the PAR. Thus, most of the X and Y chromosomal arms remain unsynapsed, when all autosomes achieve full synapsis. This can be visualized by immunostaining for SYCP3, a protein that lo-

calizes to the axial elements of the synaptonemal complex. When the autosomes are synapsed, only one SYCP3 stretch can be observed between the two homologous chromosomes, while separate SYCP3 stretches are detected on the heterologous X and Y chromosomes, respectively. The unsynapsed XY chromatin is sequestered in the nuclear periphery, and MSCI initiates, forming the XY body, when the autosomes engage in a transcriptional burst (Monesi, 1965). MSCI depends on the accumulation of a phosphorylated form of the H2A variant H2AX, termed  $\gamma$ H2AX (Fernandez-Capetillo et al., 2003). In mouse,  $\gamma$ H2AX decorates the XY body from early pachytene up to the first meiotic metaphase (Mahadevaiah et al., 2001).

MSCI is thought to be a specialization of a more general mechanism, named meiotic silencing of unsynapsed chromatin (MSUC). When autosomal chromosomes fail to synapse, for example in case of a translocation,  $\gamma$ H2AX accumulates and MSUC is initiated (Baarends et al., 2005; Turner et al., 2005). MSUC has been reported to occur in both spermatocytes and oocytes. The initiation of both MSCI and MSUC depends on meiosis-specific proteins (HORMADs) that recognize unsynapsed axes, most likely in combination with the presence of unrepaired meiotic DNA double strand breaks (DSBs) (Carofiglio et al., 2013; Daniel et al., 2011; Turner et al., 2006). These DSBs are induced throughout the genome early in meiotic prophase, and are required for initiation of meiotic homologous recombination, and also help in the establishment of homologous chromosome interactions (Baudat et al., 2000; Mahadevaiah et al., 2001; Romanienko and Camerini-Otero, 2000). Activation of the kinase ATR along chromatin associated with unsynapsed chromosomal axes, acting together with the checkpoint protein MDC1, then mediates accumulation of  $\gamma$ H2AX (Ichijima et al., 2011; Royo et al., 2013; Turner et al., 2004). If MSCI fails, spermatocytes arrest and enter an apoptotic pathway due to illegitimate toxic expression of X- and Y-encoded genes (Royo et al., 2010). This pathway functions as a “pachytene checkpoint”, as follows: when overall chromosome pairing and/or DSB repair are affected, the proteins that mediate MSCI are redistributed to many autosomal sites and fail to accumulate to a high enough density at the sex chromosomes, leading to incomplete silencing of X and Y gene transcription, which then kills the cells. In spermatocytes, MSUC is also associated with exchange of H3.1/2 by nucleosomes containing the H3.3 histone variant (van der Heijden et al., 2007). The temporal overlap between MSUC/MSCI and this nucleosome renewal suggests a causal link between these events. However, it is not clear whether this is the case. In addition, there is a tight connection between the repair of meiotic DSBs, nucleosome exchange, and both MSCI and MSUC.

Here, we aimed to obtain more information about the possible mechanism of H3.1/2 eviction, and its biological relevance. We made use of *Spo11*, *H2ax* and *Mdc1* knockout mouse models to determine the prerequisites for nucleosome exchange. In addition we used a comparative approach, between sexes and between species, to study the evolutionary conservation

of this mechanism, to assess its possible biological relevance. We show that  $\gamma$ H2AX is essential but not sufficient for nucleosome exchange, since no H3.1/2 eviction is observed in MSUC regions that also accumulate  $\gamma$ H2AX in oocytes, and *Spo11*<sup>-/-</sup> spermatocytes. Absence of this chromatin remodelling process in female MSUC suggests a sex-specific difference in response to unsynapsed chromatin. Furthermore, we observed XY body associated nucleosome exchange among 5 different eutherian mammals tested (each representing a different mammalian order), which indicates a functional conservation. However, among the marsupials, we observed XY body associated nucleosome exchange in opossum (*Monodelphis domestica*), but not in Bennet's wallaby (*Macropus rufogrisus*). The *Macropus* lineage diverged from the *Monodelphis* lineage, approximately 70 million years ago (O'Leary et al., 2013). Thus it appears that the nucleosome exchange on the XY body chromatin may have evolved prior to the eutherian-metatherian split, some 165 million years ago (O'Leary et al., 2013) and was not maintained in the *Macropus* lineage.



## RESULTS

### Histone eviction depends on $\gamma$ H2AX formation

H3.1/2 exchange for H3.3 is initiated in early-to-midpachytene spermatocytes in mouse, and thus appears to be a relatively early event in the MSCI pathway (van der Heijden et al., 2007). The earliest known marker of MSCI is  $\gamma$ H2AX, and the phosphorylation of H2AX has been shown to be essential for MSCI (Royo et al., 2013). To assess the role of  $\gamma$ H2AX formation in H3.1/2 eviction we used two mouse models: the *H2ax* knockout (Fernandez-Capetillo et al., 2003) and the *Mdc1* knockout (Lou et al., 2006). In *H2ax* knockout males, autosomal chromosome pairing and meiotic recombination are normally initiated and completed, but the X and Y chromosomes remain frequently asynapsed and fail to undergo MSCI (Fernandez-Capetillo et al., 2003). As a consequence, there is an arrest of spermatogenesis at midpachytene, when the spermatocytes enter an apoptotic pathway. Mediator of DNA damage checkpoint 1 (MDC1) interacts with  $\gamma$ H2AX and is required for complete activation of the H2AX phosphorylating cascade, leading to robust spreading of  $\gamma$ H2AX in the chromatin surrounding DNA damage in somatic cells, and in the XY body in spermatocytes (Ichijima et al., 2011; Lou et al., 2006). In *Mdc1* knockout spermatocytes,  $\gamma$ H2AX formation on the XY body is restricted to very limited regions on the chromosomal axes, and MSCI is also not achieved (Ichijima et al., 2011). Thus, *Mdc1* knockout spermatocytes arrest at midpachytene, as *H2ax* knockout spermatocytes. When we analysed H3.1/2 staining in wild type, *H2ax* knockout, and *Mdc1* knockout pachytene spermatocytes, we observed a complete lack of H3.1/2 eviction in the two knockout models (n=100 nuclei; two animals analyzed per genotype). Remodelling was not apparent even in the most advanced pachytene nuclei present in the cell preparations, as assessed by staining for the midpachytene marker H1T (Figure 1A-C). In pachytene spermatocytes from *H2ax* heterozygous mice we observed somewhat reduced accumulation of  $\gamma$ H2AX on the XY body, but the pattern and extent of H3.1/2 eviction were indistinguishable from wild type controls (data not shown).

A histone-modifying event that follows shortly after  $\gamma$ H2AX accumulation on the XY body is histone ubiquitination by the E3 ubiquitin ligase RNF8 (Lu et al., 2010). RNF8-dependent ubiquitination of histones has been implicated in the genome-wide removal of histones prior to the incorporation of transition proteins and protamines during nuclear condensation in postmeiotic spermatids (Lu et al., 2010). In addition, in somatic cells, ubiquitination of histones by RNF8 occurs in association with chromatin remodelling events that accompany repair of DSBs (Luijsterburg et al., 2012). We sought to investigate whether histone ubiquitination was also responsible for the chromatin-wide nucleosome exchange at the XY body. In spermatocytes that were isolated from *Rnf8* knockout testes, in which histone ubiquitination

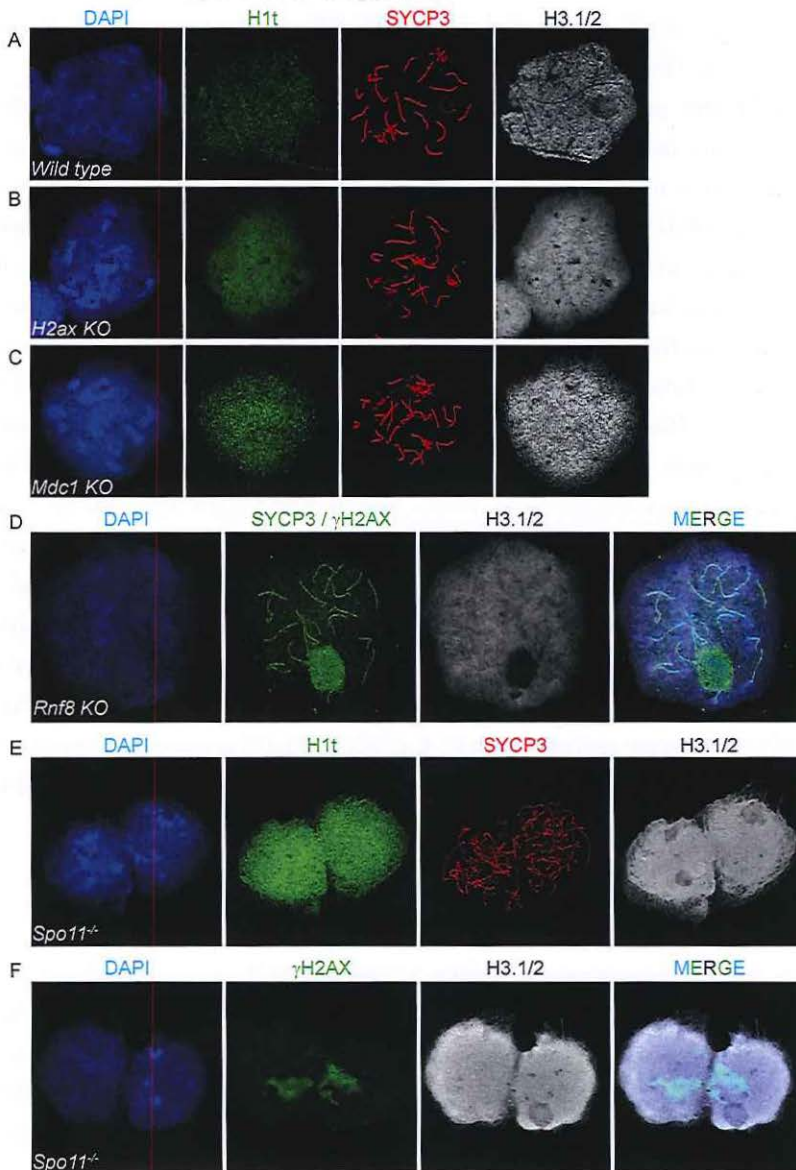


**Figure 1: H3.1/2 eviction from XY body chromatin depends on the accumulation of  $\gamma$ H2AX in this region**

Representative spread nuclei of (A) wild type, (B) *H2ax*, and (C) *Mdc1* knockout mouse spermatocytes stained with antibodies targeting H1T (green), H3.1/2 (white) and SYCP3 (red). The DNA was counterstained with DAPI (blue). (D) Spread nuclei of *Rnf8* knockout mouse spermatocytes stained with antibodies targeting SYCP3 and  $\gamma$ H2AX (green), H3.1/2 (white). The DNA was counterstained with DAPI (blue). *Spo11*<sup>-/-</sup> spread nuclei were immunostained for H1T (green), H3.1/2 (white) (E) and SYCP3 (red) and (F)  $\gamma$ H2AX (green), H3.1/2 (white) and SYCP3 (red). The DNA was counterstained with DAPI (blue).



is abolished (Lu et al., 2010), we observed normal H3.1/2 eviction (n=100 nuclei; two animals analyzed) (Figure 1D).

Since the nucleosome exchange appears to depend on  $\gamma$ H2AX accumulation, and damage-induced DSBs and associated  $\gamma$ H2AX formation also trigger nucleosome exchange in somatic cells (van Attikum and Gasser, 2005), we wondered if H3.1/2 eviction would also occur in spermatocytes of SPO11-deficient mice, where no meiotic DSBs are formed, but where a single  $\gamma$ H2AX domain is encompassing part of the asynapsed chromatin in most nuclei. This domain is referred to as a pseudo XY body, because it is generally not associated with the sex chromosomes. In mice that lack SPO11 activity, either through complete knockout (*Spo11*<sup>-/-</sup>) (Baudat et al., 2000; Romanienko and Camerini-Otero, 2000) or by point mutation of the catalytic site (*Spo11*<sup>trif</sup>) (Carofiglio et al., 2013), homologous chromosome pairing is severely disrupted and the pseudo XY body covers part of the asynapsed chromatin in association with a few endogenous DSBs (Carofiglio et al., 2013). Also in these mutant mice, the spermatocytes enter an apoptotic pathway at pachytene. We thus assessed progression of spermatocytes through pachytene by H1t staining. In *Spo11*<sup>-/-</sup> spermatocytes displaying the H1t signal, we sometimes observed one or two areas, in few nuclei, with a low level of H3.1/2 staining (Figure 1E). However, such areas never colocalized to the pseudo XY body, identified by the  $\gamma$ H2AX domain in *Spo11*<sup>-/-</sup> spermatocytes (Figure 1F) (n=100 nuclei). Although we cannot exclude that SPO11-deficient spermatocytes are lost before H3.1/2 eviction in the pseudo XY body can occur, this indicates that accumulation of  $\gamma$ H2AX by itself may not be enough to trigger the extreme H3.1/2 eviction that is observed in the XY body.

### Histone eviction is a male-specific MSUC-induced event

In males, H3.1/2 eviction occurs not only on the XY body, but also in association with MSUC, that is activated when a pairing problem is generated by the presence of chromosome translocations (van der Heijden et al., 2007). In oocytes, MSUC is activated in 10-15% of wild type oocytes, due to *de novo* induction of DNA damage, and in XO or XY oocytes, in which single sex chromosomes are frequently observed in association with markers of MSUC (Baarends et al., 2005; Carofiglio et al., 2013; Kouznetsova et al., 2009; Turner et al., 2005). It appears that oocytes with extensive accumulation of  $\gamma$ H2AX at pseudo XY bodies (this term is also used for oocytes, even if a Y chromosome is absent; a pseudo XY body can involve exclusively autosomal and X chromosomal chromatin regions) are destined to enter an apoptotic pathway (Malki et al., 2014). Surprisingly, when we analysed H3.1/2 localisation in XO E19.5 oocytes, we observed no H3.1/2 depletion in the areas that accumulated  $\gamma$ H2AX (n=20, one animal analyzed) (Figure 2). This indicates that in mouse, nucleosome remodeling in association with MSUC is male-specific, and confirms that the nucleosome exchange is not directly triggered by the accumulation of  $\gamma$ H2AX as observed in *Spo11*<sup>-/-</sup> spermatocytes.





**Figure 2: No H3.1/2 removal in XO E19.5 oocytes**

Spread nuclei isolated from XO E19.5 ovaries were stained with antibodies targeting  $\gamma$ H2AX (green), H3.1/2 (white) and SYCP3 (red). The DNA was stained with DAPI (blue).

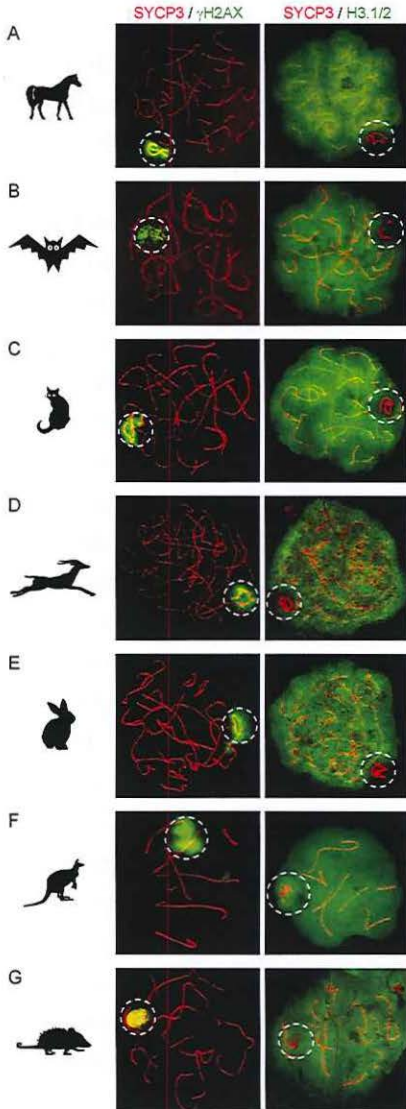


**Figure 3: H3.1/2 exchange is associated with MSCI in eutherian mammals, but is variable in pachytene spermatocytes of metatherians**

Spread pachytene nuclei from cat (A), horse (B), Egyptian fruit bat (C), springbok (D), rabbit (E), Bennet's wallaby (F) and opossum (G) stained with antibodies targeting either  $\gamma$ H2AX (left) or H3.1/2 (right, green) in combination with SYCP3 (red).

5

**XY associated histone 3.1/.2 eviction is conserved among eutherian mammals, and occurs also in the metatherian infraclass, in *Monodelphis domestica* but not in *Macropus rufogriseus*.**

Previously, it has been established that nucleosome exchange on the XY body is conserved between mouse and man, with a bit more variability in the degree of remodelling in human samples (de Vries et al., 2012). We analysed nucleosome exchange in relation to  $\gamma$ H2AX accumulation, chromosome pairing and XY body formation in five eutherian mammals (four from the Laurasiatheria superorder: cat (order Carnivora), horse (order Perissodactyla), Egyptian fruit bat (order Chiroptera), and springbok (order Artiodactyla); and one from the Euarchontoglires superorder: rabbit (order Lagomorpha). We first assessed if  $\gamma$ H2AX accumulated on the XY pair in pachytene spermatocytes, and this was clearly observed in all the species ( $n=100$  nuclei analyzed) (Figure 3A-E). In addition, we observed H3.1/2 eviction from the XY body in all investigated eutherians.

Next, we wished to investigate whether nucleosome exchange was also conserved in two marsupial species. An important difference in sex chromosome organisation between eutherians and metatherians is the lack of a pseudoautosomal region in the latter, precluding meiotic crossover formation on the XY chromosome pair in males. Instead, the X and Y are connected by a dense plate, which is built from cohesins and synaptonemal complex proteins, and remains associated with the sex chromosomes until the first metaphase-to-anaphase transition (Page et al., 2006). We assessed H3.1/2 distribution in all the substages of meiotic prophase in testis samples of a Bennet's wallaby (*Macropus rufogriseus*,  $2n=16$ ) and a grey short-tailed opossum (*Monodelphis domestica*  $2n=18$ ). Surprisingly, no H3.1/2 eviction was observed in Bennet's wallaby spermatocytes, whereas a clear H3.1/2 eviction was observed in the XY body of pachytene and diplotene spermatocytes of the opossum ( $n=100$  nuclei) (Figure 3F, G). Based on this differential XY body associated chromatin structure in the two metatherian species, we performed a further comparative analyses to assess if the lack of H3.1/2 eviction in the XY body of spermatocytes from the Bennet's wallaby was correlated to additional differences with the XY body of the opossum. The accumulation pattern of  $\gamma$ H2AX and the appearance and disappearance of the DSB marker RAD51 (Figure 4) appeared to occur in a similar manner in both species. MSCI has previously been described for the opossum (Franco et al., 2007; Namekawa et al., 2007), and was shown to be associated with H3K9me3 accumulation and lack of RNA polymerase II on the XY body. To verify MSCI in the opossum we used an antibody that recognizes the phosphorylated (active) form of RNA polymerase II only, and this staining showed a clear depletion of this form of RNA polymerase II from the XY body in pachytene spermatocytes (Figure 5A, right). Our analyses of opossum spermatocytes largely confirmed previous observations (Namekawa et al., 2007). In the Bennet's wallaby,

although phosphorylated RNA polymerase II was enriched on the part of the XY body that contained the dense plate, it was clearly depleted from the larger loops of the synaptonemal complex protein, SYCP3 (Figure 5A, left). Furthermore, the XY body region appears to have a denser DAPI staining throughout pachytene and later stages of meiotic prophase (diplotene), similar to what was observed for the opossum. Accumulation of the heterochromatin marker H3K9me3 at the XY body progressively increased, starting first on the larger SYCP3 loops, but finally covering the whole XY region, including the dense plate, that is marked by extensive SYCP3 accumulation (Figure 5B).

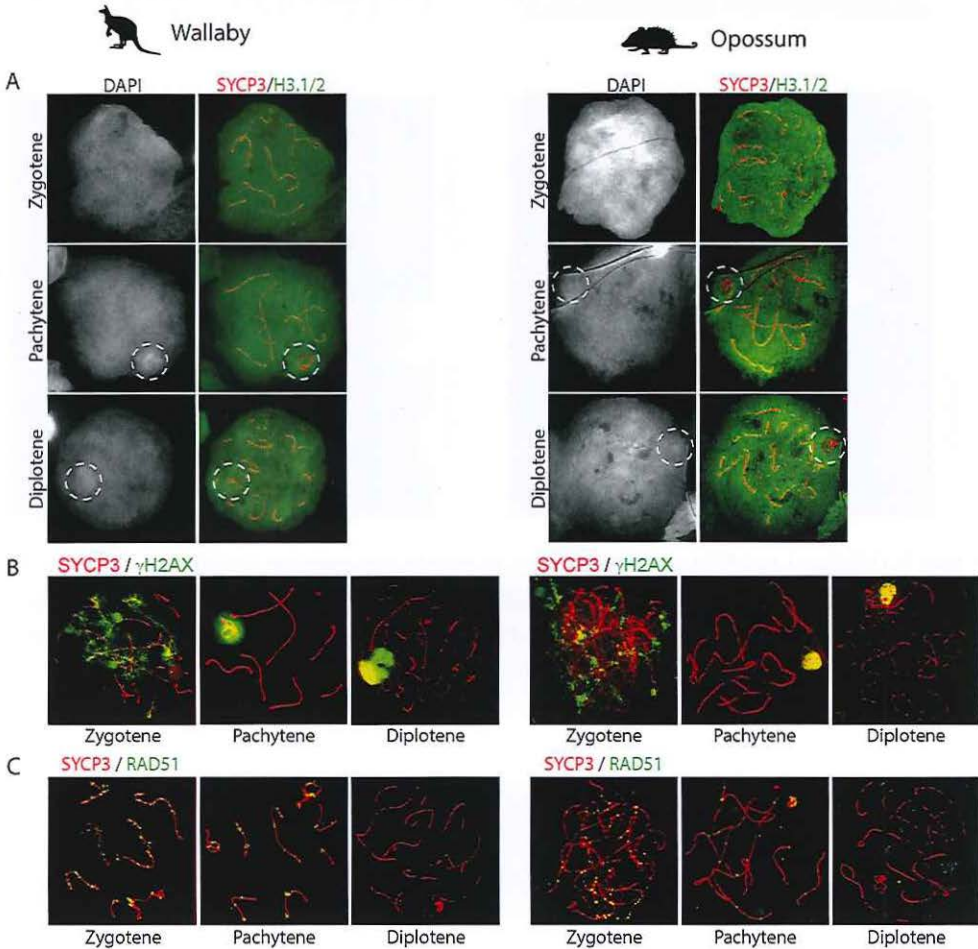


**Figure 4: Progression of histone H3.1/2 eviction, DSB repair and XY body formation in wallaby and opossum**

Spread spermatocyte nuclei from Bennet's wallaby and opossum stained with antibodies targeting H3.1/2 (green) (A),  $\gamma$ H2AX (green) (B) or RAD51 (green) (C) in combination with SYCP3 (red). The DNA was stained with DAPI (white).



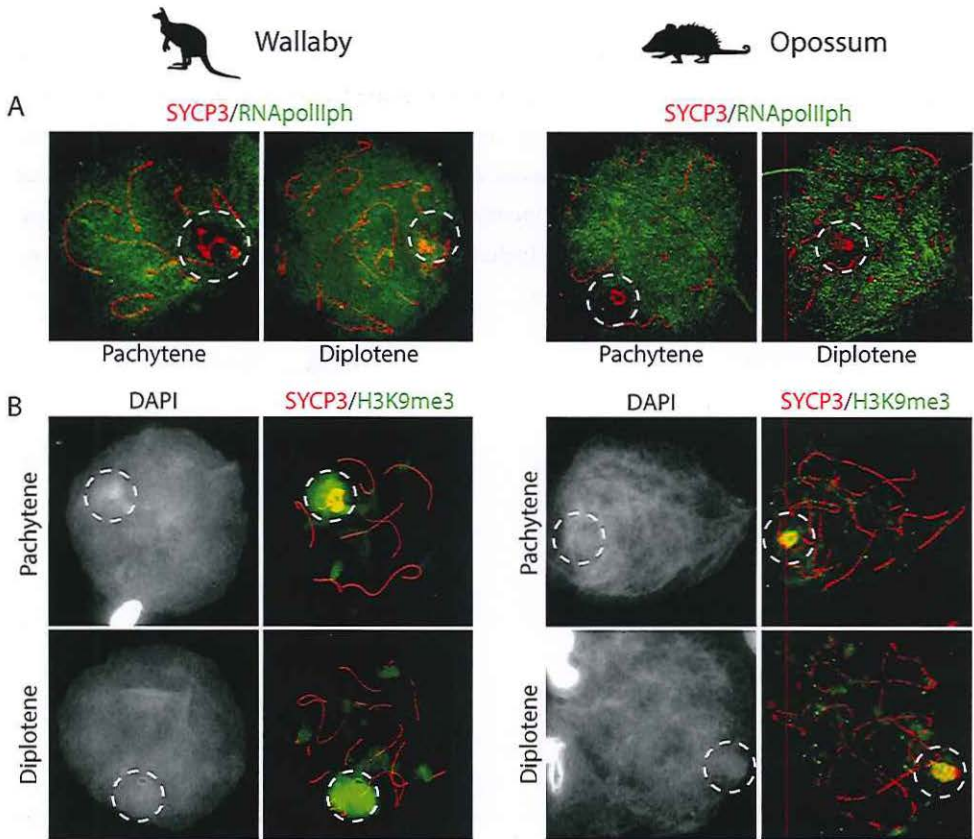


**Figure 5: H3K9me3 and RNA pol II localization in wallaby and opossum spermatocytes**

Spread spermatocyte nuclei from Benner's wallaby and opossum stained with antibodies targeting (A) phosphorylated RNA pol III (green) in combination with SYCP3 (red). (B) H3K9me3 (green) and SYCP3 (red) staining. The DNA was stained with DAPI (white).

## DISCUSSION

### MSUC associated H3.1/2 eviction constitutes a male-specific response to accumulation of $\gamma$ H2AX

MSUC in mammals is thought to be a general phenomenon, occurring in oocytes as well as in spermatocytes (Baarends et al., 2005; Turner et al., 2005). In oocytes, the presence of one or two asynapsed axes (in wild type, XO, or XY oocytes) or formation of a pseudo XY body (in SPO11-deficient oocytes) is associated with accumulation of DSB repair and DNA damage response markers such as RAD51, BRCA1, ATR, RAD18, ubiquitinated histones, and  $\gamma$ H2AX (Baarends et al., 2005; Carofiglio et al., 2013; Kouznetsova et al., 2009; Turner et al., 2005). In addition, we and others have shown global reduction of transcriptional activity in MSUC areas, as investigated through immunolocalization of RNA polymerase II or Cot-1 RNA FISH (Baarends et al., 2005; Carofiglio et al., 2013; Turner et al., 2005). However, several differences in the MSUC response between males and females have been described (Carofiglio et al., 2013; Taketo and Naumova, 2013), and it has been stated that no evidence for transcriptional silencing of unsynapsed chromosomes in oocytes could be obtained (Taketo and Naumova, 2013). One obvious difference between the MSUC response in spermatocytes and oocytes concerns its duration. In male mice, pachytene and diplotene comprise a period of approximately 210 hours, whereas in oocytes only around 60 hours pass between entry into pachytene and the diplotene arrest (Bakken and McClanahan, 1978; Oakberg, 1956). MSCI in spermatocytes is not clearly detectable in the first 50 hours after entry into pachytene, because the overall transcriptional activity is very low during this period (Page et al., 2012). Clear depletion of active RNA polymerase II from the XY body in mouse starts to become evident in midpachytene nuclei. Once MSCI is established, there is at least 150 hours of spermatocyte development during which MSCI is maintained. In oocytes, there also seems to be a relatively low overall level of gene transcription in early-midpachytene oocytes that are present at E15 and E16 (Page et al., 2012), leaving relatively little time for firm establishment of silencing on unsynapsed chromatin. However, some markers of MSCI that accumulate concomitantly with and following H3.1/2 eviction in spermatocytes, such as histone ubiquitination and the presence of the postreplication repair protein RAD18, also mark MSUC regions in pachytene oocytes isolated from E18.5 ovaries (Baarends et al., 2005). This indicates that the developmental progression of the MSUC response in oocytes does proceed up to the moment when H3.1/2 is exchanged for the H3.3 variant in males. Therefore, we conclude that MSUC-associated nucleosome exchange is a male-specific process. It requires accumulation of  $\gamma$ H2AX, as evidenced by the lack of H3.1/2 eviction in *H2ax*<sup>-/-</sup> and *Mdc1*<sup>-/-</sup> spermatocytes. However, a yet unknown downstream factor is required to trigger the eviction,

since also no nucleosome exchange was observed in *Spo11<sup>-/-</sup>* spermatocytes that do accumulate  $\gamma$ H2AX in the transcriptionally silenced pseudo XY body.

### **Nucleosome exchange is widely conserved among mammals**

The observed conservation of nucleosome exchange in association with MSCI, among mammals including the opossum, indicates that this process may have evolved before the split between the eutherian and metatherian infraclasses, some 165 million years ago. That would then also imply that nucleosome exchange on the XY body was lost in the lineage represented by Bennet's wallaby. This species is a representative of the Diprotodontia order of marsupials that split some 70 million years ago from the Didelphimorphia order to which the opossum belongs (O'Leary et al., 2013).

### **Concluding remarks**

Here we have shown that the global nucleosome exchange that occurs at the XY body and other unsynapsed chromatin regions in mouse spermatocytes is a male-specific process that requires formation of  $\gamma$ H2AX. This modification by itself is not enough to trigger the extensive remodelling, given the fact that remodelling does not occur in MSUC regions marked by  $\gamma$ H2AX accumulation that are present in SPO11-deficient spermatocytes and XO oocytes. Still, it is tempting to speculate that the nucleosome exchange process at the XY body is mechanistically related to remodelling that accompanies DSB repair in somatic cells. It might be suggested that the extreme  $\gamma$ H2AX accumulation at the XY body and in MSUC regions in mouse spermatocytes that carry certain translocation chromosomes reflects an extreme DNA damage response, resulting in the complete exchange of nucleosomes in the unsynapsed regions. This extreme response may only occur in males, because the time frame during which MSUC can establish and maintain itself is much longer in spermatocytes compared to the duration of the MSUC response in oocytes. Wallaby spermatocytes, because of the absence of MSCI associated nucleosome removal, may serve as a tool to dissect the molecular mechanism by which nucleosome exchange is achieved.



## MATERIALS AND METHODS

### Animals

#### Mice:

All mouse and opossum experiments were approved by the local animal experiments committee. Mice were killed and testes were collected and snap frozen in liquid nitrogen from 2 wt, 2 H2ax<sup>-/-</sup>, 2 H2AX<sup>+/-</sup>, 2 Mdc<sup>-/-</sup>, and 3 Rnf8<sup>-/-</sup> mice (6-9 weeks old). From adult opossum testes were collected and rapidly frozen. Spread nuclei were prepared as described below. Adult Spo11<sup>-/-</sup> mouse testes were collected and directly spread as described below.

#### Other mammalian species:

All testes were collected as remnant material following natural death, or castration of the animal as ordered by the owner. Testes were collected from adult Egyptian fruit bat after death, and adult springbok testes were collected following castration. All testes were rapidly frozen and meiotic spread nuclei were prepared as described below.

Adult horse, cat, and rabbit testes, as well as testes from a 16 month old Bennet's wallaby were collected following castration and immediately processed for meiotic spread nuclei preparation as described below.

#### Meiotic spread nuclei preparation

Fresh testis samples were mechanically disrupted to generate single cell suspensions and meiotic spread nuclei were prepared as described by Peters et al. (Peters et al., 1997). Frozen testis material was placed in a drop of phosphate buffered saline (PBS), and the thawed material was also mechanically disrupted, and for each slide, 10 µl of cell suspension was directly mixed with 20 µl 100 mM sucrose and spread on a slide covered with ample fixative (1% paraformaldehyde in 1mM sodium borate solution pH9.2 and 0.15% Triton X-100). Subsequent drying and washing of slides was performed as described for fresh material. Slides were stored at -80C.

#### Immunocytochemistry

Slides were briefly thawed at room temperature and washed in in PBS (3x10 min), and non-specific sites were blocked with 0.5% w/v BSA and 0.5% w/v milk powder in PBS. Primary antibodies were diluted in 10% w/v BSA in PBS, and incubations were performed overnight at room temperature in a humid chamber.

For primary antibodies, we used: mouse monoclonal antibodies anti-phosphorylated H2AX

(Upstate), anti-RNA polymerase II CTD repeat YSPTSPS (phospho S2) (Abcam), anti H3.1/2 (gift from dr. P. de Boer); rabbit polyclonal antibodies anti-RAD51 (Essers et al., 2002), anti-SYCP3 (gift from dr. C. Heyting), anti-H3K9me3 (Abcam); guinea pig anti-H1t (gift from dr. M.A. Handel). For secondary antibodies, we used a goat anti-rabbit IgG alexa 488/546, goat anti-mouse alexa IgG 488/546/633, goat anti-guinea pig IgG 488/546 (Molecular Probes).

Subsequently, slides were washed (3x10 min) in PBS, blocked in 10% v/v normal goat serum (Sigma) in blocking buffer (supernatant of 5% w/v milk powder in PBS centrifuged at 14,000 rpm for 10 min), and incubated with secondary antibodies in 10% normal goat serum in blocking buffer at room temperature for 2 hours. Finally, slides were washed (3x10 min) in PBS (in the dark) and embedded in Prolong Gold with or without DAPI (Invitrogen). In cases where two rabbit antibodies needed to be combined, first a single first and second antibody staining was performed followed by a second procedure targeting the other antigen, and an anti-rabbit labeled by a different fluorophore. Fluorescent observation of slides obtained through this procedure thus provide information about the localisation of the protein that was detected in the first round of staining in one channel, and both proteins in the other channel. Fluorescent images were observed by using a fluorescence microscope (Axioplan 2; Carl Zeiss) equipped with a digital camera (Coolsnap-Pro; Photometrics). Alternatively, Confocal imaging was performed on a Zeiss LSM700 microscope (Carl Zeiss, Jena): we used a 63x oil immersion objective lens (N.A. 1.4), pinhole 1AU. DAPI was excited at 405 nm and imaged with a short pass filter (SP) 490 nm; Alexa 488 was excited at 490 nm and imaged SP 555 nm; Alexa 546 was excited at 555 nm and imaged SP 640 nm; Alexa 633 was excited at 639 nm and for the imaging no filter was required.

## REFERENCES

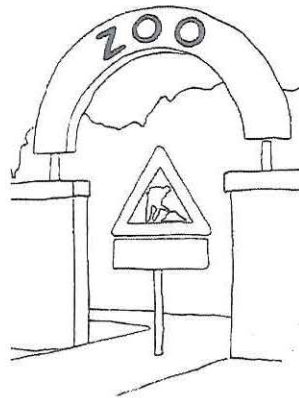
- Baarends, W.M., Wassenaar, E., van der Laan, R., Hoogerbrugge, J.W., Sleddens-Linkels, E., Hoeijmakers, J.H., de Boer, P., and Grootegoed, J.A. (2005). Silencing of unpaired chromatin and histone H2A ubiquitination in mammalian meiosis. *Mol Cell Biol* 25, 1041-1053.
- Bakken, A.H., and McClanahan, M. (1978). Patterns of RNA synthesis in early meiotic prophase oocytes from fetal mouse ovaries. *Chromosoma* 67, 21-40.
- Baudat, F., Manova, K., Yuen, J.P., Jasin, M., and Keeney, S. (2000). Chromosome synapsis defects and sexually dimorphic meiotic progression in mice lacking spo11. *Mol Cell* 6, 989-998.
- Carofiglio, F., Inagaki, A., de Vries, S., Wassenaar, E., Schoenmakers, S., Vermeulen, C., van Cappellen, W.A., Sleddens-Linkels, E., Grootegoed, J.A., Te Riele, H.P., et al. (2013). SPO11-Independent DNA Repair Foci and Their Role in Meiotic Silencing. *PLoS Genet* 9, e1003538.
- Daniel, K., Lange, J., Hached, K., Fu, J., Anastasiadis, K., Roig, I., Cooke, H.J., Stewart, A.F., Wassmann, K., Jasin, M., et al. (2011). Meiotic homologue alignment and its quality surveillance are controlled by mouse *HORMAD1*. *Nat Cell Biol* 13, 599-610.
- de Vries, M., Vosters, S., Merckx, G., D'Hauwers, K., Wansink, D.G., Ramos, L., and de Boer, P. (2012). Human male meiotic sex chromosome inactivation. *PLoS One* 7, e31485.
- Essers, J., Hendriks, R.W., Wesoly, J., Beerens, C.E., Smit, B., Hoeijmakers, J.H., Wyman, C., Dronkert, M.L., and Kanaar, R. (2002). Analysis of mouse *Rad54* expression and its implications for homologous recombination. *DNA Repair (Amst)* 1, 779-793.
- Fernandez-Capetillo, O., Mahadevaiah, S.K., Celeste, A., Romanienko, P.J., Camerini-Otero, R.D., Bonner, W.M., Manova, K., Burgoyne, P., and Nussenzweig, A. (2003). H2AX is required for chromatin remodeling and inactivation of sex chromosomes in male mouse meiosis. *Dev Cell* 4, 497-508.
- Franco, M.J., Sciarano, R.B., and Solari, A.J. (2007). Protein immunolocalization supports the presence of identical mechanisms of XY body formation in eutherians and marsupials. *Chromosome Res* 15, 815-824.
- Ichijima, Y., Ichijima, M., Lou, Z., Nussenzweig, A., Camerini-Otero, R.D., Chen, J., Andreassen, P.R., and Namekawa, S.H. (2011). MDC1 directs chromosome-wide silencing of the sex chromosomes in male germ cells. *Genes Dev* 25, 959-971.
- Kouznetsova, A., Wang, H., Bellani, M., Camerini-Otero, R.D., Jessberger, R., and Hoog, C. (2009). BRCA1-mediated chromatin silencing is limited to oocytes with a small number of asynapsed chromosomes. *J Cell Sci* 122, 2446-2452.
- Lou, Z., Minter-Dykhouse, K., Franco, S., Gottissa, M., Rivera, M.A., Celeste, A., Manis, J.P., van Deursen, J., Nussenzweig, A., Paull, T.T., et al. (2006). MDC1 maintains genomic stability by participating in the amplification of ATM-dependent DNA damage signals. *Mol Cell* 21, 187-200.
- Lu, L.Y., Wu, J., Ye, L., Gavrulina, G.B., Saunders, T.L., and Yu, X. (2010). RNF8-dependent histone modifications regulate nucleosome removal during spermatogenesis. *Dev Cell* 18, 371-384.
- Luijsterburg, M.S., Acs, K., Ackermann, L., Wiegant, W.W., Bekker-Jensen, S., Larsen, D.H., Khanna, K.K., van Attikum, H., Mailand, N., and Dantuma, N.P. (2012). A new non-catalytic role for ubiquitin ligase RNF8 in unfolding higher-order chromatin structure. *EMBO J* 31, 2511-2527.
- Mahadevaiah, S.K., Turner, J.M., Baudat, F., Rogakou, E.P., de Boer, P., Blanco-Rodriguez, J., Jasin, M., Keeney, S., Bonner, W.M., and Burgoyne, P.S. (2001). Recombinational DNA double-strand breaks in mice precede synapsis. *Nat Genet* 27, 271-276.
- Malki, S., van der Heijden, G.W., O'Donnell, K.A., Martin, S.L., and Bortvin, A. (2014). A role for retrotransposon LINE-1 in fetal oocyte attrition in mice. *Dev Cell* 29, 521-533.
- Monesi, V. (1965). Differential rate of ribonucleic acid synthesis in the autosomes and sex chromosomes during male meiosis in the mouse. *Chromosoma* 17, 11-21.
- Montellier, E., Boussouar, F., Rousseaux, S., Zhang, K., Buchou, T., Fenaille, F., Shiota, H., Debernardi, A., Hery, P., Curtet, S., et al. (2013). Chromatin-to-nucleoprotamine transition is controlled by the histone H2B variant TH2B. *Genes Dev* 27, 1680-1692.



- Namekawa, S.H., VandeBerg, J.L., McCarrey, J.R., and Lee, J.T. (2007). Sex chromosome silencing in the marsupial male germ line. *Proc Natl Acad Sci U S A* 104, 9730-9735.
- O'Leary, M.A., Bloch, J.I., Flynn, J.J., Gaudin, T.J., Giallombardo, A., Giannini, N.P., Goldberg, S.L., Kraatz, B.P., Luo, Z.X., Meng, J., et al. (2013). The placental mammal ancestor and the post-K-Pg radiation of placentals. *Science* 339, 662-667.
- Oakberg, E.F. (1956). Duration of spermatogenesis in the mouse and timing of stages of the cycle of the seminiferous epithelium. *Am J Anat* 99, 507-516.
- Page, J., de la Fuente, R., Manterola, M., Parra, M.T., Viera, A., Berrios, S., Fernandez-Donoso, R., and Rufas, J.S. (2012). Inactivation or non-reactivation: what accounts better for the silence of sex chromosomes during mammalian male meiosis? *Chromosoma* 121, 307-326.
- Page, J., Viera, A., Parra, M.T., de la Fuente, R., Suja, J.A., Prieto, I., Barbero, J.L., Rufas, J.S., Berrios, S., and Fernandez-Donoso, R. (2006). Involvement of synaptonemal complex proteins in sex chromosome segregation during marsupial male meiosis. *PLoS Genet* 2, e136.
- Peters, A.H., Plug, A.W., van Vugt, M.J., and de Boer, P. (1997). A drying-down technique for the spreading of mammalian meiocytes from the male and female germline. *Chromosome Res* 5, 66-68.
- Rathke, C., Baarends, W.M., Awe, S., and Renkawitz-Pohl, R. (2014). Chromatin dynamics during spermiogenesis. *Biochim Biophys Acta* 1839, 155-168.
- Romanienko, P.J., and Camerini-Otero, R.D. (2000). The mouse *spo11* gene is required for meiotic chromosome synapsis. *Mol Cell* 6, 975-987.
- Royo, H., Polikiewicz, G., Mahadevaiah, S.K., Prosser, H., Mitchell, M., Bradley, A., de Rooij, D.G., Burgoyne, P.S., and Turner, J.M. (2010). Evidence that meiotic sex chromosome inactivation is essential for male fertility. *Curr Biol* 20, 2117-2123.
- Royo, H., Prosser, H., Ruzankina, Y., Mahadevaiah, S.K., Cloutier, J.M., Baumann, M., Fukuda, T., Hoog, C., Toth, A., de Rooij, D.G., et al. (2013). ATR acts stage specifically to regulate multiple aspects of mammalian meiotic silencing. *Genes Dev* 27, 1484-1494.
- Tagami, H., Ray-Gallet, D., Almouzni, G., and Nakatani, Y. (2004). Histone H3.1 and H3.3 complexes mediate nucleosome assembly pathways dependent or independent of DNA synthesis. *Cell* 116, 51-61.
- Taketo, T., and Naumova, A.K. (2013). Oocyte heterogeneity with respect to the meiotic silencing of unsynapsed X chromosomes in the XY female mouse. *Chromosoma* 122, 337-349.
- Trostle-Weige, P.K., Meistrich, M.L., Brock, W.A., and Nishioka, K. (1984). Isolation and characterization of TH3, a germ cell-specific variant of histone 3 in rat testis. *J Biol Chem* 259, 8769-8776.
- Turner, J.M., Aprelikova, O., Xu, X., Wang, R., Kim, S., Chandramouli, G.V., Barrett, J.C., Burgoyne, P.S., and Deng, C.X. (2004). BRCA1, histone H2AX phosphorylation, and male meiotic sex chromosome inactivation. *Curr Biol* 14, 2135-2142.
- Turner, J.M., Mahadevaiah, S.K., Ellis, P.J., Mitchell, M.J., and Burgoyne, P.S. (2006). Pachytene asynapsis drives meiotic sex chromosome inactivation and leads to substantial postmeiotic repression in spermatids. *Dev Cell* 10, 521-529.
- Turner, J.M., Mahadevaiah, S.K., Fernandez-Capetillo, O., Nussenzweig, A., Xu, X., Deng, C.X., and Burgoyne, P.S. (2005). Silencing of unsynapsed meiotic chromosomes in the mouse. *Nat Genet* 37, 41-47.
- van Attikum, H., and Gasser, S.M. (2005). ATP-dependent chromatin remodeling and DNA double-strand break repair. *Cell Cycle* 4, 1011-1014.
- van der Heijden, G.W., Derijck, A.A., Posfai, E., Giele, M., Pelczar, P., Ramos, L., Wansink, D.G., van der Vlag, J., Peters, A.H., and de Boer, P. (2007). Chromosome-wide nucleosome replacement and H3.3 incorporation during mammalian meiotic sex chromosome inactivation. *Nat Genet* 39, 251-258.

# 6

## General discussion







Through the life cycle of mammalian species, the sex chromosomes are subject to very specific transcriptional regulation events at different time points and in a sex-specific manner (as represented in Figure 1A). In particular, also from an epigenetic point of view, it is quite remarkable that only the X and Y chromosomes, unlike any of the other chromosomes, become entirely silenced in the male germ line, by a process named meiotic sex chromosome inactivation (MSCI). In addition, in the somatic cells of female embryos, the X chromosome is specifically targeted in a process termed X chromosome inactivation (XCI) (Figure 1A).

Cells that are immortalized and grown in culture, can survive with an aberrant copy number of any chromosome (Stepanenko and Kavsan, 2012). However, cells in the developing embryo are very sensitive to gene dosage, and an extra copy or the lack of a single autosome usually leads to very early embryonic death. Proper paternal and maternal genomic imprinting is also required for early development. Together, this indicates that embryonic cells are very sensitive to changes in gene expression levels, and this is most likely the reason why the XCI dosage compensation mechanism, to equalize X-linked gene expression, between the sex chromosomes and the autosomes, and between males and females, has evolved.

For a few genes, functional alleles or homologs still exist on both the human X and Y chromosomes. In the recombining pseudoautosomal regions these are real alleles, but on the non-recombining male-specific region of the Y chromosome (MSY) these are the so-called X-degenerate genes, which are functional homologs of the respective X-linked genes. All these genes escape X-inactivation in female cells and are most likely very dosage-sensitive (reviewed by Berletch et al., 2011; Disteche et al., 2002)). The importance of such X- and Y-linked genes is illustrated by the fact that human XO embryos, in which these genes are present as a single allele, have a poor survival rate (Ashworth et al., 1991).

Compared to XCI, the complete inactivation of both sex chromosomes in male meiotic prophase by the MSCI mechanism is even more astonishing, since many important house-keeping genes reside on the X chromosome. As described in the Introduction, testis-specific expression of retroposed autosomal copies of such genes provides at least a partial escape from the detrimental effects of global X chromosome inactivation in spermatocytes (Khil et al., 2005). It is clear that MSCI did not evolve as a dosage compensation mechanism, but developed as a consequence of a different driving force, related to the origin of heterologous sex chromosomes. Thus, it is not surprising that the molecular mechanisms that operate either to achieve silencing of the X and Y chromosomes during male meiosis, or to mediate inactivation of one of the two X chromosomes in female embryos, are very different from each other (as represented in Figure 1B). In mouse, XCI is mediated by genes that reside in the X-inactivation center, and whose activation depends on the X-to-autosome ratio, leading to transcription of the long noncoding RNA *Xist*, which coats the future inactive chromosome and

recruits epigenetic modifiers that establish a silenced chromatin structure. In contrast, MSCI is initiated in response to activation of components of the DNA damage response pathway (DDR) and meiosis-specific proteins which localize to the unsynapsed XY axes. Although the exact sequence of events that leads to global inactivation of X and Y is not known, ATR-mediated phosphorylation of the H2AX histone variant has been proven to be an essential mark of the sex body (Fernandez-Capetillo et al., 2003). MSCI does not require *Xist* (Turner et al., 2002), and so far, there is no evidence for a role of other noncoding RNAs in this mechanism.

Both XCI and MSCI have been reported to occur in all mammals that were investigated. However, the dynamics of sex chromosome regulation appear to vary considerably between different mammalian species. For example, imprinted XCI (iXCI) of the paternal X chromosome has been observed in female pre-implantation embryos and extra-embryonic tissues of mouse, but doesn't seem to occur in human (Migeon et al., 2002). Moreover, the *Xist* gene is conserved within the eutherian lineage, but a different noncoding RNA that can also mediate X chromosome silencing has evolved independently in metatherians (Grant et al., 2012). Also MSCI displays some variation between mouse and human, and there is only limited overlap in the identity of the genes that escape post-meiotic sex chromatin repression (PSCR) and become specifically reactivated after meiosis in mouse and human (Sin et al., 2012). To understand the relevance of different aspects of MSCI and XCI, it is of pivotal importance to study these mechanisms in different mammalian species, from an evolutionary perspective. This might also allow us to identify the unifying properties of MSCI and PSCR mechanisms in different species, which would then help us to unravel the driving forces for evolution of MSCI.

In this thesis, we investigated the cycles of X chromosome activity and inactivity in its journey from the male developing germline, through meiosis, to the gamete and into the early female embryo, in different mammalian species. The following discussion will focus on the implications of our findings for some central questions that have arisen during the course of the work described in this thesis. We will start at the moment when the X chromosome undergoes a round of inactivation together with the Y chromosome, in meiotic prophase spermatocytes.

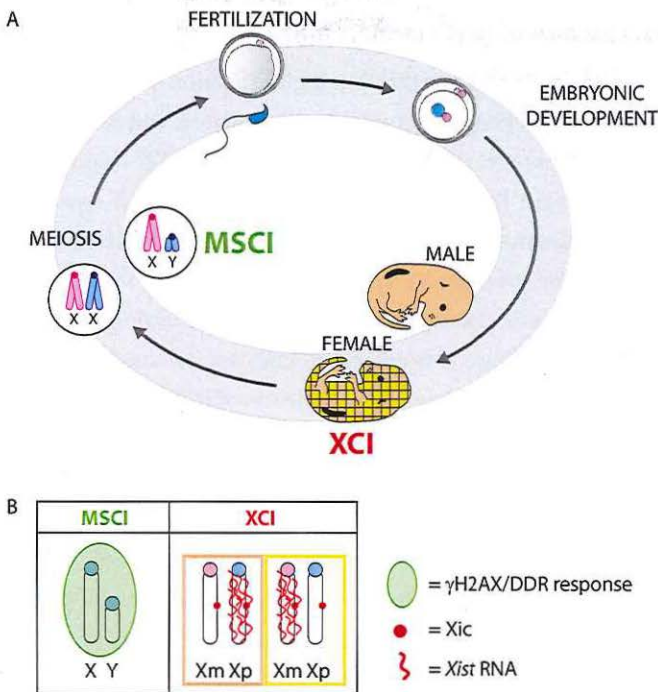


**Figure 1: Regulation of sex chromosomes through the mammalian life cycle**

(A) Through the life cycle of mammalian species, the sex chromosomes are subject to specific transcriptional regulation at different developmental time points and in a sex-specific manner. During meiosis, while in the female germline both X chromosomes are active, in the male germline, the non-homologous regions of the X and Y chromosomes undergo meiotic sex chromosome inactivation (MSCI). After fertilization, female embryos inactivate one of the two inherited X chromosomes to achieve balanced dosage of X-linked genes. In the embryo proper, either the paternal (Xp) or the maternal (Xm) X chromosome can be inactivated. Because of this randomness, and clonal inheritance of the inactivated X chromosome when cells divide, female embryos are natural mosaics of cells expressing genes from one or the other X chromosome (graphically represented as a chessboard pattern of pink and yellow areas in the female body). The inactive X chromosome is maintained throughout the life of a female. Only in the cell lineage that gives rise to the primordial germ cells (PGCs), the inactive X chromosome is reactivated. The presence of two active X chromosomes may be required for oogenesis and also may ensure transmission of an equally active Xm and the Xp to the zygote. PGCs in both male and female embryos migrate to the genital ridges (here represented as black bean-shaped structures), where meiosis takes place and a new cycle of sex chromosome inactivation begins.

(B) Silencing of the sex chromosomes by MSCI depends on accumulation of DNA damage response (DDR) proteins and phosphorylation of the histone variant H2AX ( $\gamma$ H2AX) (represented as red circle encompassing the X and Y chromatin). On the other hand, X chromosome inactivation (XCI) starts with the expression of the Xist long non-coding RNA (red wave line) from the future inactive X chromosome. When in an embryonic cell the Xp becomes inactivated, as represented in the pink boxed area on the left, this is going to be transmitted clonally in the pink patches of the female embryo represented in (A). The inactive Xm, represented in the yellow boxed area on the right, will be transmitted clonally in the yellow patches of the female embryo represented in (A).



### 6.1 Does synapsis allow escape of MSCI in mammals?

The X and Y chromosomes undergo MSCI together, but their regulation in meiotic prophase still seems to be somewhat different. When meiotic prophase is initiated, and SPO11 induces hundreds of meiotic DSBs in the genome, the X chromosome displays DSBs along its entire length, while only a single prominent RAD51 focus, marking a site of DSB repair, can be observed on the tip of the Y chromosome, most likely residing in the pseudoautosomal region (Page et al., 2012). Then, as meiotic prophase initiates, the overall level of transcription genome-wide becomes low, and only by midpachytene reactivation of transcription is observed on autosomes, when also RNA polymerase II becomes enriched on the autosomes. At that time, the XY body is subjected to MSCI and shows clear depletion of RNA polymerase II. The sex chromosomes remain largely unsynapsed during the meiotic prophase. In early pachytene, the X and Y in mouse and man achieve a quite advanced degree of synapsis, which includes almost 90% of the Y chromosomal axis (Solari, 1970; Tres, 1977). Clearly this must involve for the greater part heterologous synapsis, which is very unstable, and occurs only transiently. Subsequently, XY synapsis is limited to the chromosomal tips during the rest of pachytene. The unsynapsed parts of the X and Y chromosomes trigger MSCI (Turner et al., 2006), so it might be suggested that, if heterologous synapsis is achieved, removal of HORMADs, the proteins that specifically localize to asynapsed axes, from these regions would allow escape from MSCI. Since heterologous XY synapsis is only rarely observed in mouse and man, and occurs only when overall transcription is still low early in meiotic prophase, this precludes any analyses of the link between synapsis and MSCI escape. In the dog, the pseudoautosomal region (PAR) is much larger than that of human and mouse, and we anticipated that this might be associated with stable homologous synapsis of the X and Y PARs throughout the meiotic prophase, and that genes within the PAR would escape from MSCI. However, as described in Chapter 4, this does not appear to be the case. Rather, the dog PAR is characterized by a very low overall transcriptional activity in both spermatocytes and round spermatids. Interestingly, the additional self-synapsis we observed in dog spermatocytes concerns only the X chromosome, and correlated to a higher overall transcriptional activity of the Xp-arm compared to the Xq-arm, as observed from the RNA sequencing data. This might suggest that XY synapsis reduces the efficiency of MSCI, but we cannot exclude that MSCI is less complete in dog compared to mouse due to other, unknown differences between these species. Also in human, MSCI appears to be less stringent compared to mouse. A link between synapsis and escape from silencing appears to be more clear on autosomes that fail to complete synapsis and are thus subjected to the more general mechanism of meiotic silencing of unsynapsed chromatin (MSUC). Previously we have shown that when autosomes with translocations achieve stable

heterologous synapsis in males, this is invariably associated with lack of markers of MSUC, and conversely, failure of synapsis leads to MSUC and preferential localization of the unsynapsed chromatin in the vicinity of the XY body (Baarends et al., 2005).

In marsupials, the X and Y chromosomes do not have PARs and do not display any synapsis, but they are connected by the dense plate. In addition, although the sex chromosomes do not form a crossover site, meiotic DSB repair sites can be observed on the sex chromosomes in early pachytene. Microscopically, markers of MSCI are clearly present, but RT-PCR analysis of mRNA expression of selected X-linked genes in isolated spermatocytes and spermatids showed that, for most of the analyzed genes, reduced expression became apparent only in the spermatid mRNA sample, whereas these genes showed reduced mRNA levels in both spermatocyte and spermatid mRNA samples of the mouse (Hornecker et al., 2007). This may indicate incomplete MSCI in the marsupial, but a more global analyses of mRNA expression from autosomes and sex chromosomes in purified samples of developing marsupial germ cells would be required to provide more insight in this matter.

## 6.2 Some considerations on MSCI and MSUC

In male meiotic prophase, MSCI and MSUC can occur within one and the same nucleus, but the fact that they share mechanistic components then results in a reduction of the efficiency of MSCI, when MSUC is also occurring. Yet, it appears likely that MSCI has evolved into a more efficient mechanism compared to MSUC, and might be triggered by specific properties of the sex chromosomes, in addition to the combined response to asynapsis and persistence of DSBs. In particular, in the mouse, the existence of a pachytene checkpoint, which senses aberrant chromosomal composition (and thus aberrant synapsis) and leads to apoptotic elimination of the respective cells, may have advanced evolution of changes that favor robust and complete transcriptional silencing of the sex chromosomes in this species. It remains to be established if MSCI has evolved in a similar, hypothetical, way also in other mammalian species, and if the pachytene checkpoint in these species functions as strictly as in mouse.

In oocytes, MSCI does not occur, but others and we have previously observed accumulation of known MSUC/MSCI markers on unsynapsed chromosomes in pachytene oocytes isolated from mouse embryonic ovaries. Unlike MSCI in spermatocytes, which allows meiotic progression, MSUC in spermatocytes and oocytes marks an unwanted event (failure of completion of synapsis and/or meiotic DSB repair), and in the ovary this results in depletion of such cells from the ovarian pool (Malki et al., 2014). Although MSUC areas in spermatocytes and oocytes share some chromatin marks, it is clear from data presented in the literature and the findings in this thesis, that mechanistically MSUC in spermatocytes and oocytes differ to some extent. In particular, as described in Chapter 5, nucleosome renewal appears to be a male-specific adaptation of MSUC into MSCI.



### 6.3 Is nucleosome exchange essential for MSCI?

Chromatin remodeling normally occurs locally within a nucleus, in relation to gene transcription or DNA repair events, in many cell types of different vertebrate and invertebrate species. The chromosome-wide H3.1/2 depletion and incorporation of H3.3 observed at the XY body and regions of MSUC during male meiosis, has not been described in any other context in mammalian cells. It might be suggested, that the XY body-associated nucleosome exchange represents an extreme form of a type of nucleosome exchange that can occur locally on autosomes in somatic cells. However, it is unlikely that it is related to the very limited nucleosome eviction that generally occurs in conjunction with transcriptional activation (Wirbelauer et al., 2005), since this nucleosome exchange at the XY body initiates concomitant with establishment of MSCI. Based on the tight link between MSCI and meiotic DSB repair, it might be suggested that the XY body-associated nucleosome exchange is related to nucleosome exchange that occurs during DSB repair in somatic cells (van Attikum and Gasser, 2005a; Yang et al., 2013). One way to obtain more insight into the relevance of this phenomenon during MSCI, would be to analyze, in mutant mouse models, if absence of H3.3 would affect nucleosome exchange at the XY body, and then also would impair MSCI. The mouse genome contains the *H3f3a* and *H3f3b* genes which encode two H3.3 variants. Knockouts of either *H3f3a* or *H3f3b* are sublethal (Bush et al., 2013; Couldrey et al., 1999). An *H3f3a* hypomorphic mutant has been generated by a gene trap insertion, and both male and female surviving mutants were reported to show reduced fertility (Couldrey et al., 1999). When the male reproductive tract was analyzed more specifically, no obvious differences in the testes were noticed and sperm numbers appeared normal. It might be that depletion for H3.3A in the paternal genome accounts for developmental problems only later, in the developing embryo. The exact cause for the reduced fertility in this mutant is not well established. Furthermore, *H3f3a* transcripts are expressed throughout the spermatogenic epithelium (spermatogonia, spermatocytes, and spermatids) at low levels, whereas *H3f3b* is most highly expressed specifically in spermatocytes (Bramlage et al., 1997). This might suggest that depletion for H3.3B would possibly cause problems already in spermatogenesis. This was indeed reported in a recent detailed analyses of the infertility phenotype in *H3f3b*<sup>-/-</sup> males, where testis size of the mutant mice was significantly smaller compared to controls, and sperm concentration was also 2-fold lower than in control samples. Surprisingly, gene expression microarray analysis revealed only relatively modest effect of H3.3B depletion on overall gene expression levels, and MSCI failure was not detected (Yuen et al., 2014). In spermatocytes of *H3f3b* knockout males, overall H3.3 levels were reduced, but the dynamics of XY body-associated remodeling were not investigated in this study (Yuen et al., 2014).



A possible functional redundancy between the H3.3 variants encoded by the *H3f3a* and *H3f3b* genes may allow normal H3.1/2 nucleosome exchange by H3.3 in the single *H3f3* gene knockout models. To dissect this further, a conditional double knockout mouse model for *H3f3a* and *H3f3b* might help us to investigate the role of extensive nucleosome replacement at the XY body and provide a definitive answer on a possible link to MSCI.

Alternatively, or in addition, determining which ATP-dependent chromatin remodeling complex is functional in the chromatin make-over of the sex chromosomes during meiosis would be particularly interesting. To this end, the high degree of evolutionary conservation of H3.1/2 eviction during XY body formation (described in Chapter 5) can be used to select candidate remodelers that may be involved in this process. We would expect the responsible remodeler to accumulate in a timely manner in all species that replace H3.1/2 by H3.3 on the sex chromosomes. Furthermore, since a known function of  $\gamma$ H2AX in DSB repair is to attract chromatin remodelers (reviewed by (van Attikum and Gasser, 2005b)), we speculated that an analogous role for  $\gamma$ H2AX during MSCI would be probable. Thus  $\gamma$ H2AX accumulation in the XY body might be functionally connected to the recruitment of a specific chromatin remodeler and to the induction of nucleosome replacement (as suggested in Chapter 5), although nucleosome replacement may or may not be needed for proper establishment of XY silencing.

There are four families of ATP-dependent chromatin remodeling complexes that are known to be able to mediate nucleosome removal and exchange, and thus could act together with a chaperone in the XY body-associated chromatin remodeling process: the NuRD/Mi-2/CHD family, the INO80 (inositol requiring 80) family, the ISWI (imitation-SWI) family, and the SWI/SNF (switching defective/sucrose non-fermenting) family (reviewed in (Lusser and Kadonaga, 2003)).

Regarding the NuRD/Mi-2/CHD complex, it has been previously shown that in mouse the CHD3/CHD4 components of this complex specifically accumulate on the sex chromosomal PARs starting in leptotene nuclei, and later spread to the XY body chromatin in midpachytene (Bergs et al., 2014), which would correspond to the time frame of remodeling.

With respect to the SWI/SNF complex, immunolocalization patterns of key components of both SMARCA4 (BRG1) and SMARCA2 (BRM) (mutually exclusive ATPase subunits of the SWI/SNF complex) in spermatocytes of mouse indicate that these two remodelers are not likely to accumulate at the XY body at the time when remodeling is initiated (Wang et al., 2012). However, previous work has shown that although BRG1 is depleted from the XY body, the SWI/SNF core subunit SNF5/INI1 is enriched (Costa et al., 2006). Therefore, the SWI/SNF complex might still be involved, and analysis of Brm knockout spermatocytes might provide more insight in this matter.

At present, no data about the immunolocalization patterns of key components of the INO80 complex and of the SMARCA5 (SNF2H) (ISWI complex), in spermatocytes of mouse, are available.

After assessing which of these chromatin remodelers would be the best candidates to perform the XY nucleosome remodelling, the remodeler specifically involved in H3.1/2 eviction should not show any specific enrichment on the XY body of Bennet's wallaby spermatocytes, nor on the pseudo XY bodies in XO E19.5 mouse oocytes, because, as described in Chapter 5, we did not detect any nucleosome eviction in these cells. Mouse knockout models of most chromatin remodelers are embryonically lethal, and conditional deletion of the candidate remodeler in the mouse germ line would be extremely helpful to study this further.

#### **6.4 Basic aspects of PSCR from an evolutionary perspective**

From the ROSI experiment described in Chapter 3, we learned that perhaps it is not the inactive status of the Xp in post-meiotic cells that is relevant to the next generation, but rather the post-meiotic re-expression of certain X-linked genes that might have to be transmitted in an active state to the zygote. Although ROSI does not represent the natural situation, sex-linked genes that are active in round spermatids may be at least in part protected from the histone-to-protamine transition. This would allow to maintain an "epigenetic memory" on genes exerting an important role during early embryonic development (Erkek et al., 2013; Hammoud et al., 2009).

Immunocytochemical or histochemical enrichment of specific histone marks in certain chromatin domains, doesn't necessarily give a representative image of what is really happening at the single gene level in those domains. Furthermore, despite what can be seen as a global transcriptional inactivation process at the immunocytochemical level on the post-meiotic X and Y chromosomes, the majority of X- and Y-linked multi-copy genes (Mueller et al., 2008) and a significant number of single-copy genes are reactivated during the post-meiotic phase in mouse (Hendriksen et al., 1995; Mulugeta Achame et al., 2010), showing that PSCR is not as strict as MSC1. Based on these findings, it might be suggested that PSCR is not mediated by an active process, and that genes which encode products required for development of the haploid spermatids (spermiogenesis) or for early embryonic development can be normally re-activated. Furthermore, it remains to be established whether PSCR is a general phenomenon among mammals. To this end, the detailed analysis of the canine species (described in Chapter 4) provides additional valuable information. As also observed for human compared to mouse, PSCR is less stringent in dog compared to mouse. Identification of common genes that are reactivated in all these species can point to a specific role for these genes during spermiogenesis or early embryonic development.



## 6.5 PSCR and iXCI: does any transgenerational epigenetic effect play a role?

A longstanding question in the XCI field concerns the mechanism by which iXCI, the biased imprinted inactivation of the X chromosome of paternal origin (Xp), is achieved in mouse pre-implantation female embryos. While it appears more and more clear, that the *Xist* promoter region of the X chromosome of maternal origin (Xm) is imprinted to remain transcriptionally repressed (Fukuda et al., 2014), the contribution of epigenetic marks eventually carried by the Xp to iXCI initiation has not been definitely assessed.

In Chapter 3, we investigated whether transmission of a round spermatid paternal X chromosome, that already carries some heterochromatic marks and is largely transcriptionally repressed because of PSCR, by round spermatid injection (ROSI) into mouse oocytes, would be sufficient to establish iXCI. Using round spermatids from male mice lacking a functional *Xist* gene ( $Xp\Delta Xist$ ) for ROSI, we ruled out the possibility that *Xist* could take part into establishing an inactive status on the Xp during iXCI. After natural mating,  $Xp\Delta Xist$  female embryos die early during embryonic development, because of lack of iXCI in their extraembryonic tissues. Hence, if the Xp transmitted by a round spermatid would already be sufficiently silenced, we were expecting to rescue the female embryonic lethality caused by lack of a functional paternal *Xist* allele.

As reported in Chapter 3, by performing ROSI, we could obtain for the first time live born female pups carrying an  $Xp\Delta Xist$ . In this experiment, the observation that, instead of achieving *Xist*-independent Xp inactivation, Xm was inactivated via *Xist* expression was really surprising.

Based upon these results, it cannot be excluded that initially the Xp is partially inactive in early female embryos, but such an initial silencing would not be efficient enough or may be maintained only transiently. In this scenario, limited X-linked gene expression from Xp would allow some female embryos to reach the morula stage in "better shape", when the Xm loses the repressive imprint on the *Xist* promoter region and can eventually become inactivated (Fukuda et al., 2014). Moreover, as described in Chapter 3, we propose that active transcription of genes encoding XCI-activators from the ROSI-derived Xp might also help to overcome the maternal imprint, and stimulate *Xist* expression from Xm.

To assess X-linked gene expression levels from the Xp compared to Xm in ROSI-derived female embryos, we made use of an  $Xp\Delta Xist$  mouse line on Castaneus (Cast) genetic background. The C57Bl6 (B6) and Cast mouse strains are highly polymorphic, and can thus be used to facilitate studies aimed at examining allele specific gene expression levels. In our experimental setting, oocyte donors had a B6/DBA2 genetic background, while the round spermatid donors were Cast.



Although we performed all ROSI experiments with Cast Xp $\Delta$ Xist round spermatids following the same procedure applied for those with Xp $\Delta$ Xist on B6 genetic background (as described in the Addendum to Chapter 2), we could not rescue the Xp $\Delta$ Xist female embryonic lethality (Table 1). These results precluded any further analysis. We suggest that strain specific differences in gene expression levels could be responsible for these controversial results. X-linked XCI trans-activators might not reach an adequate and properly timed threshold for Xm inactivation, on a Cast genetic background for the round spermatid donor.

Based on immunocytological studies, the maintenance of a partially inactive state of the

**Table 1: ROSI experimental outcomes**

	ROSI Cast (E15)	ROSI B6 (E15)
N of independent experiments	3	4
N of 2-cell embryos transferred	112	163
N of pups	12	17
Males	12	12
Females	0	4
XO females	0	1

Xp in ROSI-derived embryos might be a plausible possibility. The X and Y chromosomes in round spermatids are largely depleted for histone H3.1/2, as a consequence of the extensive chromatin remodeling that has taken place during MSCI establishment (Figure 3C of Chapter 1). In ROSI-derived zygotes arrested at the pro-metaphase of the first mitotic division (as described in Chapter 3), we observed that the H3.1/2 replication-dependent histone variants are not incorporated into the X chromosome, even after DNA replication (Figure 2A). This might indicate that the Xp is late-replicating and that the replication dependent H3.1/2 are most probably not incorporated at high enough levels, leaving H3.3 as the main histone variant present. Similarly, the late-replicating pericentromeric regions of mouse pre-implantation embryos are enriched for H3.3 during the S phase (Santenard et al., 2010).

By using an antibody that recognizes the H3.3 specific modification of S31 when H3.3 is phosphorylated at mitosis (H3.3S31ph), it appears that H3.3 is indeed abundantly present on the Xp of ROSI-derived female zygotes at the first mitotic division (Figure 2B). Through which mechanism the enrichment for the histone variant H3.3 would influence the Xp at the transcriptional level, and how long the asymmetry for this variant is maintained compared to rest of the paternal genome, are some aspects that would be interesting to investigate in further experiments.

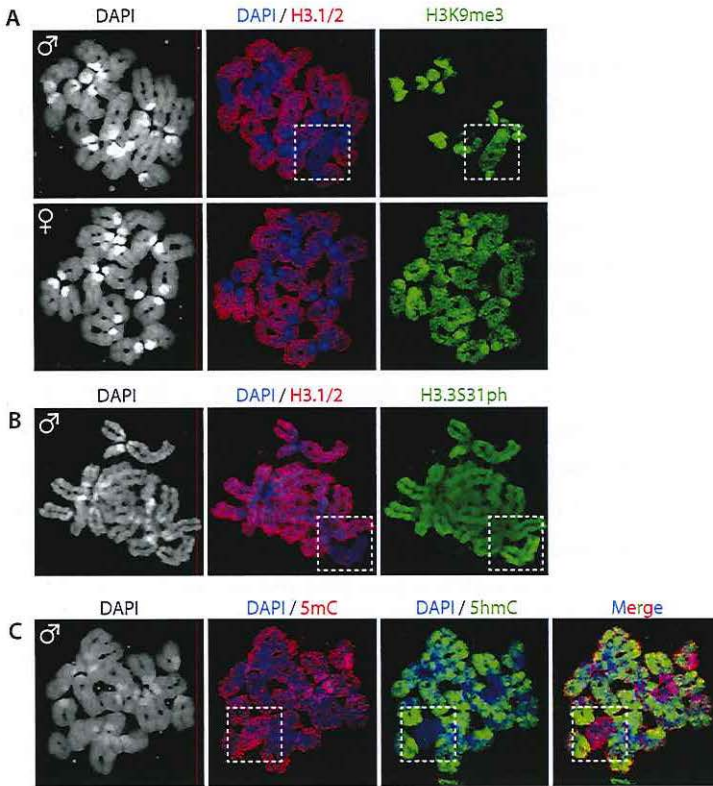


**Figure 2: Chromatin remodeling in ROSI-derived embryos**

Chromosome spreads of prometaphase-arrested zygotes obtained by ROSI.

(A) The condensed chromosomes of paternal and maternal origin are cutouts from the whole zygote image (paternal chromosome set on top; maternal below). Immunolocalization of H3.1/2 (red) merged to DAPI staining (blue) shows depletion for H3.1/2 on the entire X chromosome (delimited by white dashed square box). Paternal and maternal pericentromeric regions are also depleted for H3.1/2. On the right, staining for H3K9me3 (green) confirms that the chromosome depleted for H3.1/2 is indeed the X chromosome (as described in Chapter 3).

(B) Only the condensed chromosomes of paternal origin are shown. At amino acid position 31, the histone variant H3.3 contains a serine residue (S) instead of the alanine (A) contained in H3.1/2. During mitosis, H3.3S31 becomes phosphorylated (H3.3S31ph). Staining for H3.3S31ph (green) is enriched along the entire X chromosome (delimited by white dashed square box) depleted for H3.1/2 (red) compared to autosomes.

(C) Only the condensed chromosomes of paternal origin are shown. DNA methylation levels visualized by immunostaining for 5mC (red) are higher on one paternal chromosome (delimited by white dashed square box). The same chromosome (supposedly the X) is depleted for 5hmC (green).

ROSI-derived embryos represent a very interesting model, also to investigate the role of the specific paternal DNA hydroxymethylation that takes place in mouse zygotes. This global oxidation of 5-methylcytosines (5-mC) to 5-hydroxymethylcytosines (5-hmC) occurs selectively in the paternal pronucleus before the first cell division. Recent work has shown that the maternal genome is protected from this remodelling step by an interaction between a modified histone, H3K9me2, and the oocyte-derived factor Stella (PGC7). Based upon this, we thought that something similar might also happen for ROSI embryos, in view of the observation that round spermatids have not only a high H3K9me3 level on the pericentromeric area and the sex chromosomes (as shown in Chapter 3), but also high H3K9me2 levels (Namekawa et al., 2006). If H3K9me3 is maintained in early zygotes, as shown in Chapter 3, the same might happen for H3K9me2. Hence, we checked methylcytosine and hydroxymethylcytosine levels in ROSI-derived zygotes. We found low levels of hydroxymethylation on the Xp in ROSI-derived zygotes (Figure 2C). This would point to the possibility that some specific regions in the paternal DNA derived from a round spermatid would be protected from being hydroxymethylated by a mechanism similar to that which is protecting the maternal genome from being demethylated. In the model proposed in Figure 3, the presence of H3K9me2 on the Xp of ROSI-derived zygotes, protects the entire Xp from TET3-mediated conversion to 5hmC, while normal levels of 5hmC are detected on paternal autosomes (Figure 3B).

Through what type of mechanism DNA methylation levels would influence Xp at the transcriptional level is not exactly clear. It has been suggested that DNA hydroxymethylation on specific gene enhancers or promoters, could have a role in activating gene expression (Jin et al., 2011; Song et al., 2011). If such a function would be relevant also for activating gene expression from the paternal genome in mouse zygotes, X-linked gene expression in ROSI-derived embryos might be affected by the absence of 5hmC at specific genomic locations. In this respect, in further studies it would be particularly interesting to apply genome-wide RNA sequencing analysis and compare the gene expression profiles of ROSI-derived embryos to those of ICSI-derived embryos. This could certainly provide additional valuable information and help us also to understand more precisely how the transcriptional regulation of the paternal genome in Xp $\Delta$ Xist ROSI-derived female embryos might allow to achieve stable Xm inactivation in the extra-embryonic tissues (as described in Chapter 3).

Additionally, it is important to note that, although it has not been specifically addressed in this thesis work, the Y chromosome from a round spermatid in ROSI-derived male embryos displays epigenetic features similar to the X chromosome. The application of such genome-wide RNA sequencing analysis might also provide some interesting insight into Y-linked gene expression regulation in ROSI-derived embryos compared to controls.



The joint or separate journeys of the X and Y chromosomes through the life cycle of mammals have profound consequences for the regulation of both. Here, we focused on the X chromosome, which travels through both the male and female life cycle. Our findings have not only shed light on the peculiar aspects of the regulation of this sex chromosome, but may also be relevant to our general understanding of epigenetic regulation, in particular during spermatogenesis and in early embryonic development.

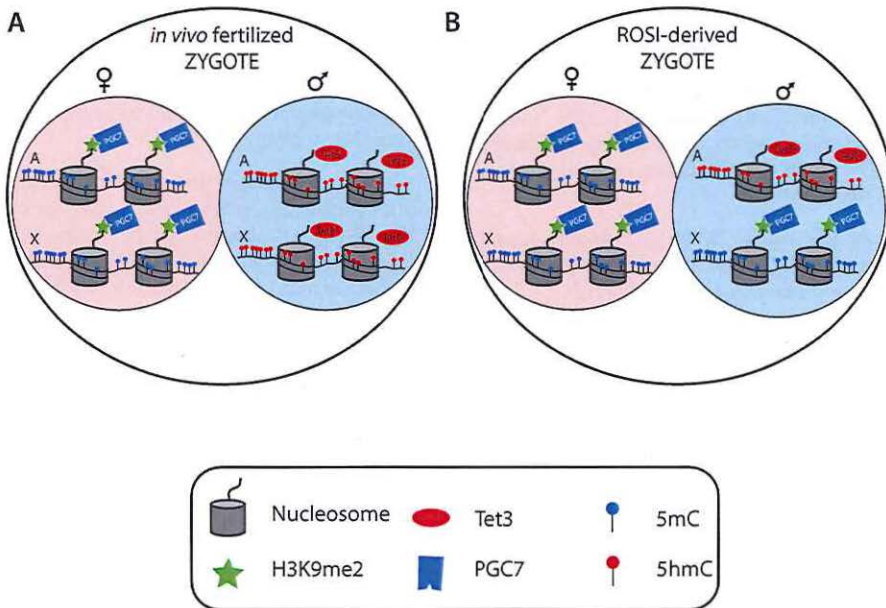


**Figure 3: Schematic view of paternal and maternal genomes soon after *in vivo* fertilization or ROSI**

Paternal and maternal pronuclei are indicated with light blue and light pink colors, respectively.

(A) In an *In vivo* fertilized zygote, PGC7 binds H3K9me2 in the maternal pronucleus, regulating chromatin organization to interfere with TET3 accessibility. The paternal pronucleus is devoid for H3K9me2, thus TET3 can convert 5mC into 5-hydroxymethylcytosine (5hmC).

(B) In a ROSI-derived female zygote, PGC7 binds H3K9me2 in the maternal pronucleus, regulating chromatin organization to interfere with TET3 accessibility. In the paternal pronucleus, the X chromosome, contrary to the autosomes, is also enriched for H3K9me2, so that the X<sub>p</sub> is protected from TET3-dependent 5mC conversion into 5-hydroxymethylcytosine (5hmC).

## REFERENCES

- Ashworth, A., Rastan, S., Lovell-Badge, R., and Kay, G. (1991). X-chromosome inactivation may explain the difference in viability of XO humans and mice. *Nature* 351, 406-408.
- Baarends, W.M., Wassenaar, E., van der Laan, R., Hoogerbrugge, J.W., Sleddens-Linkels, E., Hoeijmakers, J.H., de Boer, P., and Grootoeged, J.A. (2005). Silencing of unpaired chromatin and histone H2A ubiquitination in mammalian meiosis. *Mol Cell Biol* 25, 1041-1053.
- Bergs, J.W., Neuendorff, N., van der Heijden, G., Wassenaar, E., Rexin, P., Elsasser, H.P., Moll, R., Baarends, W.M., and Brehm, A. (2014). Differential expression and sex chromosome association of CHD3/4 and CHD5 during spermatogenesis. *PLoS One* 9, e98203.
- Berlitch, J.B., Yang, F., Xu, J., Carrel, L., and Disteche, C.M. (2011). Genes that escape from X inactivation. *Hum Genet* 130, 237-245.
- Bramlage, B., Kosciassa, U., and Doenecke, D. (1997). Differential expression of the murine histone genes H3.3A and H3.3B. *Differentiation* 62, 13-20.
- Bush, K.M., Yuen, B.T., Barrilleaux, B.L., Riggs, J.W., O'Geen, H., Cotterman, R.F., and Knoepfler, P.S. (2013). Endogenous mammalian histone H3.3 exhibits chromatin-related functions during development. *Epigenetics Chromatin* 6, 7.
- Costa, Y., Speed, R.M., Gautier, P., Semple, C.A., Maratou, K., Turner, J.M., and Cooke, H.J. (2006). Mouse MAELSTROM: the link between meiotic silencing of unsynapsed chromatin and microRNA pathway? *Hum Mol Genet* 15, 2324-2334.
- Couldrey, C., Carlton, M.B., Nolan, P.M., Colledge, W.H., and Evans, M.J. (1999). A retroviral gene trap insertion into the histone 3.3A gene causes partial neonatal lethality, stunted growth, neuromuscular deficits and male sub-fertility in transgenic mice. *Hum Mol Genet* 8, 2489-2495.
- Disteche, C.M., Filippova, G.N., and Tsuchiya, K.D. (2002). Escape from X inactivation. *Cytogenet Genome Res* 99, 36-43.
- Erkek, S., Hisano, M., Liang, C.Y., Gill, M., Murr, R., Dieker, J., Schubeler, D., van der Vlag, J., Stadler, M.B., and Peters, A.H. (2013). Molecular determinants of nucleosome retention at CpG-rich sequences in mouse spermatozoa. *Nat Struct Mol Biol* 20, 868-875.
- Fernandez-Capetillo, O., Mahadevaiah, S.K., Celeste, A., Romanienko, P.J., Camerini-Otero, R.D., Bonner, W.M., Manova, K., Burgoyne, P., and Nussenzweig, A. (2003). H2AX is required for chromatin remodeling and inactivation of sex chromosomes in male mouse meiosis. *Dev Cell* 4, 497-508.
- Fukuda, A., Tomikawa, J., Miura, T., Hata, K., Nakabayashi, K., Eggan, K., Akutsu, H., and Umezawa, A. (2014). The role of maternal-specific H3K9me3 modification in establishing imprinted X-chromosome inactivation and embryogenesis in mice. *Nat Commun* 5, 5464.
- Grant, J., Mahadevaiah, S.K., Khil, P., Sangrithi, M.N., Royo, H., Duckworth, J., McCarrey, J.R., VandeBerg, J.L., Renfree, M.B., Taylor, W., et al. (2012). Rxs is a metatherian RNA with Xist-like properties in X-chromosome inactivation. *Nature* 487, 254-258.
- Hammoud, S.S., Nix, D.A., Zhang, H., Purwar, J., Carrell, D.T., and Cairns, B.R. (2009). Distinctive chromatin in human sperm packages genes for embryo development. *Nature* 460, 473-478.
- Hendriksen, P.J.M., Hoogerbrugge, J.W., Themmen, A.P.N., Koken, M.H.M., Hoeijmakers, J.H.J., Oostra, B.A., Van der Lende, T., and Grootoeged, J.A. (1995). Postmeiotic transcription of X and Y chromosomal genes during spermatogenesis in the mouse. *Dev Biol* 170, 730-733.
- Hornecker, J.L., Samollow, P.B., Robinson, E.S., Vandeberg, J.L., and McCarrey, J.R. (2007). Meiotic sex chromosome inactivation in the marsupial *Monodelphis domestica*. *Genesis* 45, 696-708.
- Jin, S.G., Wu, X., Li, A.X., and Pfeifer, G.P. (2011). Genomic mapping of 5-hydroxymethylcytosine in the human brain. *Nucleic Acids Res* 39, 5015-5024.
- Khil, P.P., Oliver, B., and Camerini-Otero, R.D. (2005). X for intersection: retrotransposition both on and off the X chromosome is more frequent. *Trends Genet* 21, 3-7.
- Lusser, A., and Kadonaga, J.T. (2003). Chromatin remodeling by ATP-dependent molecular machines. *Bioessays* 25, 1192-1200.
- Malki, S., van der Heijden, G.W., O'Donnell, K.A., Martin, S.L., and Bortvin, A. (2014). A role



for retrotransposon LINE-1 in fetal oocyte attrition in mice. *Dev Cell* 29, 521-533.

Migeon, B.R., Lee, C.H., Chowdhury, A.K., and Carpenter, H. (2002). Species differences in TSIX/Tsix reveal the roles of these genes in X-chromosome inactivation. *Am J Hum Genet* 71, 286-293.

Mueller, J.L., Mahadevaiah, S.K., Park, P.J., Warburton, P.E., Page, D.C., and Turner, J.M. (2008). The mouse X chromosome is enriched for multi-copy testis genes showing postmeiotic expression. *Nat Genet* 40, 794-799.

Mulugeta Achame, E., Wassenaar, E., Hoogerbrugge, J.W., Sleddens-Linkels, E., Ooms, M., Sun, Z.W., van, I.W.F., Grootegoed, J.A., and Baarends, W.M. (2010). The ubiquitin-conjugating enzyme HR6B is required for maintenance of X chromosome silencing in mouse spermatocytes and spermatids. *BMC Genomics* 11, 367.

Namekawa, S.H., Park, P.J., Zhang, L.F., Shima, J.E., McCarrey, J.R., Griswold, M.D., and Lee, J.T. (2006). Postmeiotic sex chromatin in the male germline of mice. *Curr Biol* 16, 660-667.

Page, J., de la Fuente, R., Manterola, M., Parra, M.T., Viera, A., Berrios, S., Fernandez-Donoso, R., and Rufas, J.S. (2012). Inactivation or non-re-activation: what accounts better for the silence of sex chromosomes during mammalian male meiosis? *Chromosoma* 121, 307-326.

Santenard, A., Ziegler-Birling, C., Koch, M., Tora, L., Bannister, A.J., and Torres-Padilla, M.E. (2010). Heterochromatin formation in the mouse embryo requires critical residues of the histone variant H3.3. *Nat Cell Biol* 12, 853-862.

Sin, H.S., Ichijima, Y., Koh, E., Namiki, M., and Namekawa, S.H. (2012). Human postmeiotic sex chromatin and its impact on sex chromosome evolution. *Genome Res* 22, 827-836.

Solari, A.J. (1970). The spatial relationship of the X and Y chromosomes during meiotic prophase in mouse spermatocytes. *Chromosoma* 29, 217-236.

Song, C.X., Yu, M., Dai, Q., and He, C. (2011). Detection of 5-hydroxymethylcytosine in a combined glycosylation restriction analysis (CGRA) using restriction enzyme Taq(alpha)I. *Bioorg Med Chem Lett* 21, 5075-5077.

Stepanenko, A.A., and Kavsan, V.M. (2012). Immortalization and malignant transformation of eukaryotic cells. *Tsitol Genet* 46, 36-75.

Tres, L.L. (1977). Extensive pairing of the XY bivalent in mouse spermatocytes as visualized by whole-mount electron microscopy. *J Cell Sci* 25, 1-15.

Turner, J.M., Mahadevaiah, S.K., Elliott, D.J., Garchon, H.J., Pehrson, J.R., Jaenisch, R., and Burgoyne, P.S. (2002). Meiotic sex chromosome inactivation in male mice with targeted disruptions of Xist. *J Cell Sci* 115, 4097-4105.

Turner, J.M., Mahadevaiah, S.K., Ellis, P.J., Mitchell, M.J., and Burgoyne, P.S. (2006). Pachytene asynapsis drives meiotic sex chromosome inactivation and leads to substantial postmeiotic repression in spermatids. *Dev Cell* 10, 521-529.

van Attikum, H., and Gasser, S.M. (2005a). ATP-dependent chromatin remodeling and DNA double-strand break repair. *Cell Cycle* 4, 1011-1014.

van Attikum, H., and Gasser, S.M. (2005b). The histone code at DNA breaks: a guide to repair? *Nat Rev Mol Cell Biol* 6, 757-765.

Wang, J., Gu, H., Lin, H., and Chi, T. (2012). Essential roles of the chromatin remodeling factor BRG1 in spermatogenesis in mice. *Biol Reprod* 86, 186.

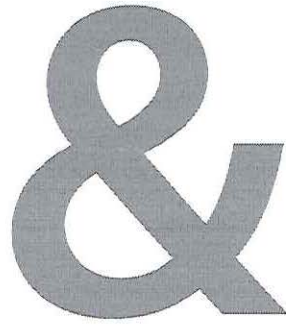
Wirbelauer, C., Bell, O., and Schubeler, D. (2005). Variant histone H3.3 is deposited at sites of nucleosomal displacement throughout transcribed genes while active histone modifications show a promoter-proximal bias. *Genes Dev* 19, 1761-1766.

Yang, X., Li, L., Liang, J., Shi, L., Yang, J., Yi, X., Zhang, D., Han, X., Yu, N., and Shang, Y. (2013). Histone acetyltransferase 1 promotes homologous recombination in DNA repair by facilitating histone turnover. *J Biol Chem* 288, 18271-18282.

Yuen, B.T., Bush, K.M., Barrilleaux, B.L., Cotterman, R., and Knoepfler, P.S. (2014). Histone H3.3 regulates dynamic chromatin states during spermatogenesis. *Development* 141, 3483-3494.







Summary  
Samenvatting  
Abbreviation list  
Curriculum vitae  
PhD Portfolio  
Acknowledgements





## SUMMARY

In mammals, individuals having two X chromosomes (XX) are female, while individuals having one X and one Y chromosome (XY) are male. This inequality in sex chromosome constitution, with marked differences in genetic composition and overall structure of the X and Y chromosomes, has evolved in association with the evolution of sex specific regulatory mechanisms. During male meiotic prophase, the X and Y chromosomes are faced with pairing problems, due to their largely heterologous nature. As a consequence, they are subjected to transcriptional repression by meiotic sex chromosome inactivation (MSCI), and this is associated with chromosome-wide replacement of nucleosomes. Post-meiotically, the repressed state is largely maintained through post-meiotic sex chromosome repression (PSCR). Following fertilization, the presence of a single X chromosome in male embryos and two X chromosomes in female embryos requires dosage compensation, to balance X-to-autosomal gene expression and to prevent an imbalance in X-linked gene expression between the sexes. To establish this balance, one of the two X chromosomes in female embryos is inactivated through a process described as X chromosome inactivation (XCI). The non-coding RNA transcribed from the X-linked regulatory *Xist* gene is responsible for XCI initiation.

In mouse, there are two developmental waves of XCI. The first wave takes place in pre-implantation embryos and is defined as imprinted XCI (iXCI), where it is always the X chromosome of paternal origin that becomes inactivated. The second wave occurs only in the cells of the epiblast, which will give rise to the embryo proper. Here, the Xp becomes reactivated and random XCI of either one of the two X chromosomes is established *de novo*. Once an X chromosome is turned off in an epiblast cell, its inactive state will be stably maintained upon cell division. However, the inactive X chromosome will later be reactivated in female germ cells, before the onset of meiosis, which may play an essential role in oogenesis and also may preset the maternal X chromosomes to be passed on to the next generation in a transcriptionally active state. Currently available evidence suggests that the paternal X is reactivated in female embryos upon zygotic genome activation (ZGA) at the two-cell stage, but the possibility that some specific marks related to MSCI and PSCR persist on the Xp and may have a transgenerational effect on iXCI cannot be definitely excluded. Correct regulation of the epigenetic constitution of the X chromosome in gametogenesis and embryogenesis is essential for fertility and overall survival of the embryo, respectively. Studies on the molecular basis and evolutionary conservation of the mechanisms that underlay the epigenetics of the X chromosome, during its journey through the male and female germ lines and in consecutive generations, can provide new insight in key aspects of epigenetic transgenerational inheritance. In this thesis we have focused on X chromosome regulation in the male germ line and in relation to early



embryonic development. We have investigated evolutionary conservation of aspects of MSCI during spermatogenesis, and examined effects of an aberrant epigenetic constitution of the paternally inherited genome on iXCI.

First, the general theoretical concepts addressed in this thesis are described and explained in **Chapter 1**. Furthermore, in **Chapter 2** we have reviewed how the vastly different chromatin organization of immature round spermatids compared to that of spermatozoa impacts on the epigenetic regulation of the paternally inherited chromatin and other aspects of embryonic development. We report that the use of round spermatid injection (ROSI) into mouse oocytes results in embryos which develop normally. Some misregulation of embryonic ZGA, paternal DNA demethylation, and heterochromatin marks was observed, but major epigenetic abnormalities were absent. Hence, we proposed that ROSI can be used as an experimental tool to investigate the consequences of inheritance of an irregular paternal epigenetic constitution.

In **Chapter 3** we have used ROSI in mouse, to investigate if bypassing the histone-to-protamine and protamine-to-histone transitions affects iXCI. First, we have analysed if heterochromatic marks that are present in round spermatids are maintained in pre-implantation embryos. In *in vivo* fertilized mouse zygotes, only maternal constitutive heterochromatin is marked by tri-methylated histone H3 lysine 9 (H3K9me3), whereas sperm DNA acquires newly deposited histones, lacking most heterochromatic marks. ROSI-derived zygotes and 2-cell embryos showed H3K9me3 also at paternal pericentromeric regions and on the paternal X (Xp) and Y chromosomes. This result shows that the epigenetic state of the sex chromosomes of round spermatids can be carried-over and maintained in the early embryo. Next, we investigated the timing of *Xist* expression in ROSI embryos. We observed normal *Xist* RNA clouds in 4-cell stage female ROSI embryos, and absence of such clouds from the male ROSI embryos, indicating that the histone/protamine/histone transitions are not required for activation of the paternal *Xist* gene.

We have then investigated whether injection of round spermatids with a pre-inactivated Xp (inactivated by MSCI and PSCR) might help to establish inactivation of Xp, in the absence of a paternal *Xist* gene ( $\Delta Xist$ ). In *in vivo* fertilized female embryos, paternal inheritance of an *Xist* deletion ( $\Delta Xist$ ) abolishes iXCI, and leads to complete reabsorption of mutant female embryos. By performing ROSI with round spermatids obtained from  $\Delta Xist$  mice we could prevent this lethality, meaning that the Xp $\Delta Xist$  female embryos achieved X-dosage compensation successfully. ICSI did not prevent lethality of XmXp $\Delta Xist$  female embryos. We observed that the ROSI-mediated rescue occurred because XCI was established through *Xist*-mediated inactivation of the X chromosome of maternal origin. Although the molecular mechanism through which this can be achieved by ROSI remains to be specifically addressed, this work provides more insight in the general biological relevance of paternally inherited histone mod-



ifications for gene expression regulation in the early embryo.

The work presented in this thesis has also focused on studying the possible variation in the regulation and pairing behavior of the heterologous sex chromosomes among different mammalian species. In **Chapter 4** we have described the regulation and pairing behavior of the XY pair during spermatogenesis in the domestic dog (*Canis familiaris*). We have observed that, in contrast to the mouse XY pair, the canine X and Y chromosomes manage to synapse extensively. Moreover, meiotic synapsis partially extends to the X chromosome singularly, most likely involving either heterologous self-synapsis or synapsis between sister chromatids. Although extensive synapsis persists only transiently, it leads to rapid loss of known markers of DNA double strand break repair (DSB repair) and MSCI. By performing sequencing analysis of RNA isolated from purified spermatocytes and spermatids, we determined that MSCI is properly established in dog spermatocytes. However, the region of the X that showed self-synapsis displayed higher levels of X-linked gene expression compared to the unsynapsed area, and was more prone to post-meiotic reactivation. We conclude that MSCI and PSCR are incomplete in the dog. In addition, through comparative analysis of dog, mouse, and human post-meiotically down- and up-regulated genes, we have identified new candidate X-linked genes potentially relevant for male fertility.

In mouse spermatocytes, persistence of unsynapsed chromatin in meiotic cells leads to transcriptional silencing (by MSCI), but also triggers a chromosome-wide histone exchange of H3.1/2 by the variant H3.3 for both the X and Y chromosomes. In **Chapter 5**, we aimed to unravel the relevance and conservation of this remodeling event on unsynapsed chromatin during male meiosis in different species, including two marsupials (representing the metatheria), and in female mouse meiosis. We have demonstrated that histone exchange of H3.1/2 by the variant H3.3 is a male-specific event, which is conserved among all investigated eutherian mammals. Furthermore, MSCI-associated nucleosome remodeling, involving the above-described exchange of histone variants, was found also in *Monodelphis domestica* (opossum), one of the two examined marsupial species, indicating that this remodelling may have evolved before the split between metatherians and eutherians. Absence of this histone-based remodeling in the metatherian *Macropus rufogrisus* (Bennet's wallaby) may serve as a tool to dissect the molecular mechanism by which nucleosome exchange is achieved.

To conclude, in **Chapter 6**, we have discussed our results in light of the current knowledge concerning the initiation of MSCI, the evolutionary conservation of meiotic silencing and the possible transgenerational effects of PSCR. Finally, we propose future experimental approaches directed in particular towards understanding the relation between chromatin structure of the paternally inherited genome and early embryo development, including the regulation of X chromosome silencing.





## SAMENVATTING

In zoogdieren bepalen de geslachtschromosomen het geslacht. Naast 22 paar autosomen dragen vrouwen twee X chromosomen in hun lichaamcellen, terwijl bij mannen één X en één Y chromosoom samen de set van 46 chromosomen bij de mens completeren. Deze ongelijkheid in chromosoomsamenstelling, met grote verschillen in de lengte, structuur en genetische samenstelling van de X en Y chromosomen, heeft zich in de evolutie geleidelijk ontwikkeld in samenhang met het ontstaan van specifieke regulatiemechanismen. Een duidelijk voorbeeld van een dergelijk mechanisme is te vinden in de meiose, het proces waarbij in een reductiedeling de homologe chromosomen worden gescheiden om een haploïde geslachtscel te vormen uit een diploïde voorlopercel. Meiose is noodzakelijk voor de vorming van zowel eicellen als spermacellen. Echter, de grote verschillen tussen de X en Y chromosomen in voorlopercellen van de spermatozoa geven een probleem bij de chromosoomparing. Chromosoomparing is noodzakelijk in de voorbereiding op de meiotische reductiedeling, die wordt gevolgd door de tweede meiotische deling. Alle autosomen paren over de gehele lengte van de assen van de chromosomen, terwijl de X en Y chromosomen slechts voor een klein gedeelte overeenkomen en stabiel kunnen paren. Dit heeft als consequentie dat transcriptie van praktisch alle genen op het XY chromosomenpaar wordt onderdrukt door een mechanisme dat “*meiotic sex chromosome inactivation*” (MSCI) wordt genoemd. In samenhang met deze transcriptionele repressie, worden alle nucleosomen die het DNA van de X en Y chromosomen inpakken vervangen door nucleosomen met een iets andere samenstelling. Na de voltooiing van de meiotische delingen blijft de transcriptie van de meeste X- of Y-chromosoom-gebonden genen onderdrukt door “*postmeiotic sex chromosome repression*” (PSCR). Na de bevruchting bevat het menselijke embryo naast 44 autosomen één X en één Y chromosoom (mannelijke embryo's) of twee X chromosomen (vrouwelijke embryo's), afhankelijk van de aanwezigheid van een X of een Y chromosoom in de bevruchtende spermacel. Om voor deze ongelijkheid tussen de seksen te compenseren is er een mechanisme beschikbaar dat zorgdraagt voor de juiste balans in expressie van genen die gecodeerd worden door het X chromosoom ten opzichte van genen op de andere chromosomen (autosomen), en in mannelijke embryo's ten opzichte van vrouwelijke embryo's. Dit mechanisme houdt onder andere in dat in vrouwelijke embryo's één van de twee X chromosomen wordt uitgeschakeld. Dit wordt X chromosoom inactivatie (XCI) genoemd. Deze inactivatie is afhankelijk van de functie van een lang RNA molecuul, dat niet codeert voor een eiwit, en dat wordt afgeschreven van het *Xist* gen op het verder inactieve X chromosoom. Het *Xist* RNA bindt aan het X chromosoom waarvan het is afgeschreven en dit is essentieel voor de totstandkoming van XCI.

Bij het onderzoek beschreven in dit proefschrift hebben wij ons gericht op enkele verschillende zoogdieren, met de muis als de meest naaste verwant van de mens. In de muis zijn er twee rondes van XCI tijdens de embryonale ontwikkeling. De eerste ronde vindt plaats in pre-implantatie



## ADDENDUM

embryo's en wordt gedefinieerd als *imprinted XCI* (iXCI), omdat tijdens dit proces altijd het X chromosoom dat van vader afkomstig is (de paternale X; X<sub>p</sub>) wordt geïnactiveerd. De tweede ronde van XCI wordt alleen geïnitieerd in cellen van de epiblast, die het daadwerkelijke embryo gaan vormen. Eerst wordt dan X<sub>p</sub> gereactiveerd, waarna op willekeurige wijze het X chromosoom afkomstig van vader of moeder wordt geïnactiveerd. Zodra één van de twee X chromosomen in een bepaalde epiblastcel is geïnactiveerd wordt dit een stabiele situatie; in de dochtercellen die na opeenvolgende delingen uit deze cel ontstaan zal dan altijd dezelfde X inactief zijn. Alleen in de vrouwelijke germinale cellen, die zich later tot oöcyt zullen ontwikkelen in het ovarium, wordt de inactieve X weer gereactiveerd, en dat is mogelijk noodzakelijk voor een correct verloop van de oögenese, het proces van eicelvorming dat plaatsvindt tijdens de embryonale ontwikkeling. Daarnaast zorgt deze reactivatie er mogelijk voor dat de rijpe eicel in het latere volwassen leven, tijdens de reproductieve periode, altijd een actief X chromosoom (de latere maternale X (X<sub>m</sub>) in het embryo) zal bevatten. De X<sub>p</sub> wordt waarschijnlijk gereactiveerd wanneer het hele diploïde genoom van de zygote actief wordt in het twee-cellig stadium bij de muis. Het is echter niet uitgesloten dat bepaalde epigenetische markeringsaanwezig zijn op X<sub>p</sub>, die het gevolg zijn van MSCI en PSCR en die een transgenerationeel effect op iXCI zouden kunnen hebben. Correcte epigenetische regulatie van het X chromosoom tijdens de gametogenese en embryogenese is van essentieel belang voor respectievelijk vruchtbaarheid (van vrouwen en mannen) en de overleving van embryo's.

Het onderzoek naar de moleculaire basis en evolutionaire conservering van de mechanismen die ten grondslag liggen aan de epigenetica van het X chromosoom tijdens zijn reis via de mannelijke en vrouwelijke germinale routes en in zich opeenvolgende generaties kan nieuw inzicht verschaffen in belangrijke aspecten van epigenetische transgenerationele overerving. In dit proefschrift hebben we ons gericht op de regulatie van het X chromosoom tijdens de spermatogenese en in relatie met iXCI in het vroege embryo. We hebben de evolutionaire conservering van aspecten van MSCI tijdens de spermatogenese onderzocht en effecten van een afwijkende epigenetische structuur van het paternale genoom op iXCI bestudeerd.

In **Hoofdstuk 1** beschrijven we de algemene theoretische achtergrond van de onderwerpen die in dit proefschrift aan de orde komen. Daarnaast hebben we in **Hoofdstuk 2** een meer gedetailleerd overzicht gegeven van de grote verschillen in chromatinestructuur tussen onrijpe spermatiden en rijpe zaadcellen. Vervolgens wordt hier uitgelegd hoe de epigenetische regulatie van het paternale genoom en de vroege embryonale ontwikkeling kunnen worden beïnvloed na bevruchting met een onrijpe zaadcel. De globale ontwikkeling van een muizenembryo blijkt normaal te verlopen na bevruchting door injectie van een ronde spermatide (haploïde voorlopercel van de rijpe spermaceel) in een oöcyt (ROSI). Er is echter wel gerapporteerd dat een aantal processen, zoals de activatie van het genoom van de zygote, de demethylering van het paternale DNA, en bepaalde kernmerken van de chromatinestructuur afwijkend zijn na ROSI. Toch lijkt dit niet tot belangrijke epigenetische afwijkingen in het embryo of nageslacht. De in de literatuur



gerapporteerde bevindingen en de toepasbaarheid van ROSI bij de muis zijn voor ons reden om ROSI voor te stellen als bruikbaar model om de gevolgen van epigenetische afwijkingen in het paternale genoom en chromatine op embryo-ontwikkeling te onderzoeken.

In **Hoofdstuk 3** hebben we ROSI toegepast bij de muis om te onderzoeken of het omzeilen van de histon-naar-protamine en protamine-naar-histon transitities (die normaal gesproken respectievelijk in de laatste stadia van de spermatogenese en direct na de bevruchting plaatsvinden) een effect heeft op *iXCI*. Als eerste hebben we onderzocht of de histonmarkeringen van het heterochromatine in ronde spermatiden persisteren in pre-implantatie embryo's. Na normale *in vivo* bevruchting bevat alleen het maternale constitutieve heterochromatine (zoals het pericentromere heterochromatine) nucleosomen waarvan het histon H3 een trimethylering op lysine 9 bevat (H3K9me3). Het paternale DNA wordt ingepakt door maternale histonen die niet of nauwelijks gemodificeerd zijn. In zygoten en 2-cellige embryo's die waren ontstaan na ROSI vonden we echter wel H3K9me3 op het paternale pericentromere heterochromatine, en op de gehele Xp of het Y chromosoom. Dit resultaat toont aan dat de epigenetische markeringen die aanwezig zijn in ronde spermatiden overgedragen kunnen worden naar het embryo en daarin enige tijd aanwezig blijven. Vervolgens hebben we de timing van *iXCI* in ROSI-embryo's onderzocht. We detecteerden een normaal wolk-vormig *Xist* RNA signaal in 4-cellige vrouwelijke ROSI-embryo's en een dergelijk RNA signaal was afwezig in de mannelijke ROSI-embryo's. Dit resultaat toont aan dat de histon-protamine-histon transitities niet noodzakelijk zijn voor een correcte timing van activatie van paternale *Xist* RNA expressie.

Vervolgens hebben we onderzocht of injectie van ronde spermatiden met een X chromosoom (dat in feite pre-inactief is vanwege de effecten van MSCI en PSCR) kan bijdragen aan de totstandkoming van inactivatie van Xp, rond het moment van de embryonale ontwikkeling waar bij normale bevruchting (of bij toepassing van ICSI) *iXCI* zou optreden, wanneer dit X chromosoom een deletie heeft waardoor het *Xist* gen is verwijderd ( $\Delta Xist$ ). Normaal gesproken, wanneer een  $\Delta Xist$  Xp aanwezig is in een *in vivo* bevrucht muizenembryo, zal *iXCI* niet kunnen worden geïnitieerd en zal het embryo worden gesorbeerd. Dit was ook het geval in onze experimenten wanneer ICSI werd uitgevoerd met  $\Delta Xist$  sperma. Echter, door ROSI uit te voeren met ronde spermatiden van een  $\Delta Xist$  muis, konden we letaliteit van de vrouwelijke embryo's voorkomen, wat bewijst dat met behulp van ROSI er toch X-dosis-compensatie kon worden bewerkstelligd in deze mutante embryo's. We hebben vastgesteld dat de dosis-compensatie het resultaat was van activatie van het intacte maternale *Xist* gen, resulterend in inactivatie van Xm in plaats van Xp. Alhoewel we de precieze moleculaire basis van de capaciteit van deze ROSI embryos met een  $\Delta Xist$  Xp om het maternale *Xist* gen te activeren nog niet hebben kunnen ontrafelen, toont dit onderzoek wel aan dat overerving van afwijkende histonmodificaties geassocieerd met het paternale genoom een belangrijk effect kan hebben op regulatie van genexpressie tijdens de embryo-ontwikkeling.

In dit proefschrift hebben we ons ook gericht op de mogelijke variatie in de regulatie en par-



ing van de heterologe geslachtschromosomen tussen verschillende diersoorten. In **Hoofdstuk 4** wordt de XY paring en regulatie tijdens de spermatogenese bij de hond beschreven (*Canis familiaris*). We hebben waargenomen dat, in vergelijking met wat bekend was voor muizen X en Y chromosomen, het XY paar in hondenspermatocyten over een veel grotere lengte aan elkaar geritst lijkt te zijn, door het synaptonemale complex. Dit is een eiwitcomplex dat de verbinding tussen de assen van gepaarde chromosomen tot stand brengt in een proces dat synapsis genoemd wordt. Nadere beschouwing gaf aan dat de synapsis voor een deel niet het XY paar maar het X chromosoom zelf betrof, mogelijk via heterologe zelf-synapsis of synapsis tussen de zusterchromatiden. Deze uitgebreide synapsis is tijdelijk van aard, maar is wel geassocieerd met een sneller verlies van eiwitten van de geslachtschromosomen die het meiose-specifieke DNA dubbelstrengsbreukherstelproces en MSCI kenmerken, in vergelijking met een langzamer verloop van deze gebeurtenissen in muizenspermatocyten. We hebben de nucleotidevolgorde van alle mRNAs bepaald die geïsoleerd waren uit gezuiverde spermatocyten en spermatiden celpopulaties van de hond en we konden uit deze informatie vaststellen dat MSCI ook plaatsvindt in hondenspermatocyten. Het was wel opvallend dat de genen die gelokaliseerd zijn in de gebieden op het X chromosoom die tijdelijke meiotische synapsis vertoonden gemiddeld actiever waren in de spermatocyten, vergeleken met de genen in andere delen van het X chromosoom. Bovendien waren meer van die genen, uit de synapsis-gebieden, duidelijker gereactiveerd in spermatiden. Hieruit concluderen we dat MSCI en PSCR incompleet zijn in de hond. We hebben ook nog een vergelijking gemaakt tussen mRNA expressie gegevens van muis, mens en hond, voor genen op het X chromosoom die in spermatiden hoger of lager tot expressie komen dan in spermatocyten, en hieruit genen geselecteerd die mogelijk van belang zijn voor mannelijke fertiliteit bij de mens.

In spermatocyten van de muis leidt de afwezigheid van synapsis in grote delen van het XY paar niet alleen tot MSCI, maar ook tot een volledige vervanging van alle nucleosomen met histonen van het type H3.1/2 door nucleosomen met de H3.3 variant op de geslachtschromosomen. In **Hoofdstuk 5** hebben we beschreven hoe wij wilden onderzoeken wat de biologische relevantie is van dit mechanisme, en in hoeverre dit is geconserveerd in de evolutie. Hiervoor hebben we het al dan niet optreden van deze uitwisseling van nucleosomen op de (grotendeels) ongepaarde geslachtschromosomen onderzocht in spermatocyten van verschillende placentaire zoogdieren en twee buideldieren, en tevens in oöcyten met slechts één X chromosoom van een speciale XO muis. Het bleek dat de nucleosoomuitwisseling op de geslachtschromosomen een spermatogenese-specifiek proces is dat sterk geconserveerd is in de evolutie, en waarschijnlijk is ontstaan in een gemeenschappelijke voorouder van zowel de buideldieren als de placentaire zoogdieren. In spermatocyten van de wallabie (*Macropus rufogrisus*), één van de twee onderzochte buideldiersoorten, vonden we geen vervanging van de nucleosomen op de X en Y chromosomen. In toekomstig onderzoek kan dit gegeven mogelijk gebruikt worden om tot een betere selectie te komen van kandidaateiwitten die betrokken zouden kunnen zijn bij het bewerkstelligen van de nucleosoomuitwisseling.

In het concluderende **Hoofdstuk 6** bediscussiëren we onze resultaten in het licht van de huidige kennis betreffende de initiatie van MSCI, de evolutionaire conservering van dit proces en de mogelijke transgenerationele effecten van PSCR. Tot slot worden suggesties gegeven voor toekomstig onderzoek gericht op het begrijpen van de relatie tussen de chromatinestructuur van het paternaal overgeërfde genoom en de vroege embryo-ontwikkeling, inclusief de regulatie van het uitschakelen van het X chromosoom in vrouwelijke embryo's.





ADDENDUM

## LIST OF ABBREVIATIONS

ACS	abnormal chromosome segregation
ANC	adenine nucleotide carrier
AE	axial elements
ARTs	Assisted reproductive technologies
ATM	ataxia telangiectasia mutated
ATR	ATM- and RAD3-related
BrUTP	5-bromouridine-5'-triphosphate
BSA	bovine serum albumin
cDNA	complementary DNA
CE	central elements
DAPI	4',6-Diamidino-2-Phenylindole
DNA	deoxyribonucleic acid
DNMT	DNA methyltransferase
dpc	days post coitum
DSB	double strand break
ELSI	elongating spermatid injection
FC	fold-change
FISH	fluorescence in situ hybridization
FITC	fluorescein isothiocyanate
fg	fully grown
FPKM	Fragments Per Kilobase of transcript per Million fragments mapped
HDAC	histone deacetylase
HR	homologous recombination
IAP	intracisternal A particle
ICM	inner cell mass
ICSI	intracytoplasmatic sperm injection
IVF	in vitro fertilization
iXCI	imprinted X chromosome inactivation
LE	lateral elements
Mb	megabase
MDC1	mediator of DNA-damage checkpoint 1
MNase	micrococcal nuclease
MSCI	meiotic sex chromosome inactivation
MSUC	meiotic silencing of unsynapsed chromatin
ng	non-growing



ADDENDUM

PAR	pseudoautosomal region
PBS	phosphate buffered saline
PE	primitive endoderm
PFA	paraformaldehyde
PRC	Polycomb repressive complex
Prm	Protamine
PSCR	postmeiotic sex chromatin repression
RNA	ribonucleic acid
RNA pol II	RNA polymerase II
RNF	RING finger protein
ROSI	round spermatid injection
RS	round spermatid
rXCI	random X chromosome inactivation
SC	synaptonemal complex
SIM	structured illumination microscopy
Sp	spermatocyte
StCl <sub>2</sub>	strontium chloride
SUZI	subzonal insemination
TE	transverse element
TE	trophectoderm
TESE	testicular sperm extraction
Tet	ten-eleven translocation
Tsix	X inactive specific transcript, antisense
WT	wild type
XAR	X-added region
XCI	X chromosome inactivation
XCR	X-conserved region
Xic	X inactivation center
Xist	X inactive specific transcript
Xm	maternal X chromosome
Xp	paternal X chromosome
ZGA	zygotic genome activation
ZP	zona pellucida
γH2AX	phosphorylated H2AX



**CURRICULUM VITAE**

Name: Federici Federica  
 Date of birth: July 28<sup>th</sup> 1984  
 Place of birth: San Doná di Piave  
 Email address: f.federici@erasmusmc.nl

**Education**

2010-2015 PhD in Reproduction and Development  
 Erasmus University Medical Center, Rotterdam

2007-2009 MSc. Molecular Biology  
 University of Padua (Italy), degree obtained 2009

2003-2007 BSc. Molecular Biology  
 University of Padua (Italy), degree obtained 2007

**Research experience**

Aug 2010 - Mar 2015 *PhD: Reproduction and Development, Erasmus MC Rotterdam*  
 Life cycle of the X chromosome

Oct 2008 - Aug 2009 *MSc. internship in Cytogenetic, Würzburg University, Germany*  
 Genomic *in situ* hybridization (GISH) in the unisexual hybrid fish *Poecilia formosa*

May 2007 - Sep 2007 *BSc. Internship in Human Genetics, University of Padua, Italy*  
*LICAM* gene analysis in three Italian families with reported cases of spastic paraplegia



ADDENDUM

## PHD PORTFOLIO

### Summary of PhD training and teaching

Name PhD student	Federica Federici
Erasmus MC Department	Reproduction and development
Research School	Biomedical Sciences
PhD period	August 2010 - March 2015
Promotor(s)	Prof. dr. J.A. Grootegoed Prof. dr. J.S.E. Laven
Supervisor	dr. W.M. Baarends

### 1. PhD training

#### Courses

	Year
- Safely Working in the Laboratory	2011
- Biochemistry and Biophysics	2010
- Cell and Developmental Biology	2011
- Genetics	2011
- Working with test animals (Artikel 9, proefdierkunde cursus)	2010
- OIC course "Practical introduction to laser scanning microscopy"	2011
- Literature course	2012
- OIC course " <i>In vivo</i> imaging: from molecule to organism"	2011
- AMS course	2011

#### Seminars and workshops

- Adobe Photoshop and Illustrator CS5 Workshop	2011
- 18 <sup>th</sup> MGC workshop, Maastricht	2011
- 19 <sup>th</sup> MGC workshop, Düsseldorf	2012
- Winterschool Kleinwalsertal (oral presentations)	2011/2012

#### (Inter)national conferences

- "Chromatin changes in differentiation and malignancies", Giessen	2011
- EMBO Meiosis Meeting, Capaccio, Italy (poster presentation)	2011
- 10 <sup>th</sup> Dutch chromatin meeting, Amsterdam (poster presentation and selected blitz oral presentation)	2012
- Stem cells, development and regulation, Amsterdam (poster presentation)	2013
- "Chromatin changes in differentiation and malignancies", Egmond aan Zee (poster presentation)	2013
- 11 <sup>th</sup> Dutch chromatin meeting, Rotterdam (poster presentation)	2013
- Keystone symposium "Chromatin Mechanisms and Cell Physiology", Oberstdorf (poster presentation and selected oral presentation)	2014

### 2. Teaching

#### Supervising practicals and excursions, Tutoring

- Teaching assistant in "VO Vroege embryos cloning and transgenese"	2012
- Junior Science Program, Erasmus MC, 2 high school students	2011





ADDENDUM

## ACKNOWLEDGMENTS

Eh eh, hier zijn we eindelijk!

I must admit that writing these last pages brings up a lot of mixed feelings...I am definitely very happy and excited to have reached this goal and to start a new chapter of my life, but at the same time sad to leave all the people that in these years have become family to me. I am honored to have shared these years with you, and I would like to thank you all from the bottom of my heart!

Dear Willy, I will never thank you enough for allowing me to undertake this adventure, for your constant support and for taking care of me not only on a professional level, but also on a personal one. You never stop surprising me with your load of energy and enthusiasm, not even the peaks of the Giro d'Italia can stop you! Thank you for having guided me up to this point and for all the effort and time you have put in the work we can finally present in this thesis.

Geachte promotoren, dear Anton and Joop, I am deeply grateful to you for giving me the opportunity to carry out this research project, for the many inspiring discussions and for sharing your deep knowledge with me. Your valuable comments helped me enormously to improve this manuscript.

Furthermore, I would like to thank the members of the thesis committee, Dr.ir. Tokameh Mahmoudi, Prof.dr. Sjoerd Repping and Prof.dr. Bas van Steensel for their insightful comments and suggestions.

Thanks also to Joost, Esther and Maureen for being always very helpful and for finding time whenever I needed it to discuss research projects or to find solutions to any kind of technical problem with me. Your ideas and suggestions have contributed greatly to my work.

An enormous GRAZIE/BEDANKT to my paranympths!

Cara Agnese, aka *Paranympth of March 2015*, sei una forza della natura! Trovare un'amica così é come vincere la lotteria: raro ed una gran fortuna! Ti sono infinitamente grata per essermi stata vicina quotidianamente in questi anni, ne abbiamo passate un bel po' insieme, eh?! E non finisce qui, ne sono certa!

Lieve Evelyne, dankzij jou zijn lange ROSI secties in een stinkend muishuis een plezier geweest. Ik ga de gezelligheid zeker missen! Bedankt voor jouw hulp en inzet, zonder jouw steun zou ik nooit zo ver gekomen zijn.

With my paranympths, I would also like to thank my "extraordinary" paranympths: Aristea, Fabrizia, Friedemann and Godfried.



Dear Aris, thanks for being such a good friend. I've the feeling words are not even necessary between us, we simply understand each other. I look forward to the day you will be also done, soon we will be in the sun!

Cara Fa, grazie mille per essere stata non solo un'ottima collega, ma soprattutto una cara amica. Sono proprio felice che tu abbia deciso di restare ancora per un po'! Grazie anche per tutte le dritte ed il tuo aiuto, questa tesi non sarebbe mai stata impaginata così bene senza il tuo contributo!

Dear Friedo, so nice we are finishing together. March is going to be hardcore party time! Finally! Thanks for all your patience with these noisy Italians that keep invading your house. And thanks for asking your father to take us on his "vessel", that was fun!

Beste Godfried, van jouw heb ik de eerste (van alle tijden!) Nederlandse worden geleerd, dat ga ik nooit meer vergeten! Bedankt voor alles wat je mij over wetenschap hebt geleerd en voor alle boeiende discussies. Het is altijd leuk om met jou te praten!

Furthermore, I would like to thank all my colleagues and friends from lab 902, the coolest of the entire building ☺: Akiko, Andrea, Annagien, Bas, Catherine, Cheryl (and Peanut!), Cristina, Daphne, Dimitar, Eskeww, Esther, Eveline, Hegias, Joke, Jos, Marja, Nathalie, Nhilan, Pang, Ruben, Sam, Sarra, Selma and Stefan. Thanks to all of you for the help at the bench, the fun and the great company. You have enriched me a lot, and not only as a scientist!

Ik ben ook John (the master injector!), Helen, Alex, Iris, Suzette en Patrik ontzettend dankbaar voor alle huis-gerelateerde hulp.

Thanks to Christine, Margarida, Cindy, and to Alex, Gert, Gert-Jan, Johan and the whole OIC group for the nice collaborations and for your help.

And thanks to all the friends I made on the way: Ainoha, Luca ed Iria (é sempre bello venire a "svernare" da voi!), Angy (come sono felice di averti vicino anche in questa occasione!), Dani (al fin, después de más de diez años, nos vemos!), Jovana ed Enrico (forza Meolo! C'è sempre piú aria di casa da quando ci siete voi!), Fanny (we need do make the ratatouille again!), Giulia (non credo di aver mai scritto così tanto nemmeno in 5 anni di liceo! E tu lo sai bene!), Gloria, Davi e Cali (il tempo passa, ma con voi si ride sempre come ai tempi di Alfredo!), Isa (la persona piú zen che abbia mai conosciuto! Riesci sempre ad avere un'influenza così positiva sulle persone!), Jessica e Thomas (it's nice to know that either in Rotterdam, Padova, Amersfoort or Freiburg we will keep seeing each other!), Linda e Vale (adesso dobbiamo proprio riuscire a trovarci...basta essere così cialtrone! ☺), Luca (in quel di Amersfoort stiamo solo aspettando i primi tepori primaverili per dar fuoco alle grigie,



tienti pronto!), Nesrin (keep strong, you are almost there as well! Thanks for all the laughs!), Rachael en Rik (ik vind het echt vet dat jullie bij mijn feest zijn en dank voor de muziek!), Sander (het is altijd lachen met jou!), Simone e Flavia (grazie per tutte le belle serate passate insieme!), molte grazie anche alla sempre crescente comunità italiana and thanks to many other colleagues spread around the building. I will be happy to celebrate the end of my PhD with all of you!

E adesso tocca proprio a te, caro Ale! Grazie mille per avermi sopportata in questi mesi, in cui sono stata piú come uno dei tuoi pazienti, che come una morosa! Grazie per avermi ricordato, ogniqualvolta la frustrazione prendeva il sopravvento, quali fossero le cose veramente importanti (e riuscire ad isolare dell'RNA certamente non lo é! Ma sei servito tu a mettere le cose bene in prospettiva...). Mi sento la persona piú fortunata al mondo ad averti al mio fianco...ma ora basta con le smancerie! Prepara la motorina, che é arrivato il momento di partire! Un ringraziamento speciale anche alla tua famiglia, a Nicola, Lizzy, Marco, Giorgia e Gian. Na Natale 2014, hoor ik er echt bij! ☺

Infine voglio ringraziare di cuore la mia famiglia, i capisaldi della mia vita: mia mamma, mio papà e mia sorella. Senza il vostro supporto non sarei mai riuscita a completare questa tesi, e non sto esagerando! Quantomeno sarebbe stata una tesi senza copertina! Grazie mille per tutto il tempo impiegato a disegnarla papà! E grazie a voi, mamma e Nena, per aver tenuto d'occhio i colori ☺!

Grazie per avermi fatto vivere, seppur a distanza, la vostra quotidianità e per avermi sempre lasciata libera di scegliere la mia strada...vi voglio bene!

*fede*



